UNIVERSIDAD COMPLUTENSE DE MADRID
FACULTAD DE CIENCIAS BIOLÓGICAS
Departamento de Genética

TESIS DOCTORAL

Efectos de parámetros ambientales en interacciones compatibles entre plantas y virus de RNA y su relación con los supresores de silenciamiento virales y sus propiedades

MEMORIA PARA OPTAR AL GRADO DE DOCTOR

PRESENTADA POR

Francisco Javier del Toro Serna

Director
Tomás Canto Ceballos

Madrid, 2016

TESIS DOCTORAL

Efectos de parámetros ambientales en interacciones compatibles entre plantas y virus de RNA y su relación con los supresores de silenciamiento virales y sus propiedades

Francisco Javier del Toro Serna

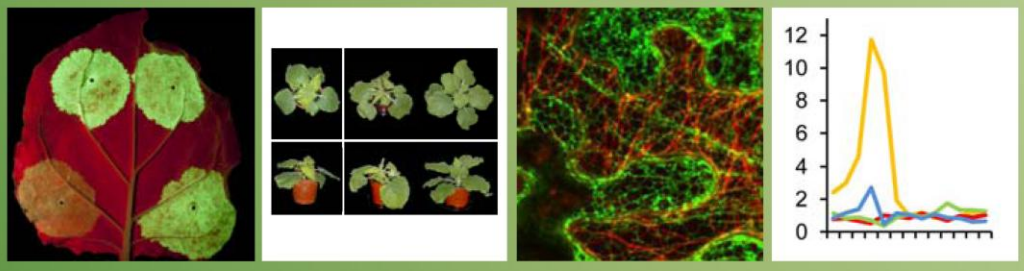

UNIVERSIDAD COMPLUTENSE DE MADRID
FACULTAD DE CIENCIAS BIOLÓGICAS
DEPARTAMENTO DE GENÉTICA

CONSEJO SUPERIOR DE INVESTIGACIONES CIENTÍFICAS
CENTRO DE INVESTIGACIONES BIOLÓGICAS
DEPARTAMENTO DE BIOLOGÍA MEDIOAMBIENTAL

Madrid, 2015

A mi amada reina, mi dulce y única
A mi familia
A mis amigos

UNIVERSIDAD COMPLUTENSE DE MADRID
FACULTAD DE CIENCIAS BIOLÓGICAS
DEPARTAMENTO DE GENÉTICA

TESIS DOCTORAL

Efectos de parámetros ambientales en interacciones compatibles entre plantas y virus de RNA y su relación con los supresores de silenciamiento virales y sus propiedades

MEMORIA PARA OPTAR AL GRADO DE DOCTOR
PRESENTADA POR

Francisco Javier del Toro Serna

Director

Dr. Tomás Canto Ceballos

Madrid, 2015

UNIVERSIDAD COMPLUTENSE DE MADRID
FACULTAD DE CIENCIAS BIOLÓGICAS
DEPARTAMENTO DE GENÉTICA

CONSEJO SUPERIOR DE INVESTIGACIONES CIENTÍFICAS
CENTRO DE INVESTIGACIONES BIOLÓGICAS
DEPARTAMENTO DE BIOLOGÍA MEDIOAMBIENTAL

TESIS DOCTORAL

Efectos de parámetros ambientales en interacciones compatibles entre plantas y virus de RNA y su relación con los supresores de silenciamiento virales y sus propiedades

Effects of environmental parameters on compatible interactions between plants and RNA viruses, and their relation to viral suppresors of silencing and their properties

Francisco Javier del Toro Serna

Madrid, 2015

AGRADECIMIENTOS

Esta tesis se ha llevado a cabo en el Centro de Investigaciones Bilógicas (CIB) perteneciente al Consejo Superior de Investigaciones Científicas (CSIC) y ha sido financiada por los proyectos "Prediction of the impact of climate change on the outcome of diseases caused by plant RNA viruses" (PJ00946102) de la Rural Development Administration de la República de Corea en cooperación con el CSIC y por el proyecto "Función de determinantes de patogenicidad viral en los balances que se establecen en interacciones compatibles virus RNA-planta" del Ministerio de Economía y Competitividad (MINECO) de España.

Durante la realización de esta tesis he tenido la oportunidad de compartir experiencias con mucha gente a la que desde aquí me gustaría enviar mis agradecimientos.

En primer lugar no sólo tengo que agradecer sino que estoy encantado de hacerlo, a mi director, el Dr. Tomás Canto. Muchas gracias por permitirme trabajar contigo y realizar esta tesis. Muchas gracias por tu ayuda, dedicación y sobre todo paciencia. Gracias por tus críticas que tanto me han enseñado y por tu profunda visión científica. Gracias por tu apoyo y confianza. Gracias, de todo corazón. También debo agradecer al Dr. Francisco Tenllado por su ánimo, sus consejos y por ejemplificar algo que admiro, la vívida búsqueda de los entresijos biológicos que subyacen al resultado. I could never forget Dr. Bong-Nam Chung, partner researcher in the project in collaboration with the RDA, whom always brought me good advices and whose visit was a breath of fresh and a revitalizing experience. I cannot also forget Dr. Kyung-San Choi, partaker researcher in the same project, and that was always as cheerful and happy as educational. También quiero agradecer al Dr. César Llave por una tremenda oportunidad concedida aunque brindara ríos oscuros necesarios.

A la Dra. Maite Serra, de la que admiro su alma infatigable y su capacidad para ser encantadora. A Virginia por ser tan afable.

También debo agradecer mucho a otra tanta gente que sin ser científicos titulares siempre trataron de brindarme sus altos conocimientos científicos además de su cariño. No sabría por dónde empezar y mucho menos como continuar, así que lo intentaré hacer lo mejor posible… empecemos por Livia, maravillosa compañera, maestra de poyata y de vida. Cualquier cosa que diga de ella nunca será suficiente. Alberto, un ídolo, un ejemplo *in vivo* de la paz kármica que solo la experiencia proporciona. Gosia, una chica de valor (no solo científico) incalculable y apoyo incondicional. Meme, siempre sonriente y animosa, cargada del encanto de un espíritu libre. Anita Manzano, alegre como un sol de primavera. Gracias. Fátima, con una sonrisa siempre dispuesta a alegrar los corazones. Sin ti esto no existiría. Gracias. Ana Castro, ejemplo de esfuerzo y alegría. Una esclava a la que echo mucho de menos. Loïc, que tantos buenos ratos me hizo pasar entre malos momentos. Lourdes, tan polite y formal como llena de amor. Nacho por su vivo desparpajo. Llucia, critica sociopolítica de nuestros tiempos. A Inmaculada con la que he acabado compartiendo jefe y sprint en el depósito. Gracias también a Montse por sus "píldoras de realidad" y apoyo técnico. A los "salinos" que siempre que se lo pedí me ofrecieron su ayuda. A Andrés Requena por ser mi primer contacto con el mundo de los virus.

Gracias a la renovación de los tiempos llegaron nuevos espíritus al CIB a los que tanto tengo que agradecer. Emmunué… has sido un compañero fantástico, compartiendo siempre visión científica y dosis de cariño a partes iguales. A ver cuando limpias el labo. David, figura, gracias…sí, sí, ¿pero por qué? Fran2, por esos inolvidables buenos momentos de compañerismo sincero. Laura, una liliflor de realidad ácida. Irene, siempre sonriente. A los "niños" del 205, Raúl, Arantxa y Miguel, a los que fue tan fácil coger cariño. A los fantásticos Miguel y Javi,

estudiantes de Mª Cristina Vega con los que compartí labo, que fueron luego reemplazados por los maravillosos fungers Vero, Iván y Javi.

Gracias también a la gente de la Facultad de Biología de la UCM; profesores que me hicieron enamorarme de la ciencia, de los que me gustaría recalcar el papel del Dr. Marcelino Bañuelos y de las buenas gentes del departamento de genética (de los que hacer una lista sería imposible); así como gente con la que interactué por diversas tramitaciones como el Dr. Javier Gallego por hacer que todo fuese tan fácil; y Rosa M. Rodríguez por su paciencia con las millones de dudas sobre papeleos.

Además de esta gente tan maravillosa han habido otras personas sin las que esto no habría sido posible porque soy quien soy gracias a ellos.

A mis amigos. Todos habéis sido un pilar de mi vida. Un pilar inquebrantable de afecto, apoyo y alegrías. No voy a escribir aquí vuestros nombres porque de sobra sé que sabéis quien sois. Que nada nos cambie.

A mi familia. Vosotros no solo sois los primeros artífices de este cuerpo (que yo me he ocupado de agrandar), sino que habéis modelado mi espíritu a base de amor para tratar de hacer de mi alguien de provecho. Si en lo más mínimo he sido capaz de adoptar los valores que me tratasteis de inculcar la aventura habrá valido la pena.

A Rebe. Porque te quiero tanto que las palabras no son capaces de expresarlo. Has aguantado en los momentos buenos y en los "reguleros". Si he sido capaz de seguir en pie ha sido porque estabas a mi lado y tu sonrisa me quitaba las penas. Aún nos quedan muchos amaneceres por disfrutar.

A todos os debo mi más sincero GRACIAS

INDEX

RESUMEN

La presente memoria de investigación presenta y discute los resultados de trabajos que estudian, por un lado, los efectos de dos factores ambientales, la temperatura y los niveles de CO_2 en infecciones compatibles de plantas por virus de RNA de polaridad positiva, y también en el silenciamiento antiviral y en su supresión por factores virales. Y por otro lado estudia las propiedades del supresor de silenciamiento viral HCPro del Virus Y de la patata (*Potato virus Y*, PVY), mediante aproximaciones de biología celular y molecular.

Para estudiar cómo incrementos en los valores de estos factores ambientales pueden afectar a las infecciones virales de plantas se estudió su efecto por separado en la infección de la planta *Nicotiana benthamiana* por varios de estos virus: el Virus del mosaico del pepino (*Cucumber mosaic virus*, CMV), PVY, y un vector de expresión derivado del Virus X de la patata (*Potato virus X*, PVX) vacio, o expresando los supresores de silenciamiento de PVY o de CMV, HCPro y la proteína 2b, respectivamente. En condiciones de elevada temperatura (30 ºC) o de elevados niveles de CO_2 (970 partes por millón, ppm) se analizaron la acumulación viral sistémica, los síntomas de infección, y la actividad de los supresores de silenciamiento de estos virus, comparándolos con los obtenidos en las condiciones "normales" de 25 ºC y 401 ppm de CO_2.

A 30 ºC la acumulación de PVY y las de las tres construcciones de PVX se vieron disminuidas a aproximadamente la mitad. La severidad de los síntomas también se redujo mucho en la infección por PVY e incluso no hubo síntomas en las infecciones por los virus derivados de PVX. Por el

contrario ni la acumulación viral ni los síntomas asociados se vieron afectados por la elevada temperatura en la infección por CMV.

En condiciones de elevado CO_2 no se observaron cambios en la intensidad o en el momento de la aparición de los síntomas derivados de las infecciones virales estudiadas. Sin embargo, bajo estas circunstancias ambientales la acumulación de PVY así como las de las construcciones de PVX se vieron ligeramente disminuidas en discos foliares, pero se incrementaron al relativizarlas a las proteínas totales contenidas en los discos foliares. Esto fue así porque las plantas de *N. benthamiana* crecidas bajo condiciones de elevados niveles de CO_2 ambiental alcanzaron mayor tamaño que el de las plantas crecidas en condiciones normales, pero con una cantidad de proteína total en discos de tejido foliar que fue aproximadamente la mitad que la encontrada en discos equivalentes de plantas crecidas en condiciones normales. Por otra parte, la acumulación de CMV aumentó en un ambiente de alto CO_2 en discos foliares equivalentes, e incluso más relativizándola a proteínas totales. Los virus analizados se pudieron pues separar en dos grupos según su respuesta, tanto a la elevada temperatura como al elevado CO_2 ambiental: PVY y los vectores de PVX por un lado, CMV por el otro.

La técnica de la agroinfiltración ha sido ampliamente utilizada para expresar transitoriamente ácidos nucleicos y las proteínas que puedan codificar en plantas. La técnica permite estudiar y cuantificar algunas actividades biológicas, como por ejemplo la supresión del silenciamiento antiviral por ciertas proteínas virales. Sin embargo, un inconveniente de la agroinfiltración es que temperaturas superiores a 29 ºC impiden la transferencia de información genética desde la bacteria a las células vegetales. Dado que uno de los objetivos de este trabajo era el estudio de

la actividad de los supresores de silenciamiento virales HCPro y proteína 2b a la temperatura de 30 ºC, se tuvo que diseñar un procedimiento que permitiera su uso. Se razonó que si se permitía una ventana temporal a 25 °C después de la agroinfiltración, la transferencia de información de la bacteria a la planta tendría lugar, y al elevar la temperatura a 30 °C las proteínas expresadas se acumularían y realizarían su función a dicha temperatura. No se obtuvieron resultados satisfactorios dando un lapso de 12 horas a 25 ºC previo al emplazamiento de las plantas a 30 ºC. Sin embargo, un lapso de 24 horas a 25 ºC después de la agroinfiltración permitió la acumulación de varias proteínas, incluyendo la de un marcador fluorescente, comparable a las observadas en ensayos realizados a 25 ºC.

Este procedimiento permitió evaluar la actividad biológica a 30 ºC de los supresores de silenciamiento HCPro y la proteína 2b. Estos supresores se expresaron bajo el control de promotores eucariotas, o como parte de amplicones virales agroinfiltrados (construcciones de PVX). Los resultados obtenidos demostraron que ambas proteínas eran capaces de suprimir el silenciamiento de un gen reportero de forma tan efectiva a 30 °C como a 25 ºC. En los ensayos de expresión mediante vectores basados en PVX ni la expresión de HCPro ni la de la proteína 2b favorecieron la acumulación viral, a pesar de haberse demostrado su efectividad como supresores a 30 ºC.

También se empleó la agroinfiltración para comprobar si un ambiente enriquecido en CO_2 alteraba la actividad supresora de HCPro o de la proteína 2b. Los resultados demostraron que ambos factores virales eran tan efectivos en la supresión del silenciamiento sobre un gen reportero en condiciones de elevado CO_2 como en las condiciones normales. De igual modo a lo observado a elevada temperatura, la expresión de los

mencionados supresores de silenciamiento mediante vectores basados en PVX tampoco favoreció la acumulación viral en condiciones de alto CO_2.

De todo esto se infiere que ninguno de los factores ambientales estudiados es capaz de afectar negativamente a la eficiencia de dichos supresores para neutralizar el silenciamiento antiviral bajo dichas condiciones, al menos por separado. Por ello, los efectos observados tanto en la infección por PVY como por las construcciones de PVX parecen no estar relacionados con el silenciamiento génico antiviral o con su supresión por factores virales.

Para avanzar en el estudio del supresor de silenciamiento viral HCPro de PVY se siguieron dos aproximaciones: una de estudio de su localización y dinámicas subcelulares; y otra de caracterización de los RNAs que pudieran estar unidos a la misma *in vivo* en el curso de una infección.

Para estudiar las dinámicas subcelulares de HCPro *in vivo* mediante microscopía confocal, éste se expresó en células epidérmicas de *N. benthamiana* fusionado a distintos marcadores para emitir fluorescencia, bien en su forma monomérica o como homodímero. En paralelo se caracterizaron las actividades funcionales de las proteínas de fusión para determinar si los marcajes afectaban a las funciones de HCPro. La microscopía confocal reveló una diversidad de patrones de distribución subcelular que incluyen una distribución difusa de HCPro por todo el citoplasma, o la presencia de inclusiones irregulares que contenían, al menos algunas de ellas α-tubulina, y cuyo tamaño y número pueden estar condicionados por factores externos. Además se descubrió un patrón de estructuras de tamaño y distribución regulares asociadas tanto al retículo endoplásmico como a los microtúbulos (MTs). La exposición de las células a ciertos estreses originó que HCPro se translocara desde estas

estructuras regulares (y quizás también desde otras partes del citoplasma) hacia el citoesqueleto de MTs, hasta cubrirlo completamente. No se observó que HCPro se localizase asociado con los filamentos de actina o con el aparato de Golgi. A pesar de esta asociación con los MTs, la integridad de este citoesqueleto celular no es requerida para que HCPro medie la transmisión de PVY por su insecto vector *Myzus persicae*, ni tampoco para su supresión del silenciamiento de un gen reportero en ensayos agroinfiltración. La razón funcional de estos patrones y dinámicas subcelulares de HCPro permanece pues por aclarar.

Para caracterizar si HCPro une RNAs *in vivo* y la naturaleza de dichos RNAs se purificó esta proteína marcada con una cola de seis histidinas a partir de tejido de plantas infectadas por un vector viral basado en PVX, que la expresaba. La purificación se realizó en condiciones no desnaturalizantes mediante una resina de agarosa cargada de níquel, y como control el mismo proceso se realizó con plantas infectadas con el vector viral PVX vacio. Los RNAs menores de 500 nucleótidos (nts) se extrajeron de ambas muestras, se procedió a la secuenciación masiva de los mismos. Mediante herramientas bioinformáticas se analizaron y compararon las secuencias obtenidas de ambas muestras.

Los resultados muestran que HCPro une RNAs pequeños (sRNAs) de 21 y 22 nts, mostrando preferencia por aquellos de secuencia viral (vsRNAs) sobre los de secuencia de la planta, a pesar de ser estos últimos mucho más numerosos. También une en mucha menor medida algunos RNAs de tamaños mayores, también con secuencias virales. Además, se encontró que los vsRNAs de 21 y 22 nts unidos a HCPro estaban enriquecidos en secuencias que tenían una adenina en su extremo 5', hecho que no se observó en los RNAs de otros tamaños de secuencia viral o en los sRNAs

con secuencias de la planta. Estos resultados sugieren que una forma en la que HCPro podría realizar su función de supresor de silenciamiento sería mediante el secuestro de sRNAs específicos: de 21 y 22 nts, secuencia viral y con adeninas en sus extremos 5', que de otro modo podrían incorporarse al efector antiviral Argonauta2.

SUMMARY

This Research Report presents and discusses results obtained in work that on the one hand studies effects that the environmental factors temperature and ambient CO_2 levels cause on compatible infections of plants by positive-sense RNA viruses and also on the antiviral silencing defense and its suppression by viral factors. And on the other hand, studies the properties of the viral suppressor of silencing HCPro from *Potato virus Y* (PVY), using cell and molecular biology experimental approaches.

To study how increases in the values of those two environmental factors could affect viral infections of plants we addressed each separately in infections of the host *Nicotiana benthamiana* by several viruses: *Cucumber mosaic virus* (CMV), PVY, and a viral expression vector derived from *Potato virus X* (PVX) either empty, or expressing the suppressors of silencing of PVY or CMV, HCPro and 2b protein, respectively. Systemic viral accumulation levels, infection symptoms, and the activities of the viral suppressors were analyzed under elevated temperature conditions (30 ºC) or under elevated ambient levels of CO_2 (970 parts per million, ppm) and were compared to those found at the "normal" conditions of 25 ºC and 401 ppm levels of CO_2.

At 30 °C the accumulation of PVY and those of the three PVX constructs roughly halved. The severity of symptoms was also much reduced in infections by PVY and symptoms were even absent in plants infected with any of the PVX-derived constructs. By contrast, neither viral accumulation nor its associated symptoms were affected by the elevated temperature in CMV infections.

Under elevated CO_2 conditions no changes were observed in the intensity of infection symptoms or in their timing of appearance, for any of the viruses studied. However, under those same circumstances the accumulation of PVY and also those of the three PVX constructs was slightly reduced in leaf discs, but it increased with regard to the total protein content contained in those leaf discs. This was so because *N. benthamiana* plants grown under elevated CO_2 conditions grew larger in size than plants grown under normal conditions, but the former contained approximately half the total protein content than the latter in equivalent leaf discs. On the other hand, the accumulation of CMV at elevated CO_2 levels increased in both, equivalent leaf discs, and even further with regard to total protein content. Thus, the five viruses analyzed could be clustered into two separate groups based on in their response to elevated temperature or ambient CO_2 levels: PVY and the three PVX constructs on the one hand, CMV on the other.

The agroinfiltration technique has been widely used to transiently express in plants nucleic acids and the protein products that they may encode. The technique allows the study and quantification of some of the biological properties of those proteins, such as for example the suppressor of antiviral silencing activities of certain viral factors. However, one drawback of the technique is that at temperatures above 29 °C the transfer of genetic information from the bacteria to plant cells is prevented. As one of the objectives of this research was to study the biological activities of the viral silencing suppressors HCPro and the 2b protein at the temperature of 30 °C, a procedure had to be envisaged to allow its use at this non-permissive temperature. It was reasoned that if a time window at 25 °C was allowed after infiltration, some transfer of information from the

bacteria to the plant cell would take place, and afterwards when increasing temperature to 30 °C the proteins expressed would accumulate and perform their functions at that temperature. A window time of just 12 hours before placing the plants at 30 °C gave unsatisfactory results, but a 24 hour window at 25 °C allowed the accumulation of several proteins, including a fluorescent protein reporter, comparable to those observed in assays performed all the time at 25 °C.

This procedure allowed the evaluation of the biological activities of the viral suppressors HCPro and 2b protein. Those suppressors were expressed either under the controls of eukaryotic promoters, or as part of agroinfiltrated viral amplicons (PVX constructs). The results obtained showed that both proteins were capable of suppressing the silencing of a reporter gene as effectively at 30 °C as at 25 °C. The expression assays from PVX-based constructs showed that neither HCPro nor the 2b protein helped the virus construct to accumulate further at 30°C, in spite of both proteins being affective suppressors at that temperature.

Agroinfiltration was also employed to test whether an enriched CO_2 environment altered the suppressor activities of HCPro and of the 2b protein. Results showed that both viral factors were as effective in silencing suppression of a reporter gene at elevated CO_2 levels as in normal conditions. Similarly to what was found at elevated temperature, expression of either suppressor from PVX vectors failed to favor viral accumulation at elevated CO_2 levels.

From all this it can be concluded that neither of the two environmental parameters separately had a negative effect on the effectiveness of these suppressors to neutralize the antiviral silencing defense. Because of this,

the effects on infection by PVY or by the three PVX constructs seem to be unrelated to antiviral gene silencing or its suppression by viral factors.

To study further the viral suppressor of silencing HCPro from PVY two approaches were followed: one that studied its subcellular localization and dynamics *in vivo*; and another one that characterized the RNAs that could be bound to this protein also *in vivo* during the course of infection.

To study HCPro subcellular dynamics *in vivo* by confocal microscopy, the protein was expressed in *N. benthamiana* epidermal cells fused to different tags, in order to emit fluorescence either as a monomer, or as a homodimer. In parallel to this, the functional activities of these fusion proteins were characterized, to determine how these tags affected HCPro biological functions. Confocal microscopy observations revealed a diversity of subcellular distribution patterns that included HCPro diffuse distribution throughout the cell cytoplasm, or its presence in irregular inclusions that also contained, at least some of them, α-tubulin, and whose size and number could be influenced by external factors. In addition, a pattern of structures of regular size and distribution was discovered, associated to the endoplasmic reticulum, as well as to microtubules (MTs). Exposure of cells to some stresses caused HCPro to translocate from these regular structures (perhaps also from other parts of the cytoplasm) towards the MT cytoskeleton, coating it completely. No association of HCPro to actin filaments or to the Golgi was observed. In spite of its association with MTs, the integrity of this cellular cytoskeleton was found not to be required for HCPro-mediated transmission of PVY by its insect vector *Myzus persicae*, or for its suppression of the silencing of a reporter gene in agropatch assays. The functional reasons of these distribution patterns and their dynamics remain thus to be explained.

To characterize whether HCPro would bind to RNAs *in vivo*, and the nature of those bound RNAs the protein tagged with six histidines was purified from leaf tissue of plants infected with a PVX-based vector that expressed it. The purification was performed under non-denaturing conditions using a nickel charged resin, and as control, the same procedure was followed using tissue from plants infected with the empty PVX vector. RNAs of less than 500 nucleotides (nts) were extracted from both samples and deep sequenced. The sequences obtained were analyzed and compared using bioinformatic tools.

Results show that HCPro binds to small RNAs (sRNAs) of 21 and 22 nts in length, preferentially to those that have a virus-derived sequence (svRNAs) over those that are of plant sequence, in spite of the latter being much more abundant than the former. It also appears to bind to larger RNAs also of viral sequence, to a much lesser degree. In addition to this, the svRNAs of 21 and 22 nts bound to HCPro were found to be enriched in sequences that had adenines at their 5'-ends. This did not occur in bound RNAs of other sizes or of plant sequence. These results suggest that a way by which HCPro could perform its suppressor function could be through the sequestration of specific types of sRNAs: of 21 and 22 nts in length, of viral sequence and with 5'-end adenines, which could otherwise incorporate into the antiviral Argonaute2 effector.

ABBREVIATIONS AND ACRONYMS LIST

General abbreviations and acronyms

6x: hexahistidine tag

aas: amino acids

ABA: abscisic acid

AGO: Argonaute protein

Avr gene: *Avirulence* gene

BiFC: bimolecular fluorescence complementation

CI: cylindrical inclusion protein

CP: coat/capsid protein

C-terminus/terminal: carboxyl terminus/terminal

DCL: Dicer-Like protein

dpa: days post-agroinfiltration

dpi: days post-inoculation

ds: double-stranded

ER: endoplasmic reticulum

ET: ethylene

GFP: Green Fluorescent Protein

h: hour/hours

HA: Hemagglutinin epitope tag

HCPro: Helper component proteinase

HEN1: Hua Enhancer1 methyltransferase

HIP2: HCPro-Interacting protein 2

hpi: hours post-infiltration

HR: hypersensitive response

HSP: Heat Shock protein

IPCC: Intergovernmental Panel on Climate Change

JA: jasmonic acid

MP: movement protein

miRNA: microRNA

NIa/NIb: Nuclear Inclusion protein a/b

NPR1: Non-expressor of PR genes1 protein

nt: nucleotide

N-terminus/terminal: amino-terminus/terminal

ORF: Open reading frame

PR: Pathogenesis-Related protein

R gene*:* *Resistance* gene

RAV2: Related to ABI3/VP1 protein

RDR: RNA-dependent RNA polymerase

RISC: RNA-induced silencing complex

ROS: reactive oxygen species

SA: salicylic acid

SAR: systemic acquired resistance

sgRNA: subgenomic RNA

SGS3: Suppressor of Gene Silencing3

siRNA: small interfering RNA

sRNA: small RNA

ss: single-stranded

st: standard conditions (25 ºC and 401 ppm of CO_2)

T-DNA: Transferred DNA

TGB: *Triple gene block*

VIGS: Virus-Induced Gene Silencing

VPg: Viral genome-linked protein

vsiRNA: virus-derived siRNA

VSR: viral suppressor of RNA silencing

Y2H: yeast two-hybrid assays

Viruses:

BYDV:	*Barley yellow dwarf virus*
CaMV:	*Cauliflower mosaic virus*
CMV:	*Cucumber mosaic virus*
PMMoV:	*Pepper mild mottle virus*
PPV:	*Plum pox virus*
PVX:	*Potato virus X*
PVY:	*Potato virus Y*
RDV:	*Rice dwarf virus*
SPCSV:	*Sweet potato chlorotic stunt virus*
TAV:	*Tomato aspermy virus*
TBSV:	*Tomato bushy stunt virus*
TCV:	*Turnip crinkle virus*
TEV:	*Tobacco etch virus*
TMV:	*Tobacco mosaic virus*
ToRSV:	*Tomato ringspot virus*
TRV:	*Tobacco rattle virus*
TuMV:	*Turnip mosaic virus*
TYLCV:	*Tomato yellow leaf curl virus*
TYMV:	*Turnip yellow mosaic virus*
ZYMV:	*Zucchini yellow mosaic virus*

CHAPTER 1

GENERAL INTRODUCTION

1.1- Plant-virus interactions

Plant viruses are obligate intracellular parasites that in some cases constitute important pathogens that inflict economic losses to crops. The rather genetically homogeneous crops with introgressed resistances to specific viruses that are common to modern agriculture can increasingly become exposed to new viral outbreaks, through global trade and a changing climate environment. This affects the security of our food supplies at a time of population pressure. Hence the importance of understanding the mechanisms and processes by which viruses interact with plants and cause disease.

Plant viruses are composed of ribonucleic acid genomes that encode proteins with different functionalities that are required to complete the viral infectious cycle, and in most viruses a capsid protein (CP) that encapsidates the viral genome into virions. A common feature shared among many plant virus genomes is that of their compactness. Another relevant feature that may derive from this compactness is that many plant viral proteins have a multifunctional nature. Based on the types of the nucleic acids that constitute their genomes, plant viruses are grouped into single-stranded (ss) RNA viruses of either positive or negative sense polarity; double-stranded (ds) RNA viruses; and DNA viruses, either ss or ds (Hull, 2002). The most frequent ones in number of species, and probably also in global frequency are those that have positive-sense ssRNA genomes (Hull, 2002).

Because plants have a first physical defensive barrier to infection that is composed by their external cuticle and the individual cell walls, viruses can only infect them through wounds caused by mechanical damage, or more frequently through vectors, such as insects, mites, nematodes, fungi or

other organisms that allow them to be transferred into the plant. These plant-virus-vector interactions are the products of long co-evolutions throughout time, and require specific interactions at the molecular level involving viral proteins. Once a plant is exposed to a virus different outcomes can be reached that will define the type of interaction. In many cases a plant species will not become infected by a specific virus. That plant is described as non-host and this type of resistance to the virus is referred to as non-host resistance (Mysore and Ryu, 2004; Palukaitis and Carr, 2008). The mechanisms that prevent viral infection of a non-host plant are very varied, and although the non-host could have escaped virus attack through certain passive mechanisms, such as physical barriers or the lack of plant factors essential for virus propagation, an increasing number of virus-non-host interactions are being shown to involve active defense responses mounted by the non-host plants (Fujisaki *et al.*, 2009; Ishibashi *et al.*, 2009; Jaubert *et al.*, 2011; Nieto *et al.*, 2011).

When a plant species is susceptible to become infected at the point of entry by a certain virus species it is said that this plant species is a host to this virus. At this point, if the plant is able to detect the virus and is capable of displaying a set of mechanisms that prevent the local and systemic spread of the virus the interaction is deemed as incompatible. In most cases an incompatible plant-virus interaction is based on the so-called gene-for-gene resistance (Flor, 1971; Gassmann and Bhattacharjee, 2012). This is because in this type of resistance the result of an infection attempt is prevented by the existence of specific disease *resistance* (*R*) genes in the plant and *avirulence* (*Avr*) genes in the virus that need to interact with each other, although more complex interactions have been demonstrated (Gassmann and Bhattacharjee, 2012). The incompatible interaction is

frequently, although not always, associated with a hypersensitive response (HR) that causes cell necrosis and tissue death at the point of infection, and the elicitation of a systemic acquired resistance (SAR) state that contributes to the containment of the virus (Kang *et al.*, 2005).

Conversely, if a plant host is not able to specifically identify the intrusion of a certain virus as alien, or if the mechanisms of defense that it elicits are not able to effectively contain the spread of the infection, the interaction is deemed to be compatible. Local and systemic hosts are distinguished within compatible plant–virus interactions, depending on whether the infection is able to spread systemically or not (Takács *et al.*, 2014).

All the work presented here was performed with three positive-sense ssRNA viruses, or their encoded protein factors, in a common, compatible systemic host, *Nicotiana benthamiana.*

When a virus infects a plant, viral proteins and nucleic acids are expressed from its genome to perform the multiple functions that will allow for viral replication, movement and spread within the host and eventually the horizontal dispersal of the virus to new plants to occur (Whitham *et al.*, 2006). To do all this, viruses will need also to overcome host defenses, and to hijack host cellular functions and resources. All these events have consequences on the modulation of the host´s gene expression, development and metabolism, which may lead in some cases to the onset of disease and its symptoms (Whitham *et al.*, 2006). Besides the costs to the plant of diversion of resources towards viral multiplication, infections produce additional energetic costs to the plant because of the triggering of defense responses (Berger *et al.*, 2007). They promote the accumulation in infected tissues of several compounds such as soluble sugars and amino acids (aas) as energy sources, and also as signaling molecules in plant

defense responses and in the maintenance of the cellular homeostasis (Berger *et al.*, 2007; Fernández-Calvino *et al.*, 2014)

There are several changes in gene expression commonly associated with plant-virus interactions, such are those affecting defense and stress genes, genes associated with metabolic processes and genes whose expression is modulated by hormones or by small interfering RNAs (siRNAs), among others (Whitham *et al.*, 2006). Changes in the expression of genes associated with stresses are not only triggered by viral infections but usually also by other biotic as well as by abiotic stresses (Fernández-Calvino *et al.*, 2015; Kadioglu *et al.*, 2012; Rodrigo *et al.*, 2012; Whitham *et al.*, 2006; Yue *et al.*, 2015). These stress-like responses in viral infections are characterized by the expression of Heat Shock proteins (HSPs). The expression of this HSPs due to accumulation of misfolded viral proteins make them likely a generic response to viral infections (Aparicio *et al.*, 2005).

The production of reactive oxygen species (ROS) is known as oxidative burst, and is one of the earliest cellular responses to infection. An incompatible interaction displays a biphasic ROS accumulation, with a first low-amplitude phase, characterized by a rapid but weak transient accumulation of oxidants, followed by a second phase of much higher amplitude in time and ROS accumulation, that is absent in compatible interactions (Torres *et al.*, 2006). This response, together with the expression of genes as a result of the oxidative burst, suggest that the first phase of ROS production, rather than being an effector of immunity acts instead as signal inducer of antiviral responses (Torres *et al.*, 2006). Furthermore, the oxidative burst enhances not only the transcription of stress responsive genes but it also participates in a cross-talk with

hormones related to antiviral defense, such as salicylic acid (SA; Alazem and Lin, 2014).

Some transcription factors induce both, the expression of senescence and of defense genes (Robatzek and Somssich, 2001). Furthermore, senescence processes can elicit the expression of defense related genes without the participation of any pathogen and even SA signaling (Quirino *et al.*, 1999). Cellular stresses could be a likely reason that explains why senescence-related genes are activated during pathogen-activated responses (Gepstein *et al.*, 2003; Weaver *et al.*, 1998), and the interplay between expression of senescence-related genes and cellular homeostasis can be a relevant factor in the susceptibility of plants to viral infections (Fernández-Calvino *et al.*, 2015).

1.1.1- Antiviral defense mechanisms in plants

In addition to the expression of genes associated with stresses as a general response of plants to viral infections, plants can display more specific defense responses against viruses. This section describes some of these mechanisms of defense during plant-virus compatible interactions.

Ubiquitin-proteasome has been postulated as an important pathway of antiviral defense. In turn, viruses use a plethora of strategies to modulate and circumvent it. Ubiquitin-proteasome is a pathway that conducts protein degradation and intervenes in the regulation of a wide range of cellular activities, such as cell cycle, transcription, and signal transduction (Hershko and Ciechanover, 1998). But this pathway also participates in the degradation of targeted viral proteins through their ubiquitination and ulterior proteolysis in proteasomes. Examples of these are the movement proteins of *Tobacco mosaic virus* (TMV) and of *Turnip yellow mosaic virus*

(TYMV) (Drugeon and Jupin, 2002; Reichel and Beachy, 2000). Nevertheless, viruses have developed strategies to counteract any antiviral role of this system and in some cases to use the ubiquitin-proteasome pathway to their own advantage, by directing towards degradation cellular components that participate in antiviral responses. Such is the case of potexviruses, whose P25 protein induce the protesome-mediated degradation of some Argonaute (AGO) proteins (Chiu *et al.*, 2010).

Plant hormones activate a series of signaling mechanisms that can initiate antiviral defenses. Hormones such as SA have been shown to be signals that trigger resistance against biotrophic and hemibiotrophic pathogens, whereas jasmonic acid (JA) and ethylene (ET) have been associated with resistances against necrotrophic pathogens (Glazebrook, 2005). In addition to its role in the cascade of responses to biotrophic pathogens, SA is a phytohormone that has relevance in antiviral defenses: it promotes the mobilization of NPR1 (Non-expressor of PR genes1) to the cell nucleus where it activates the transcription factors that trigger the expression of a number of defense genes (Dempsey, 2011; Dong, 2004; Vlot *et al.*, 2009). However, a SA-induced, NPR1-independent pathway has also been reported, suggesting that other proteins related with SA perception are also involved in this process (Blanco *et al.*, 2005). SA not only participates in responses to viruses during compatible interactions but also has been observed to have key role in incompatible interactions (Baebler *et al.*, 2014). JA on the other hand, although initially associated to responses to necrotroph pathogens, has also been shown to intervene in the establishment of SAR in plant-virus interactions (Zhu *et al.*, 2014) and in early phases of some viral infections (Kovač *et al.*, 2009). As with any other antiviral mechanism evolved by plants, some plant viruses have

counteracted the hormone-mediated antiviral defenses. For example, the P6 protein of *Cauliflower mosaic virus* (CaMV) inhibits the SA-activated defenses through NPR1, by exploiting the antagonistic effects of the SA and JA pathways (Love *et al.*, 2012).

Viruses in compatible infections cause the expression of defense- and pathogenesis-related (PR) proteins (van Loon *et al.*, 2006; Wise *et al.*, 2007). Expression of these genes is again associated with molecular signals, such as hormones (Dempsey, 2011; Dong, 2004; Vlot *et al.*, 2009) and ROS (Alazem and Lin, 2014). The large number of *PR* genes present in plants is classified into 17 families, based on the functions of the proteins encoded that encompass from glucanases and chitinases to peroxidases, ribonucleaes and proteinases, among others (van Loon *et al.*, 2006).

Other plant mechanism of defense against viruses include non-sense mediated decay, a plant quality control system for mRNAs that can detect and degrade viral RNAs with internal termination codons or with long 3'-end untranslated regions (Garcia *et al.*, 2014); or the targeted degradation of viral proteins by the autophagy pathway, such as some suppressors of the antiviral RNA silencing defense (Nakahara *et al.*, 2012).

1.1.2- RNA silencing

RNA silencing is a conserved mechanism of genetic regulation in eukaryotic organisms. This mechanism plays an important role in developmental regulation, stress responses or defense against nucleic acids like transposons, or those from invading viruses (Voinnet, 2009). One of the first evidences of the existence of mechanisms of RNA silencing was obtained in the early 90s. Petunia plants in which a gene causing

pigmentation was introduced by stable transformation resulted paradoxically not in a more intense pigmentation, as expected, but in its loss. This suggested the existence of a mechanism that had silenced both, the transgene as well as of the corresponding endogenous gene responsible for pigmentation (Napoli *et al.*, 1990; van der Krol *et al.*, 1990). Later on, the antiviral role of RNA silencing was observed in diverse biological groups, from plants to invertebrates (Bronkhorst and Van Rij, 2014; Pumplin and Voinnet, 2013) and also in mammals (Burgess, 2013; Cullen *et al.*, 2013; Li *et al.*, 2013).

The initial trigger of the RNA silencing-based antiviral defense in plants is the formation of dsRNAs. These are recognized as foreign or defective by the plant and can be formed by different mechanisms. In those viruses whose genome is constituted by ssRNA, they appear as transient intermediates during viral replication, or by the pairing of genomic regions that have a degree of self-complementarity that intervene in the secondary structures of the viral RNAs. In dsDNA viruses, they can occur by the overlapping of bidirectional read-through transcripts (Blevins *et al.*, 2011; Donaire *et al.*, 2008; Molnár *et al.*, 2005). Whichever their origin, those dsRNAs structures are recognized and sliced by the different Dicer-like proteins (DCLs) of the plant in a hierarchical manner into primary virus-derived small interfering RNAs (vsiRNAs), of between 21 and 24 nucleotides (nts) in length (Donaire *et al.*, 2008). In infections by many RNA viruses, DCL4 appears to be the main DCL that conducts the processing of the viral dsRNAs into vsiRNAs, although in a *dcl4* mutant background DCL2 becomes relevant (Deleris *et al.*, 2006; Donaire *et al.*, 2008; Garcia-Ruiz *et al.*, 2010; Qu *et al.*, 2008). Other DCLs that have been shown to have an important role in viral infections are DCL3 in dsDNA

virus infections (Akbergenov *et al.*, 2006) or DCL1 as a positive regulator that makes dsRNAs accessible to other DCLs (Blevins *et al.*, 2006). The Hua enhancer1 (HEN1) methylase is then required for the methylation and stabilization of those vsiRNAs (Vogler *et al.*, 2007; Zhang *et al.*, 2012).

The next step of the antiviral RNA silencing-mediated defense is called the effector phase (Carbonell and Carrington, 2015; Csorba *et al.*, 2015). This phase requires the participation of proteins of the AGO family. The vsiRNAs are loaded into AGO-containing RNA-induced silencing complexes (RISCs) (Azevedo *et al.*, 2010; Carbonell *et al.*, 2012; Garcia-Ruiz *et al.*, 2015; Wang *et al.*, 2011). Viral RNAs are then sliced by the activities of these complexes, which target them by complementarity of sequence to those of the vsiRNAs they carry (Carbonell and Carrington, 2015) leading to their destruction, although translational repression activity could also be playing some antiviral role in defined cases (Ghoshal and Sanfaçon, 2014). The antiviral role of different AGOs is tissue-dependent (Garcia-Ruiz *et al.*, 2015), and although historically it was shown first that AGO1 is a main effector of the antiviral silencing in ssRNA viruses, other AGO proteins, such as AGO2, AGO5, AGO7 and AGO10 have been shown to play important roles in it, depending on the virus and also on the plant and/or tissue (Garcia-Ruiz *et al.*, 2015; Jaubert *et al.*, 2011; Qu *et al.*, 2008).

Another process involved in the antiviral RNA silencing-mediated defense is the amplification of the response by the generation of secondary vsiRNAs. These vsiRNAs are the synthesis products of plant RNA-dependent RNA polymerases (RDRs) using as templates products of RISC slicing activities (Bologna and Voinnet, 2014), although not always (Wang *et al.*, 2011). RDR6 and RDR1 have both been shown to be the

main polymerases responsible for the formation of secondary vsiRNAs, and experiments conducted with loss of function mutants showed that RDR6 acted as a surrogate when RDR1 function was disrupted (Qu, 2010). The activities of plant RDRs produce viral-derived dsRNAs with are processed by DCL4 and DCL2 into 21–22 nt long vsiRNAs, respectively (Csorba *et al.*, 2015). These vsiRNAs are loaded into RISCs to participate in antiviral defense.

1.1.3- Viral suppressors of RNA silencing

To avoid the mechanism of antiviral defense based on RNA-mediated gene silencing that plants have developed, some viruses have adapted to replicate inside specialized subcellular structures or organelles that provide shelter form this defense, or to replicate and spread inside the cells fast, before the silencing defense overrides them (Schwartz *et al.*, 2002). On the other hand, to directly counteract this mechanism most, if not all, viruses have evolved proteins with silencing suppressor properties, of varying strengths, to neutralize or mitigate this host defense against viral infection (Lakatos *et al.*, 2006). Otherwise, the strength and specificity of this resistance would in many cases not allow for the infection to proceed successfully, including reaching the viral titer and host alterations required for their horizontal dispersal.

Despite having a common function, the viral suppressors of RNA silencing (VSRs) can have different evolutionary origins in different viruses, and evidence shows that they also display different functional approaches to perform their function (Csorba *et al.*, 2015). This also implies that the silencing pathway steps affected by them may not be the same for different suppressors and viruses. In fact, the different VSRs

could interfere with virtually any step of the silencing pathway to perform their function (Csorba *et al.*, 2015).

A first step of interference could be with that of vsiRNA making by the plant DCLs. However, that some plant virus VSRs interfere directly with the functions of DCLs has yet to be shown. This Dicer-interfering strategy has, nevertheless, been demonstrated in viruses that infect insects (Bronkhorst and Van Rij, 2014), and it had been suggested for the P38 protein of *Turnip crinkle virus* (TCV) (Azevedo *et al.*, 2010; Deleris *et al.*, 2006). However, its effect on DCLs was latter attributed to be an indirect one, through AGO1-mediated DCL homeostasis (Zhang *et al.*, 2012).

The formation of functionally active antiviral vsiRNAs requires in a following step their methylation by HEN1, in order to be loaded into AGO proteins. Otherwise any unmethylated siRNAs would by susceptible to degradation by endonucleases (Ramachandran and Chen, 2008). This step could be target for VSRs. Indeed, it has been demonstrated that some VSRs cause the lack of methylation of vsiRNAs by their sequestration (Csorba *et al.*, 2007; Lózsa *et al.*, 2008; Vogler *et al.*, 2007). In other cases, a direct interaction between HEN1 and VSRs, such as has the one shown for potyviral HCPro *in vitro*, inhibiting the methylase activity, is very likely to occur also *in vivo* (Jamous *et al.*, 2011).

The next step of antiviral RNA silencing is the assembly of the RISC effectors of this defense. Different ways by which VSRs can interfere with this process have been demonstrated. One such way is the slicing of vsiRNAs into smaller RNAs, preventing their load into RISCs, followed by RNase3 of *Sweet potato chlorotic stunt virus* (SPCSV) (Cuellar *et al.*, 2009). A more common way of interference with the effector step is the sequestration of the vsiRNAs by VSRs (Mérai *et al.*, 2006). It prevents the

incorporation of vsiRNAs into the AGO-containing RISCs, and could also prevent their methylation. Evidence has been gathered for some VSRs that either demonstrates that they perform their functions by sequestering vsiRNAs, as in the case of the tombusviral P19 suppressor (Silhavy *et al.*, 2002), or strongly supports it, as are the cases of potyviral HCPro (Garcia-Ruiz *et al.*, 2015), cucumoviral 2b protein (González *et al.*, 2012, 2010; Goto *et al.*, 2007; Hamera *et al.*, 2012). While some VSRs bind specific-size siRNAs others sequestrate siRNAs with a wider size-range (Mérai *et al.*, 2006; Hamera *et al.*, 2012; García-Ruíz *et al.*, 2015). Additionally, differential sequestration preferences based on the 5'-end nt of the vsiRNA that would load otherwise into specific AGO protein-containing RISCs have also been observed for a VSR, 2b (Hamera *et al.*, 2012); and in the present work is shown an evidence toward that preference for potyviral suppressor HCPro.

In the effector assembly step another way by which VSRs can perform their function is by direct interaction with RISC components. In some cases this interaction leads to the degradation of the component with which it interacts. These are the situations described for the P0 VSRs of poleroviruses that interact with AGO components of the RISC machinery promoting their degradation (Baumberger *et al.*, 2007; Bortolamiol *et al.*, 2007); for the potexviral P25 (also denominated TGB1) VSRs, that interacts with some AGOs to conduct their degradation through the ubiquitination-proteasome pathway (Chiu *et al.*, 2010); or for the CP suppressor of *Tomato ringspot virus* (ToRSV) that promotes degradation of AGO1 via autophagy (Karran and Sanfacon, 2014). In other cases, these interactions may not lead to the degradation of RISC components but nevertheless inactivate the effector complex. Such could be the cases of

the cucumoviral 2b protein (Duan *et al.*, 2012; González *et al.*, 2010; Zhang *et al.*, 2006), of the ipomoviral P1 protein (Giner *et al.*, 2010) or of the tombusviral P38 protein (Azevedo *et al.*, 2010), among others (Csorba *et al.*, 2015).

VSRs can also alter the antiviral RNA silencing amplification step that requires the activities of the plant RDRs. This has been shown for example in the cases of the geminiviral V2 protein of *Tomato yellow leaf curl virus* (TYLCV), and of the potexviral P25 protein, which inhibit both the RDR6-Suppressor of gene silencing 3 (SGS3) pathway (Glick *et al.*, 2008; Okano *et al.*, 2014).

1.2- Description of the viruses used in this study and of their suppressors of silencing

Three ssRNA viruses and their corresponding three VSRs are used in the studies presented in this PhD Thesis. They are *Potato virus Y* (PVY), *Cucumber mosaic virus* (CMV) and *Potato virus X* (PVX). PVY, CMV and PVX happen to be the type members of the *Potyvirus, Cucumovirus* and *Potexvirus* genera, respectively (Hull, 2002). Their genome organization is shown in Fig. 1. and brief description of these viruses follows.

1.2.1- Potyviruses

Viruses of the genus *Potyvirus* (family *Potyviridae*) were described for the first time in the 1930s (Smith, 1931). They are distributed world-wide, representing about 30% of the plant viruses in number of species (Talbot, 2004), infecting a wide range of monocot and dicot plants, many of them of agricultural, horticultural or ornamental, importance (Ward and Shukla, 1991).

Although potyviral infections in plants can cause very different symptoms, such as ringspots, necrosis and stunting, among others, which will depend on the virus species, the host and the environment, all members of the genus *Potyvirus* form cylindrical inclusion bodies in infected cells and before the genetic information was available this was the most important criterion for assigning viruses to the group (Edwardson and Christie, 1978; Rubio-Huertos and López-Abella, 1966; Ward and Shukla, 1991).

Potyviruses have a virion characterized for being rod shaped and flexuous, of 600-900 nm in length and 12-15 nm of diameter, composed by the genomic RNA molecule encapsidated by multiple copies of the CP and covalently linked at its 5'-end with viral genome-linked protein (VPg) (Fig. 1; Shukla *et al.*, 1994). Potyviruses have a monopartite genome of ssRNA of approximately 9.7 kb with a polyadenylate tail in the 3'-end. This RNA molecule is of positive sense and encodes a single large open reading frame (ORF) flanked by untranslated regions. The large ORF its polycistronic and encodes a polyprotein processed by three virus-encoded proteolitical activities into 10 multifunctional proteins (Fig. 1; Carrington and Dougherty, 1987; Carrington *et al.*, 1989; García *et al.*, 1989; Riechmann *et al.*, 1992; Verchot *et al.*, 1991): P1, helper component proteinase (HCPro), P3, 6K1, cylindrical inclusion (CI) protein, 6K2, VPg, nuclear inclusion protein a (NIa), nuclear inclusion protein b (NIb), and the CP. The small "pretty interesting *Potyviridae* ORF" (PIPO) is expressed by a ribosomal frameshifting of +2 nts that occurs inside the third cistron (P3) of the polyprotein, resulting in a functional protein fused to the N-terminal region of P3 (P3N-PIPO) (Chung *et al.*, 2008; Vijayapalani *et al.*, 2012; Wen and Hajimorad, 2010).

The P1 protein has a protease domain in the C-terminal region that performs its cleavage from the adjacent HCPro downstream (Fig. 1; Verchot and Carrington, 1995). It has been shown to be involved in genome amplification (Pasin *et al.*, 2014; Verchot and Carrington, 1995), to be able to bind RNA (ss and dsRNAs) (Brantley and Hunt, 1993; Soumounou and Laliberté, 1994) and its presence in tandem with HCPro as a fusion protein enhances the suppression of RNA silencing by the latter (Anandalakshmi *et al.*, 1998; Kasschau and Carrington, 1998) because of *cis*-acting translational enhancing effects (Tena Fernández *et al.*, 2013). HCPro will be described in a separate section. The P3 protein has been proposed as a membrane protein (Eiamtanasate *et al.*, 2007; Restrepo-Hartwig and Carrington, 1994) and several studies have implicated this protein in viral replication, systemic infection, pathogenicity and movement (Chu *et al.*, 1997; Cui *et al.*, 2010; Johansen *et al.*, 2001; Merits *et al.*, 1999). The P3N- PIPO protein participates in cell-to-cell movement, together with the CI protein, and it has been shown to be located in the plasmodesmata (Wei *et al.*, 2010b). The 6K1 protein has an unknown defined function but had been associated to host adaptation (Calvo *et al.*, 2014; Gibbs *et al.*, 2015). The 6K2 integral membrane protein is required for the formation of cortical endoplasmic reticulum (ER)–associated viral replication vesicles that will afterwards become translocated towards the chloroplasts (Wei *et al.*, 2013). The CI protein, component of the pinwheel-shaped inclusion bodies characteristic of potyviruses(Lawson and Hearon, 1971; Rubio-Huertos and López-Abella, 1966) has been associated to viral replication and their ER-associated

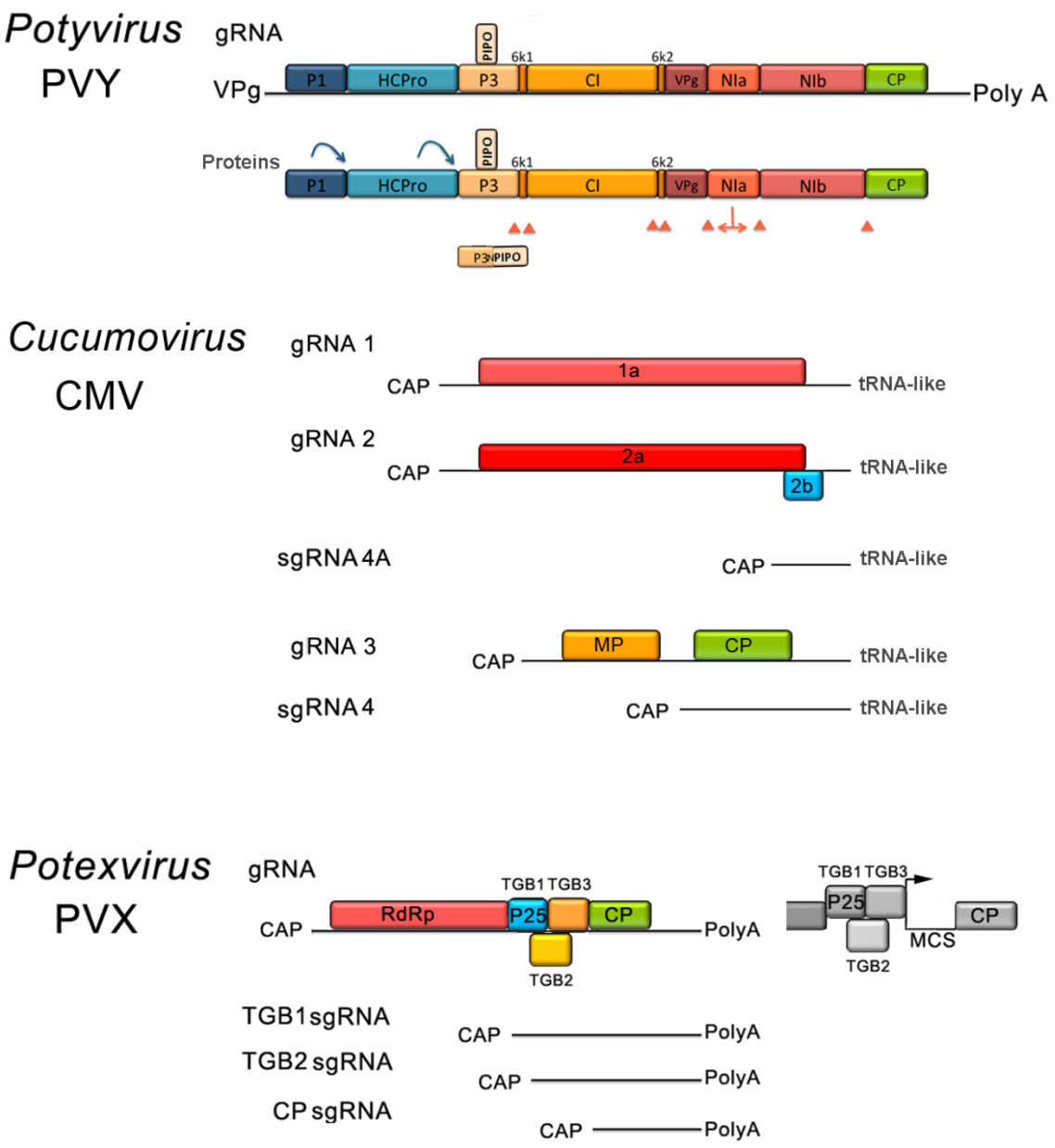

Fig 1. Genome organization of potyviruses, cucumoviruses and potexviruses. Genomes of *Potato virus Y* (PVY), *Cucumber mosaic virus* (CMV) and *Potato virus X* (PVX). Genomic RNA (gRNA) of PVY has two open reading frames (ORFs), the larger encodes potyviral polyprotein, and the smaller is expressed by a ribosomal frameshifting that occurs inside the third cistron (P3), both shown below. The polyprotein is processed by three virus-encoded proteolitical activities which cleavage sites are shown by blue arrows for P1 and HCPro and red arrowheads for NIa. Genomic RNAs (gRNA) of CMV and subgenomic RNAs (sgRNAs) derived from those shown just bellow. gRNA 1 encodes one ORF, whereas gRNAs 2 and 3 each encode two ORFs. The 1a, 2a and 3a (MP) are expressed directly from their respective gRNAs,

(Continuation of Fig 1) while 2b and 3b (CP) proteins are expressed from the sgRNAs 4A and 4, respectively. Genomic RNA (gRNA) of PVX has five ORFs. The RdRp is encoded by ORF most close to 5'-end and is expressed directly from the genomic RNA. The following three ORFs downstream in the genome are the three *TGB* genes (*TGB1, 2* and *3*) where *TGB2* overlaps with those of *TGB1* and *TGB3*. This ORFs could be expressed directly from gRNA or by any of the sgRNAs containing them and shown bellow. The last ORF encodes viral CP, and is expressed trough sgCP RNA. On the right of gRNA of PVX is shown in gray colors position of multiple cloning site (MCS) were silencing suppressors of PVY and CMV (HCPro and 2b, respectively) has been cloned in the present work. RNA sizes are not shown on the same scale.

vesicles, as well as to plasmodesmata and to viral trafficking (Lawson and Hearon, 1971; Sorel *et al.*, 2014). The VPg protein has been involved in viral translation as well as replication within the viral replication factories (Jiang and Laliberté, 2011). The NIa protein is the last of the proteases encoded by the viral genome and is responsible for conducting the proteolytic cleavage that allows its own excision and those of 6K1, CI, 6K2, VPg, NIb and the CP (Fig. 1; Carrington and Dougherty, 1987; García *et al.*, 1989; Verchot *et al.*, 1991), and it has also been related with the fecundity of insect vectors (Casteel *et al.*, 2014). The NIb protein is the viral RNA-dependent RNA polymerase responsible of the viral replication (Hong and Hunt, 1996), using the VPg as primer (Anindya *et al.*, 2005; Puustinen and Mäkinen, 2004). The CP has been associated with protection of viral RNA from degradation and to participate in viral cell-to-cell and systemic movement, as well as from host to host through its role in the non-persistent transmission by aphids of virions, together with HCPro (Besong-Ndika *et al.*, 2015).

Potyviral RNA replication occurs in association with membrane vesicles and large perinuclear ring-like structures (Cotton *et al.*, 2009; Cui *et al.*, 2010; Grangeon *et al.*, 2010; Wei and Wang, 2008; Wei *et al.*, 2010a). In

addition to the RNA-dependent RNA polymerase activity of the NIb and of the priming activity of the VPg, NTPase and RNA helicase activities of the CI protein are required for viral replication (Fernández *et al.*, 1995; Laín *et al.*, 1991, 1990). The CI protein appears to be also related with P3N-PIPO in the form of conical structures at plasmodesmata associated cell-to-cell spread (Wei *et al.*, 2010b).

PVY is a major viral threat to many crops besides potato cultivation, where it affects both yield and tuber quality, and results in yield losses of up to 80% (De Bokx and Huttinga, 1981). Potyviruses are able to be transmitted vertically through infected tubers or seeds (Simmons *et al.*, 2013; Draper *et al.*, 2002), and horizontal transmissions has been observed to take place through more than 40 aphid species in a non-persistent, non-circulative manner (Boquel *et al.*, 2011; Edwardson and Christie, 1978; Radcliffe and Ragsdale, 2002). In the transmission process HCPro is also required, although the mechanism by which this happens is not elucidated as yet.

1.2.2- Cucumoviruses

Viruses of the genus *Cucumovirus* (family *Bromoviridae*) generally possess a broad range of hosts. Only the type member *Cucumber mosaic virus* (CMV) is able to infect more than 1200 plant species in over 100 families, including many plant species of economic interest, both monocots and dicots (Scholthof *et al.*, 2011). *Cucumovirus*-infected symptoms can range from light mosaic to necrosis, leaf curling and stunting, among others, as well as ringspot symptoms in fruits (Palukaitis and García-Arenal, 2003; Roossinck, 1999).

Virions are icosahedral particles of approximately 29 nm in diameter, composed by 180 units of the CP that encapsidate separately each of the three genomic RNAs, althougt RNA 3 encapsidates together with the subgenomic RNA 4, itself derived from RNA 3 (Habili and Francki, 1974; Lot and Kaper, 1976). The type member species CMV has a tripartite genome of ssRNAs (Fig. 1), named RNAs 1, 2, and 3, in order of decreasing size [of approximately 3.4, 3.1 and 2.2 kbs, respectively (Palukaitis and García-Arenal, 2003)]. RNA 1 has one ORF that encodes the 1a protein. The RNA 2 has two ORFs, a large one that encodes the 2a protein, and a small one towards the 3'-end of the viral RNA that overlaps with the 5'-end of the *2a* but in a +1 nt reading frame, which encodes the 2b protein. RNA 3 encodes the 3a and CP proteins in two non-overlapping reading frames separated by a non-coding, intercistronic region.

The 1a, 2a, and 3a proteins are translated directly from genomic RNAs 1, 2, and 3, respectively (Schwinghamer and Symons, 1977), whereas the CP is translated through the subgenomic RNA 4 derived from RNA 3, and the 2b protein is expressed through a small subgenomic RNA 4A derived from RNA 2 (Fig. 1). In some *cucumovirus* species another two subgenomic RNAs (RNA 3B and 5) could be generated during the infective process (Li *et al.*, 1999; Lucy *et al.*, 2000; Palukaitis and García-Arenal, 2003). The 1a protein and 2a proteins, together with host-encoded components constitute the viral replicase. The 1a protein has a methyltransferase domain in its N-terminal domain and a helicase domain in its C-terminal domain (Choi *et al.*, 2011; Habili and Symons, 1989; O'Reilly *et al.*, 1998; Rozanov *et al.*, 1992). The 2a protein contains a number of motifs characteristic of RNA-dependent RNA polymerases (Choi *et al.*, 2011;

Nitta *et al.*, 1988; Palukaitis and García-Arenal, 2003; Pita *et al.*, 2015). The 2b protein is a suppressor of posttranscriptional gene silencing (Li *et al.*, 1999; Lucy *et al.*, 2000; Palukaitis and García-Arenal, 2003). The posttranscriptional gene silencing function of the 2b protein could be related with its ability to bind to AGO proteins and/or to small RNAs *in vivo* and *in vitro* (González *et al.*, 2012, 2010; Goto *et al.*, 2007; Hamera *et al.*, 2012; Zhang *et al.*, 2006). It has also a nucleolar localization (Lucy *et al.*, 2000; Mayers *et al.*, 2000) that although unnecessary for antiviral silencing suppression (González *et al.*, 2012) may yet be related with other silencing functions of the protein, such as involvement in RNA-directed DNA methylation (Nakahara *et al.*, 2012). The 2b protein cytoplasm-nuclear balance affects suppression strength and pathogenicity (Du *et al.*, 2014). The 3a protein is the movement protein (MP) of CMV, and it is essential for virus cell-to-cell, as well as for long-distance movement (Canto and Palukaitis, 2005; Canto *et al.*, 1997; Ding *et al.*, 1995; Kim *et al.*, 2004; Nagano *et al.*, 2001). The 3a protein has been located to plasmodesmata between infected cells (Blackman *et al.*, 1998; Itaya *et al.*, 2002; Vaquero *et al.*, 1996) and was able to gate the movement through plasmodesmata of itself, RNA, or fluorescent dyes (Canto *et al.*, 1997; Ding *et al.*, 1995; Vaquero *et al.*, 1997) and to form filaments that protrude from plant protoplasts in the same manner as MPs from some other viruses (Canto and Palukaitis, 1999). The viral CP is the sole protein associated with virus particles, but it has been shown to be also required for cell-to-cell and long-distance movement as well as for viral transmission via aphid vectors (Palukaitis and García-Arenal, 2003; Requena *et al.*, 2006).

In subcellular fractionation studies, CMV replication activity was found associated with the membrane-bound fraction (Jaspars *et al.*, 1985). Later

on it was shown that it specifically associated with the tonoplast (Cillo *et al.*, 2002; Huh *et al.*, 2011; Jacquemond, 2012; Kim *et al.*, 2006).

CMV and other cucumoviruses are mainly transmitted horizontally between hosts by over 80 aphid species (Palukaitis *et al.*, 1992) in a non-persistent manner (Edwardson and Christie, 1991). The CP is the only virus determinant of aphid transmissibility and vector specificity (Chen and Francki, 1990; Ng *et al.*, 2000, 2005). Depending on the host and *Cucumovirus* species infection can also occur in some cases vertically through seeds (Ali and Kobayashi, 2010; Palukaitis *et al.*, 1992; Yang *et al.*, 1997)

1.2.3- Potexviruses

Viruses of the genus *Potexvirus* (family *Alphaflexiviridae*) have as type member the *Potato virus X* (PVX). Potexviral infection affects both monocots and dicots plants and can cause chlorosis, mosaicism, necrotic lesion, decreased leaf size and ringspot symptoms (Alam *et al.*, 2014). Potexviruses can cause severe infection symptoms in some plants, particularly when they are part of mixed infections with potyviruses (González-Jara *et al.*, 2005; Pruss *et al.*, 1997). The synergistic effect of potyviruses on PVX symptoms and titers has been mapped to the potyviral HCPro cistron and the potexviral P25 protein (Aguilar *et al.*, 2015b; González-Jara *et al.*, 2005; Pruss *et al.*, 1997).

Potexviruses have a rod-shaped virion of about 13 nm in diameter and 470–580 nm in length, shorter and less flexuous than those of potyviruses. The potexviral genome is monopartite and it is composed by a positive polarity ssRNA molecule of 5.9–7.0 kb with a 5'-cap structure and a 3'-poly(A) tail (Fig. 1). The virions are composed by this RNA coated by

multiple copies of the coat protein in a helical arrangement (Atabekov *et al.*, 2007; Kendall *et al.*, 2008).

The genome has five ORFs (Fig. 1). The first ORF, starting from the 5'-end, does not overlap with any other one and is expressed directly from the genomic RNA. It encodes the viral replicase protein. This replicase contains several domains associated with RNA capping, helicase and RNA-dependent RNA polymerase activities (Huang *et al.*, 2009; Li *et al.*, 2001, 1998). The following three ORFs downstream in the genome are the three *TGB* genes (TGB1, 2 and 3). The ORF of *TGB2* overlaps with those of *TGB1* and *TGB3* but the latter two do not overlap with each other. *TGB1* is translated through a subgenomic (sg) RNA named TGB-CP and encodes the P25 protein, which regulates plasmodesmata size exclusion limits and participates in viral translocation across them, has silencing suppressor activity (Bayne *et al.*, 2005; García-Marcos *et al.*, 2013; Pacheco *et al.*, 2012; Voinnet *et al.*, 2000) and has been associated with synergies observed in mixed infections with potyviruses (Aguilar *et al.*, 2015b). The *TGB2* and *TGB3* genes encode the P12 and P8 proteins, respectively. Both can be expressed from the sgTGB-CP RNA, and also from a second sgTGB2-CP RNA. Both have been shown to participate in the cell-to-cell and long-distance movement of the virus (Park *et al.*, 2014). The last ORF does not overlap with any other one and encodes the viral CP, which is expressed from its own third sgCP RNA (Tilsner *et al.*, 2013).

Potexviruses replicate in association with ER membranes (Doronin and Hemenway, 1996) and in a perinuclear viral replication complex found at late infection stages (Linnik *et al.*, 2013; Tilsner *et al.*, 2012). Not only the viral replicase but also the P12 and P8 proteins co-localize in granules anchored to the ER, suggesting their possible association with viral

replication (Bamunusinghe *et al.*, 2011). Following replication, the viral RNA is conveyed towards the plasmodesmata by the P25 and CP proteins, and moves through them with the help of the P12 and P8 proteins (Park *et al.*, 2014).

Potexviruses are efficiently transmitted mechanically by abrasion, so their spread occurs mainly by contact between plants, although in some cases insects and fungus have been identified as the epidemiological factors associated with the transmission (Nienhaus and Stille, 1965; Walters, 1952).

1.2.4- The viral silencing suppressors of potyviruses, cucumoviruses and potexviruses

The genomes of PVY, CMV and PVX viruses express the suppressors of silencing HCPro, 2b protein, and P25 protein, respectively. Two of the chapters of this PhD Thesis deal specifically with PVY HCPro: Chapter 5 investigates cell biology and functional properties of this protein, while Chapter 6 deals with its RNA binding properties *in vivo*. Both chapters already contain specific Introductions about the protein, with regard to the issues investigated in them. Therefore it only will be summarized in this General Introduction the description of HCPro and its properties.

Potyviral HCPro is a non-structural cytoplasmic protein of around 50 kDa in size that was initially described as necessary for the transmission of viruses by aphid vectors, hence its original name of "helper component" (Govier and Kassanis, 1974). HCPro is now known to be a multifunctional protein that participates in several steps of the viral cycle, such as aphid transmission, polyprotein processing and suppression of antiviral RNA silencing, among others (Anandalakshmi *et al.*, 1998; Kasschau and Carrington, 1998; Pruss *et al.*, 1997).

The N-terminal domain of HCPro has been associated to its function in the transmission of these viruses by aphids (Blanc *et al.*, 1997; Canto *et al.*, 1995). HCPro requires to be taken by the aphid prior to or simultaneously with the virions for the transmission to take place (Blanc *et al.*, 1997; Canto *et al.*, 1995). The mechanism by which this happens is largely unknown. The N-terminus of HCPro interacts also with some components of the proteasome (Ballut *et al.*, 2003; Jin *et al.*, 2007; Sahana *et al.*, 2012). The central domain of HCPro has been associated to the suppression of silencing function (Shiboleth *et al.*, 2007). The C-terminal domain of HCPro resembles those of papain-like proteases, and upon translation its proteolytic activity self-detaches HCPro from the rest of the polyprotein downstream (Carrington and Herndon, 1992; Carrington and Oh, 1999).

In vitro retardation gels have shown that plant-expressed HCPros of some, but not all potyviruses, successfully bound to synthetic ds siRNAs (Lakatos *et al.*, 2006; Mérai *et al.*, 2006). Also *in vitro* it was observed that HCPro could interact with longer ssRNAs, of approximately 200 nts (Maia and Bernardi, 1996; Urcuqui-Inchima *et al.*, 2000). Therefore, binding to RNAs could be the basis of a strategy of interference with antiviral silencing. However, the HCPro of *Zucchini yellow mosaic virus* (ZYMV) has been shown to interact with the component of the silencing machinery HEN1 *in vitro*, inhibiting its siRNA methylation function (Jamous *et al.*, 2011). Thus HCPro reduction of siRNA methylation during viral infections (Ebhardt *et al.*, 2005) could therefore provide another strategy of interference with silencing. To perform its silencing suppression function HCPro may require host cofactors (Lakatos *et al.*,

2006). On the other hand, no interaction of HCPro with AGO proteins has been reported to the date.

With regard to the cellular estate of the HCPro molecule, it is a cytoplasmic protein that size chromatography fractionation or analytic centrifugation of soluble plant extracts had shown to be in the form of homodimers and further aggregates (Ruiz-Ferrer *et al.*, 2005; Thornbury *et al.*, 1985). Self-interaction of HCPro has been also observed by yeast two-hybrid assays (Y2H) (Urcuqui-Inchima *et al.*, 1999) and by bimolecular fluorescence complementation (BiFC) (Ala-Poikela *et al.*, 2011; Sahana *et al.*, 2012; Zheng *et al.*, 2011; Zilian and Maiss, 2011).

In contrast to HCPro, the 2b protein of CMV is much smaller, of around 16 kDa in size and of mainly nuclear presence (Lucy *et al.*, 2000). Within the nucleus, it has been shown that it specifically targets the nucleolus and Cajal bodies (González *et al.*, 2010). The 2b protein of CMV is a suppressor of RNA silencing and a pathogenicity determinant (Lucy *et al.*, 2000). With regard to its functional form, in the orthologous protein of the *Tomato aspermy cucumovirus* (TAV) the 2b protein was demonstrated to dimerize *in vitro* (Chen *et al.*, 2008). The dimerisation was later visualized *in vivo* for the 2b protein of CMV (González *et al.*, 2010). With regard to how it performs it silencing suppression function, the 2b protein was shown to interact with AGO1, both *in vivo* and *in vitro*, and that interaction inhibited the RNA cleavage activity of the latter in RISC reconstitution assays, *in vitro* (Zhang *et al.*, 2006). However, the 2b protein of CMV has been also shown to bind to different types of siRNAs, including miRNAs, both *in vivo* and *in vitro* (González *et al.*, 2010; Goto *et al.*, 2007). When the kinetics of these bindings were characterized they were found to occur *in vitro* at protein:small RNA (sRNA) molar ratios of 2:1, with high affinity

(González *et al.*, 2012), supporting the model previously proposed by Chen *et al.*, (2008) of a protein dimer binding to a single molecule of sRNA. The use of an extensive battery of functionally characterized 2b protein mutants showed that a strong correlation existed between their ability to bind to sRNAs *in vitro* at these 2:1 protein:RNA ratios and the suppressor function. Furthermore, nuclear accumulation was not needed for suppressor function (González *et al.*, 2012), but could by contrast be related to genomic DNA modifications (Nakahara *et al.*, 2012), and the balance between nuclear and cytoplasmic protein could be modulating the severity of symptoms in virus infections, and the overall suppressor strength (Du *et al.*, 2014). These sRNA binding data *in vitro* were further confirmed by the characterization of sRNA populations bound to the 2b protein in infected plants, which showed some preference for ds siRNAs of 24 nt in length and with 5'-end adenosines (Hamera *et al.*, 2012). Thus, the 2b protein could be acting as suppressor of silencing either by siRNA sequestering, by interference with AGO activities, or by both of these mechanisms.

In addition to silencing suppression, the 2b protein has other functions. Among them, it could be noted its role in the horizontal transmission of CMV by aphids: CMV does not need additional non-structural proteins other than those in the virion to be transmitted by these insects. However, it has been observed that alterations in the profiles of volatile emissions from infected plants can alter the behavior of aphids that feed on them, facilitating their dispersal to other plants, and with them that of the viruses they acquired (Mauck *et al.*, 2010; Ziebell *et al.*, 2011). In this way the protein could be considered as a helper in CMV transmission, just as

HCPro is in that of potyviruses, but with a very different functional approach.

The P25 protein of PVX is a 25 kDa protein encoded by the TGB1 with the sole suppressor of silencing function of this type of viruses (Senshu *et al.*, 2009). Contrary to HCPro and the 2b protein, the P25 protein has historically been considered a weak suppressor of silencing. Despite its reputation, the P25 protein can suppress silencing in agropatch assays (Senshu *et al.*, 2009). The reasons to consider the P25 a comparatively weaker suppressor are: 1) that in mixed infections with potyviruses, or in a HCPro-expressing background, PVX titers and the symptoms the virus induces increased markedly (Vance, 1991; Vance *et al.*, 1995), suggesting that the endogenous suppressor was unable to keep PVX RNAs from being partially silenced; and 2) that the P25 protein has been shown to be the trigger of a systemic necrosis response in *Nicotiana* plants that is dose-dependent. For that threshold to be reached the presence of strong heterologous suppressors, such as HCPro or 2b protein are required, thus contributing to the severity of symptoms reported in mixed infections.

1.3- Virus-induced symptoms in compatible interactions

Disease symptoms are phenotypic manifestations that often appear as the result of the plant–virus interplay, although in some instances virus infection can have no apparent pathological effects. Development of disease symptoms can be the outcome of the viral exploit of host resources, the physiological alterations associated with defensive responses in the plant and/or the counter-defensive mechanisms deployed by the virus to offset these defenses.

As biotrophic entities viruses need live cells to accomplish their biological cycles. In that way, one mechanism displayed by plants to defend them from viral infections is the activation of different cell death programs to impede viral propagation. Within these types of mechanisms it can be found the HR which occurs when there is a specific recognition of pathogen.

Some symptoms are derived from the replication of the virus. That is the case of NIb replicase of a *Plum pox virus* (PPV) adapted by serial passages in the laboratory to *Pisum sativum*, leading to an increase in viral titer associated with the enhancement of disease symptoms (Wallis *et al.*, 2007). In other examples, mutations of the viral replicase can cause reductions in viral titers, together with attenuation of symptoms. This was observed in TMV (Lewandowski, 1993), *Pepper mild mottle virus* (PMMoV) (Yoon *et al.*, 2006) and CMV (Choi *et al.*, 2005). However, severity of symptoms does not necessarily correlate with virus titer as it is shown in the present work.

Since hormone signaling mechanisms can be involved in antiviral defenses, the viral counter-defense mechanisms based in hormone modulation can cause the development of infection symptoms. In this way the CP of TMV that negatively regulates the SA-mediated defense reduces plant growth and delays the timing of floral transition (Rodriguez *et al.*, 2014). Or the P2 protein from *Rice dwarf virus* (RDV) reduces the biosynthesis of gibberellins and causes stunting (Zhu *et al.*, 2005).

Movement of viruses among cells also can lead to pathogenesis processes. It has been observed that the expression of some viral MPs in uninfected plants can trigger typical symptoms of virus infections, such as sugar accumulation, photosynthesis repression, chlorosis and stunting (Balachandran *et al.*, 1995).

RNA silencing acts as a defensive mechanism against viral infections. Nevertheless, this mechanism plays a main regulatory role in plant development and in responses to environmental stresses. Therefore, VSRs can potentially interfere with the plant physiological processes that also depend for their regulation on RNA silencing. This disrupts plant development and homeostasis and causes disease symptoms (Silhavy and Burgyán, 2004). Because of this, VSRs are among the most important determinants of pathogenicity and in many cases before being shown to suppress silencing they had been identified previously as pathogenicity determinants. Transgenic expression of these proteins can cause developmental abnormalities resembling infection disease symptoms (Anandalakshmi *et al.*, 1998; Chapman *et al.*, 2004; Shiboleth *et al.*, 2007; Silhavy and Burgyán, 2004; Stav *et al.*, 2010).

But not only viral proteins can be associated with disease symptoms. Viral nucleic acids can also be themselves pathogenicity determinants. For example tombusviral defective interfering RNAs ameliorates symptoms in infected plants (Havelda *et al.*, 2005). And also a viral satellite RNA (Y-sat) from CMV produces specific disease symptoms (yellowing) that are caused by the RNA silencing of an endogenous gene that is directed by a small RNA derived from the satellite RNA (Shimura *et al.*, 2011).

1.4- The influence of environmental parameters on compatible plant-RNA virus interactions

Environmental abiotic factors affect plant infections by viruses in different ways. This influence can be reached by their affection on any of the participants in the interaction, i.e. the plant, the virus, or in some cases the transmitting agent. This particular study will be focused in two environmental parameters that affect the interactions between an

experimental compatible plant host and several positive-sense ssRNA viruses.

Earth regions constantly experience climate change (Norse and Gommes, 2003). At present the planet is in a markedly fast warming that has important implications for life, including mankind. Compared with previous episodes of warming, the current one is occurring at an unprecedented pace, supported by the anthropogenic emissions of "greenhouse gases" such as carbon dioxide, methane and nitrous oxide thrown into the atmosphere that trap heat from the sun radiation inside the atmosphere system. The 1990s was the warmest decade of the last 1,000 years (Norse and Gommes, 2003). The Intergovernmental Panel on Climate Change (IPCC) in its last report of 2014 has shown that increases of global temperature are following those predicted by improved models and envisage a progressive increase of global average temperature of between 0.3 to 4.8 ºC from now to the end of the current century (differences depending of the model of prediction). Therefore, it appears relevant to know how compatible plants will respond to infection by viruses under scenarios of increased atmospheric CO_2 levels to which they will very likely be exposed at the end of the century and to the higher average temperatures that will derive from the greenhouse effect of that and other gases.

Plants exposed to high temperatures display cellular alterations in homeostasis which include among others, the change in the fluidity of membranes that leads to activation of lipid-based signaling cascades and to an increased Ca^{2+} influx that conduct to organelles and cytoskeleton reorganization (Saidi *et al.*, 2009; Weis and Berry, 1988). But high temperatures also produce metabolic responses in plants that repress

general protein synthesis and the expression in extreme conditions of HSPs (Bray *et al.*, 2000). Heat also represses genes involved in carbohydrate metabolism, and affects the activities of enzymes involved in carbon metabolism, starch accumulation, and sucrose synthesis (Ruan *et al.*, 2010). Heat stress modifies also phytohormone levels leading to increases of SA, ET and abscisic acid (ABA), and to decreases of others such as cytokinins, auxins, and gibberellic acids (Larkindale and Huang, 2004; Larkindale *et al.*, 2005). Similarly to in other types of stresses, high temperature results in the production of ROS and of oxidative stress responses (Potters *et al.*, 2007).

The increase in temperature may lead to either increased or decreased disease resistance, reflecting a differential influence of the same temperature variation in different plant-pathogen systems (Wang *et al.*, 2009). It is known that plant–virus interactions are affected by temperature (Broderick and Jones, 2014; Szittya *et al.*, 2003). At high temperature, viral infection symptoms are often attenuated in a phenomenon so-called heat masking (Hull, 2002; Johnson, 1922). At high temperature viruses can encounter difficulties to proliferate because of the increased antiviral effects of the metabolic changes caused by elevated temperature, but also because RNA silencing appears to be stronger at temperatures higher than the standard 25 °C laboratory room temperature (Chellappan *et al.*, 2005; Szittya *et al.*, 2003). But virus accumulation can also be affected by temperature due to modification of biochemical efficiency of its own components that affect their replication or movement (intracellular, local cell-to-cell, or long distance). Such are for example the cases of the replicase activities of tobamoviruses and bromoviruses at high temperatures (Dawson, 1976; Dawson *et al.*, 1978).

Elevated levels of environmental CO_2 cause also changes to plants. The experimental increase of atmospheric CO_2 has been shown to generally increase photosynthesis (Amthor, 1995) and water use efficiency (Rogers and Dahlman, 1993) and therefore plant growth. Increase of photosynthesis efficiency directly increases the production of photoassimilates that could act as signaling molecules in plant defense responses (Berger *et al.*, 2007; Fernández-Calvino *et al.*, 2014). In the end, elevated CO_2 levels lead to increases in the C:N ratios in plant tissues (Gifford *et al.*, 2000). Furthermore, they cause an increase in plant size that can be attributed to increases of chloroplast density within cells, to increases of cell sizes, and also of the number of individual cells (Madsen 1971, 1973).

Other changes produced by elevated CO_2 in plants include the general increase of SA levels and the induction of genes associated with this hormone (Zhang *et al.*, 2015). Furthermore, it has been demonstrated that because in plants there is cross-talk between SA and JA, elevated CO_2-induced accumulation of SA is associated with the inhibition of JA signaling (Spoel *et al.*, 2007). Because SA is also associated with defense against biothrophic pathogens, and JA against necrothrophs, elevated CO_2 may imply alterations in the intensities of plant defense responses against these different types of pathogens. In this way changes in the susceptibility to disease of a plant are likely to be observed under elevated CO_2 (Zhang *et al.*, 2015). In this regard, Zhang and colleages (2015) observed that tomato plants under elevated CO_2 levels were less susceptible to TMV infection, measured as a decrease in viral titer in infected tissue and milder symptoms. This, decrease correlated with an increase in SA levels. A similar decrease of viral titers was observed for PVY-infected tobacco

plants under elevated CO_2 conditions, which was similarly shown to correlate with an increase in the levels of SA (Matros *et al.*, 2006). Nevertheless, increases of CO_2 levels can also lead to increased plant susceptibility to viral infections. Such is the case of wheat infected with *Barley yellow dwarf virus* (BYDV) which accumulates higher viral titers under elevated CO_2 conditions (Trębicki *et al.*, 2015).

1.5- Transient expression in plants of transcript RNAs and of their encoded protein products for plant-virus interaction studies

To study mechanism and processes in plant-virus interactions at the molecular and cellular levels the expression of viral and of plant factors in plants is often required. These factors can be expressed either in their native form, or modified by mutations or by the addition of different tags. There are actually very few means by which this can be accomplished in a differentiated plant. One such is the constitutive expression of those genes by stable transformation. The drawbacks of the technique for research purposes are many and important. Stable transformation requires lengthy periods of time to regenerate the plants, bring them to homozygosis and characterize the expression properties of the integrated transgenes. Although some experimental plants like arabidopsis are rather amenable to transformation, most of the others require more time and work. For example, tomato plants require at least a year to produce and characterize transgenic lines. Experimental plants from *Nicotiana* genus also require several months (Canto and Palukaitis, 1998). For some plant species there are simply no procedures to perform a transformation. And in some cases, transgene expression interferes with the normal regeneration of a differentiated plant.

Leaving aside stable transgenesis, and also ultra-specialized and cumbersome microinjection techniques of single cells (Canto *et al.*, 1997) the alternative is to use approaches that transiently express genes in plant cells. In contrast to animal cells that can be cultured and easily transfected, plant cells cannot be cultured in the same way because their being encased in the cell walls that they produce. It is true that cell wall-stripped protoplasts isolated from adult plant leaves can often be electroporated with DNA, RNA and proteins, but their average life is measured in hours, at best up to a few days.

To express genes in a tissue-differentiated plant researchers are then limited to basically three transient expression systems, or their combinations thereof: the first one is the gene gun or biolistic delivery system based on mechanical bombardment of plant tissues with plasmids that carry the genes to be expressed under the control of a eukaryotic promoter; the second one is the delivery into plant cells of the DNA fragments from binary vectors that carry the genes of interest, also under control of eukaryotic promoters, by agroinfiltration; the third one is the use of viral vectors. Each has its pros and cons. In addition, the three delivery systems for transient expression could be combined. Several RNA virus vectors that initially were infectious by mechanical inoculation of *in vitro*-made transcripts have now been transferred to binary vectors for delivery by agroinfiltration or bombardment.

Bombardment by mechanical means of metal particles coated with plasmid DNA or with RNAs causes damage to leaf tissue, only a few epidermal and mesophyll cells receive the particles and survive the mechanical damage, to express those genes (Canto *et al.*, 1997; Gal-On *et al.*, 1997, 1995; Sikorskaite *et al.*, 2010). On the advantages side, the genes

introduced are expressed in absence of alien biological delivery agents (bacteria, viruses).

Gene expression through viral vectors has been used with success to analyze the functions of genes involved in plant-virus interaction. Viruses can be used not only for the expression of the inserted nucleic acids and of their encoded genes, but also by taking advantage of the RNA silencing machinery, to trigger the silencing of endogenous genes, the so called Virus-Induced Gene Silencing or VIGS (Ruiz *et al.*, 1998). Infectious clones from several viruses have been obtained and modified to become transient expression vectors and/or to conduct VIGS. Examples of some RNA virus vectors are *Tobacco rattle virus* (TRV) (Padmanabhan and Dinesh-Kumar, 2009), PVX (Chapman *et al.*, 1992), CMV (Fujiki *et al.*, 2008) and potyviruses, such as TEV or PPV (Bedoya and Daròs, 2010; Dolja *et al.*, 1992; García *et al.*, 2006). Some viral vectors can move systemically with their insert, others are cell-limited amplicons often for encapsidation limitation reasons. A downside to the use of virus vectors is that the genes of interest are being expressed in the context of a viral infection, which can lead to difficulties discerning between the effects or properties of our gene of interest in such altered cellular backgrounds. Of course, on the other hand it is often very useful in virus studies to express the gene from the same (modified) virus that is being investigated, as it is also shown in some of the experimental results presented here.

Agroinfiltration is a technique commonly used in plant research and in plant virology (Fig. 2). This technique is employed to introduce in the plant cell a Transferred DNA (T-DNA) that will express the gene it harbors for a period of time in the cells of the infiltrated tissue region (Gelvin, 2003). The delivery is achieved by needle-less injection of a

culture of disarmed (devoid of some tumorigenic genes) *Agrobacterium tumefaciens* that harbors the T-DNA-containing binary vector, which has been cloned and manipulated previously in *Escherichia coli*. This methodology has been successfully used to express ectopic genes *in planta*. Transient levels of expression in some hosts, such as the experimental *N. benthamiana* are rather high and allow for several types of assays to be performed. One such is confocal microscopy of fluorescently tagged proteins, in epidermal cells, as it is shown in some of the results of the present work.

The versatility of the agroinfiltration system is remarkable, as it also allows for several T-DNAs to be co-infiltrated in the same cells and therefore the co-expression of different products. This is not achievable with a plant viral vector, as cross-protection prevents that two viruses with high homology accumulate in the same cell at comparable levels. A key aspect of the technique is that plants recognize transcripts from the infiltrated T-DNA fragments as foreign for reasons not very clear, but that may be related to promoter-less bi-directional transcript synthesis. This triggers the partial silencing of the expressed transcript and depresses the transient steady-state levels of RNA and its encoded protein products, which would otherwise be reached in this expression system. However, far from this being a problem it can be used to advantage: silencing can be prevented by the co-expression of a suppressor (Canto *et al.*, 2002; Johansen and Carrington, 2001), and furthermore, the suppression of the silencing of a reporter gene can be quantified, providing a functional assay to test for suppression of silencing function and its strength (the agropatch assay), as it is also shown in this work. Drawbacks of the technique are that many plant species are not amenable to mechanical agroinfiltration, and even

Fig 2. Picture of the agroinfiltration technique. The tip of the syringe without a needle is pressed against the underside of a leaf while simultaneously applying gentle counterpressure to the other side of the leaf, making the *Agrobacterium* solution get injected into the leaf.

if they are, the levels of transient expression from T-DNAs are comparatively low (in tobacco they are roughly 1/10th of those achieved in *N. benthamiana;* T. Canto, personal observation). Another limitation is that Agrobacterium delivery is temperature-constrained to less than 29 °C, and at relatively elevated temperatures the technique cannot be used (Fullner and Nester, 1996; Gelvin, 2003). In this respect the present study shows one approach to circumvent in part this limitation.

CHAPTER 2

OBJECTIVES

The broad objectives of this work were four:

1. To study at the whole plant level the effects of environmental parameters on the outcomes of the infections by different positive-sense RNA viruses of a compatible common host.

2. To assess the roles of antiviral silencing and its suppression by viral factors on these outcomes, in fully developed plants.

3. To study the subcellular distribution and dynamics of the silencing suppressor HCPro by cell biology means.

4. To determine whether HCPro binds to small RNAs *in vivo*, and if so, characterize the properties of the bound RNA populations.

For the first and second points the following specific objectives were pursued:

- To develop a procedure that allows the use of the agroinfiltration technique for the transient expression of proteins in plants at non-permissive temperatures above 29 °C.
- To compare infections of the common host *N. benthamiana* by the positive-sense RNA viruses *Cucumber mosaic virus* (CMV), *Potato virus Y* (PVY), and by a *Potato virus X* (PVX) vector, the latter either unaltered or expressing the CMV 2b protein or the PVY HCPro suppressors of silencing, at 25 °C vs. 30 °C, or at standard (~401 parts per million, ppm) vs. elevated (970 ppm) CO_2 levels.
- To measure the efficiency of the suppressors of RNA silencing of these viruses under the above altered environmental conditions and determine whether infection outcomes derive in part from their inability to neutralize antiviral silencing.

For the third point the following specific objective was pursued:

- To visualize *in vivo* the subcellular distribution and dynamics of HCPro from PVY and of its homodimers using fluorescent tags and find out their biological implications through function and activity assays.

For the fourth point the following specific objectives were pursued:

- To purify HCPro under non-denaturing conditions and the nucleic acids associated to the purified preparation.
- To deep-sequence and analyze the populations of short RNAs of less than 500 nucleotides in length that might be bound to HCPro and determine their characteristics.

CHAPTER 3

A PROCEDURE FOR THE TRANSIENT EXPRESSION OF GENES BY AGROINFILTRATION ABOVE THE PERMISSIVE THRESHOLD TO STUDY TEMPERATURE-SENSITIVE PROCESSES IN PLANT–PATHOGEN INTERACTIONS

Article published in Molecular Plant Pathology in 2014; 15(8):848-57.

doi: 10.1111/mpp.12136.

Molecular Plant Pathology

MOLECULAR PLANT PATHOLOGY (2014) 15(8), 848–857 DOI: 10.1111/mpp.12136

Technical advance

A procedure for the transient expression of genes by agroinfiltration above the permissive threshold to study temperature-sensitive processes in plant–pathogen interactions

FRANCISCO DEL TORO[1], FRANCISCO TENLLADO[1], BONG-NAM CHUNG[2,*] AND TOMAS CANTO[1,*]

[1]*Environmental Biology Department, Centro de Investigaciones Biológicas, CIB-CSIC, Ramiro de Maeztu 9, 28040 Madrid, Spain*

[2]*National Institute of Horticultural & Herbal Science, Agricultural Research Center for Climate Change, 281, Ayeon-ro, Jeju 690-150, Jeju Island, South Korea*

SUMMARY

Localized expression of genes in plants from T-DNAs delivered into plant cells by *Agrobacterium tumefaciens* is an important tool in plant research. The technique, known as agroinfiltration, provides fast, efficient ways to transiently express or silence a desired gene without resorting to the time-consuming, challenging stable transformation of the host, the use of less efficient means of delivery, such as bombardment, or the use of viral vectors, which multiply and spread within the host causing physiological alterations themselves. A drawback of the agroinfiltration technique is its temperature dependence: early studies have shown that temperatures above 29 °C are nonpermissive to tumour induction by the bacterium as a result of failure in pilus formation. However, research in plant sciences is interested in studying processes at these temperatures, above the 25 °C experimental standard, common to many host–environment and host–pathogen interactions in nature, and agroinfiltration is an excellent tool for this purpose. Here, we measured the efficiency of agroinfiltration for the expression of reporter genes in plants from T-DNAs at the nonpermissive temperature of 30 °C, either transiently or as part of viral amplicons, and envisaged procedures that allow and optimize its use for gene expression at this temperature. We applied this technical advance to assess the performance at 30 °C of two viral suppressors of silencing in agropatch assays [*Potato virus Y* helper component proteinase (HCPro) and *Cucumber mosaic virus* 2b protein] and, within the context of infection by a *Potato virus X* (PVX) vector, also assessed indirectly their effect on the overall response of the host *Nicotiana benthamiana* to the virus.

Keywords: agroinfiltration, plant virology, plant–virus interactions, transient expression.

INTRODUCTION

Agrobacterium tumefaciens is one of the few bacteria capable of delivering DNAs into plant cells. In nature, the transferred DNA fragment (T-DNA) of the tumour-inducing plasmids delivered by the agrobacterium into plant nuclei encodes genes required for crown gall tumour formation as part of the bacterial life cycle. However, laboratory modifications have created versatile binary vector systems in which the T-DNA, free of tumour-inducing genes, can express any desired gene or sequence fragment under the control of a eukaryotic promoter, the most common of which for research purposes is the *Cauliflower mosaic virus* 35S promoter. Some of the T-DNA molecules delivered into a plant cell can integrate stably by recombination into the plant genome, thus becoming inheritable. This constitutes the basis of current techniques for plant transformation (Gelvin, 2003). More recently, transient, localized expression of genes and their products in plants from the bulk of nonintegrated T-DNAs delivered into the plant cell by the bacterium has become a widely used tool in plant pathology and cell biology studies. This technique is commonly known as agroinfiltration or agroinjection, and ways to enhance the levels of expression or its large-scale use have been envisaged employing a variety of approaches (Chen *et al*., 2013; Voinnet *et al*., 2003).

Transient, steady-state levels of gene products expressed from T-DNAs delivered into the agroinfiltrated leaf patch (agropatch) are influenced by several factors, one of which is their recognition as foreign by the host, which elicits a silencing response that depresses both the transcript messenger RNA (mRNA) levels and those of their encoded protein products (Johansen and Carrington, 2001). The trigger of this silencing response is probably the presence of double-stranded transcripts derived from sense and antisense transcription of the T-DNA sequences, causing the generation of small interfering RNAs (siRNAs) to promoter sequences, or to promoterless T-DNAs, in theory expected not to be transcribed (Canto *et al*., 2002). The co-expression of viral suppressors of gene silencing that prevent the targeting and degradation of T-DNA-derived transcripts arose as a strategy to counteract this partial silencing of T-DNA gene expression (Canto *et al*., 2002; Johansen and Carrington, 2001; Voinnet *et al*., 2003).

Another important factor in agroinfiltration efficiency is the type of plant host. Some plant species are not physically amenable to the efficient infiltration of their leaves with *Agrobacterium*

*Correspondence: Email: tomas.canto@cib.csic.es; chbn7567@korea.kr

cultures. The experimental plant species *Arabidopsis thaliana*, *Nicotiana tabacum* and *Nicotiana benthamiana* are all readily infiltrated, but differences in the respective transient levels of the gene products achieved can be large: the latter host expresses higher levels of transcript mRNAs and their products than the first two (Andrews and Curtis, 2005). This may be related to the fact that, in *N. benthamiana*, the salicylic acid- and virus-inducible RNA-dependent RNA polymerase 1 (RdRP1), involved in antiviral defences, is naturally truncated, possibly causing its hypersusceptibility to many different plant viruses (Yang *et al*., 2004; Ying *et al*., 2010). Thus, unless a study requires a specific plant species, *N. benthamiana* is the usual host of choice for agroinfiltration assays in experimental studies.

Temperature is another factor affecting the efficiency of agroinfiltration as a tool for gene expression in plants. Optimal temperatures for transient gene expression through agroinfiltration appear to be in the 25 ± 0.5 °C region in *N. benthamiana* (Chen *et al*., 2013; Lai and Chen, 2012), although the tumour induction optimum of the bacterium may be lower, 22 °C, in other hosts (Fullner and Nester, 1996). The transfer of T-DNAs into plant cells involves a complex set of bacterial genes and the physical formation of a pilus structure to allow for the physical transfer of bacterial DNA into the plant. Temperatures of 29 °C and above completely prevent the development of tumours as certain proteins involved in the transfer machine are not functional and, critically, pilus formation also does not take place (Fullner and Nester, 1996; Gelvin, 2003). In addition, it has been shown that the strength of the plant silencing defence response that targets both viruses and T-DNA transcripts steadily increases with temperature (Chellappan *et al*., 2005; Qu *et al*., 2005; Szyttia *et al*., 2003; Velázquez *et al*., 2010). Thus, in addition to failure in the T-DNA transfer process, a stronger silencing defence response could have a further negative effect on any expression from agrodelivered T-DNAs. Therefore, agroinfiltration as a technique to transiently express genes in plants at temperatures above 29 °C would appear to be a nonviable option.

In this work, we first assessed the efficiency and viability of agroinfiltration for the expression of genes from T-DNAs at 30 °C, either transiently or as part of a viral *Potato virus X* (PVX)-based amplicon. We then devised and optimized a procedure that allows its use for gene expression at this temperature and characterized its properties and parameters. With this procedure, we assessed the performance at 30 °C of two viral suppressors of silencing in agropatch assays [*Potato virus Y* helper component proteinase (HCPro) and *Cucumber mosaic virus* (CMV) 2b protein] and found that, at least for HCPro, its suppressor of silencing activity in agropatch assays is as strong at 30 °C as it is at 25 °C. Within the context of infection by a PVX vector, we also found that the strength of the overall response of the host *N. benthamiana* to the virus at high temperatures overcomes the effect of either 2b or HCPro on the neutralization of host defences.

RESULTS

Poor steady-state levels of a reporter expressed at 30 °C from agroinfiltrated T-DNAs

A green fluorescent protein (GFP) reporter was agroinfiltrated at standard (25 °C) temperature into *N. benthamiana* leaf patches, together with empty construct pROK2 or pROK2 constructs expressing P1-hexahistidine-tagged HCPro (P1-6×-HCPro) from *Potato virus Y* (PVY), 2b protein from CMV or P19 from *Tomato bushy stunt virus* viral suppressors of silencing (Fig. 1A, agropatches labelled C, 1, 2 and 3, respectively). Within a few minutes after infiltration, plants were moved to growth cabinets at either 25 or 30 °C. After 3 days at standard temperature, GFP-derived fluorescence in the patches in which the viral suppressors of silencing were present was much more intense than in the patch in which GFP was being expressed alone under the UV lamp (Fig. 1A, left leaf, patches 1, 2 and 3 versus patch C), as partial silencing of the T-DNA-derived GFP transcript was relieved by the viral factors. Both the visual intensity of fluorescence and the amounts of GFP detected by Western blot in the presence of the three different viral suppressors were similar (Fig. 1A, left leaf; Fig. 1B, top left Western blot, compare 1, 2 and 3), indicating that 6×-HCPro (P1 and 6×-HCPro separated by proteolytic cleavage) and 2b displayed suppressor strengths comparable with that shown by tombusviral P19, usually considered to be a strong suppressor of silencing in this type of assay. Both HCPro and 2b were also detected serologically by Western blot in their corresponding patches (Fig. 1B, bottom left and right panels, respectively).

By contrast, in those plants kept for 3 days at 30 °C, GFP-derived fluorescence in infiltrated patches was visualized very poorly and unevenly (Fig. 1A, right leaf). Western blot analysis of the infiltrated patches showed the presence of very low, but comparable, amounts of GFP in all four patches, with no dependence on whether or not a viral suppressor was co-infiltrated (Fig. 1B, top right Western blot panel). GFP levels in the C patch in this leaf were lower than in the left leaf that had been kept at 25 °C (Fig. 1B, lanes labelled C in top Western blot panels). Interestingly, neither HCPro nor 2b could be detected serologically (Fig. 1B, bottom left and right panels, respectively).

We concluded that, in leaves kept at 30 °C after infiltration, transient GFP and suppressor expression, as well as suppressor function, were compromised. Given the published literature, a likely cause for this outcome could be an inefficient transfer of T-DNA. However, it could also be the case that other factors, such as host processes at that temperature having a negative effect on the steady-state levels of T-DNA transcripts or their protein products, could also influence this outcome. In this regard, we also tested whether the transfer of plants from 25 to 30 °C after infiltration could have affected negatively their efficiency in

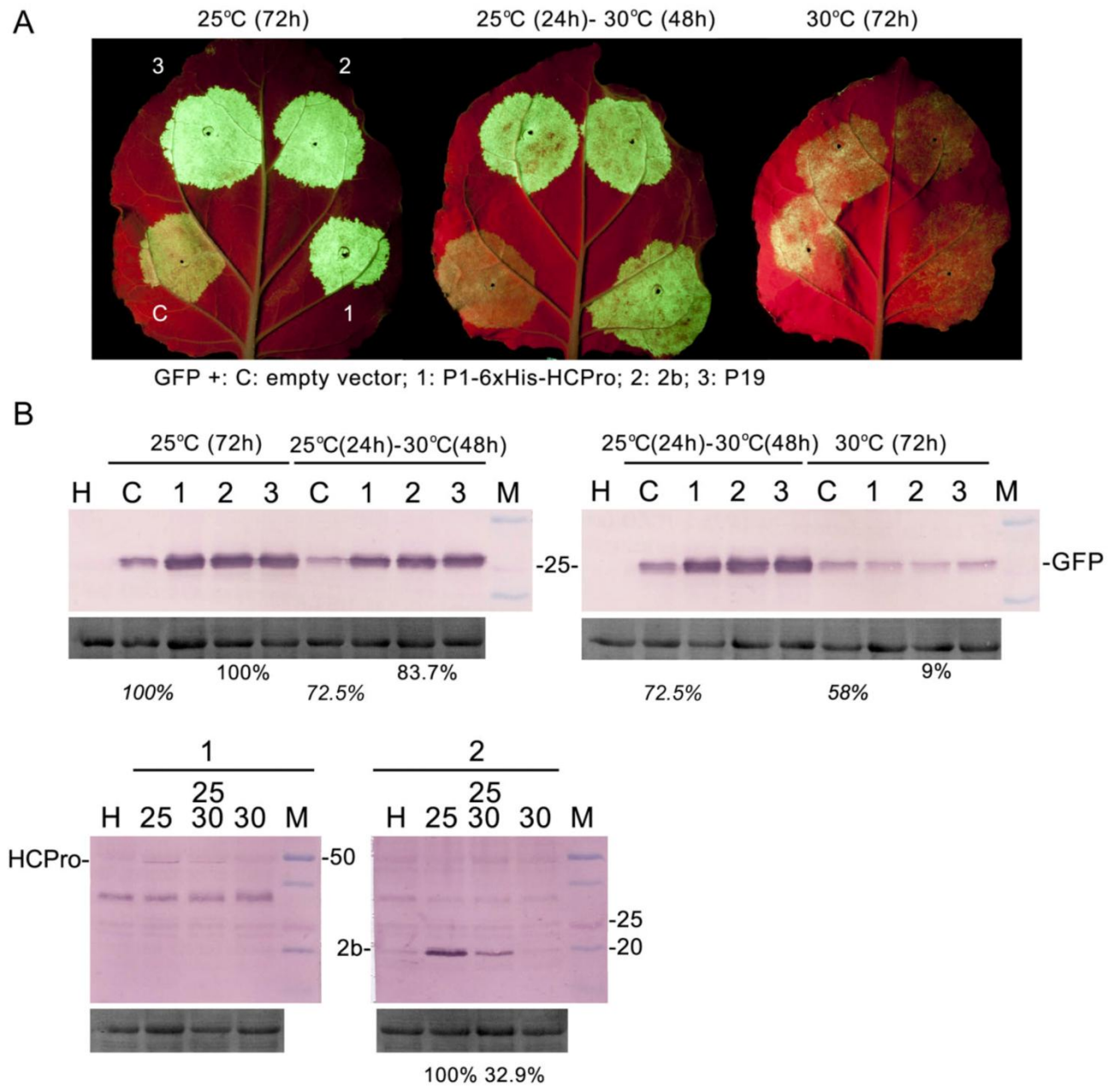

Fig. 1 Assessment of the efficiency of agroinfiltration to transiently express a green fluorescent protein (GFP) reporter in infiltrated *Nicotiana benthamiana* patches at different temperatures at 72 h post-infiltration (hpi). The GFP reporter vector was co-infiltrated together with empty vector (patches and Western blot lanes labelled C), or together with vectors expressing P1-6×-HCPro, 2b protein or P19 suppressors of silencing (patches and Western blot lanes labelled 1, 2 and 3, respectively). (A) Visualization of GFP-derived fluorescence under a UV lamp in a leaf kept at 25 °C for 72 hpi (left leaf), in a leaf kept for 72 hpi at 30 °C (right leaf) and in a leaf kept for the first 24 hpi at 25 °C and the following 48 hpi at 30 °C (central leaf). (B) Western blot analysis using total extracts of the accumulation in the infiltrated patches of the GFP reporter (top panels) and of the suppressors 6×-HCPro and 2b protein (bottom panels) using antibodies against GFP and 6×histidine tags, respectively. Below the selected lanes is a densitometric analysis of the protein bands (protein levels in leaf samples kept for 72 hpi at 25 °C are given the arbitrary value of 100%). Note that the same samples from the central leaf patches appear duplicated in both top left and right Western blots. This is because densitometric analysis requires bands to be in the same membrane to eliminate the effect of differences between membranes in blotting efficiency or in antibody binding. Lane M in the blots shows the molecular weight markers in kilodalton (kDa), and the small panels below the Western blots show the membranes stained with Ponceau-S after blotting, as controls of loading.

agropatch assays as a consequence of heat shock. To do this, we compared 25 °C plants with those that had been placed at 30 °C 3 days prior to their agroinfiltration, and found no difference in their performance (data not shown).

Twenty-four hours at 25 °C after infiltration allowed T-DNA transfer into plant cells and restored transient gene expression at 30 °C

We hypothesized that, if T-DNA transfer into plant cell nuclei was being prevented by a temperature of 30 °C, the provision of a window of time after infiltration at standard temperature, sufficiently long to allow for transfer to occur, but sufficiently short that most T-DNA-derived protein accumulation and functional action would take place at 30 °C, would allow us to perform studies on protein function at high temperatures using the agroinfiltration technique. For this reason, we tested keeping plants for 24 h at 25 °C after infiltration, followed by 48 h at 30 °C (Fig. 1A, centre leaf). With this procedure, at 72 h post-infiltration (hpi), we obtained levels of expression of the GFP reporter that were on the order of those seen in leaves kept all the time at 25 °C (Fig. 1A, central versus left leaf; Fig. 1B top left Western blot panel). As an example, quantification of the GFP band density corresponding to patch 2 showed that, in the central leaf patch, there was 83.7% of the protein found in the left leaf. This was in contrast with the meager 9% obtained at 30 °C in the equivalent sample (Fig. 1B, top Western blot panels). Both HCPro and 2b proteins were also detected serologically in their corresponding patch samples in the central leaf, although in a smaller proportion relative to the protein found in the equivalent patch in the left (25 °C) leaf than for the GFP reporter (Fig. 1B; bottom Western blot panel). As an example, quantification of the 2b protein band density corresponding to patch 2 in the left and central leaves showed that the latter accumulated one-third (32.9%) of the suppressor found in the former. The reason for this disparity between the accumulation of the reporter and of the two suppressors could lie in the existence of host processes that specifically target the suppressor but not the reporter (Nakahara *et al*., 2012).

Thus, as expected, T-DNA transfer was critically affected by the 30 °C temperature and the provision of a 24-h 25 °C window after infiltration overcame this obstacle. We tested a window of only 12 h, but the results were unsatisfactory (Fig. S1A, see Supporting Information).

We then determined the maximum proportion of protein found at 72 hpi that could have accumulated in the initial 24 h. For this purpose, we performed a time course experiment to analyse the protein accumulation at 24, 48 and 72 hpi of the GFP reporter co-infiltrated with empty vector or with vectors expressing either 6×-HCPro or 2b protein, for which we had means of serological detection (Fig. 2). We tested the protein accumulation in plants

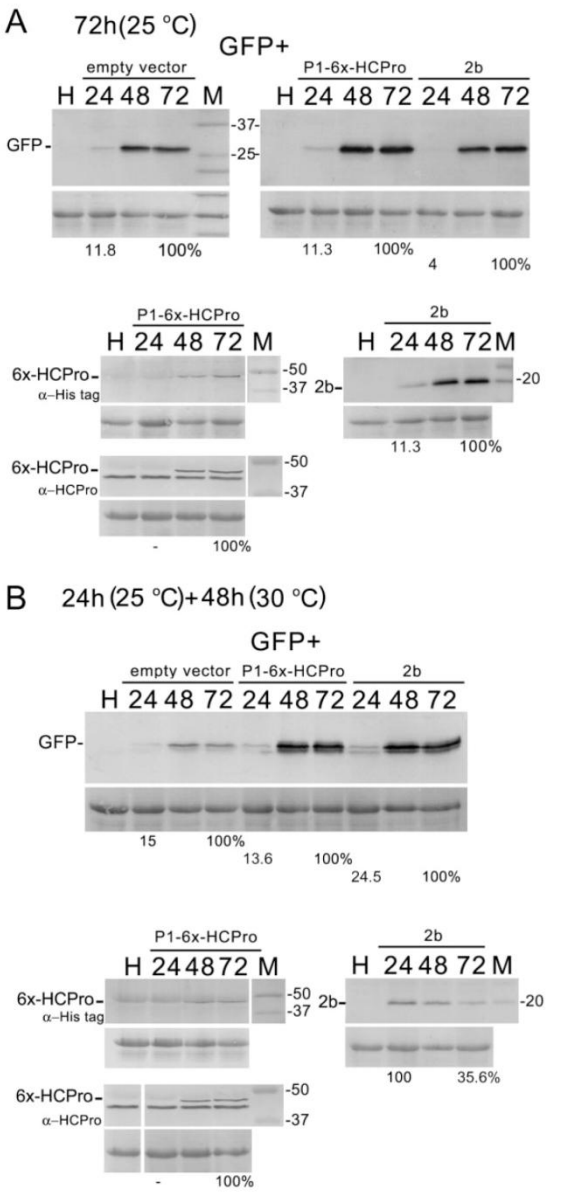

Fig. 2 Time course analysis by Western blot of green fluorescent protein (GFP) reporter and of suppressor accumulation in infiltrated patches at 24, 48 and 72 h post-infiltration (hpi). (A) Agroinfiltrated *Nicotiana benthamiana* leaves were kept at 25 °C for the whole 72 hpi. (B) Agroinfiltrated leaves were kept at 25 °C for the first 24 h and then at 30 °C for the following 48 h. The GFP reporter construct was co-infiltrated together with empty vector or with *Potato virus Y* (PVY) P1-6×-HCPro or *Cucumber mosaic virus* (CMV) 2b protein suppressors of silencing. Total patch extracts were analysed by Western blot for GFP (top panels, using an antibody against GFP), 6×-HCPro (bottom left panels, using antibodies against 6×histidines or against HCPro) and 2b protein (bottom right panel, using an antibody against 2b protein). Below the selected lanes are densitometric analyses of protein bands (protein levels in leaf samples collected at 72 hpi are given the value of 100%). Lane M in the blots shows molecular weight markers in kilodalton (kDa), and the small panels below the Western blots show the membranes stained with Ponceau-S after blotting, as controls of loading.

kept all the time at 25 °C (Fig. 2A) and in plants kept for the first 24 h at 25 °C and the following 48 h at 30 °C (Fig. 2B). In both cases, at 24 h, we detected the accumulation of the GFP reporter and 2b suppressor, but failed to detect the accumulation of 6×-HCPro using two separate antibodies. For the GFP reporter, accumulation in the first 24 h at 25 °C was limited to 15% or less of the total found at 72 hpi (Fig. 2A, B, top right panels). The same pattern was found for the 2b suppressor in plants kept all the time at 25 °C: 2b accumulation at 24 hpi was also less than 12% of the protein found at 72 hpi (Fig. 2A). However, in the case of plants kept for 24 h at 25 °C and the following 48 h at 30 °C, 2b accumulation declined after the initial 24 h and, at 72 hpi, it was only 35.6% of that found at 24 h (Fig. 2B, bottom right panel). We found the same pattern in a modified 2b tagged with six histidines and an HA peptide (Tyr-Pro-Tyr-Asp-Val-Pro-Asp-Tyr-Ala) at its N- and C-termini, respectively (construct 6×-2b-HA; Fig. S1B). By contrast, 6×-HCPro accumulation followed a similar pattern in plants kept all the time at 25 °C and in plants kept for the first 24 h at 25 °C and the following 48 h at 30 °C. No clear decline from 48 to 72 h was observed, in contrast with the observations for the 2b protein (Fig. 2B). These data clearly indicate differences between 2b and 6×-HCPro in their speed of expression and maturation, stability and turnover in a similar cellular environment.

Thus, in both situations, most of the accumulation of our GFP reporter (over 85%) and of 6×-HCPro took place at 30 °C, as did whatever functionality the latter might have had at that temperature. This allowed us to conclude that, in our particular experiment, HCPro displayed suppressor of silencing activities at 30 °C that were at least as strong as those displayed at 25 °C in the agropatch assay system. The case of 2b protein, native or tagged, was different, as its accumulation declined substantially after the initial 24 h if plants were transferred to 30 °C. Remarkably, even these lower levels of suppressor were sufficient to suppress efficient silencing of the GFP reporter [Figs 1, 2A versus 2B (top GFP Western blot panels), S1A].

Viable expression of viral amplicons at 30 °C through agroinfiltration

We tested how binary constructs expressing viral amplicons would perform in our system. For this, we used a construct expressing a PVX vector, and PVX vectors expressing either PVY P1-6×-HCPro (construct PVX-P1-6×-HCPro) or CMV 6×-2b-HA protein (construct PVX-6×-2b-HA). After agroinfiltration at 25 °C, plants were kept at either 25 °C for 7 days or 25 °C for 24 h and then transferred to 30 °C for the remaining 6 days. Plants were monitored daily for the appearance of systemic infection symptoms during this period (Table 1) and, at the end of the seventh day, samples were taken from systemic tissue to monitor viral coat protein (CP) levels. In plants kept at 25 °C, symptoms appeared on the fifth day in all three cases, and increased with time. Symptoms were more severe in the case of PVX-P1-6×-HCPro and PVX-6×-2b-HA, and particularly strong in the case of PVX-6×-2b-HA, leading, on the seventh day, to the start of necrosis in apical leaves (Table 1 and Fig. 3A). By contrast, in all three cases, plants kept at 30 °C remained visually symptomless (Table 1 and Fig. 3A). Western blot analysis of systemic tissue revealed that, regardless of the absence of symptoms, all plants were infected with the virus. Densitometric analysis of the Western blot CP bands revealed that, at 25 °C, tissue infected with PVX or PVX-6×-2b-HA contained comparable levels of protein, and greater levels than in tissue infected with PVX-P1-6×-HCPro (Fig. 3B, top panels). In the symptomless plants kept at 30 °C, CP levels in the three viruses were lower, and differences among them were less marked (Fig. 3B, top panels). This is somewhat surprising as it occurred despite the fact that two of the constructs expressed 6x-2b-HA and P1-6x-HCPro, both strong suppressors of gene silencing in agropatch assays, as shown previously (González *et al*., 2012 and Tena *et al*., 2013, respectively), and, at least for 6×-HCPro, functionally as active at 30 °C as at 25 °C (this work). That both suppressors accumulated at 30 °C in virus-infected tissue was confirmed serologically (Fig. 3B, bottom panels).

Table 1 Visual assessment of systemic infection symptoms in plants infected with *Potato virus X* (PVX)-based vectors (PVX, PVX-P1-6×-HCPro or PVX-6×-2b-HA) at 4–7 days post-infiltration (dpi).

	4 dpi		5 dpi		6 dpi		7 dpi	
	25 °C	25 °C (24 h)–30 °C (48 h)	25 °C	25 °C (24 h)–30 °C (48 h)	25 °C	25 °C (24 h)–30 °C (48 h)	25 °C	25 °C (24 h)–30 °C (48 h)
PVX	No symptoms	No symptoms	Curling in apical leaves, mosaic	No symptoms	Curling in apical leaves increased	No symptoms	Curling in apical leaves increased	No symptoms
PVX-P1-6×-HCPro	No symptoms	No symptoms	Curling in apical leaves, mosaic	No symptoms	Curling in apical leaves increased	No symptoms	Curling in apical leaves increased	No symptoms
PVX-6×-2b-HA	No symptoms	No symptoms	Curling in apical leaves, mosaic	No symptoms	Curling in apical leaves increased	No symptoms	Curling in apical leaves increased. Start of necrosis in leaves 3–6 above infiltrated ones	No symptoms

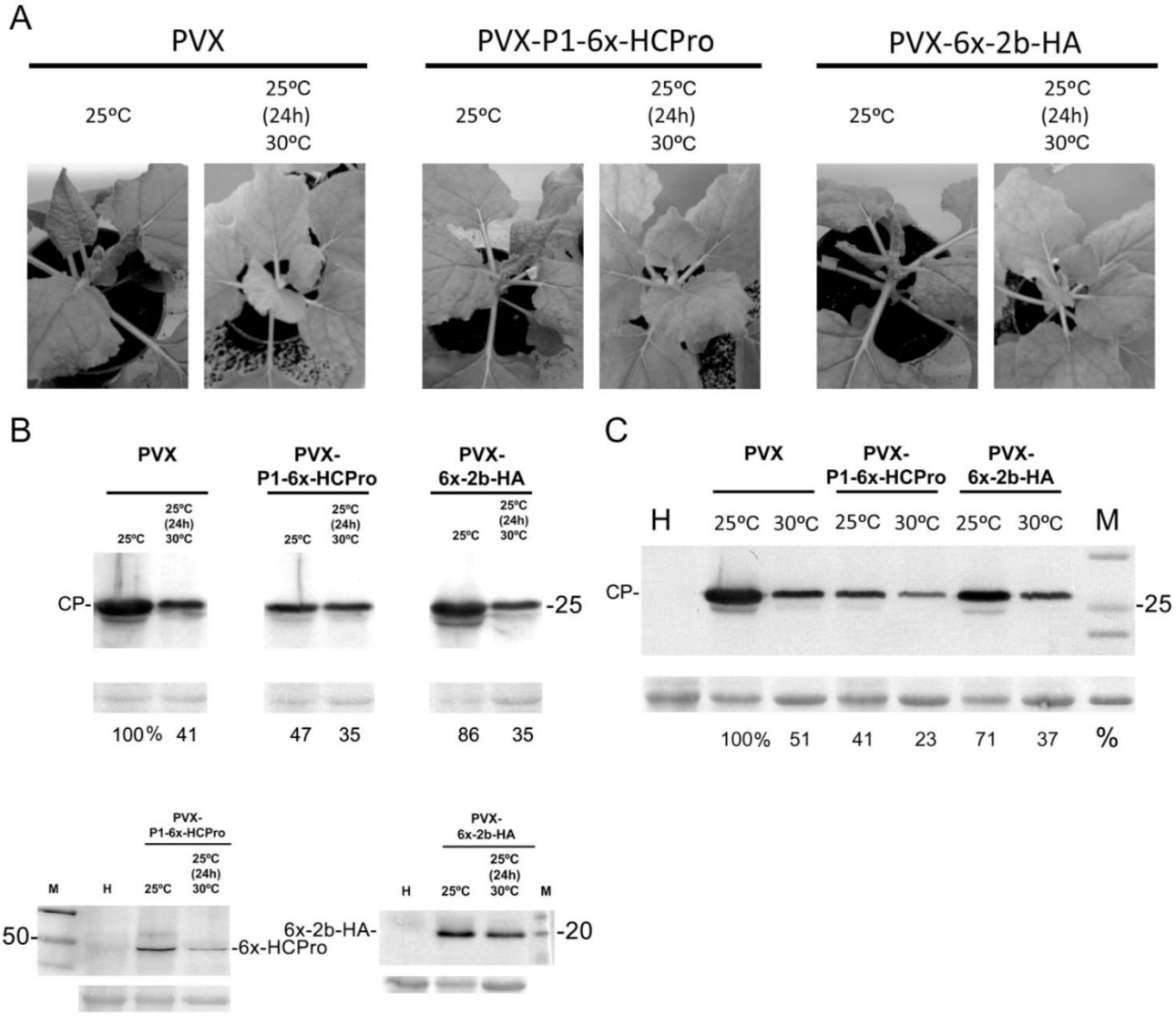

Fig. 3 Assessment of the efficiency of agroinfiltration to deliver *Potato virus X* (PVX)-based amplicons to *Nicotiana benthamiana* plants, and their accumulation at different temperatures, at 7 days post-infiltration. (A) Symptoms found in systemic leaves of plants infiltrated with a PVX amplicon, or with PVX amplicons expressing either P1-6×-HCPro or 6×-2b-HA protein (PVX-P1-6×-HCPro and PVX-6×-2b-HA, respectively). At 25 °C, plants showed systemic symptoms in the three cases (first, third and fifth images from the left). Symptoms were more severe if a suppressor was expressed, in particular 6×-2b-HA (third and fifth images versus first image from the left). Plants kept at 30 °C after an initial 24 h at 25 °C appeared symptomless (second, fourth and sixth images from the left). (B) Western blot analysis of viral coat protein (CP; top panels), 6×-HCPro (bottom left panel) and 6×-2b-HA (bottom right panel) accumulation in systemic tissue (fifth leaf above the infiltrated ones) of the plants shown in (A) using antibodies against PVX CP, 6×histidines and 2b protein, respectively. CP and suppressor accumulation were lower in samples kept at 30 °C after an initial 24 h at 25 °C than in plants kept all the time at 25 °C. (C) Western blot analysis of viral CP accumulation in systemic tissue (fifth leaf above the infiltrated ones) in plants kept for 7 days after infiltration at 30 °C versus plants kept all the time at 25 °C. In both (B) and (C), CP protein accumulation was similar between virus treatments, but lower in the plants kept at 30 °C than in those kept at 25 °C. Below the selected lanes are densitometric analyses of CP bands as a measure of virus titres. Protein levels in plants kept at 25 °C infected with the PVX construct are given the value of 100%. Lane M in the blots shows molecular weight markers in kilodalton (kDa), and the small panels below the Western blots show the membranes stained with Ponceau-S after blotting, as controls of loading.

As even a very low transfer of T-DNA by the agrobacterium could be sufficient to allow the viral amplicon to replicate independently, and given that we observed a low level of expression of the GFP reporter even in plants transferred to 30 °C immediately after agroinfiltration (Fig. 1, right leaf and right Western blot panel), we tested whether infiltration of the viral amplicons at 30 °C would cause plants to become infected. At 7 days after agroinfiltration, plants remained symptomless (data not shown),

but Western blot analysis of the viral CP in systemic tissue revealed that they were infected, although CP levels were again lower than those found in plants kept at 25 °C (Fig. 3C). Furthermore, the levels of CP in all cases were very similar to those found in plants kept for the first 24 h after infiltration at 25 °C prior to their transfer to 30 °C for 6 days (Fig. 3C versus 3B). However, repeated tests showed that, in some instances, PVX infection failed to occur in plants transferred to 30 °C immediately after agroinfiltration (Fig. S1C). Therefore, even for T-DNAs expressing viral amplicons, a 24-h window at 25 °C is advisable.

DISCUSSION

Most research in laboratories investigating the mechanisms and processes underlying plant–virus interactions takes place at the standard room temperature, usually 25 °C. One of the main tools in plant pathology for functional studies is agroinfiltration, a technique that has its optimal working temperature precisely at 25 °C (Chen *et al*., 2013). At temperatures of 29 °C and above, it is nonfunctional (Fullner and Nester, 1996; Gelvin, 2003). However, plants interact with their environment under seasonal and daily changes in temperature that, within a crop growing season, can span from a low of 10 °C or less to a high in the upper 30 °C region. Thus, there is interest in studying plant processes at 30 °C and above, especially as agriculture in warm and highly populated regions is becoming increasingly important, and as climate models forecast future increases in both average and extreme temperatures in most areas. The use of agroinfiltration as a fast and versatile tool to express proteins in native or modified form, or to transiently silence any gene at elevated temperatures, would be very useful.

However, in plant–virus interactions, increased temperature leads, in general, to weaker infection symptoms (Hull, 2002). In this regard, there is documented evidence that gene silencing-based defence processes that are key to the infection outcome show a positive correlation with temperature: it has been reported that antiviral silencing becomes progressively stronger against RNA viruses and agroinfiltrated T-DNAs from 15 to 24 °C (Szyttia *et al*., 2003), against positive-sense RNA viruses from 21 to 27 °C (Qu *et al*., 2005), against negative RNA viruses from 26/18 °C to 32/26 °C (day/night; Velázquez *et al*., 2010) and against DNA geminiviruses from 25 to 30 °C (Chellappan *et al*., 2005). In all cases, this coincides with a decrease in the accumulation of corresponding viral titres, their mRNAs or the products they encode, and with an increase in the levels of siRNAs to these sequences. This observation has been used to advantage to transform plants at higher temperatures to constitutively express a potyvirus-based viral amplicon vector, avoiding its pathological effects. When transformation, regeneration and plant growth take place at high temperature, the amplicon fails to replicate and plants avoid virus-derived pathological effects during their regeneration and development. Lowering the temperature in full-grown, symptomless plants allows the amplicon vector to express any potential product at high levels in some of the transgenic lines (Dujovny *et al*., 2009).

In contrast with gene silencing, less is known about the effect of temperature on other defence processes targeting viruses, such as proteasome or autophagy routes. Temperature can, however, also affect the biological activities of viral factors involved in processes such as movement (Boyko *et al*., 2000) and replication (Ohsato *et al*., 2003), although, for the latter, to discriminate it from gene silencing is problematic. To date, there is little evidence regarding the temperature dependence of the activity of viral suppressors of silencing, but as this takes place through binding to nucleic acids or to host factors, within and/or interacting with physical subcellular structures/compartments, it could be the case.

Here, we have developed a procedure that allows the use of the agroinfiltration technique for the expression of genes at 30 °C in virus–plant interaction studies. We first characterized the efficiency of agroinfiltration to express proteins at 30 °C and found that, at this temperature, the accumulation of a GFP reporter and of the viral proteins tested was either very poor or undetectable (Fig. 1). By providing a 24-h period post-infiltration at 25 °C before placing the plants at 30 °C, we allowed sufficient time for T-DNA transfer and subsequent gene expression to occur, whereas a shorter window of 12 h was found to be inefficient (Figs 1 and S1). In this way, and by co-expression of our reporter with any of three viral suppressors of silencing, we were able to achieve levels of accumulation that were over 83% of those obtained in similarly agroinfiltrated plants kept at 25 °C (Fig. 1B).

In contrast with our GFP reporter, the accumulation of both viral HCPro and 2b suppressor proteins was lower than that found in plants kept all the time at 25 °C (33% in the case of 2b protein; visually lower, but not quantified, in the case of 6×-HCPro; Fig. 1B). The reason for this disparity with the reporter could be the intrinsic stability or, unlike the reporter, the viral suppressors may be differentially targeted by host processes that negatively affect their steady-state levels, such as the proteasome (Ballut *et al*., 2005; Dielen *et al*., 2011; Jin *et al*., 2007; Sahana *et al*., 2012), or in the case of both HCPro and 2b protein, through their binding to a calmodulin-related protein that may direct them to degradation via autophagy (Nakahara *et al*., 2012).

Although 24 h is usually insufficient for protein accumulation after agroinfiltration (Voinnet *et al*., 2003), we tested, in a time course, the levels of accumulation of proteins in our system from 24 to 72 hpi. We found that we could detect both GFP reporter and 2b suppressor at 24 hpi. They are small proteins of 25 and 16 kDa, respectively. By contrast, we failed to detect accumulation after 24 h of the much larger (50 kDa) 6×-HCPro, which was also expressed as a polyprotein downstream of the self-cleaving potyviral P1 factor. In any case, the levels of accumulation of GFP and 2b protein at 24 hpi were less than 12% of those found at

72 hpi (Fig. 2). Therefore, the vast majority of proteins were actually expressed at 30 °C, as were their biological activities, if any. Our data from 6×-HCPro and 2b (or 6×-2b-HA) show that the former requires more time to be translated and accumulated than the latter (Fig. 2B), and also suggest that its stability is greater than that of the 2b protein and its turnover is slower. It may also be possible that the 2b protein is targeted for degradation in a more efficient manner than is HCPro by autophagy. These results also suggest that not all 'strong' suppressors may perform in the same manner in our agroinfiltration procedure to express proteins at high temperatures, although, in our conditions (30 °C and 72 hpi), we observed no difference in the suppressor effect on GFP reporter levels using either 6×-HCPro or 2b protein, or P19 (Fig. 1). The fact that the steady-state levels of 2b protein decreased much more rapidly than those of 6×-HCPro (Fig. 2B) suggests that, if the experiment was performed at higher temperatures or for a longer period of time (4–5 days), differences in suppressor activity may arise, and the more stable suppressor would be preferable.

We also tested how our procedure would help express viral PVX amplicons from binary vectors. We found that, although the 24-h window at 25 °C is not strictly necessary for the amplicon to successfully take hold in a plant, it is necessary to ensure that all plants become infected. When we tested PVX and PVX expressing either 6×-HCPro or 6×-2b-HA protein, we found that, regardless of the differences between the three in the symptoms they induced and in their CP titres in plants kept at 25 °C, at 30 °C, all plants were asymptomatic and CP levels were more uniform in the three cases, roughly between 25% and 50% of those found in systemic tissue of PVX-infected plants kept at 25 °C (Table 1 and Fig. 3A, B). This may indicate that defence responses against PVX are stronger at 30 °C than at 25 °C or, alternatively, that viral replication is negatively affected by the higher temperature. Neither of the suppressors expressed by PVX-P1-6×-HCPro or PVX-6×-2b-HA increased CP levels from those found in tissue infected with PVX at 25 or 30 °C (Fig. 3B, C), despite 6×-HCPro being a strong suppressor at 30 °C. This is in agreement with the observations that PVX RNA did not increase in plants infected with a PVX recombinant virus expressing the *Plum pox virus* HCPro compared with plants infected with the PVX vector (González-Jara *et al*., 2005).

In conclusion, we have designed a procedure that allows the use of the agroinfiltration technique for the efficient expression of genes in plants for scientific studies at 30 °C. This technical advance allows: (i) studies *in vivo* at these temperatures of, for example, fluorescently tagged proteins and their interactions with subcellular structures or other proteins, and their dynamics; (ii) the performance of biological assays, such as reported here, on the suppression of the silencing of a reporter by viral factors; or (iii) comparative studies of the synthesis and turnover of proteins. We have also shown the viability of the agroinfiltration of binary vectors for the expression of viral amplicons at 30 °C. With this tool, we were able to monitor the effect of heterologous viral suppressors of silencing, whose activities were previously assessed at high temperatures, on the overall response of the host to the virus.

EXPERIMENTAL PROCEDURES

Binary vector constructs

Reporter and viral proteins were transiently expressed in plants from corresponding gene sequences expressed from caulimovirus 35SP-driven, pROK2-based binary vectors: vectors expressing the free GFP reporter and CMV (Fny) 2b protein have been described in González *et al*. (2010); the binary vector expressing PVY P1-6×-HCPro (construct P1-6×-HCPro) has been described in Tena *et al*. (2013); the binary vector expressing TBSV P19 suppressor has been described in Canto *et al*. (2006). To generate the pROK2 binary vector that expressed 2b protein with six histidines fused at its N-terminus and an HA peptide (Tyr-Pro-Tyr-Asp-Val-Pro-Asp-Tyr-Ala) fused to its C-terminus, used in Fig. S1 (construct 6×-2b-HA), the 2b coding sequence was amplified in sequential polymerase chain reaction (PCR) events with flanking oligos that contained the HA peptide and 6×histidine sequences, resulting in a 2b sequence that had attached, at its 3' end, an *Asc*I site plus that of the HA peptide in frame and a *Sac*I site plus a stop codon at its end, and, at its 5' end, an *Xba*I site followed by an ATG, the sequence coding for 6×histidine and a *BamH*I site in frame with the following sequence coding for 5' end nucleotides of the 2b sequence. The fragment was cloned between the *Xba*I and *Sac*I sites of pROK2.

With regard to the three PVX viral amplicons, binary vector pgR 107 was used to express infectious PVX that contains an additional CP promoter and a polylinker for the insertion and expression of foreign genes (Lu *et al*., 2003). PVX expressing PVY P1-6×-HCPro has been described previously (Tena *et al*., 2013). To create PVX expressing 6×-2b-HA, the tagged 2b protein was amplified by PCR with appropriate oligos and cloned into *Cla*I/*Sal*I-linearized construct pgR 107.

All PCRs were performed with Phusion™ DNA polymerase (Finnzymes, Keilaranta, Finland). All constructs were confirmed by sequencing of the inserted fragments and of the vector flanking regions.

Transient expression of genes in plants and local suppression of silencing in agroinfiltration patch assays

For transient expression assays (patch assays) of single proteins expressed from binary vectors, the latter were transferred to nononcogenic electrocompetent *A. tumefaciens* strain C58C1 derived from a single colony to prevent bacterial variability. Cultures were grown to exponential phase in Luria–Bertani medium with antibiotics at 28 °C. For infiltration, each bacterial culture was diluted to a final optical density of 0.3 at 600 nm. Different cultures harbouring different T-DNAs were then combined, and infiltration of the mixtures was performed as described by Canto *et al*. (2002). In silencing suppression assays, a free *GFP* reporter gene expressed from a binary vector under the control of the 35S promoter was expressed transiently in an *N. benthamiana* leaf, co-infiltrated with

either the empty binary vector pROK2 or with another vector expressing a protein to be tested for the suppression of silencing activity. Leaves were then illuminated at 72 hpi with a Blak Ray® long-wave UV lamp (UVP, Upland, CA, USA) to visualize the fluorescence derived from the transiently expressed free enhanced GFP as described by González *et al*. (2010).

In the case of PVX amplicons, the binary vectors expressing them were electroporated into electrocompetent *A. tumefaciens* strain GV3101 already containing a pJIC SA_Rep that conferred tetracycline resistance, kindly provided by Professor D. C. Baulcombe's group (University of Cambridge, Cambridge, UK). For infiltration, *Agrobacterium* cultures were grown as described in the previous paragraph.

Agroinfiltrations were performed on the laboratory bench at 25 °C. Immediately after infiltrations (no more than 15 min on the bench), plants were transferred to Controlled Environment Plant Growth chambers (SANYO Electronic Co.; Panasonic Corp., Osaka, Japan), where they were maintained in a 16-h/8-h day/night photoperiod and at temperatures of 25 °C or 30 °C, or combinations thereof, depending on the experiment. In addition to the chamber's own temperature controls, temperature accuracy was independently monitored with a PCE HT-71 datalogger sensor (PCE Instruments Ltd., Southampton, UK).

Immunoblot detection of proteins and densitometric analysis

Infiltrated fresh leaf tissue discs of 25 mm in diameter were separated from the leaf with a borer (0.05–0.1 μg of fresh leaf tissue). Total proteins were extracted by grinding the nitrogen-frozen discs with a pestle in 400 μL of extraction buffer [0.1 M tris(hydroxymethyl)aminomethane (Tris)-HCl, pH 8, 10 mM ethylenediaminetetraacetic acid (EDTA), 0.1 M LiCl, 1% β-mercaptoethanol and 1% sodium dodecylsulphate (SDS)], and the samples were boiled and fractionated by SDS-polyacrylamide gel electrophoresis (PAGE) in 10% (for HCPro detection) or 15% (for GFP and 2b protein detection) gels. Gels were wet blotted in Tris-glycine buffer onto Hybond-P poly(vinylidene difluoride) (PVDF) membranes (Amersham, GE Healthcare, Little Chalfont, Buckinghamshire, UK). For immunological detection of GFP, a rabbit anti-GFP, N-terminal antibody was used (Sigma-Aldrich, St Louis, MO, USA; Cat. G1544). For detection of 6×-HCPro, a mouse monoclonal antiserum to six histidines was used (Sigma-Aldrich; Cat. H1029). In addition, a mouse monoclonal antibody to PVY HCPro (Ab 1A11; Canto *et al*., 1996) was used for its detection in the panels shown in Fig. 2, indicated as α-HCPro. For the detection of 2b protein, a mouse polyclonal serum was used (González *et al*., 2010). For the detection of PVX by Western blot, a commercial rabbit antibody was used (No. 070375/500; Loewe Biochemica GmbH, Sauerlach, Germany). Blotted proteins were detected using commercial secondary antibodies and SigmaFast™ 5-bromo-4-chloro-3-indolylphosphate/nitroblue tetrazolium (BICP/NBT) substrate tablets (Sigma-Aldrich). Comparative protein densitometric analysis of blotted proteins was made with Quantity One 4.6.3 1-D analysis software (Bio-Rad Laboratories, Hercules, CA, USA). The numbers shown in the figures represent the quantification of protein amounts in individual Western blot bands, and the values given are percentages relative to the value found in the internal control within the same blot. Densitometric comparisons were only made between bands within the same membrane and not between bands that corresponded to different blots or antibodies, unless internal controls were taken into account.

ACKNOWLEDGEMENTS

This work was funded by a grant from the Rural Development Administration (RDA) of the Republic of Korea, in cooperation with the Spanish Council for Scientific Research (CSIC). The authors wish to thank Professor D. C. Baulcombe (University of Cambridge, UK) for the kind provision from his laboratory to our group of the binary construct pgR107 and helper plasmid pJICSA_Rep.

REFERENCES

Andrews, L.B. and Curtis, W.R. (2005) Comparison of transient protein expression in tobacco leaves and plant suspension culture. *Biotechnol. Prog.* **21**, 946–952.

Ballut, L., Drucker, M., Pugniére, M., Cambon, F., Blanc, S., Roquet, F., Candresse, T., Schmid, H.-P., Nicolas, P., Le Gall, O. and Badaoui, S. (2005) HcPro, a multifunctional protein encoded by a plant RNA virus, targets the 20S proteasome and affects its enzymatic activities. *J. Gen. Virol.* **88**, 2595–2603.

Boyko, V., Ferralli, J. and Heinlein, M. (2000) Cell-to-cell movement of TMV RNA is temperature-dependent and corresponds to the association of movement protein with microtubules. *Plant J.* **22**, 315–325.

Canto, T., Ellis, P., Bowler, G. and López-Abella, D. (1996) Production of monoclonal antibodies to Potato virus Y helper component-protease and their use for strain differentiation. *Plant Dis.* **79**, 234–237.

Canto, T., Cillo, F. and Palukaitis, P. (2002) Generation of siRNAs by T-DNA sequences does not require active transcription nor homology to sequences in the plant. *Mol. Plant–Microbe Interact.* **15**, 1137–1146.

Canto, T., Uhrig, J., Swanson, M., Wright, K. and MacFarlane, S. (2006) Translocation of Tomato bushy stunt virus P19 protein into the nucleus by ALY proteins compromises its suppressor of silencing activity. *J. Virol.* **80**, 9064–9072.

Chellappan, P., Vanitharani, R., Ogbe, F. and Fauquet, C.M. (2005) Effect of temperature on geminivirus-induced RNA silencing in plants. *Plant Physiol.* **138**, 1828–1841.

Chen, Q., Lai, H., Hurtado, J., Stahnke, J., Leuzinger, K. and Dent, M. (2013) Agroinfiltration as an effective and scalable strategy of gene delivery for production of pharmaceutical proteins. *Adv. Tech. Biol. Med.* **1**, 103.

Dielen, A.-S., Sassaki, F.T., Walter, J., Michon, T., Menard, G., Pagny, G., Krause-Sakate, R., Maia, I., Badaoui, S., Le Gall, O., Candresse, T. and German-Retama, S. (2011) The 20S proteasome α_5 subunit of *Arabidopsis thaliana* carries an RNAse activity and interacts *in planta* with the *Lettuce mosaic potyvirus* HcPro protein. *Mol. Plant Pathol.* **12**, 137–150.

Dujovny, G., Valli, A., Calvo, M. and García, J.A. (2009) A temperature-controlled amplicon system derived from *Plum pox potyvirus*. *Plant Biotechnol. J.* **7**, 49–58.

Fullner, K.J. and Nester, E.W. (1996) Temperature affects the T-DNA transfer machinery of *Agrobacterium tumefaciens*. *J. Bacteriol.* **178**, 1498–1504.

Gelvin, S. (2003) *Agrobacterium*-mediated plant transformation: the biology behind 'gene-jockeying' tool. *Microbiol. Mol. Biol. Rev.* **67**, 16–37.

González, I., Martínez, L., Rakitina, D., Lewsey, M.G., Atienzo, F.A., Llave, C., Kalinina, N., Carr, J.P., Palukaitis, P. and Canto, T. (2010) *Cucumber mosaic virus* 2b protein subcellular targets and interactions: their significance to its RNA silencing suppressor activity. *Mol. Plant–Microbe Interact.* **23**, 294–303.

González, I., Rakitina, D., Semashko, M., Taliansky, M., Praveen, S., Plaukaitis, P., Carr, J., Kalinina, N. and Canto, T. (2012) RNA binding is more critical to the suppression of silencing function of *Cucumber mosaic virus* 2b protein than nuclear localization. *RNA*, **18**, 771–782.

González-Jara, P., Atencio, F.A., Martínez-García, B., Barajas, D., Tenllado, F. and Díaz-Ruíz, J.R. (2005) A single nucleotide mutation in the *Plum pox virus* HC-Pro gene abolishes both synergistic and silencing suppression activities. *Phytopathology*, **95**, 894–901.

Hull, R. (2002) *Matthews Plant Virology*. San Diego, CA: Academic Press.

Jin, Y., Ma, D., Dong, J., Jin, J., Li, D., Deng, C. and Wang, T. (2007) HC-Pro protein of *Potato virus Y* can interact with three *Arabidopsis thaliana* 20S proteasome subunits in planta. *J. Virol.* **81**, 12 881–12 888.

Johansen, L.K. and Carrington, J.C. (2001) Silencing on the spot. Induction and suppression of RNA silencing in the *Agrobacterium*-mediated transient expression system. *Plant Physiol.* **126**, 930–938.

Lai, H. and Chen, Q. (2012) Bioprocessing of plant-derived virus-like particles of Norwalk virus capsid protein under current good manufacture practice regulations. *Plant Cell Rep.* **31**, 573–584.

Lu, R., Malcuit, I., Moffett, P., Ruíz, M.T., Peart, J., Wu, A.J., Rathjen, J.P., Bendahmane, A., Day, L. and Baulcombe, D.C. (2003) High throughput virus-induced gene silencing implicates heat shock protein 90 in plant disease resistance. *EMBO J.* **22**, 5690–5699.

Nakahara, K.S., Masuta, C., Yamada, S., Shimura, H., Kashihara, Y., Wada, T.S., Meguro, A., Goto, K., Tadamura, K., Sueda, K., Sekiguchi, T., Shao, J., Itchoda, N., Matsumara, T., Igarashi, M., Ito, K., Carthew, R.W. and Uyeda, I. (2012) Tobacco calmodulin-like protein provides secondary defense by binding to and directing degradation of virus RNA silencing suppressors. *Proc. Natl. Acad. Sci. USA*, **109**, 10 113–10 118.

Ohsato, S., Miyanishi, M. and Shirako, Y. (2003) The optimal temperature for RNA replication in cells infected by *Soil-borne wheat mosaic virus* is 17 °C. *J. Gen. Virol.* **84**, 995–1000.

Qu, F., Ye, X., Hou, G., Sato, S., Clemente, T.E. and Morris, T.J. (2005) RDR6 has a broad-spectrum but temperature-dependent antiviral defense role in *Nicotiana benthamiana*. *J. Virol.* **79**, 15 209–15 217.

Sahana, N., Kaur, H., Raj, B., Tena, F., Kumar, R.J., Palukaitis, P., Canto, T. and Praveen, S. (2012) Inhibition of the host proteasome facilitates papaya ringspot virus accumulation and proteosomal catalytic activity is modulated by viral factor HcPro. *PLoS ONE*, **7**, e52546.

Szyttia, G., Silhavy, D., Molnár, A., Havelda, Z., Lovas, A., Lakatos, L., Bánfaldi, Z. and Burgyán, J. (2003) Low temperature inhibits RNA silencing-mediated defence by the control of siRNA generation. *EMBO J.* **22**, 633–640.

Tena, F., González, I., Doblas, P., Rodríguez, C., Sahana, N., Kaur, H., Tenllado, F., Praveen, S. and Canto, T. (2013) The influence of cis-acting P1 protein and translational elements on the expression of *Potato virus Y* HCPro in heterologous systems and its suppression of silencing activity. *Mol. Plant Pathol.* **14**, 530–541.

Velázquez, K., Renovell, A., Comellas, M., Serra, P., García, M.L., Pina, J.A., Navarro, L., Moreno, P. and Guerri, J. (2010) Effects of temperature on RNA silencing of a negative-stranded RNA plant virus: *Citrus psorosis virus*. *Plant Pathol.* **59**, 982–990.

Voinnet, O., Rivas, S., Mestre, P. and Baulcombe, D. (2003) An enhanced transient expression system in plants based on suppression of gene silencing by the P19 protein of tomato bushy stunt virus. *Plant J.* **33**, 949–956.

Yang, S.-J., Carter, S.A., Cole, A.B., Cheng, N.-H. and Nelson, R.S. (2004) A natural variant of a host RNA-dependent RNA polymerase is associated with increased susceptibility to viruses by *Nicotiana benthamiana*. *Proc. Natl. Acad. Sci. USA*, **101**, 6297–6302.

Ying, X.-B., Dong, L., Zhu, H., Duan, C.-H., Du, Q.-S., Lv, D.-Q., Fang, Y.-Y., García, J.A., Fang, R.-X. and Guo, H.-S. (2010) RNA-dependent polymerase 1 from *Nicotiana tabacum* suppresses RNA silencing and enhances viral infection in *Nicotiana benthamiana*. *Plant Cell*, **22**, 1358–1372.

SUPPORTING INFORMATION

Additional Supporting Information may be found in the online version of this article at the publisher's web-site:

Fig. S1 (A) Assessment of the efficiency of agroinfiltration to transiently express a green fluorescent protein (GFP) reporter in infiltrated *Nicotiana benthamiana* patches at different temperatures. The GFP vector was co-infiltrated together with an empty vector (patches labelled C) or with vectors expressing *Potato virus Y* P1-6×-HCPro (patch labelled 1), *Cucumber mosaic virus* (CMV) 2b protein or a modified 2b protein with both a hexahistidine tag and an HA peptide tag at the N- and C-termini, respectively (6×-2b-HA) (patches labelled 2 and 3, respectively). The top panel shows the visualization of GFP-derived fluorescence under the UV lamp in a leaf kept at 25 °C for 72 h post-infiltration (72 hpi; left leaf), in a leaf kept at 30 °C for 72 hpi (right leaf) and in a leaf kept for the first 24 hpi at 25 °C and the following 48 hpi at 30 °C (central leaf). Note the similarity in fluorescence between the left and central leaves. The bottom panel show the visualization of GFP-derived fluorescence under a UV lamp in a leaf kept at 25 °C for 60 hpi (left leaf), in a leaf kept for 60 hpi at 30 °C (right leaf) and in a leaf kept for the first 12 hpi at 25 °C and the following 48 hpi at 30 °C (central leaf). Note that, in this case, fluorescence in the central leaf is much weaker than that in the left leaf. (B) Time course accumulation of the 6×-2b-HA protein at 24, 48 and 72 hpi by Western blot analysis using an antibody against the 2b protein. During the first 24 h, the plant was kept at 25 °C, and afterwards transferred to 30 °C. Note that the highest accumulation of 6×-2b-HA occurred at 24 hpi. (C) Detection of the presence of the virus in plant tissues agroinfiltrated with binary vectors that expressed three *Potato virus X* (PVX) amplicons by Western blot analysis using an antibody against PVX coat protein (CP). Immediately after infiltration plants were kept at either 25 °C or 30 °C. Note that, in one case (PVX-P1-6×-HCPro), infiltration on leaves transferred to 30 °C failed to initiate infection. Lane M in the blots shows molecular weight markers in kilodalton (kDa), and the small panels below the Western blots show the membranes stained with Ponceau-S after blotting, as controls of loading.

Supporting information

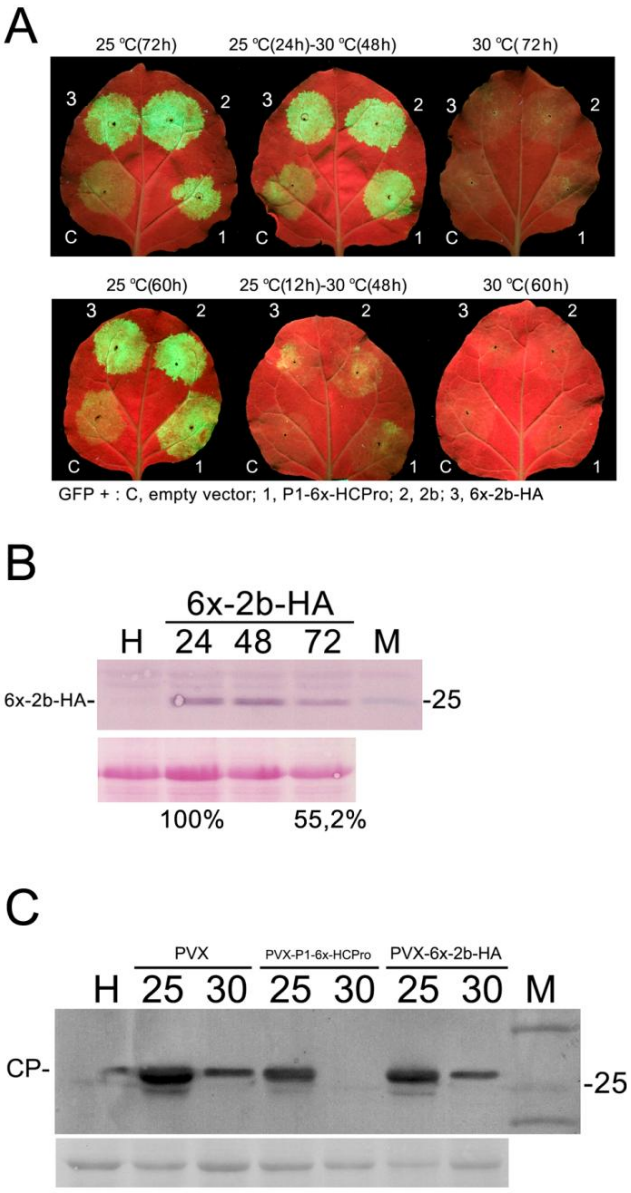

Fig. S1 (A) Assessment of the efficiency of agroinfiltration to transiently express a green fluorescent protein (GFP) reporter in infiltrated *Nicotiana benthamiana* patches at different temperatures. The GFP vector was co-infiltrated together with an empty vector (patches labelled C) or with vectors expressing *Potato virus Y* P1-6×-HCPro (patch labelled 1), *Cucumber mosaic virus* (CMV) 2b protein or a modified 2b protein with both a hexahistidine tag and an HA peptide tag at the N- and C-termini, respectively (6×-2b-HA) (patches labelled 2 and 3, respectively). The top panel shows the visualization of GFP-derived fluorescence under the UV lamp in a leaf kept at 25 °C for 72 h post-infiltration (72 hpi; left leaf), in a leaf kept at 30 °C for 72 hpi (right leaf) and in a leaf kept for the first 24 hpi at 25 °C and the following 48 hpi at 30 °C (central leaf). Note the similarity in fluorescence between the left and central leaves. The bottom panel show the visualization of GFP-derived fluorescence under a UV lamp in a leaf kept at 25 °C for 60 hpi (left leaf), in a leaf kept for 60 hpi at 30 °C (right leaf) and in a leaf kept for the first 12 hpi at 25 °C and the following 48 hpi at 30 °C (central leaf). Note that, in this case, fluorescence in the central leaf is much weaker than that in the left leaf. (B) Time course accumulation of the 6×-2b-HA protein at 24, 48 and 72 hpi by Western blot analysis using an antibody against the 2b protein. During the first 24 h, the plant was kept at 25 °C, and afterwards transferred to 30 °C. Note that the highest accumulation of 6×-2b-HA occurred at 24 hpi. (C) Detection of the presence of the virus in plant tissues agroinfiltrated with binary vectors that expressed three *Potato virus X* (PVX) amplicons by Western blot analysis using an antibody against PVX coat protein (CP). Immediately after infiltration plants were kept at either 25 °C or 30 °C. Note that, in one case (PVX-P1-6×-HCPro), infiltration on leaves transferred to 30 °C failed to initiate infection. Lane M in the blots shows molecular weight markers in kilodalton (kDa), and the small panels below the Western blots show the membranes stained with Ponceau-S after blotting, as controls of loading.

CHAPTER 4

HIGH TEMPERATURE, HIGH AMBIENT CO2 AFFECT THE INTERACTIONS BETWEEN THREE POSITIVE-SENSE RNA VIRUSES AND A COMPATIBLE HOST DIFFERENTIALLY, BUT NOT THEIR SILENCING SUPPRESSION EFFICIENCIES

Article published in PLOs One in 2015; 10(8):e0136062

doi: 10.1371/journal.pone.0136062

PLOS ONE

RESEARCH ARTICLE

High Temperature, High Ambient CO_2 Affect the Interactions between Three Positive-Sense RNA Viruses and a Compatible Host Differentially, but not Their Silencing Suppression Efficiencies

Francisco J. Del Toro[1], Emmanuel Aguilar[1], Francisco J. Hernández-Walias[1], Francisco Tenllado[1], Bong-Nam Chung[2]*, Tomas Canto[1]*

1 Departamento de Biología Medioambiental, Centro de Investigaciones Biológicas, CSIC, Ramiro de Maeztu 9, 28040, Madrid, Spain, **2** National Institute of Horticultural & Herbal Science, Agricultural Research Center for Climate Change, 281, Ayeon-ro, 690–150, Jeju, Jeju Island, Republic of Korea

* chbn7567@korea.kr (BNC); tomas.canto@cib.csic.es (TC)

OPEN ACCESS

Citation: Del Toro FJ, Aguilar E, Hernández-Walias FJ, Tenllado F, Chung B-N, Canto T (2015) High Temperature, High Ambient CO_2 Affect the Interactions between Three Positive-Sense RNA Viruses and a Compatible Host Differentially, but not Their Silencing Suppression Efficiencies. PLoS ONE 10(8): e0136062. doi:10.1371/journal.pone.0136062

Editor: Mikhail M. Pooggin, University of Basel, SWITZERLAND

Received: June 5, 2015

Accepted: July 29, 2015

Published: August 27, 2015

Data Availability Statement: All relevant data are within the paper and its Supporting Information files.

Funding: This work was supported by grant PJ009461 from the Rural Development Administration (RDA) of the Republic of Korea (http://www.rda.go.kr/foreign/eng/), in cooperation with the Spanish Council for Scientific Research (CSIC; www.csic.es), and also by grant BIO2013-47940-R from the Spanish Ministry of Economy and Competitiveness (MINECO; http://www.mineco.gob.es/). The funders had no role in study design, data

Abstract

We compared infection of *Nicotiana benthamiana* plants by the positive-sense RNA viruses *Cucumber mosaic virus* (CMV), *Potato virus Y* (PVY), and by a *Potato virus X* (PVX) vector, the latter either unaltered or expressing the CMV 2b protein or the PVY HCPro suppressors of silencing, at 25°C vs. 30°C, or at standard (~401 parts per million, ppm) vs. elevated (970 ppm) CO_2 levels. We also assessed the activities of their suppressors of silencing under those conditions. We found that at 30°C, accumulation of the CMV isolate and infection symptoms remained comparable to those at 25°C, whereas accumulation of the PVY isolate and those of the three PVX constructs decreased markedly, even when expressing the heterologous suppressors 2b or HCPro, and plants had either very attenuated or no symptoms. Under elevated CO_2 plants grew larger, but contained less total protein/unit of leaf area. In contrast to temperature, infection symptoms remained unaltered for the five viruses at elevated CO_2 levels, but viral titers in leaf disks as a proportion of the total protein content increased in all cases, markedly for CMV, and less so for PVY and the PVX constructs. Despite these differences, we found that neither high temperature nor elevated CO_2 prevented efficient suppression of silencing by their viral suppressors in agropatch assays. Our results suggest that the strength of antiviral silencing at high temperature or CO_2 levels, or those of the viral suppressors that counteract it, may not be the main determinants of the observed infection outcomes.

collection and analysis, decision to publish, or preparation of the manuscript.

Competing Interests: The authors have declared that no competing interests exist.

Introduction

Anthropogenic releases of CO_2 and of other gases very likely increase global temperatures and may lead to changes in local climates (http://www.ipcc.ch/). In this context, modern agriculture becomes exposed to losses from outbreaks of viral diseases that derive from increased global trade and warmer environments [1]. Among plant viruses, single-stranded, positive-sense RNA (ssRNA+) viruses are taxonomically the largest group and some, such as cucumoviruses and potyviruses cause relevant economic losses [2]. The outcomes of any virus/plant compatible infection also depend on the physiological state that environment parameters, such as temperature or CO_2 levels induce in the host, which provoke changes affecting plant growth rate and shape, carbon:nitrogen ratios, and in the molecular pathways that modulate responses to both, external biotic or abiotic factors [3, 4, 5, 6, 7]. Knowledge gained on compatible viral infections when these parameters alter, and on the molecular mechanisms underpinning them is therefore of interest. With regard to elevated environment CO_2 levels our knowledge on compatible plant-virus interactions it is still limited: CO_2 levels of 1000 parts per million (ppm) reduced *Potato virus Y* (PVY) titers in tobacco fresh weight samples [4], and 750 ppm alleviated the damage this virus caused in the same host [8]. The latter levels also decreased both symptom severity and virus titers in the infection of tomato by the geminivirus *Tomato yellow leaf curl virus* and also of *Tobacco mosaic virus* in the same plant [3, 7] respectively, probably because of alterations in the levels of salicylic acid (SA) and jasmonic acid (JA). In this regard, elevated CO_2 decreased JA but increased SA levels in uninfected arabidopsis plants [9]. With regard to temperature, it is known from early works that increases in temperature can lead to weaker infection symptoms (heat masking effect) [2]. Interestingly, more recent reports also indicate that a main defense of plants against viruses, small interfering RNA (siRNA)-mediated gene silencing, increases in strength with temperature. In a number of compatible infections, weaker symptoms correlated with slight-to-marked decreases in the accumulation of the corresponding viruses, and with an increase in the ratios of small RNAs to viral sequences: in ssRNA+ viruses *Turnip crinkle carmovirus* and *Cymbidium ringspot tombusvirus*, when increasing temperatures from 21 to 27°C in *Nicotiana benthamiana* [10, 11], for the negative ssRNA *Citrus psorosis virus* in sweet orange, from a range of 26/18°C (day/night) to 32/26°C [12], or for several DNA geminiviruses from 25 to 30°C in cassava and *N. benthamiana* [13]. The molecular basis for this effect of temperature on antiviral gene silencing is being investigated, but could be related to increased biological activities at higher temperatures of some protein components of its molecular pathways. This was proposed for host RdRp and/or Dicer-like (DCL) activities [13] and was demonstrated for DCL 2, which at 26°C (vs. 20°C) increases synthesis of 22-nucleotide small RNAs to positive-sense RNA virus *Turnip crinkle virus* sequences in arabidopsis plants [14]. However, high temperatures (30 vs. 22°C) reduced the silencing induced on endogenous genes by homologous integrated sense transgenes in arabidopsis plants, possibly as the levels of *Suppressor of gene silencing 3* gene product (SGS3) involved in formation of secondary siRNAs, diminished at 30°C in this host [15]. SiRNA-based silencing strength against mRNAs expressed from transient agroinfiltrated T-DNAs, as well as against integrated antisense transgenes has also been shown to increase gradually with temperature, from 15 to 24°C in *N. benthamiana* [11], likely for the same underlying reasons than for viruses. It has been hypothesized that heat masking (decreased viral titers and symptoms) at high temperature derive from enhanced antiviral gene silencing defenses overcoming the counteracting activities of virus-encoded suppressors of silencing [10, 11, 13].

On the virus side, the effects of either temperature or CO_2 levels on the biological activities of the viral suppressors that neutralize the host antiviral silencing defenses are little known. Recently, two viral suppressors, HCPro from PVY and the 2b protein from the cucumovirus

Cucumber mosaic virus (CMV), both ssRNA+ viruses were shown to suppress in *N. benthamiana* agroinfiltration patch assays the partial silencing of a green fluorescent protein (GFP) reporter at high temperature (30°C) [16].

Processes other than RNA silencing also intervene in defending plants against viruses and could be susceptible to temperature or CO_2 levels: degradation of viral factors through proteasome or autophagy, or elicitation of generic responses by phytohormones, such as SA or JA, or non-sense mediated decay [17, 18, 19, 20, 21, 22]. In addition, plant viruses must carry out processes involving viral and host components to successfully infect the plant, disperse and complete their infectious cycles. Current knowledge is limited on the effects of temperature, CO_2 levels on any of these processes.

In this work we have characterized infection of *N. benthamiana* plants with five ssRNA + viruses, at 25 vs. 30°C, or at standard (st) vs. potential end-of-the-century atmospheric CO_2 levels [401 vs. 970 parts per million (ppm); http://www.ipcc.ch]. We found that alterations in severity of symptoms and virus titers were characteristic for each individual virus, but also that their encoded suppressors of silencing could prevent efficiently the host silencing response under those same conditions. These results suggest that the strength of antiviral silencing by the host or those of the viral suppressors that neutralize it cannot explain the differences in the outcomes of infection observed in these environment conditions, and therefore that other processes relevant to the viral cycle must be more determinant.

Materials and Methods

Plants and viruses

Plants: *N. benthamiana* plants were used, as they become systemically infected by the five viruses/virus vectors used in this study and are also amenable to transient gene expression by agroinfiltration. Transgenic *N. benthamiana* [23] expressing an inverted repeat fragment of its *RNA-dependent RNA polymerase 6 (RDR6)* gene that reduced the levels of the endogenous transcript mRNA to 4% of that found in non-silenced plants was also used, kindly provided by Prof. D. C. Baulcombe (University of Cambridge, UK). Viruses: we used an aphid transmissible PVY isolate (Scottish ordinary variety PVY-O, Scottish Agricultural Science Agency) from which the P1-6x-HCPro sequence contained in the binary constructs P1-6x-HCPro and PVX-P1-6x-HCPro [24, 25], respectively, and described below derive. We used a cloned CMV isolate, strain Fny, obtained by inoculating combined in vitro transcripts of full-length infectious clones of viral RNAs 1, 2, and 3 [24]. We also used three PVX vectors that were expressed from binary constructs (see below).

Binary constructs for agroinfiltration

A GFP reporter and viral proteins were transiently expressed in plants from caulimovirus 35SP-driven, pROK2-based binary vectors: a vector expressing a free GFP reporter described in [26]; the binary vector expressing PVY P1-6x-HCPro (construct P1-6x-HCPro), described in [27]. The binary vector that expressed 2b protein with six histidines fused at its N- terminus, described by in [16].

Binary vector pgR107 kindly provided by Prof. D. C. Baulcombe group (University of Cambridge, UK) was used to express a modified infectious PVX that contains an additional CP promoter and a polylinker for the insertion and expression of foreign genes [28]. PVX expressing PVY P1-6x-HCPro was described in [27] and PVX expressing Fny CMV 2b protein with 6 histidines fused at its N terminus and an HA peptide at its C- terminus was described in [16].

Delivery and expression of genes in plants by agroinfiltration, and local suppression of silencing in agropatch assays

For transient expression of proteins in plants by agroinfiltration, the corresponding binary constructs were transferred to non-oncogenic *Agrobacterium tumefaciens* strain C58C1, grown and infiltrated as described [16]. In the case of infectious PVX constructs, the binaries expressing them were expressed from *A. tumefaciens* strain GV3101 already containing a complementing pJIC SA_Rep plasmid [28].

In silencing suppression assays (agropatch assays), the free *GFP* reporter was co-expressed transiently in a *N. benthamiana* leaf patch, either with an empty binary vector, or with another vector expressing a protein to be tested for suppression of silencing activity. Leaves were then illuminated at 72 hours post infiltration (hpi) with a Blak Ray long wave UV lamp (UVP, Upland, CA, USA) to visualize and photograph the fluorescence derived from the transiently expressed free eGFP, and infiltrated patch disks were collected for protein analysis and quantification by western blot as described [26].

Agroinfiltrations were performed at lab room temperature (around 25°C). Immediately after infiltrations (no more than 15 minutes on the bench) plants were transferred to controlled plant growth chambers. In those cases where transient expression was to take place at higher temperatures (30°C), plants were maintained during the first 24 hpi at 25°C to allow for the agrobacterium-mediated T-DNA transfer into plant tissues to take place, as described [16].

Plant inoculations and growing conditions

N. benthamiana plants were kept for the duration of the experiment in controlled growth chambers, with 16/8 hour day/night photoperiod and ~2500 lux of daylight intensity. Three environmental conditions were used: a) plants grown at 25°C and st CO_2 partial pressure (~401 ppm): b) plants grown at 30°C and st CO_2 levels; c) plants grown at 25°C and high CO_2 partial pressure (~970 ppm). In c, plants were kept for the 7 days previous to viral challenge at 25°C and ~970 ppm, to allow them to adapt to the high CO_2 environment.

Carborundum-dusted plants were inoculated with extracts at 10% (w/v) from PVY- or CMV-infected *N. benthamiana* plants, made in phosphate buffered saline, pH 6.8. For each of these two viruses, a single extract, aliquoted and kept at -80°C was used in all different experiments. For PVX constructs, plants were agroinoculated with agrobacterium containing the appropriate binary constructs as described in the previous section. In all cases, at the time of viral challenge, plants were 4–5 weeks old. Seven days after the challenge, leaf disks were collected for viral and host protein and nucleic acid assessments from the upper expanding leaves. Each type of experiment was performed at least twice

Analysis of viral proteins by SDS-PAGE plus western blot and densitometry

For agroptach assays, agroinfiltrated leaf disks of around 25 mm in diameter (0.05 to 0.1 μg of fresh leaf tissue) excised from the leaf with a borer were used. For systemic plant tissue infected with viruses, 3 combined leaf disks/plant of 9.7 mm diameter were taken from the upper expanding leaves. In both cases, disks were excised from the leaf with a cylindrical borer. Total proteins were extracted by grounding disks in nitrogen with a pestle, and adding 400 μl of extraction buffer/0.05 g of leaf tissue (0.1 M Tris-HCl PH 8, 10 mM EDTA, 0.1 M LiCl, 1% β-mercaptoethanol and 1% SDS). Samples were boiled, and fractionated in 10% (for HCPro detection) or 15% (for GFP, 2b and viral CPs) SDS-PAGE gels. Gels were wet-blotted onto Hybond-P PVDF membranes (Amersham, GE Healthcare, Buckinghamshire, UK). Antisera

used for detection of GFP, or of 2b protein bands were already described [26]. Detection of HCPro tagged with six histidines was performed using a mouse monoclonal antibody to PVY HCPro (Ab 1A11) [29]. For the detection of PVX CP a commercial rabbit antibody was used (No. 070375/500; Loewe Biochemica GmbH, Germany). For the detection of CMV CP we used a home-made rabbit polyclonal antiserum. Blotted proteins were detected using commercial secondary antibodies and SigmaFast BCIP/NBT substrate tablets (SIGMA Aldrich, Saint Louis, Missouri, USA). Densitometric analysis of blotted protein bands were performed using ImageJ (image processing and analysis in java; http://imagej.nih.gov/ij/index.htmls). The numbers that appear below selected western blot panels show quantifications of protein bands as percentages to the value of internal controls within the same blot. Densitometry analysis results are shown in some Figures as bar charts whose values appear relative to the mean intensity of the controls (arbitrary value 1). Densitometry comparisons were only made between bands within the same membrane and not between bands that corresponded to different blots or antibodies, unless internal controls in each blot were equalized.

Determination of total plant protein content in leaf disks

Total proteins in leaf disks were obtained from the same leaf disk extracts that were used for the western blot analysis. Because of the incompatibility between the 1% β-mercaptoethanol in the extraction buffer and the method used in total protein quantification, proteins in those extracts were first precipitated by adding 4 volumes of cold (-20°C) acetone, followed by centrifugation for 10 minutes at 4°C at 15,000 g and pellet resuspension in 50 mM Tris pH 8.0 with 1% SDS buffer. Protein content was then measured by a Lowry-like colorimetric assay performed in microplates with DC Protein Assay (Bio-Rad, Hercules, CA, USA) using as standards known amounts of bovine serum albumin (BSA). Absorbances were read at 750 nm in a Versamax microplate reader (Molecular Devices, Sunnyvale, CA, USA).

Quantitative RT-PCR determination of viral genomic RNA levels

For the estimation of genomic viral RNA levels in infected plants total RNAs were extracted from 3 combined leaf disks of 9.7 mm diameter taken at 7 days post-inoculation (dpi) from the same expanding analysed for viral proteins by SDS-PAGE and western blot. TRIzol reagent (Invitrogen, Carlsbad, CA, USA) was used to extract total RNA, and DNA contaminants were removed by treatment with TURBO DNA-free kit (Ambion, Austin, TX, USA). A one-step real-time quantitative reverse transcription (RT-qPCR) was performed using 15 μl of a reaction mix that contained 7.5 μl of Brilliant III Ultra-Fast RT-qPCR Master Mix (Agilent, Santa Clara, CA, USA), 1.8 μl of RNase-free water, 0.75 μl of reverse transcriptase (Agilent), 0.15 μl of 100 mM dithiothreitol (Agilent), 0.3 μM each primer, and 3 μl of total RNA extract (approximately 10 ng RNA/μl). Primers employed were PVX-Fw (5′-ATTTGGGACCAGCAACAGAG-3′) and PVX-Rv (5′-ATGCTGATTTCGGTGACTCC-3′) for PVX [30]; PVY-Fw (5′-CTGTGGGGACAAAGGGAGTA-3′) and PVY-Rv (5′-GGATGCTTGCGGATTTCATA-3′) for PVY; CMV RNA3-Fw (5′-CTGATCTGGGCGACAAGGA-3′) and CMVRNA3-Rv (5′-CGATAACGACAGCAAAACAC-3′) for RNA 3 of CMV [31]; and 18SrRNA-Fw (5′-GCCCGTTGCTGCGATGATTC-3′) and 18SrRNA-Rv (5′-GCTGCCTTCCTTGGATGTGG-3′) for 18S rRNA for normalization [30]. For the estimation of transient *GFP* transcript levels by RT-qPCR in agroinfiltrated patches for each time-point and sample in the time-course assay shown in S1 Fig, total RNAs were extracted from either two 1.5 cm diameter disks (A in S1 Fig) or from six 9.7 mm diameter leaf disks (B in S1 Fig), each from a different plant. The primers used were GFP-Fw (5′-GATGGCCCTGTCCTTTTACC-3′) and GFP-Rv (5′-CTCTCTTTTCGTTGGGATCTTTC-3′). All RT-qPCR assays were performed in a Rotor-Gene Q thermal

cycler (Qiagen. Venlo, Limburgh, Netherlands) using the following protocol: 50°C for 10 min; 95°C for 3 min; 40 cycles of 95°C for 10 s and 60°C for 20 s; and a final ramp for melting analysis from 60°C to 95°C rising 1°C every 5 s. All reactions were done in triplicate with two replicates of each sample in each run. Relative viral accumulation was determined for individual plants using the $2^{-\Delta\Delta C}{}_T$ method with Rotor-Gene Q Series Software (Qiagen). Results were analyzed with SPSS Statistics (IBM, Armonk, NY, USA).

Results

To assess how temperature or elevated CO_2 levels affect compatible plant-RNA virus interactions and gene silencing suppression, we altered each of the two environmental parameters separately: 25 vs. 30°C at st CO_2 levels, or st vs. elevated CO_2 levels at 25°C. We infected the compatible host *N. benthamiana* with CMV, PVY, or a PVX vector, and the latter either unaltered or expressing the CMV 2b protein or PVY HCPro suppressors. Then we quantified systemic viral titers (CP or genomic RNA levels). We also quantified their suppressor of silencing strength in a virus-free system (agropatch assay) under those environmental conditions.

Differential effects of temperature, CO_2 levels on viral titers and infection symptoms are specific to each virus

At 30°C plants challenged with PVY or with any of the three PVX constructs showed attenuated (PVY) or no symptoms (the three PVX constructs), in contrast to infected plants kept at 25°C. By contrast, plants at 30°C challenged with CMV displayed curling and mosaic symptoms similar in severity and in their time of appearance as those in plants kept at 25°C. (Fig 1, whole plant panels on the left side). To assess systemic viral titers in individual plants, total protein extracts from leaf disks were subjected to western blot detection of viral CPs, and the intensities of individual CP bands were measured. Results showed that in the case of CMV, viral CP levels remained comparable at 25 and at 30°C. However, in the cases of PVY or of the three PVX constructs, CP levels decreased at 30°C, with regard to the levels found at 25°C (Fig 1, central western blot panels). Presence of heterologous suppressors of silencing in the PVX vectors did not attenuate the rate of reduction in the accumulation of the corresponding constructs (Fig 1). To contrast our CP data with viral genomic RNA data we measured by RT-qPCR the levels of viral RNAs (PVY and PVX genomic RNAs, CMV genomic RNA 3) extracted from leaf disks, at 25 vs. 30°C. The results obtained showed an increase of CMV levels, whereas genomic RNAs decreased for PVY and for the three PVX vectors (Fig 2 vs. Fig 1). The trends in viral RNA accumulation broadly correlated with those from CP western blots, although the larger than expected increase in CMV RNA 3 could suggest some slowing of translation or encapsidation at the higher temperature. Thus, although either of both, the CP or the viral RNA quantitation approaches seemed adequate to assess the levels of these five viruses in this host, the serological approach appears better suited for comparisons between our five different viruses.

We also challenged *N. benthamiana* plants with each of the five viruses, at st vs. elevated CO_2 levels, in both cases at 25°C. Plants at elevated CO_2 levels grew larger than those kept at st levels, but infection symptoms remained unchanged for all five viruses (Fig 3, whole plant panels to the left). Viral titers assessed by western blot analysis of viral CPs in equivalent leaf disks showed that CMV levels increased, but PVY and PVX levels fared less well than CMV at higher CO_2 levels. However, we also noticed that the major ribulose-1,5-bisphosphate carboxylase/oxygenase (rubisco) band in the loading controls also appeared reduced in disk extracts of plants kept at high vs. st CO_2 levels (Fig 3, ponceau S-stained loading control panels below

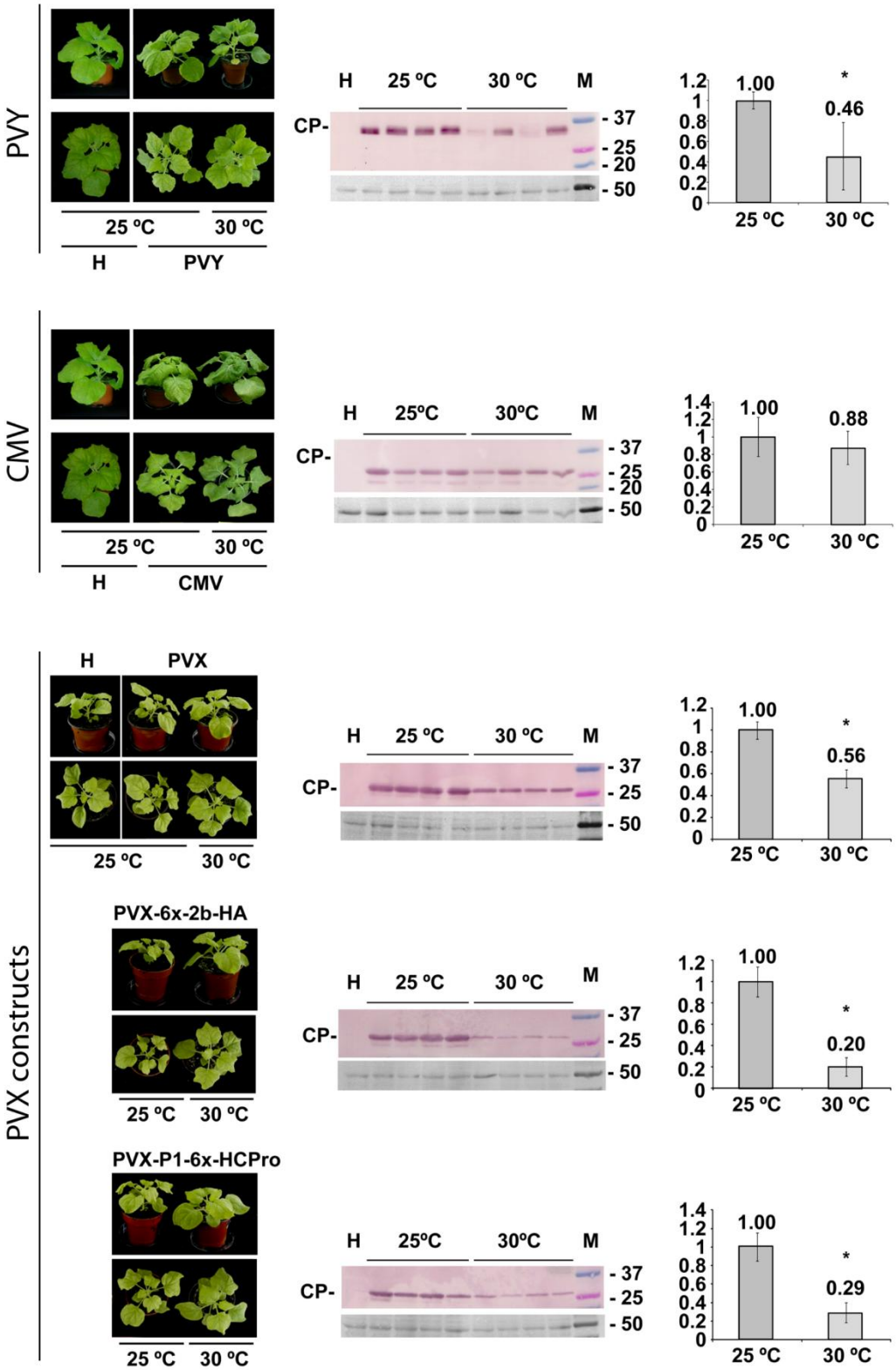

Fig 1. Systemic infection of *Nicotiana benthamiana* plants, at either 25°C or 30°C, by *Potato virus Y* (PVY), *Cucumber mosaic virus* (CMV), or a *Potato virus X* (PVX) vector, the latter either unaltered or expressing the CMV 2b protein or the PVY P1-HCPro bicistron (upper, middle and the

three lower sets of data, respectively). Whole-plant panels in the left: at seven days post inoculation (dpi), all plants displayed infection symptoms at 25°C (mosaic, curling and stunting in the case of PVY; stronger mosaic, severe curling and stunting in the case of CMV; mosaic, curling but no stunting in all three PVX constructs, more severe in those expressing 2b or HCPro). By contrast, at 30°C only plants infected with CMV displayed symptoms similar to those observed at 25°C, whereas plants infected with PVY had very mild mosaic symptoms and plants infected with any of the three PVX vectors showed no symptoms. Plants labeled H are healthy plants. The central coat protein (CP) western blot panels assess viral titers in emerging systemic tissue: levels remained comparable at both temperatures in the case of CMV in equivalent leaf disks, but decreased markedly at 30°C in the cases of PVY and the three PVX constructs. Each western blot lane represents an extract from a single plant. Lanes labeled H show extracts from healthy plants as negative control. Lanes labeled M show molecular weight markers in kilodalton (kDa), indicated to the right of the blots. The panels below each western blot show the blotted, ponceau S-stained membranes prior to antibody incubation as controls for loading. Charts to the right of the western blot panels display mean CP values obtained in the densitometry analysis of the corresponding CP bands with standard deviation bars, relative to average CP accumulation at 25°C, which was given an arbitrary value of 1. Asterisks in charts indicate significant differences (Mann Whitney U-test, P<0.05).

doi:10.1371/journal.pone.0136062.g001

each of the central western blot panels). We had not observed this difference in the loading control panels of extracts obtained from plants kept at different temperatures, shown in Fig 1.

Elevated CO_2 levels, but not high temperature, reduce total protein content in both, healthy or virus-infected *N. benthamiana* leaves

To quantify how total plant protein content changed at elevated vs. st CO_2 levels, or at 25 vs 30°C in *N. benthamiana*, and also whether viral infection might have any effect in it, total plant protein extracts used for western blots were analyzed by the Lowry method to quantify total protein amounts. The results showed that elevated CO_2 levels alone significantly decreased total protein contents in *N. benthamiana* leaf disks in healthy plants (Upper chart in Fig 4), as well as in plants infected with any of the five viruses tested (lower charts in Fig 4), and virus infection did not alter this outcome at 7 dpi. When normalizing viral accumulation to total protein content instead of to leaf disks, viral accumulation as a proportion of plant protein in leaf disks were at least maintained or increased in the high CO_2 environment, as shown in Table 1, which summarizes our results on viral accumulation.

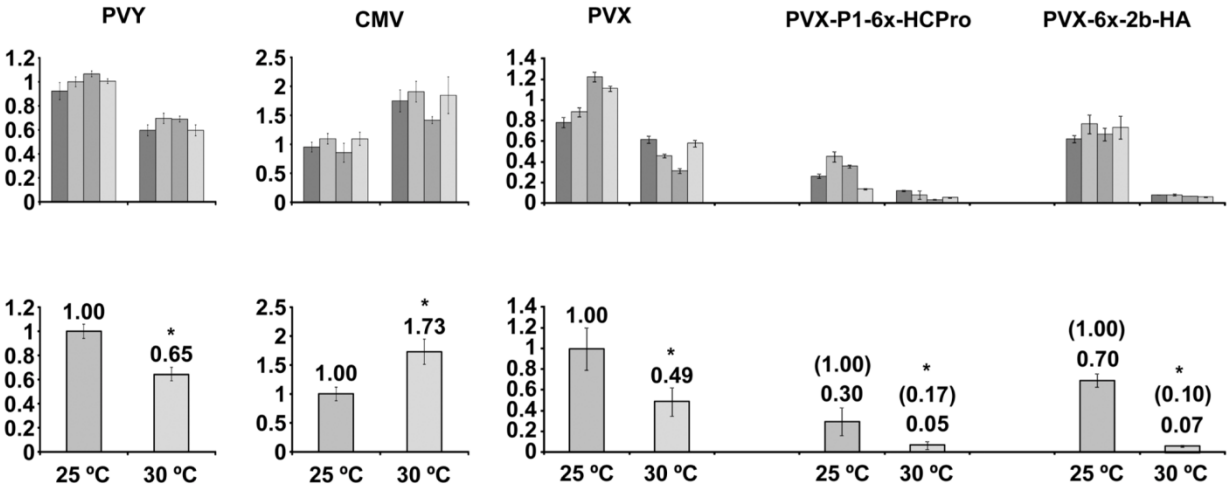

Fig 2. Assessment by RT-qPCR of genomic viral RNA levels in systemic tissue of *Nicotiana benthamiana* plants infected at either 25°C or at 30°C and standard (st; 401) parts per million (ppm) CO_2 levels with *Potato virus Y* (PVY), *Cucumber mosaic virus* (CMV) or a *Potato virus X* (PVX) vector, the latter either unaltered or expressing the *Cucumber mosaic virus* (CMV) 2b protein or the PVY P1-HCPro bicistron. The upper charts show the measurements for separate individual plants, while the lower charts show the mean values with standard deviation bars, relative to viral RNA levels of PVY, CMV or the PVX constructs at 25°C, which were given an arbitrary value of 1. In the cases of the PVX vectors expressing heterologous viral suppressors, their accumulation values at 30°C relative to their accumulation at 25°C appear between brackets, while their values relative to those of PVX at 25°C, appear below. The amplified viral RNA fragments correspond to genomic RNAs, in the case of CMV to genomic RNA 3, and do not contain subgenomic sequences. Asterisks in charts indicate significant differences (Mann Whitney U-test, P<0.05).

doi:10.1371/journal.pone.0136062.g002

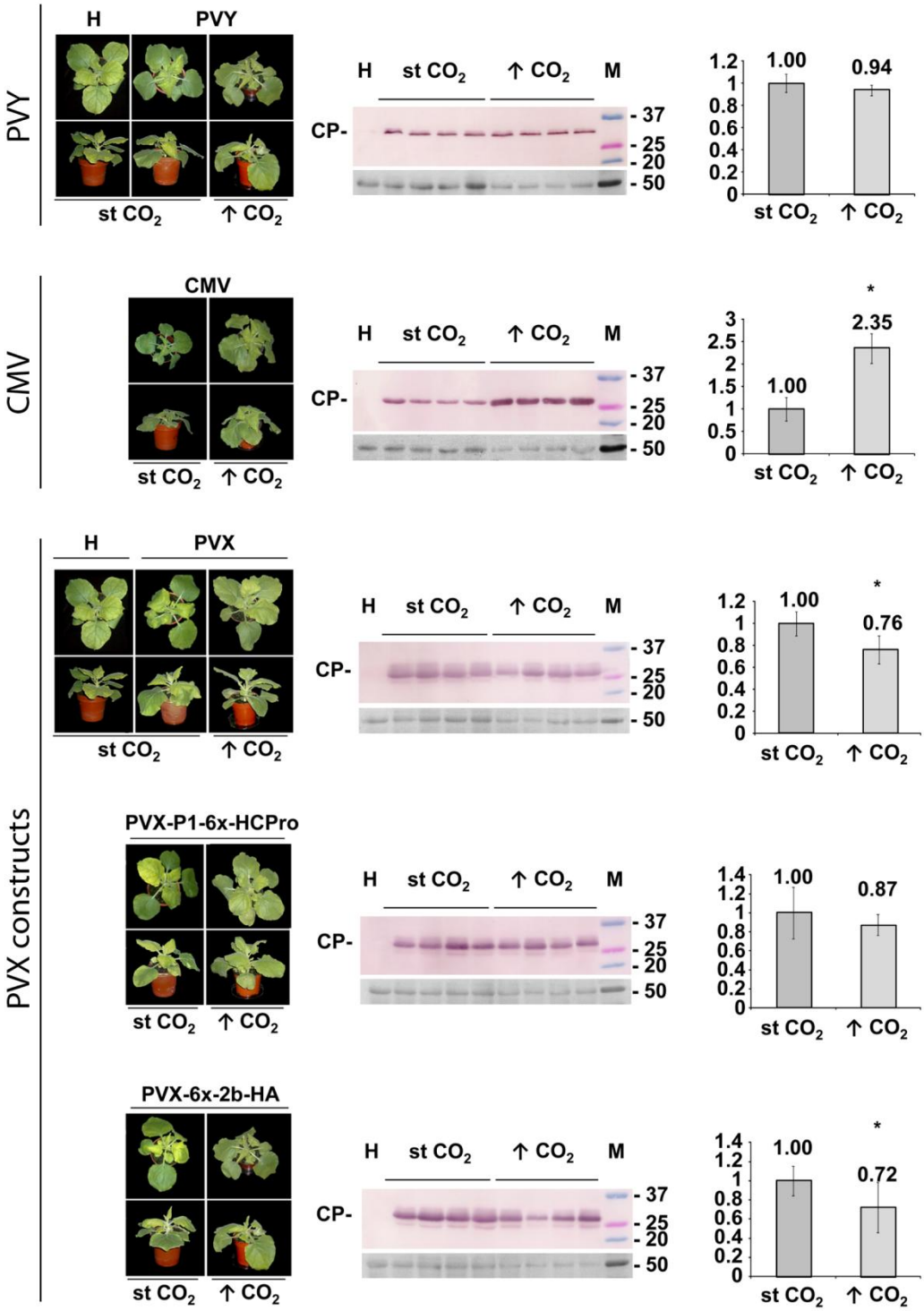

Fig 3. Systemic infection of *Nicotiana benthamiana* plants either at standard (st) or at elevated ↑CO_2 levels [401 and 970 parts per million (ppm), respectively], by *Potato virus Y* (PVY), *Cucumber mosaic virus* (CMV), or a *Potato virus X* (PVX) vector, the latter either unaltered or expressing the CMV 2b protein or the PVY P1-HCPro bicistron (upper, middle and the three lower sets of data, respectively). Whole-plants in the left panels at seven days post inoculation (dpi) showed similar infection symptoms under both CO_2 conditions (mosaic and some curling and stunting in the case of PVY; stronger mosaic, with severe curling and stunting in the case of CMV; mosaic and leaf curling but little stunting in all three PVX vectors, with more severity in those expressing heterologous suppressors of silencing 2b or HCPro). Plant panels labeled H show healthy control plants. The central coat protein (CP) western blot panels assess viral titers in emerging systemic tissue: ↑CO_2 levels increased markedly viral titers for CMV in equivalent leaf disks, but not for PVY or the

three PVX constructs. Each western blot lane represents an extract from a single plant. Lanes labeled H show an extract from a healthy plant as negative control. Lanes labeled M show molecular weight markers, indicated to the right of the blots. The panels below each western blot show the blotted, ponceau S-stained membranes prior to antibody incubation as controls for loading. Charts to the right of the western blot panels display the mean values obtained in the densitometry analysis of CP bands, with standard deviation bars relative to average CP accumulation at st CO_2, which was given an arbitrary value of 1. Asterisks in charts indicate significant differences (Mann Whitney U-test, $P<0.05$).

doi:10.1371/journal.pone.0136062.g003

Elevated temperature or CO_2 levels do not prevent the neutralization of silencing of a reporter by viral suppressors in agropatch assays

To assess whether the viral suppressors of silencing encoded by the viruses used in this study would be capable of counteracting efficiently the silencing defenses of our compatible host

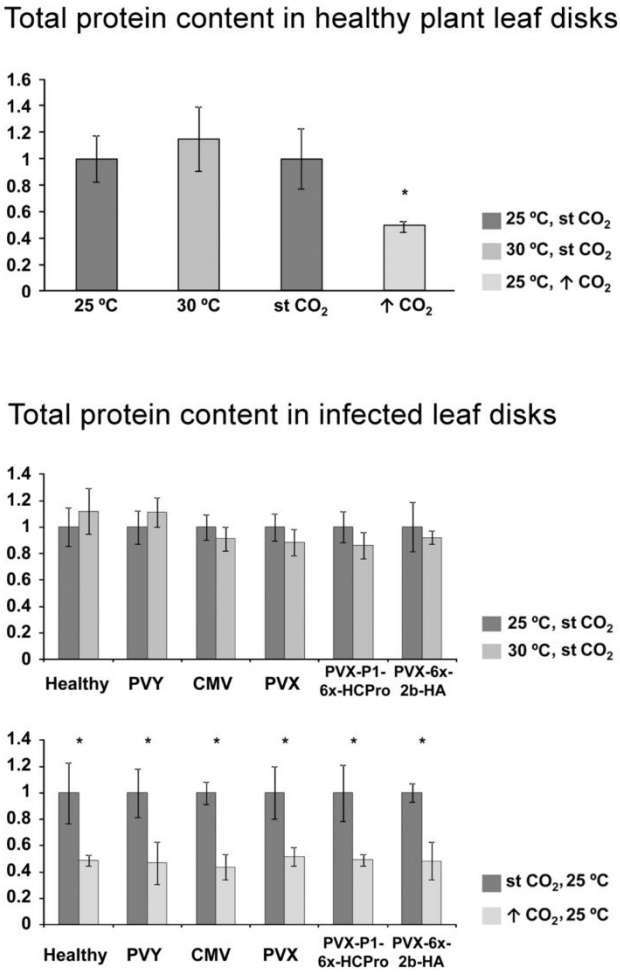

Fig 4. Quantification of total protein content in systemic leaf disks of *Nicotiana benthamiana* plants kept at either 25°C or at 30°C, or in plants kept at standard (st) or elevated ↑CO_2 levels [401 and 970 parts per million (ppm), respectively]. Plants were either healthy non-inoculated, or inoculated with *Potato virus Y* (PVY), *Cucumber mosaic virus* (CMV), or a *Potato virus X* (PVX) vector, the latter either unaltered or expressing the CMV 2b protein or the PVY P1-HCPro bicistron. Results show that total protein content decreased significantly at ↑CO_2 levels (Mann Whitney U-test, $P<0.05$, marked with asterisk). The upper chart shows the values for non-infected healthy plants, under the three ambient scenarios studied. The lower charts show the comparative total protein content of disks from healthy and from virus-infected plants. Total protein from leaf disks was extracted in all cases at seven days after challenge with viruses. An arbitrary value of 1 was given to total protein content in control conditions [25°C and st CO_2 levels of 401 parts per million].

doi:10.1371/journal.pone.0136062.g004

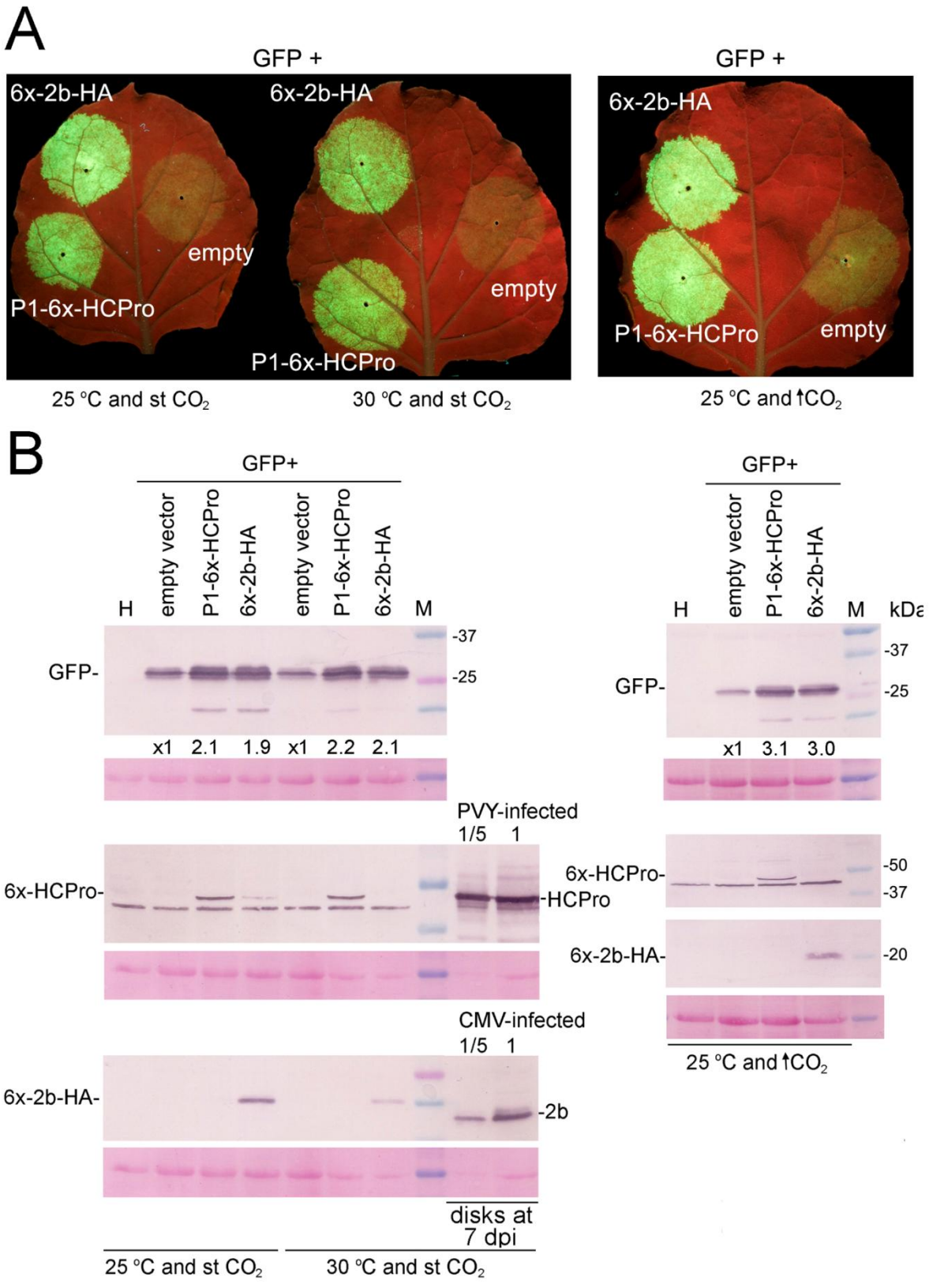
A
GFP +
6x-2b-HA
6x-2b-HA
empty
empty
P1-6x-HCPro
P1-6x-HCPro
25 °C and st CO2
30 °C and st CO2
GFP +
6x-2b-HA
P1-6x-HCPro
empty
25 °C and ↑CO2
B
GFP+
empty vector
P1-6x-HCPro
6x-2b-HA
empty vector
P1-6x-HCPro
6x-2b-HA
H
M
GFP-
-37
-25
x1 2.1 1.9 x1 2.2 2.1
PVY-infected
1/5 1
6x-HCPro-
-HCPro
CMV-infected
1/5 1
6x-2b-HA-
-2b
disks at 7 dpi
25 °C and st CO2
30 °C and st CO2
GFP+
empty vector
P1-6x-HCPro
6x-2b-HA
H
M
kDa
GFP-
-37
-25
x1 3.1 3.0
6x-HCPro-
-50
-37
6x-2b-HA-
-20
25 °C and ↑CO2

Fig 5. Assessment of the efficiency of the *Cucumber mosaic virus* (CMV) 2b protein or the *Potato virus Y* (PVY) P1-HCPro to alleviate the partial silencing of a green fluorescent protein (GFP) reporter under the three scenarios studied, at 72 hours post infiltration (hpi) in a virus-free system (agropatch assay). The binary vector expressing the GFP was co-infiltrated together with either an empty binary plasmid or together with plasmids expressing P1-6x-HCPro or 6x-2b-HA suppressors of silencing. **A,** visualization of GFP-derived fluorescence under the UV lamp from leaves kept at 25°C and standard (st; -401 part per million, ppm) CO_2 levels during the 72 hpi (left side leaf), in a leaf kept the first 24 hpi at 25°C and the following 48 hpi at 30°C at st CO_2 levels (central leaf), and from leaves kept at 25°C and elevated (↑; 970 ppm) CO_2 levels (right side leaf). **B,** western blot analysis of the accumulation in infiltrated patches of the GFP reporter (upper panels) and of the 6x-HCPro and 6x-2b-HA protein suppressors (lower panels) using antibodies against GFP, HCPro (1A11) and the 2b protein, respectively. Below selected lanes appear the values of densitometry analysis of GFP bands (steady-state levels of GFP in control patches infiltrated with the GFP + empty binary vectors are given the arbitrary value of 1). In the high temperature scenario, the accumulation of native HCPro and of 2b protein found in equivalent-size disks from virus-infected plants at 7 days post infiltration (dpi) are also shown, either undiluted or diluted five-fold, to compare their levels with those reached by 6x-HCPro and by 6x-2b-HA proteins at 3 dpi in the agropatch assays. Lanes labeled H correspond to plant extracts from non-infiltrated plants. Lanes labeled M show molecular weight markers in kilodalton (kDa). The panels below each western blot show the blotted, ponceau S-stained membranes prior to antibody incubation as controls for loading. Note that in the ↑CO_2 scenario only one ponceau S-stained blot appears because the same blotted membrane was cut in two separate strips for detection of both, HCPro and 2b protein, as they run at different heights.

doi:10.1371/journal.pone.0136062.g005

N. benthamiana, under scenarios of high temperature or CO_2 levels, we expressed transiently by agroinfiltration a GFP reporter from a binary vector, together with either an empty binary vector as control, or with binaries expressing the corresponding viral suppressors, in leaf patches. The degrees of attenuation by the suppressors of the partial silencing of the reporter could then be measured and quantified. In the case of elevated temperature, as agrobacterium-mediated delivery of T-DNAs into plant cells is prevented at temperatures above 28°C we provided a window of 24 h at 25°C to allow for efficient T-DNA transfer to take place, before rising the temperature to 30°C [16].

Both, transiently expressed constructs derived from CMV 2b protein (6x-2b-HA) and PVY HCPro (P1-6x-HCPro) increased steady-state levels of the GFP reporter three days after infiltration, at 25°C and st CO_2 levels. The rate of increase in the accumulation of GFP induced by the suppressors was similar at 30°C than at 25°C, at st CO_2 levels (Fig 5, left leaves and western blot panels, and reference [16]) and even higher at 25°C and high CO_2 levels (Fig 5, right leaf and western blot panels). Therefore, under either altered parameter, the viral suppressors of silencing were capable to overcome the host silencing on the reporter. In this agropatch assays the levels reached by HCPro at 72 hpi were comparable, but not those of the 2b protein, which were lower at 30°C, suggesting a much faster turnover for the latter (Fig 5). Even so, at high temperature transient levels of 6x-2b-HA protein or of 6x-HCPro at 3 dpi in the infiltrated patches were lower than those of 2b and HCPro found in issue systemically infected by CMV or PVY virus under the same environment conditions at 7 dpi (Fig 5, lanes in left western blot panels detecting HCPro and 2b protein from virus-infected leaf disks, vs. levels of the corresponding proteins in agropatch assay disks). In a similar way as the 2b protein and HCPro, the P25 from PVX, considered a weak suppressor of silencing also increased the levels of reporter in comparable rates at 25 and at 30°C (data not shown; Aguilar *et al.*, manuscript submitted).

Time-course analysis of *GFP* mRNA levels by RT-qPCR showed that in agropatch assays at 25°C the levels of *GFP* transcripts increased markedly in the presence of the 2b or HCPro suppressors (S1 Fig), whereas in assays at 30°C (the first 24 h at 25°C) transcripts also increased several-fold, but less so than at 25°C (more than 3 times in the case of HCPro and around 2 times in the case of the 2b protein; S1 Fig), perhaps as a consequence of the interruption of T-DNA delivery into plants cells after the initial 24 hpi at 25°C.

We also used RNA-dependent RNA polymerase 6-silenced plants (RDR6i) to test whether generation of RDR6-dependent secondary siRNAs influenced the levels of reporter in our sense T-DNA agropatch test. However, the levels of reporter and of viral suppressors were roughly comparable at 70 hpi to those found in non-silenced plants (Fig 6).

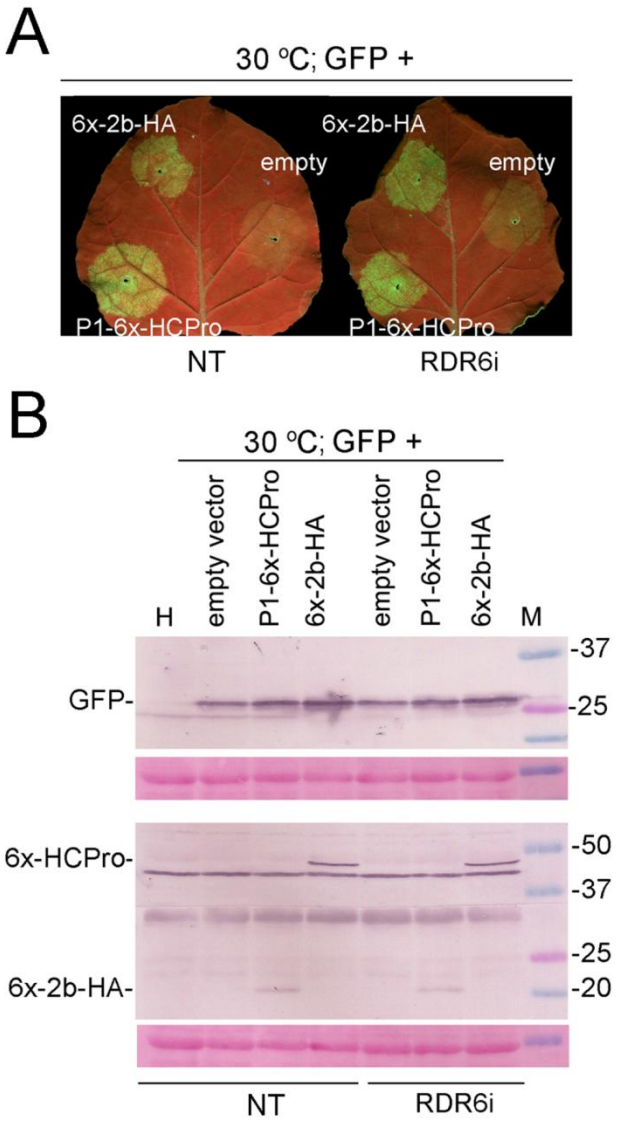

Fig 6. Assessment of the efficiency of the *Cucumber mosaic virus* (CMV) 2b protein or the *Potato virus Y* (PVY) P1-HCPro to release the partial silencing of a green fluorescent protein (GFP) reporter in a virus-free system (agropatch assay) in RNA-dependent RNA polymerase 6-silenced transgenic plants (line RDR6i) vs. non-transgenic (NT) plants at 30°C. Infiltrated plants were kept the first 24 hours post infiltration (hpi) at 25°C and the following 70 hpi at 30°C, at standard (st) CO_2 levels. The GFP reporter binary vector was co-infiltrated together with either an empty binary plasmid or together with plasmids expressing P1-6x-HCPro or 6x-2b-HA suppressors of silencing. **A,** visualization of GFP-derived fluorescence under the UV lamp from infiltrated patches in NT or RDR6i leaves. **B,** western blot analysis of the accumulation in infiltrated patches of the GFP reporter (upper panels) and of the 6x-HCPro and 6x-2b-HA protein suppressors (lower panels) using antibodies against GFP, HCPro (antibody 1A11) and the 2b protein, respectively. Lanes labeled H correspond to plant extracts from non-infiltrated plants. Lanes labeled M show molecular weight markers in kilodalton (kDa). The panels below each western blot show the blotted, ponceau S-stained membranes prior to antibody incubation as controls for loading. Only one ponceau S-stained blot appears because the same blotted membrane was cut in two separate strips for detection of both, HCPro and 2b protein, as they run at different heights.

doi:10.1371/journal.pone.0136062.g006

Discussion

We have compared infection by five different ssRNA+ viruses of *N. benthamiana* plants at 25 vs. 30°C, or at st vs. elevated CO_2 levels, and explored the relation of the infection outcome to antiviral silencing and its suppression. Systemic infections with our five RNA viruses were measured at 7 dpi in newly expanding tissue to study the initial wave of systemic infection and avoid any recovery phenotypes that could difficult our comparisons. In the three scenarios studied all plants challenged with viruses became systemically infected. However, there were stark differences with regard to severity of symptoms and virus titers. We found that at high temperature, infection by PVY resulted in very mild symptoms and reduced titers. By contrast, neither symptoms nor titers were affected in the case of Fny CMV (Figs 1 and 2). Infection by the PVX vectors followed the pattern of PVY, and the expression from the vector of the viral suppressors from CMV or PVY did not alter the disappearance of symptoms or the degree of reduction in viral titers at elevated temperature (Figs 1 and 2) suggesting that constrained PVX accumulation at high temperature was not solely caused by gene silencing or its suppression. In contrast to temperature, the effects of elevated CO_2 on infection by these five viruses were more subtle. Plants had been kept for the previous seven days before viral challenge in elevated CO_2 environments to adapt physiologically. We found that infection symptoms did not change with regard to plants at st CO_2 levels, but viral titers did, in particular when measuring CP levels relative to total plant protein content in leaf disks. This was because the latter decreased always markedly under elevated CO_2 (Fig 4 and Table 1).

As mentioned in the Introduction, high temperatures often lead to much weaker infection symptoms. This fact has been taken to advantage to transform plants with viral amplicons avoiding negative effects on plant regeneration and growth [32]. Coinciding with heat masking and lower viral titers, antiviral silencing was reported to increase in strength with temperature in some infections, with increases in the ratios of siRNAs to viral sequences. Thus, a causal link between heat masking and silencing strength has been proposed [10, 11, 13]. For this to occur,

Table 1. Summary of the effects of high temperature (30 vs. 25°C) or elevated CO_2 levels [↑; 970 vs 401 parts per million (ppm)] on viral titers in *Nicotiana benthamiana* plants infected with *Potato virus Y* (PVY), *Cucumber mosaic virus* (CMV), or a *Potato virus X* (PVX) vector, either unaltered or expressing the CMV 2b protein or the PVY P1-HCPro bicistron. Viral titers in leaf disks or relative to total protein in leaf disks are indicated as a proportion of the values reached at 25°C or at standard (st; 401 ppm) CO_2 levels (arbitrary values of 1), as well as are the symptoms caused to the plants.

Effect of high temperature (30°C vs. 25°C)			
Virus	**viral titer (25°C value = 1)**		**Symptoms**
	leaf disk	**total protein**	
PVY	0,46	0,41	attenuated
CMV	0,88	0,96	similar
PVX	0,56	0,63	symptomless
PVX-P1-6x-HCPro	0,20	0,23	symptomless
PVX-6x-2b-HA	0,29	0,31	symptomless
Effect of ↑ CO_2 (970 ppm vs. 401 ppm)			
Virus	**viral titer (401 ppm value = 1)**		**Symptoms**
	leaf disk	**total protein**	
PVY	0,94	1,51	similar
CMV	2,35	4,57	similar
PVX	0,76	1,65	similar
PVX-P1-6x-HCPro	0,87	1,64	similar
PVX-6x-2b-HA	0,72	1,48	similar

doi:10.1371/journal.pone.0136062.t001

the effectiveness of viral suppressors in an enhanced silencing situation would also need to be somehow compromised. This is difficult to assess within an infection, as other processes operating during the viral infectious cycle could also be temperature- or CO_2-sensitive. A way to assess silencing suppression separately from other viral processes is the use of virus-free agropatch assays, which can compare silencing suppression strength by measuring the transient steady-state levels reached by a reporter in the absence or the presence of a viral suppressor, and also with regard to the levels of suppressor [33, 34, 35, 36, 37]. Besides RNA silencing other host responses during viral infection may also be operative in agropatches: generic responses, such as non-sense mediated decay [20] or phytohormone-mediated, or case-specific ones, such as the targeted binding to viral suppressors potentially affecting their accumulation [17, 18; 19, 21, 22, 38]. A drawback of the technique is its narrow temperature scope, as agrobacterium-mediated T-DNA delivery into plants is prevented above 29°C. However this limitation can be overcome by providing a window of 24 h at permissible temperature to allow efficient T-DNA transfer before raising the temperature [16]. The amount of protein expressed from agro-delivered T-DNAs within the first 24 h, relative to the total found at the end of the assay varies for each protein [39]. In the case of our 6x-HCPro, it is undetectable serologically during the first 24 hpi [16], and thus, any of its effects on the reporter must derive largely from protein accumulating and functioning at high temperature.

To assess the biological activities of our viral suppressors we used therefore the agropatch technique. We used binary constructs that expressed a GFP reporter or the viral suppressors from the PVY and CMV isolates used in this study, modified with tags (hexahistidines fused to the N-termini of both 2b protein and HCPro, and a C-terminal hemagglutinin HA peptide fused to the 2b construct). These are also the exact same constructs expressed from the PVX vectors. This integrated study allowed us to compare the outcomes of infection by our virus isolates with the biological activities of their own suppressors under altered environment scenarios. We found that neither high temperature nor high CO_2 levels affected negatively the ability of the suppressors to relieve the partial silencing of the GFP reporter, compared to normal conditions (25°C and st CO_2 levels) at both, protein and transcript levels (Fig 5 and S1 Fig, respectively). *GFP* transcript accumulation in the 30°C agropatch assays had lower average levels measured at 24, 48, and 72 hpi than in the equivalent assay at 25°C. This is likely a consequence of the interruption of T-DNA delivery into plant cells after the initial 24 hpi at 25°C. We do not know why the GFP (and HCPro) product accumulated to comparable levels in both temperature assays at 72 hpi (Fig 5) despite these differences in transcript levels (S1 Fig). Perhaps lesser saturation of the translation machinery and/or higher translation rates at the higher temperature could be taking place. In any case, the presence of HCPro or the 2b protein increased transcript levels by around 3 and 2 times, respectively (S1 Fig), and these rates of increase are roughly in line with those of the GFP product shown in Fig 5.

We would expect that the same suppressor activities we found in the agropatches would operate in the context of a viral infection, as like with viruses, silencing in agropatch assays derives from plants recognizing agroinfiltration-delivered T-DNAs as foreign [33]. It could be argued that silencing at high temperature against transient T-DNA transcripts in agropatch assays could be weaker than that elicited against viruses because of insufficient secondary siRNA generation in the former. However, in RDR6i patches the levels of reporter and of viral suppressors were roughly comparable at 70 hpi to those found in non-trangenic plants (Fig 6), indicating that generation of RDR6-dependent secondary siRNAs does not determine the levels of reporter in our sense T-DNA agropatch test in the first instance. On the other hand, as transient levels of suppressor in agropatch assays were found lower than those found in virus-infected tissue (Fig 5, middle HCPro western blot panel to the left), that rules out that insufficient levels of suppressor caused the lower viral accumulation at high temperatures.

Our work therefore suggests that the lower viral titers in leaf disks that we observed for PVY and PVX in response to higher temperature or CO_2 levels were not caused by the activities of their viral suppressors being overrun by the strength of antiviral silencing under those altered environmental conditions, and that other processes that defend plants against viruses, or other viral processes must also be involved. Viral cell-to-cell or long-distance movement appear an unlikely target, since in all five cases viruses were able to establish systemic infection at 7 dpi. Replication of positive-strand RNA viruses on the other hand is closely associated with specific virus-induced intracellular membranous vesicles [40, 41] that require translation and the translocation of viral factors via the secretory and/or cytoskeleton pathways. One possibility is that disturbations of intracellular trafficking could negatively affect our PVY and PVX isolates, but not our CMV isolate. Heat can activate endoplasmic reticulum (ER)-associated degradation pathways [41, 42] and both potyviruses and PVX, but not CMV require for their replication the formation of ER-related vesicles [43, 44, 45].

Supporting Information

S1 Fig. Quantification by RT-qPCR of *GFP* transcript levels in three-day time-course agropatch assays at either 25°C or at 30°C [the latter with the first 24 hours post infiltration (hpi) at 25°C]. Two experiments were performed. In **A**, a binary vector expressing GFP was co-infiltrated together with either empty vector or with vectors expressing the viral suppressors P1-6x-HCPro or 6x-2b-HA. Two 15 mm diameter leaf disks were collected at each of three times after infiltration (24, 48 and 72 hpi). In **B**, a GFP vector was co-infiltrated with a vector expressing β-glucuronidase (GUS; Aguilar et al. 2015. J Virol 89:2090–2103) or with vectors expressing the viral suppressors. Six 9.7 mm diameter disks were collected at each of three time points after infiltration (24, 48 and 72 hpi) from three different leaves for assessment. The rates of increase in the levels of *GFP* transcript (the combined average of the 24, 48 and 72 hpi measures) with regard to the baseline controls (either GFP + empty vector in A or GFP + GUS vector in B, both given a value of x1) are indicated below each sample.
(TIF)

Author Contributions

Conceived and designed the experiments: TC FJDT BNC FT. Performed the experiments: TC FJDT EA FJHW FT. Analyzed the data: TC FJDT FT BNC. Wrote the paper: TC FJDT.

References

1. Canto T, Aranda MA, Fereres A (2009) Climate change effects on physiology and population processes of hosts and vectors that influence the spread of hemipteran-borne plant viruses. Global Change Biol 15: 1884–1894.
2. Hull R (2002) Matthews Plant Virology. Academic Press, San Diego CA USA.
3. Huang L, Ren Q, Sun Y, Ye L, Cao H, Ge F (2012) Lower incidence and severity of tomato virus in elevated CO_2 is accompanied by modulated plant induced defence in tomato. Plant Biol 14: 905–913. doi: 10.1111/j.1438-8677.2012.00582.x PMID: 22512888
4. Matros A, Amme S, Kettig B, Buck-Sorlin GH, Sonnewald U, Mock HP (2006) Growth at elevated CO_2 concentrations leads to modified profiles of secondary metabolites in tobacco cv. SamsunNN and to increased resistance against infection with Potato virus Y. Plant Cell Environ. 29: 126–137. PMID: 17086759
5. Prasch CM, Sonnewald U (2013) Simultaneous application of heat, drought, and virus to arabidopsis plants reveals significant shifts in signaling networks. Plant Physiol 162: 1849–1866. doi: 10.1104/pp.113.221044 PMID: 23753177
6. Pritchard S, Ragers H, Priar S, Petersan C (1999) Elevated CO_2 and plant structure: a review. Global Change Biol 5: 807–837.

7. Zhang S, Li X, Sun Z, Shao S, Hu L, Ye M, Zhou Y, Xia X, Yu J, Shi K (2015) Antagonism between phytohormone signaling underlies the variation in disease susceptibility of tomato plants under elevated CO_2. J Exp Botany doi: 10.1093/jxb/eru538

8. Ye LF, Fu X, Ge F (2010) Elevated CO_2 alleviates damage from Potato virus Y infection in tobacco plants. Plant Sci 179: 219–224.

9. Sun Y, Guo H, Zhu-Salzman K, Ge F (2013) Elevated CO2 increases the abundance of the peach aphid on Arabidopsis by reducing jasmonic acid defenses. Plant Sci 210: 128–140. doi: 10.1016/j.plantsci.2013.05.014 PMID: 23849120

10. Qu F, Ye X, Hou G, Sato S, Clemente TE, Morris TJ (2005) RDR6 has a broad-spectrum by temperature-dependent antiviral defense role in Nicotiana benthamiana. J Virol 79: 15209–15217. PMID: 16306592

11. Szittya G, Silhavy D, Molnár A, Havelda Z, Lovas A, Lakatos L, Bánfaldi Z, Burgyán J (2003) Low temperature inhibits RNA silencing-mediated defence by the control of siRNA generation. EMBO J 22: 633–640. PMID: 12554663

12. Velázquez K, Renovell A, Comellas M, Serra P, García ML, Pina JA, Navarro L, Moreno P, Guerri J (2010) Effects of temperature on RNA silencing of a negative-stranded RNA plant virus: Citrus psorosis virus. Plant Pathol 59: 982–990.

13. Chellappan P, Vanitharani R, Ogbe F, Fauquet CM (2005) Effect of temperature on geminivirus-induced RNA silencing in plants. Plant Physiol 138: 1828–1841. PMID: 16040661

14. Zhang X, Zhang X, Singh J, Li D, Qua F (2012) Temperature-Dependent Survival of Turnip Crinkle Virus-Infected Arabidopsis Plants Relies on an RNA Silencing-Based Defense That Requires DCL2, AGO2, and HEN1. J Virol 86: 6847–6854. doi: 10.1128/JVI.00497-12 PMID: 22496240

15. Zhong SH, Liua JZ, Jin H, Lina L, Lia Q, Chena Y, Yuana YX, Wang ZY, Huanga H, Qie YJ, Chena XY, Vaucheret H, Choryc J, Lib J, He ZH (2013) Warm temperatures induce transgenerational epigenetic release of RNA silencing by inhibiting siRNA biogenesis in Arabidopsis. Proc Natl Acad Sci USA 110: 9171–9178. doi: 10.1073/pnas.1219655110 PMID: 23686579

16. Del Toro F, Tenllado F, Chung BN, Canto T (2014a) A procedure for the transient expression of genes by agroinfiltration above the permissive threshold to study temperature-sensitive processes in plant–pathogen interactions. Mol Plant Pathol 15: 848–857.

17. Ballut L, Drucker M, Pugniére M, Cambon F, Blanc S, Roquet F, Candresse T, Schmid HP, Nicolas P, Le Gall O, Badaoui S (2005) HCPro, a multifunctional protein encoded by a plant RNA virus, targets the 20S proteasome and affects its enzymatic activities. J Gen Virol 88: 2595–2603.

18. Jin Y, Ma D, Dong J, Jin J, Li D, Deng C, Wang T (2007) HC-Pro protein of Potato virus Y can interact with three Arabidopsis thaliana 20S proteasome subunits in planta. J Virol 81: 12881–12888. PMID: 17898064

19. Dielen AS, Sassaki FT, Walter J, Michon T, Menard G, Pagny G, Krause-Sakate R, Maia I, Badaoui S, Le Gall O, Candresse T, German-Retama S (2011) The 20S proteasome α_5 subunit of Arabidopsis thaliana carries and RNase activity and interacts in planta with the Lettuce mosaic potyvirus HcPro protein. Mol Plant Pathol 12: 137–150. doi: 10.1111/j.1364-3703.2010.00654.x PMID: 21199564

20. García D, García S, Voinnet O (2014) Nonsense-mediated decay serves as a general viral restriction mechanism in plants. Cell Host Microbe 16: 391–402. doi: 10.1016/j.chom.2014.08.001 PMID: 25155460

21. Nakahara KS, Masuta C, Yamada S, Shimura H, Kashihara Y, Wada TS, Meguro A, Goto K, Tadamura K, Sueda K, Sekiguchi T, Shao J, Itchoda N, Matsumara T, Igarashi M, Ito K, Ohsato S, Miyanishi M, Shirako Y (2003) Tobacco calmodulin-like protein provides secondary defense by binding to and directing degradation of virus RNA silencing suppressors. Proc Natl Acad Sci USA 109: 10113–10118.

22. Sahana N, Kaur H, Raj B, Tena F, Kumar RJ, Palukaitis P, Canto T, Praveen S (2012) Inhibition of the host proteasome facilitates Papaya ringspot virus accumulation and proteosomal catalytic activity is modulated by viral factor HcPro. PLoS ONE 7(12):e52546. doi: 10.1371/journal.pone.0052546 PMID: 23300704

23. Schwach F, Vaistij FE, Jones L, Baulcombe DC (2005) An RNA-dependent RNA polymerase prevents meristem invasion by Potato Virus X and is required for the activity but not the production of a systemic silencing signal. Plant Physiol 138: 1842–1852. PMID: 16040651

24. Rizzo TM, Palukaitis P (1990). Construction of full-length cDNA clones of cucumber mosaic virus RNAs 1, 2 and 3: Generation of infectious RNA transcripts. Mol Gen Genet 222: 249–256. PMID: 2274028

25. Del Toro F, Tena F, Tilsner J, Wright K, Tenllado F, Chung BN, Praveen S, Canto T (2014b) Potato virus Y HCPro localization at distinct, dynamically-related and environment-influenced structures in the cell cytoplasm. Mol Plant-Microbe Interact 27: 1331–1343.

26. González I, Martínez LI, Rakitina D, Lewsey MG, Atienzo FA, Llave C, Kalinina N, Carr JP, Palukaitis P, Canto T (2010) Cucumber Mosaic Virus 2b Protein Subcellular Targets and Interactions: Their Significance to its RNA Silencing Suppressor Activity. Mol Plant-Microbe Interact 23: 294–303. doi: 10.1094/MPMI-23-3-0294 PMID: 20121451

27. Tena F, González I, Doblas P, Rodríguez C, Sahana N, Kaur H, Tenllado F, Praveen S, Canto T (2013) The influence of cis-acting P1 protein and translational elements on the expression of Potato virus Y HCPro in heterologous systems and its suppression of silencing activity. Mol Plant Pathol 14: 530–541. doi: 10.1111/mpp.12025 PMID: 23451733

28. Lu R, Malcuit I, Moffett P, Ruíz MT, Peart J, Wu AJ, Rathjen JP, Bendahmane A, Day L, Baulcombe DC (2003) High throughput virus-induced gene silencing implicates heat shock protein 90 in plant disese resistence. EMBO J 22: 5690–5699. PMID: 14592968

29. Canto T, Ellis JP, Bowler G, López-Abella D (1995) Production of monoclonal antibodies to Potato virus Y Helper Component protease and their use for strain differentiation. Plant Dis 79: 234–237.

30. Pacheco R, García-Marcos A, Manzano A, Garcia de Lacoba M, Camañes G, Pilar GA, Díaz-Ruíz JR, Tenllado F (2012) Comparative analysis of transcriptomic and hormonal responses to compatible and incompatible plant-virus interactions that lead to cell death. Mol Plant-Microbe Interact 25: 709–723. doi: 10.1094/MPMI-11-11-0305 PMID: 22273391

31. Feng JL, Chen SN, Tang XS, Ding XF, Du ZY, Chen JS (2006) Quantitative determination of cucumber mosaic virus genome RNAs in virions by real-time reverse transcription-polymerase chain reaction. Acta Bioch Bioph Sin. 38: 669–676.

32. Dujovny G, Valli A, Calvo M, García JA (2009) A temperature-controlled amplicon system derived from Plum pox potyvirus. Plant Biotechnol J 7: 49–58. doi: 10.1111/j.1467-7652.2008.00373.x PMID: 18801011

33. Canto T, Cillo F, Palukaitis P (2002) Generation of siRNAs by T-DNA sequences does not require active transcription nor homology to sequences in the plant. Mol Plant-Microbe Interact 15:1137–1146. PMID: 12423019

34. Johansen LK, Carrington JC (2001) Silencing on the spot. Induction and suppression of RNA silencing in the Agrobacterium-mediated transient expression system. Plant Physiol 126: 930–938. PMID: 11457942

35. L akatos L, Csorba T, Pantaleo V, Chapman EJ, Carrington JC, Liu Y-P, Dolja V, Fernñandez Calvino L, López-Moya J, Burgyán J (2006) SanII RNA binding is a common strategy to suppress RNA silencing by several viral suppressors. EMBO J 25: 2768–2780 PMID: 16724105

36. Pantaleo V, Szittya G, Burgyán J (2007) Molecular bases of viral RNA targeting by viral small interfering RNA-programmed RISC. J Virol 81: 3797–3806. PMID: 17267504

37. Voinnet O, Lederer C, Baulcombe DC (2000) A viral movement protein prevents spread of the gene silencing signal in Nicotiana benthamiana. Cell 103: 157–167. PMID: 11051555

38. Carthew RW, Uyeda I (2012) Tobacco calmodulin-like protein provides secondary defense by binding to and directing degradation of virus RNA silencing suppressors. Proc Natl Acad Sci USA 109: 10113–10118. doi: 10.1073/pnas.1201628109 PMID: 22665793

39. Liu L, Zhang Y, Tang S, Zhao Q, Zhang Z, Zhang H, Dong L, Guo H, Xie Q (2010) An efficient system to detect protein ubiquitination by agroinfiltration in Nicotiana benthamiana. Plant J 61: 893–903. doi: 10.1111/j.1365-313X.2009.04109.x PMID: 20015064

40. den Boon JA, Diaz A, Ahlquist P (2010) Cytoplasmic viral replication complexes. Cell Host Microbe 8: 77–85. doi: 10.1016/j.chom.2010.06.010 PMID: 20638644

41. Moreno AA, Orellana A (2011) The physiological role of the unfolded protein response in plants. Biol Res 44: 75–80. doi: 10.4067/S0716-97602011000100010 PMID: 21720684

42. Parmar VM, Schroder M (2012) Sensing endoplasmic reticulum stress. Adv Exp Med Biol 738: 153–168. doi: 10.1007/978-1-4614-1680-7_10 PMID: 22399379

43. Wei T, Huang TS, McNeil J, Laliberté JF, Hong J, Nelson RS, Wang A (2010) Sequential recruitment of the endoplasmic reticulum and chloroplasts for plant potyvirus replication. J Virol 84: 799–809. doi: 10.1128/JVI.01824-09 PMID: 19906931

44. Verchot JM (2014) The ER quality control and ER associated degradation machineries are vital for viral pathogenesis. Front Plant Sci 5: 66. doi: 10.3389/fpls.2014.00066 PMID: 24653727

45. Cillo F, Roberts IM, Palukaitis P (2002) In Situ Localization and Tissue Distribution of the Replication-Associated Proteins of Cucumber Mosaic Virus in Tobacco and Cucumber. J Virol 76: 10654–10664. PMID: 12368307

Supporting information

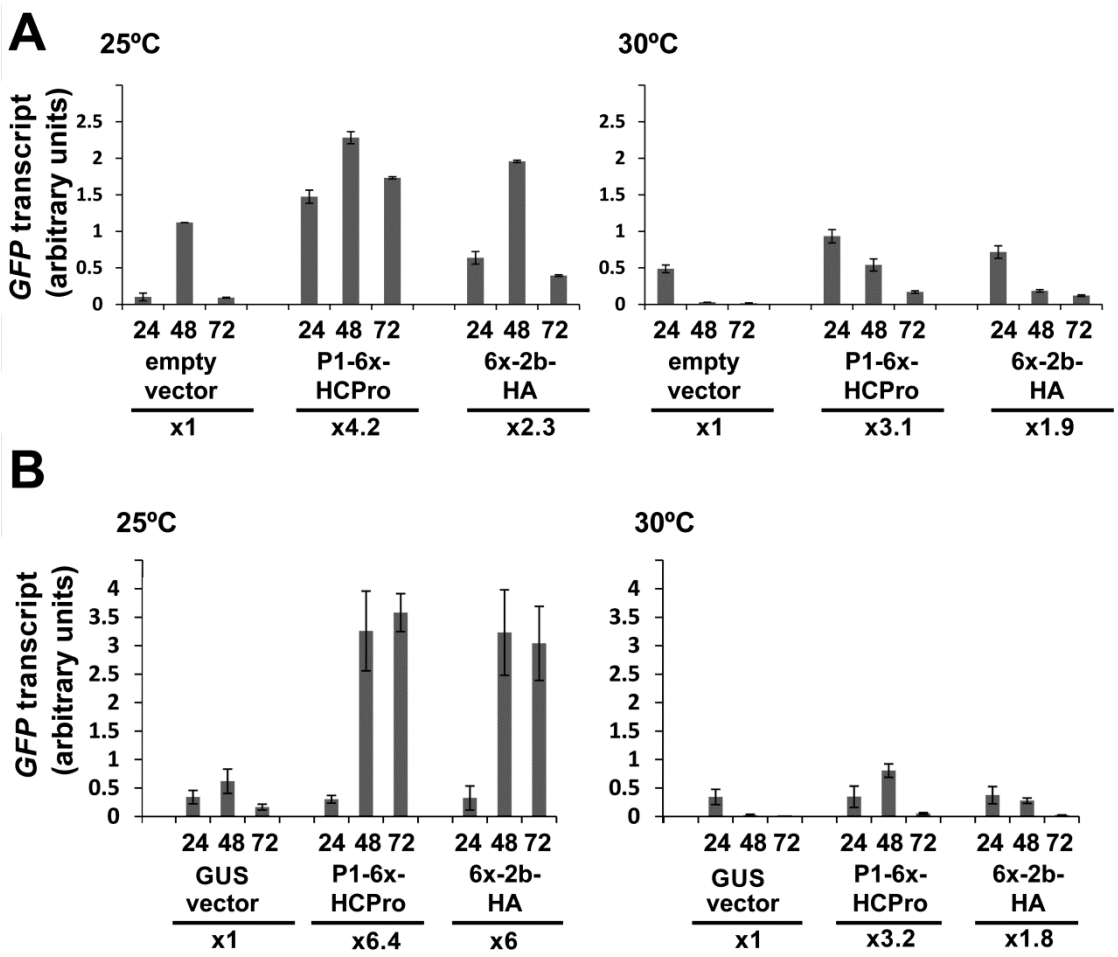

Supporting Information

S1 Fig. Quantification by RT-qPCR of *GFP* transcript levels in three-day time-course agropatch assays at either 25°C or at 30°C [the latter with the first 24 hours post infiltration (hpi) at 25°C]. Two experiments were performed. In **A**, a binary vector expressing GFP was co-infiltrated together with either empty vector or with vectors expressing the viral suppressors P1-6x-HCPro or 6x-2b-HA. Two 15 mm diameter leaf disks were collected at each of three times after infiltration (24, 48 and 72 hpi). In **B**, a GFP vector was co-infiltrated with a vector expressing β-glucuronidase (GUS; Aguilar et al. 2015. J Virol 89:2090–2103) or with vectors expressing the viral suppressors. Six 9.7 mm diameter disks were collected at each of three time points after infiltration (24, 48 and 72 hpi) from three different leaves for assessment. The rates of increase in the levels of *GFP* transcript (the combined average of the 24, 48 and 72 hpi measures) with regard to the baseline controls (either GFP + empty vector in A or GFP + GUS vector in B, both given a value of x1) are indicated below each sample.

CHAPTER 5

Potato virus Y HCPRO LOCALIZATION AT DISTINCT, DYNAMICALLY RELATED AND ENVIRONMENT-INFLUENCED STRUCTURES IN THE CELL CYTOPLASM

Article published in Mol Plant Microbe Interact in 2014; 27(12):1331-43

doi: 10.1094/MPMI-05-14-0155-R.

MPMI Vol. 27, No. 12, 2014, pp. 1331–1343. http://dx.doi.org/10.1094/MPMI-05-14-0155-R

e-Xtra*

Potato virus Y HCPro Localization at Distinct, Dynamically Related and Environment-Influenced Structures in the Cell Cytoplasm

Francisco del Toro,[1] Fátima Tena Fernández,[1] Jens Tilsner,[2,3] Kathryn M. Wright,[2] Francisco Tenllado,[1] Bong Nam Chung,[4] Shelly Praveen,[5] and Tomas Canto[1]

[1]Environmental Biology Department, Centro de Investigaciones Biológicas, CIB-CSIC, Ramiro de Maeztu 9, 28040 Madrid; [2]The James Hutton Institute, Cell and Molecular Sciences, Invergowrie, Dundee, DD2 5DA, U.K.; [3]Biomedical Sciences Research Complex, University of St Andrews, Fife KY16 9ST, Scotland, U.K.; [4]National Institute of Horticultural & Herbal Science, Agricultural Research Center for Climate Change, 281, Ayeon-ro, Jeju, 690-150, Jeju Island, Republic of Korea; [5]Division of Plant Pathology, Indian Agricultural Research Institute, 110 012 New Delhi, India

Submitted 27 May 2014. Accepted 25 July 2014.

Potyvirus **HCPro is a multifunctional protein that, among other functions, interferes with antiviral defenses in plants and mediates viral transmission by aphid vectors. We have visualized in vivo the subcellular distribution and dynamics of HCPro from *Potato virus Y* and its homodimers, using green, yellow, and red fluorescent protein tags or their split parts, while assessing their biological activities. Confocal microscopy revealed a pattern of even distribution of fluorescence throughout the cytoplasm, common to all these modified HCPros, when transiently expressed in *Nicotiana benthamiana* epidermal cells in virus-free systems. However, in some cells, distinct additional patterns, specific to some constructs and influenced by environmental conditions, were observed: i) a small number of large, amorphous cytoplasm inclusions that contained α-tubulin; ii) a pattern of numerous small, similarly sized, dot-like inclusions distributing regularly throughout the cytoplasm and associated or anchored to the cortical endoplasmic reticulum and the microtubule (MT) cytoskeleton; and iii) a pattern that smoothly coated the MT. Furthermore, mixed and intermediate forms from the last two patterns were observed, suggesting dynamic transports between them. HCPro did not colocalize with actin filaments or the Golgi apparatus. Despite its association with MT, this network integrity was required neither for HCPro suppression of silencing in agropatch assays nor for its mediation of virus transmission by aphids.**

Members of the genus *Potyvirus* are filament-shaped, plus-sense RNA viruses that express a single polyprotein that undergoes proteolytic cleavage to generate the final products, although one small essential gene (*P3N-PIPO*) expresses itself via translational frameshifting (Chung et al. 2008). The proteases involved in this processing are the P1 protein, which is the first product from the polyprotein that detaches itself at its C terminus from the following HCPro (Verchot and Carrington 1995a; Verchot et al. 1991): HCPro, a papain-like protease that detaches itself at its C terminus from the rest of the polyprotein (Carrington and Herndon 1992); and the small nuclear inclusion body protein (NIa), which cleaves the remaining sites (Carrington et al. 1988; García et al. 1989). *Potyvirus* polyprotein translation is thought to be closely coupled to viral replication which, as in many RNA viruses, takes place in replicative complexes associated with membrane vesicles that originate from the endoplasmic reticulum (ER). In the specific case of potyviruses, these vesicles are transported from the ER via actin filaments toward the chloroplasts for enhanced replication (Wei and Wang 2008; Wei et al. 2013). The transport of potyviral protein products from replication-translation vesicle factories to other parts of the cell may be mediated by routes such as the secretory pathway or the cell microtubules (MT) or microfilaments, although our knowledge of these processes is still fractionary (Sorel et al. 2014).

HCPro is a multifunctional protein that, in addition to its protease activity, is involved in the suppression of the antiviral gene silencing defenses of the host, among other functions (Anandalakshmi et al. 1998, Brigneti et al. 1998; Canto et al. 2002; Johansen and Carrington 2001; Rajamäki et al. 2005; Valli et al. 2006). It is also required in the transmission of potyviruses by their insect aphid vectors; hence its original name of "helper component" (Govier and Kassanis 1974). HCPro has been traditionally divided into three domains: the N-terminal domain associated with aphid transmission (Blanc et al. 1997; Canto et al. 1995b) and its interaction with proteasomal units (Jin et al. 2007a; Sahana et al. 2014), the central domain associated with the suppression of silencing function (Shiboleth et al. 2007), and the C-terminal domain of the protein that harbors its protease activity (Carrington and Herndon 1992) and interaction domains to plant HIP2-like MT-associated proteins (Guo et al. 2003; Haikonen et al. 2013a and b).

Soluble HCPro from several potyviruses extracted from infected plants has been shown by size chromatography to be formed mainly by homodimers and further aggregates (Plisson et al. 2003; Ruíz-Ferrer et al. 2005, Tena et al. 2013; Thornbury et al. 1985), which could be relevant to some of the biological functions of the protein. Self-interactions of HCPros have also been demonstrated by yeast two-hybrid assays (Y2H) (Urcuqui-

F. del Toro and F. Tena Fernández contributed equally to this work.

Corresponding authors: S. Praveen; E-mail: shellypraveen@hotmail.com; and T. Canto; E-mail: tomas.canto@cib.csic.es

*The *e*-Xtra logo stands for "electronic extra" and indicates that three supplementary figures are published online.

Inchima et al. 1999) or visualized in the plant cell cytoplasm by bimolecular fluorescence complementation (BiFC) (Ala-Poikela et al. 2011; Sahana et al. 2012; Zheng et al. 2011; Zilian and Maiss 2011).

Despite being one of the most studied plant virus proteins, relatively little is known about the precise modes by which HCPro undertakes these two principal functions of silencing suppression and mediation of viral transmission by vectors. As regards silencing suppression, it is known that HCPro interacts in vitro with long RNAs (approximately 200 nucleotides) and small RNAs (Chapman et al. 2004; Lakatos et al. 2006; Maia and Bernardi 1996; Mangrauthia et al. 2009; Mérai et al. 2006; Shiboleth et al. 2007; Urcuqui-Inchima et al. 2000) but at protein/RNA molar ratios much higher than the 2:1 characterized for the 2b and P19 suppressors of *Tomato bushy stunt virus* (TBSV) (González et al. 2012; Vargasson et al. 2003) and *Cucumber mosaic virus* (CMV), thus making it unlikely that HCPro interferes with antiviral silencing in the same way as P19 and 2b do; that is, by means of sequestering small interfering RNAs. On the other hand, HCPro interacts in vitro with the RNA methyltransferase HEN-1, inhibiting it (Jamous et al. 2011). Suppressor activity of HCPro also seems influenced by the P1 protein (Canto et al. 2002; Johansen and Carrington 2001; Pruss et al. 1997; Rajamäki et al. 2005; Valli et al. 2006; Verchot and Carrington 1995a and b). That P1 detachment is essential for HCPro suppressor activity in agropatch assays was recently demonstrated (Pasin et al. 2014). However, a direct role for P1 on HCPro suppressor activity either as cofactor or by influencing its conformation during translation to improve its stability has been be excluded and it appears, instead, that its effect on HCPro can be explained by cis-acting elements that favor HCPro translation in the upstream presence of P1, without ruling out a possible role of P1 in protecting HCPro from degradation (Tena et al. 2013).

As regards viral transmission by vectors, HCPro is required to be taken by the vector prior to or simultaneously with virions for transmission to occur. HCPro can interact with the homologous viral coat protein in vitro, as well as in plant extracts (Blanc et al. 1997; Roudert-Tavert et al. 2002). Of not clear significance to transmission, HCPro has been found to be present at one end of a tiny minority (less than 3%) of *Potato virus Y* (PVY) and *Potato virus A* (PVA) virions (Torrance et al. 2006).

HCPro interaction with plant factors and cytoplasmic structures involved in processes other than gene silencing is extensive: it binds a host rgs-CaM factor, which directs its degradation through autophagy (Nakahara et al. 2012) to the *Arabidopsis thaliana* transcription factor RAV2 (Endres et al. 2010) to components of the proteasome, which participate in another type of antiviral defense (Ballut et al. 2005; Dielen et al. 2011; Sahana et al. 2012), with translation initiation factors (Ala-Poikela et al. 2011; Freire 2014), with chloroplast factors (Cheng et al. 2008; Jin et al. 2007b), and with MT-binding HIP2-type proteins (Guo et al. 2003; Haikonen et al. 2013).

As regards the subcellular loci where several HCPro functions and interactions take place, early electron microscopy immunolocalization studies situated PVY HCPro in the cytoplasm of fixed infected mesophyll cells forming amorphous inclusions (Baunoch et al. 1990). Studies using fixed cowpea protoplasts found HCPro from *Cowpea aphid-borne mosaic virus* (CABMV) diffused throughout the cytoplasm (Mlotshwa et al. 2002). In live tissues, HCPro from *Turnip mosaic virus* (TuMV) tagged with green fluorescent protein (GFP) was also found to localize to the cytoplasm of epidermal *Nicotiana benthamiana* cells as filaments, around the nucleus, and in what could be the ER; whereas, in protoplasts from transgenic *N. benthamiana* plants expressing GFP targeting the ER (line 16c) (Ruíz et al. 1998), untagged HCPro from TuMV induced morphological changes in the ER structure, suggesting an interaction between HCPro and this structure (Zheng et al. 2011). Furthermore, PVA HCPro interaction with the host HIP2 factor has been visualized by BiFC, coating in vivo MT (Haikonen et al. 2013b). Thus, evidence from the literature with regard to HCPro subcellular targets and its accumulation originates from different potyviruses and hosts and is diverse, pointing at different subcellular structures and features.

In this work, we have used HCPros modified with fluorescent proteins to visualize the protein in the living cell and its dynamics in vivo, while characterizing their biological properties using activity assays. Our initial hypothesis was that this approach could allow us to link observations on subcellular targets of HCPro to its biological functions, by disrupting those targets and assessing their effect on the activity assays. Unlike previous works by others, we carried out a comparative study on the subcellular distribution of PVY HCPro using different, functionally characterized constructs fused to GFP and yellow and red fluorescent protein (YFP and RFP, respectively) tags or their split halves to obtain a more comprehensive picture of HCPro subcellular whereabouts and dynamics. We found that, in a virus-free transient expression system, HCPro distributed evenly throughout the cytoplasm. However, for some constructs and in some cells, we could also identify accumulation in distinct structures: as a few large, irregular inclusions; as numerous evenly distributed dot-shaped inclusions of similar size associated with both cortical ER and MT; and, finally, colocalizing extensively with the MT cytoskeleton. Although, in some individual cells, localization at one particular structure was prevalent, in other cells mixed and intermediate patterns could be found, suggesting that they evolved from one into another and, thus, were dynamically linked. Furthermore, the presence of these structures was influenced by environment stresses. We also tested the need for HCPro functions of its interactions with defined subcellular structures by disrupting them and performing biological activity assays. Potential biological implications of our results are discussed.

RESULTS

Fluorescent tags affect HCPro biological activities to different degrees.

To study the subcellular distribution of PVY HCPro in vivo, we tagged it with fluorescent proteins or their split parts (Fig. 1). C-terminal tagging of HCPro included GFP and monomeric (m)RFP (Fig. 1, constructs P1-HCPro-GFP and P1-HCPro-mRFP, respectively). In these C-terminal fusion constructs, the second glycine at the HCPro protease cleavage site (tyrosine-X-valine-glycine/glycine) had been replaced by tyrosine-arginine-valine-glycine/alanine, a motif shown previously not to be cleaved by *Tobacco etch virus* (TEV) HCPro in rabbit reticulocyte lysates (Carrington and Herndon 1992). However, Western blot analysis of the expressed proteins showed that both had the same size as the native protein (Supplementary Fig. S1, Western blot, third and fourth lanes versus second lane). The most likely explanation for these data is that, after translation of the fusion product, the fluorescent tags became detached from HCPro. Thus, our C-terminal tagging approach proved inefficient to its purpose.

N-terminal taggings of HCPro with GFP, mRFP, split (s)YFP (sYN and sYC), and split monomeric (sm)RFP (sRN and sRC) parts (Fig. 1) were stable, and fusion proteins had the expected size in Western blots (Fig. 2; data not shown). All the constructs had an additional hexahistidine motif in frame, located either at the end of the N terminus of the fusion construct (plus a starting methionine) in the case of GFP- or sYFP-

tagged constructs, or between the fluorescent tag and HCPro in the case of mRFP- or smRFP-tagged constructs (Fig. 1).

Suppression of the silencing of a free *GFP* reporter by these N-fusion constructs in agroinfiltration patch assays showed that tags affected this HCPro activity to varying degrees. Suppression was very weak in both of the GFP-tagged constructs (Fig. 2A, leaves in the upper panel and Western blot panel). By contrast, the sYFP-tagged constructs showed stronger suppressor activities; in particular, construct 6x-sYN-HCPro or when both N- and C-terminal parts were combined. The accumulation of construct 6x-YC-HCPro was also weak in infiltrated tissue but it rose when it was coexpressed with construct 6x-YN-HCPro (Fig. 2A, leaves in the middle panel, and Western blot panels). In contrast to the GFP constructs, the mRFP-tagged construct displayed suppression of silencing activity (Fig. 2B); in particular, that from the combined smRFP-tagged constructs (Fig. 2C). For this high preservation of suppressor activity and for their good fluorescence response under confocal microscopy, the use of BiFC smRFP-tagged HCPro constructs was preferred, when possible, in our in vivo subcellular localization studies.

Regarding mediation of virus transmission by aphids, we tested 6x-HCPro and 6x-GFP-HCPro after their large-scale purification from plant tissue infected with PVX-P1-6x-HCPro or with PVX-P1-6x-GFP-HCPro, respectively. Although purified 6x-HCPro successfully mediated transmission of PVY virions in aphid membrane feeding tests, 6x-GFP-HCPro did not (Supplementary Fig. S2). Therefore, the tagging of HCPro with GFP had a severe negative effect on both activities, silencing suppression in agropatch assays and mediation of virus transmission by insects. Tagging with mRFP and smRFP was less detrimental to suppressor activity. These two latter constructs were not tested for aphid transmission activity.

HCPros with fluorescent tags accumulate in distinct yet dynamically related as well as environment-influenced structures in epidermal cells.

We used confocal microscopy of our N-terminal tagged constructs to visualize HCPro in subcellular structures within living cells. We had GFP and mRFP-tagged constructs as well as constructs that were tagged with split parts of either YFP (sYFP) or mRFP (smRFP). In the latter two cases, visualized fluorescence would correspond only to the interacting homodimers of HCPro that had complementary tags (sYN + sYC tags; sRN + sRC tags) as a result of BiFC.

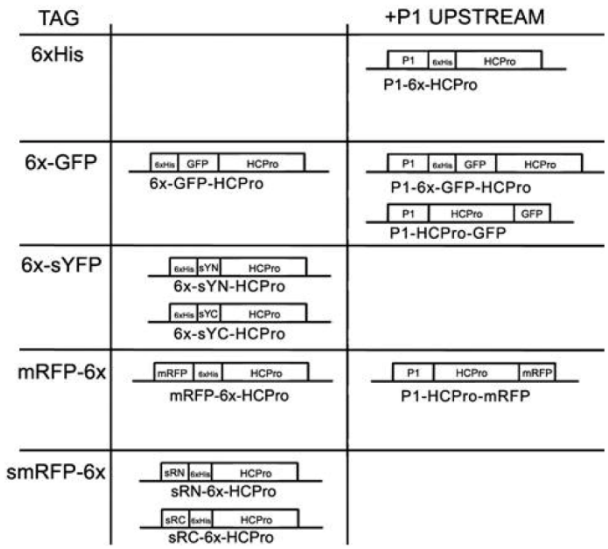

Fig. 1. N-terminal and C-terminal tagging of HCPro for fluorescence studies in vivo. Schematic representation of the different constructs tagged with green fluorescent protein (GFP), N-terminal and C-terminal split yellow fluorescent protein parts (sYN and sYC, respectively), monomeric red fluorescent protein (mRFP), or N-terminal and C-terminal split mRFP parts (sRN and sRC, respectively) at either the N or the C terminus of HCPro, and in the upstream presence or absence of P1 protein during translation.

Confocal imaging of single epidermal cells showed that, in many cells, fluorescence derived from constructs P1-6x-GFP-HCPro and mRFP-6x-HCPro distributed smoothly throughout the cytoplasm, negatively staining some unidentified vesicle structures (Fig. 3, upper panels). In addition, large irregular inclusions were observed in the case of the GFP-tagged construct but not in the case of the mRFP-tagged one (Fig. 3, upper left panel, arrows)

Confocal imaging at low magnification covering fields of approximately 20 *N. benthamiana* epidermal cells transiently expressing GFP- or sYFP-tagged HCPros showed, in both cases, a similar pattern of distribution, in which most of the fluorescence appeared distributed throughout the cytoplasm; in particular, as the large inclusions aforementioned of irregular or amorphous shape. Interestingly, the transient presence of heterologous suppressors of silencing, provided with the intention of boosting the accumulation of HCPro, such as TBSV P19 or the CMV 2b protein, had the effect of reducing both the number and size of these irregular inclusions throughout the cytoplasm without increasing the overall accumulation of HCPro (Fig. 3, second and third rows of panels from the top, respectively). At the same low magnification level, a few irregular inclusions were also found in smRFP-tagged HCPro, usually one or two inclusions per cell, much less than those found in GFP- or split YFP-tagged constructs. The presence of heterologous suppressors P19 or 2b was also detrimental to their number and size (Fig. 3, fourth row of panels from the top; data not shown). These data show that the formation of large irregular inclusions can be influenced by factors from the environment in which the constructs are expressed.

In some epidermal cells, instead of the diffuse distribution of fluorescence throughout the cytoplasm, other different and distinct patterns were found: fluorescence from smRFP-tagged constructs was found in some cells distributed as dots of similar size, regularly positioned in a mesh pattern. In some of these cells, the dots appeared interconnected by filaments of red fluorescence of a similar diameter. In other cells, only the smooth red filaments were visible (Fig. 4, second row of panels from the top). The presence of fluorescent filaments connecting dots was also demonstrated for mRFP-, sYFP-, and GFP-tagged HCPros (Fig. 4, upper and lower rows of panels, respectively; data not shown). We found cells harboring these dots and filaments plus their intermediate forms mainly but not exclusively when infiltrated tissue was exposed to some stresses; in particular, volatile components from common nail varnish used as sealant at the edges of the infiltrated plant tissue several minutes prior to confocal viewing. It must be highlighted that none of the epidermal cells imaged had direct contact with the varnish, they were fully turgent, and they had their subcellular structures visually unaltered (Fig. 5, integrity of the ER). Cells with filaments could also sometimes be found in tissue treated with saturated CO_2 atmosphere (data not shown). By contrast, 50 aphids left overnight on the infiltrated patch before confocal viewing failed to induce the filament pattern (data not shown). These responses were specific to HCPro constructs, because transiently expressed free mRFP or split mRFP-tagged 2b protein dimers did not alter their diffuse cytoplasmic and nuclear localization under the same stresses (data not shown; Supplementary Fig. S3). We did not identify which component of the nail varnish was responsible for the response. For example, one of its volatile components,

n-butyl acetate, can be a component in insect pheromones. However, we tested the two components (n-butyl acetate and ethyl acetate) separately and neither induced the HCPro filament distribution pattern in our experimental conditions (data not shown).

To identify whether the HCPro-derived fluorescence as dots or filaments or as large inclusions colocalized with defined subcellular structures, we used transgenic *N. benthamiana* plants that constitutively expressed GFP fused to *A. thaliana* α-tubulin (Tua-GFP plants) (Gillespie et al. 2002), GFP targeting the cortical ER (line 16c) (Ruíz et al. 1998), and a Lifeact TagRFP fusion targeting actin. To visualize the Golgi apparatus, we also transiently overexpressed a binary vector expressing mCherry protein with a targeting signal to this structure (Nelson et al. 2007). In the green-fluorescing backgrounds of the 16c and Tua-GFP transgenic plants, we transiently expressed split red HCPro constructs and detected the BiFC-derived fluorescence of the interacting homodimers. As we had previously seen in nontransgenic plants (Fig. 4), we could find fluorescence from sRN-6x-HCPro + sRC-6x-HCPro BiFC distributing as dots, filaments, or intermediates in some epidermal cells of both stress-treated 16c and Tua-GFP plants (Fig. 5). In 16c plants, the cortical ER fluoresced green in a characteristic polygonal net (Fig. 5, upper green and overlay panels). Although the BiFC-derived red fluorescence from interacting HCPros did not overlap with that from the ER, images showed that the red dots appeared nevertheless anchored somehow or linked to the ER scaffold (Fig. 5, overlay panels in upper row). The red filaments seemed, by contrast, unrelated to the ER structure (Fig. 5, overlay panel in second row from the top). In stressed Tua-GFP plants, many epidermal cells displayed a filamentous green fluorescent MT cytoskeleton (Fig. 5, green and overlay panels in third and fourth rows from the top). In some of the cells, the HCPro BiFC-derived red filaments but not many of the red dots matched exactly the green MT fluorescence (Fig. 5, overlay panels in third and fourth rows from the top; data

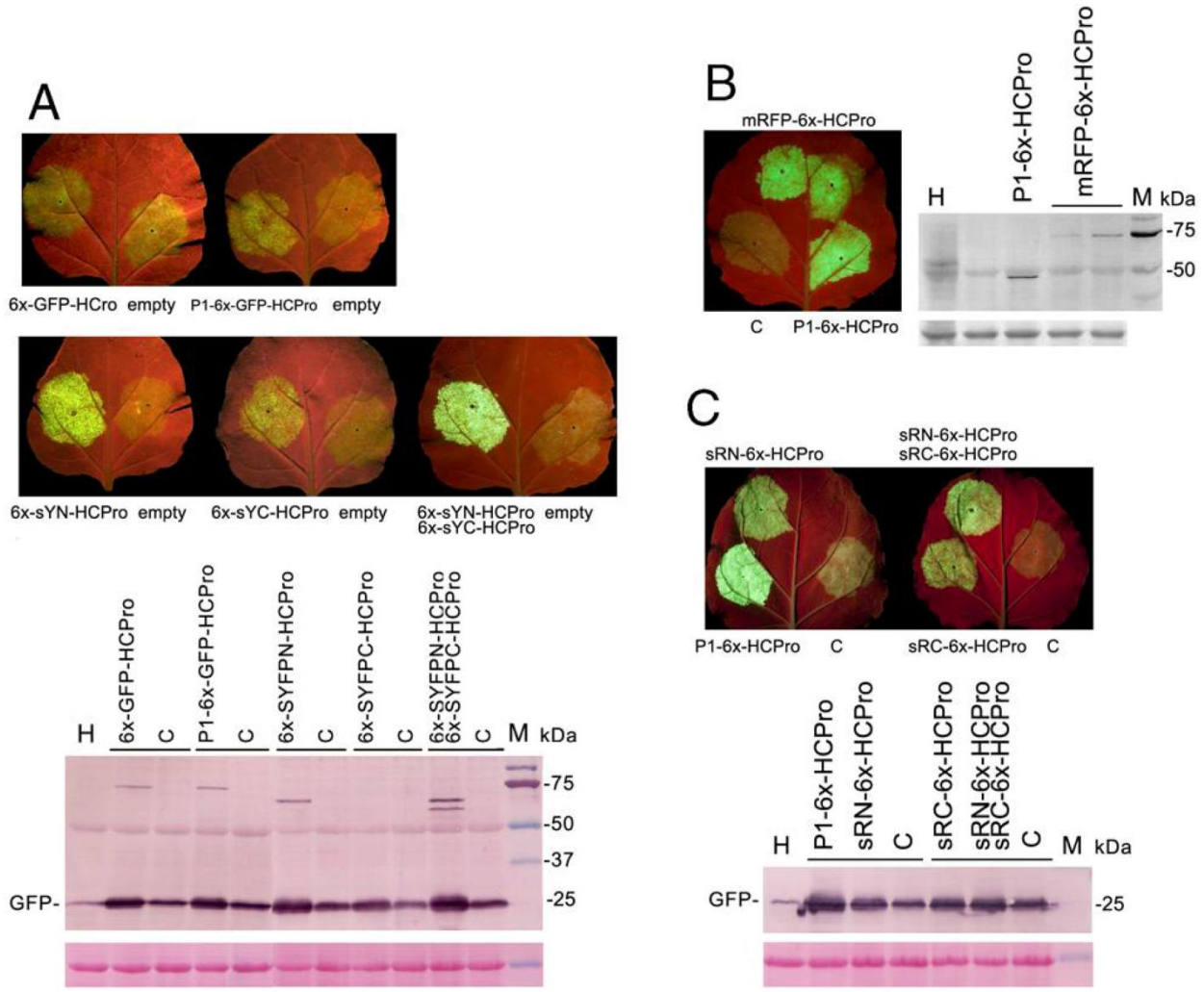

Fig. 2. Suppression of silencing in agropatch assays by N-terminally tagged HCPro constructs: a binary vector expressing a *green fluorescent protein* (*GFP*) reporter was agroinfiltrated together with the empty binary vector pROK2 (right side of leaves) or together with binary vectors expressing *Potato virus Y* (PVY)-derived constructs. **A,** P1-6x-GFP-HCPro, 6x-GFP-HCPro, 6x-sYN-HCPro, 6x-sYC-HCPro or 6x-sYN-HCPro, plus 6x-sYC-HCPro (left side of upper left to bottom right leaves, respectively) and upper Western blot panel in which a polyclonal GFP antibody was used. The increase in GFP-derived fluorescence and on its accumulation was greatest in presence of P1-6x-HCPro and of 6x-sYN-HCPro, either alone or in combination with 6x-sYC-HCPro. By contrast, GFP tagging greatly reduced or abolished HCPro suppressor activity in this type of assay. Note that the serum also detects the GFP and split yellow fluorescent protein (sYFP)-tagged HCPro constructs. **B**, P1-6x-HCPro and mRFP-6x-HCPro (lower right side of leaf and upper patches, respectively) and right side Western blot panel using an anti 6xhistidine tag antibody. **C**, P1-6x-HCPro, sRN-6x-HCPro, sRC-6x-HCPro, and sRN-6x-HCPro plus sRC-6x-HCPro (as labeled by the infiltrated patches). In contrast to the 6x-GFP tag, the monomeric red fluorescent protein (mRFP)-6x tag did not prevent suppressor activity, nor did the tags of the split mRFP parts (corresponding patches in leaves, and Western blot panel to GFP). In all Western blot panels, lane H shows a sample extracted from a healthy plant and lane M = prestained markers for molecular weight, indicated in kilodaltons (kDa).

not shown). In addition, green fluorescence derived from the GFP-tagged α-tubulin transgene product was also found in the large red irregular inclusions (Fig. 5, arrow in overlay panel in bottom row). Thus, large irregular HCPro inclusions contain tubulin.

In epidermal cells of red actin transgenic plants, green fluorescence derived from the BiFC of transiently expressed 6x-sYN-HCPro + 6x-sYC-HCPro constructs did not colocalize with the red fluorescence associated with the plant actin filaments (Fig. 6, upper panels). Likewise, coexpression of 6x-sYN-HCPro + 6x-sYC-HCPro with an m-cherry construct designed to target the Golgi stacks detected no sign of colocalization (Fig. 6, lower panels).

Disruption of the MT network does not prevent HCPro suppression of silencing activity or its mediation of viral transmission by insect vectors.

To test whether the integrity of the MT network would be required for HCPro biological activities that we could test in activity assays (suppression of silencing in patch assays or mediation of viral transmission by insect vectors), we disrupted the MT cytoskeleton using colchicine, as described by Wright and associates (2007). Three days after agroinjection of smRFP-HCPro constructs in Tua-GFP plants with colchicine in the infiltration buffer, green fluorescence derived from transgenic tubulin was distributed as dots or blobs instead of as filaments in epidermal cells, under stress conditions. By contrast, green fluorescence was distributed as filaments in the patches from the same plants injected with buffer lacking colchicine (Fig. 7A). In both cases, red fluorescence derived from BiFC of smRFP-tagged HCPros colocalized with the green tubulin, as either dots or filaments (Fig. 7A).

To test for the suppression of silencing activity of HCPro under undisrupted versus colchicine-disrupted MT cytoskeleton, we carried out a 3-day suppression of silencing patch assay using a free GFP reporter and suppressor P1-6x-HCPro, as well as CMV 2b and TBSV P19. The test was performed both in nontransgenic and in Tua-GFP-transgenic *N. benthamiana* plants. In all cases, suppression of the partial silencing of the transiently expressed GFP reporter was comparable in the presence and in the absence of colchicine (Fig. 7B, upper versus lower patches in left side of leaves; compare GFP fluorescence derived from the reporter under UV light). This happened even if the amount of colchicine injected (5 μM) was 10 times that required for efficient disruption of the MT (Fig. 7B, lower panel). Thus, integrity of the MT cytoskeleton is not required for suppressor of silencing activity in patch assays.

To test the potential requirement of intact MT cytoskeleton for HCPro to mediate aphid transmission, we injected aphid-transmissible, PVY-infected *N. benthamiana* leaves with either colchicine or buffer without this substance and, 3 days after injection, we carried out viral transmission tests with aphids. Transmission efficiencies were similar in both cases, at 100%. Furthermore, we carried out one experiment in which we injected 5 μM colchicine, 10 times the amount required to disrupt the cytoskeleton, and the results were similar (Fig. 7C).

DISCUSSION

Members of the genus *Potyvirus* are among the most successful and economically relevant plant viruses to agriculture, despite their translation strategy leading to the expression of almost all their protein factors in equimolar amounts. Because it appears that not all these proteins would be required in similar amounts at any given time during the viral infection cycle, this strategy would not seem efficient, unless turnover of the different viral products and their accumulation in specific structures for storage, removal, or degradation within the cell at different times or under different environmental conditions was closely integrated and programmed. In this regard, several potyvirus proteins are known to form inclusion structures in

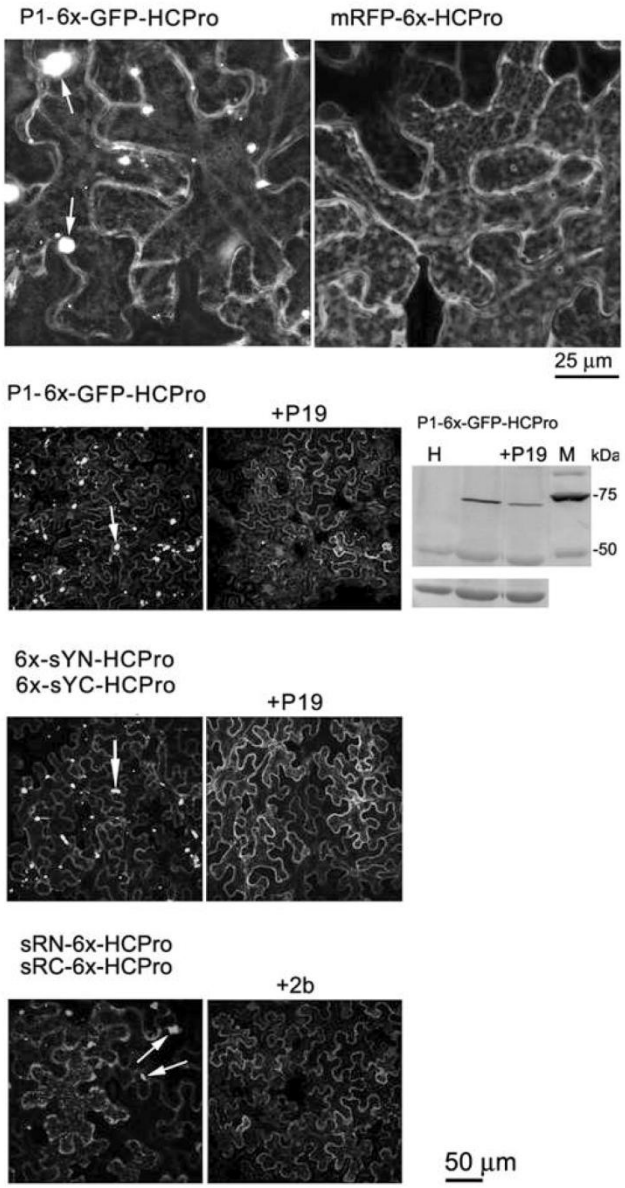

Fig. 3. Visualization of the distribution of fluorescence derived from green fluorescent protein (GFP)-tagged HCPro (construct P1-6x-GFP-HCPro) from monomeric red fluorescent protein (mRFP)-tagged HCPro (construct mRFP-6x-HCPro), or from the bimolecular fluorescence complementations (BiFC) between the two split yellow fluorescent protein (sYFP)-tagged HCPros (constructs 6x-sYN-HCPor and 6x-sYC-HCPro) or the two split monomeric red fluorescent protein (smRFP)-tagged HCPros (constructs sRN-6x-HCPro and sRC-6x-HCPro) transiently expressed by agroinfiltration in fields of epidermal cells of *Nicotiana benthamiana* leaves. Fluorescence derived from the GFP and mRFP tags is found throughout what appears as the cytoplasm; in particular, in large irregular inclusions (arrows in panels) that were absent in the case of construct mRFP-6x-HCPro (upper left and right panels, respectively). Addition of heterologous viral suppressors of silencing such as the tombusviral P19 or cucumoviral 2b protein had the effect of making these inclusions smaller, without increasing the steady-state levels of HCPro, as indicated in the Western blot panel for construct P1-6x-GFP-HCPro (third lane, P19 added versus second lane, empty vector added) or for the BiFC pairs 6x-sYN-HCPro + 6x-sYC-HCPro and sRN-6x-HCPro + sRC-6x-HCPro (third and fourth rows of panels from the top, respectively). Size bars are indicated in the bottom right corner.

different subcellular compartments such as, among others, the nuclear inclusion proteins NIa and NIb within the nucleus, the characteristic plasmodesmata (PD)-associated pinwheels formed by the cylindrical inclusion (CI) helicase protein in the cytoplasm (Sorel et al. 2014), or the cytoplasm-scattered amorphous inclusions of HCPro (Baunoch et al. 1990).

Despite extensive literature, our overall view of the turnover of potyviral proteins or the structures they form and their biological significance is rather poor. That is, are these structures functional sites or only places to remove excess protein? Are these structures reversible or do they contain host factors such as proteins or nucleic acids that may interfere with the progress of the infection or, alternatively, that may need recruiting for use at some further step of the viral infection? How do all of these proteins travel there from the translation sites? In this regard, research into the CI helicase has shown how this protein, in addition to its enzymatic role in replication, is involved in the translation of the vesicle-associated viral replication factories from the ER toward the chloroplasts membranes via actin filaments (Wei et al. 2010a), while it also translocates via the ER-Golgi secretory pathway toward the PDs, where it anchors through its interaction with viral P3N-PIPO and is involved somehow in the local movement of the virus (Wei et al. 2010b).

In contrast to the CI protein, we have a less integrated view of the subcellular dynamics of HCPro interactions, translocation pathways, accumulation, and their relation to its several functions. HCPro is a factor important to processes such as viral replication or local movement but two roles make it essential to the virus cycle: as a strong suppressor of antiviral gene silencing and as a helper factor in the horizontal transmission of the virus by vectors. Microscopy observational data from previous works with different potyviral HCPros have individually linked it to the cytoplasm, distributing diffusely or forming inclusions (Baunoch et al. 2002; Mlothswa et al. 2002; Sahana et al. 2012, 2014; Zheng et al. 2011; Zillian and Maiss 2011). It has also been suggested that it may affect ER structure (Zheng et al. 2011), and it has been found to bind in Y2H and in vivo (BiFC) to a protein (HIP2) associated with the cellular

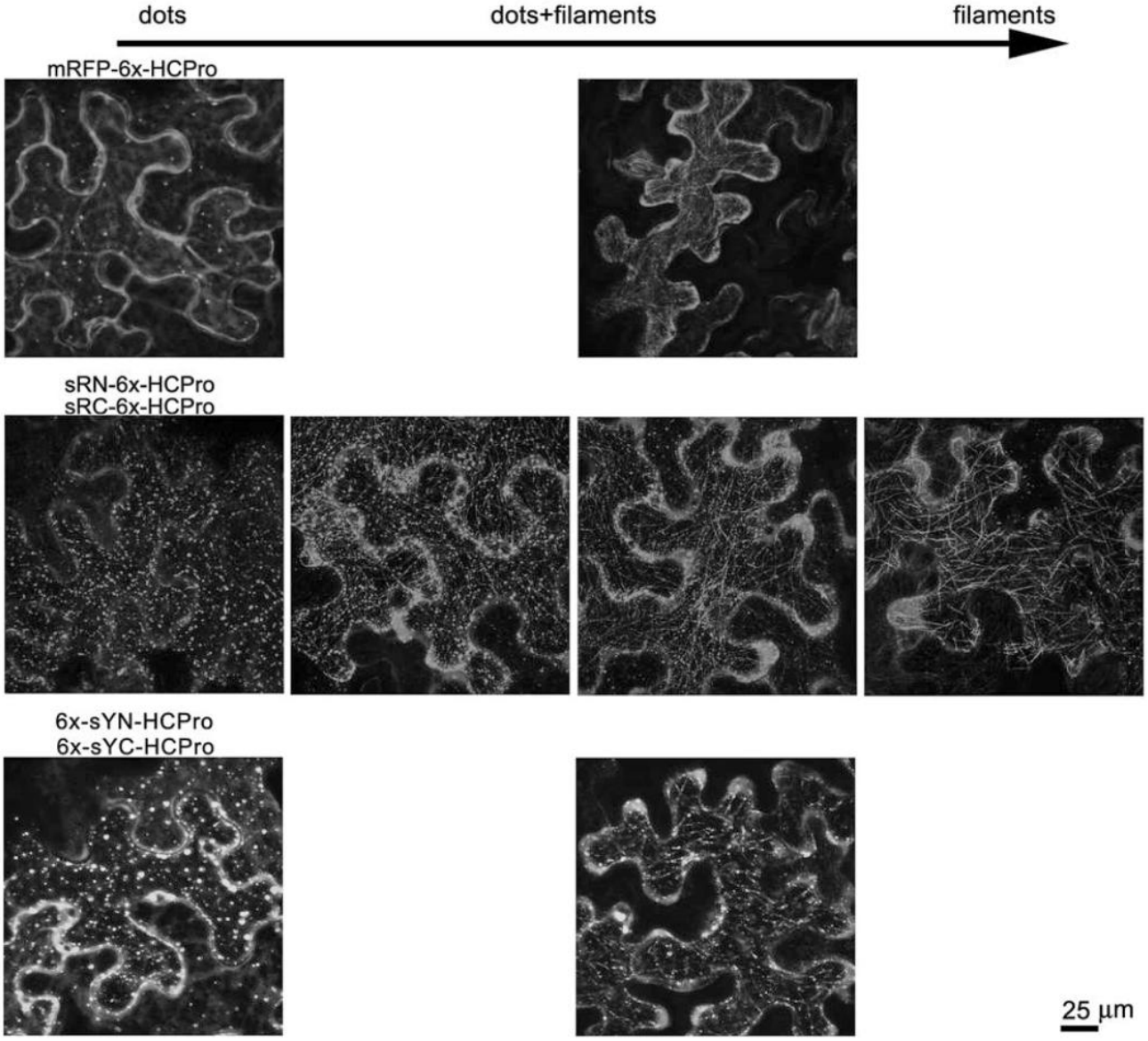

Fig. 4, Close-up view at high magnification within the cytoplasm of individual epidermal cells in which fluorescence distributes as dots of similar size arranged in a regular, reticulate pattern (leftmost panels), as combinations of fluorescent dots and connecting filaments, or mainly as filaments (central and rightmost panels, respectively). The horizontal arrow above the set of panels indicates the increase in filament- versus dot-associated fluorescence and does not suggest any direction to protein traffic. Size bars for panels are indicated in the bottom right corner.

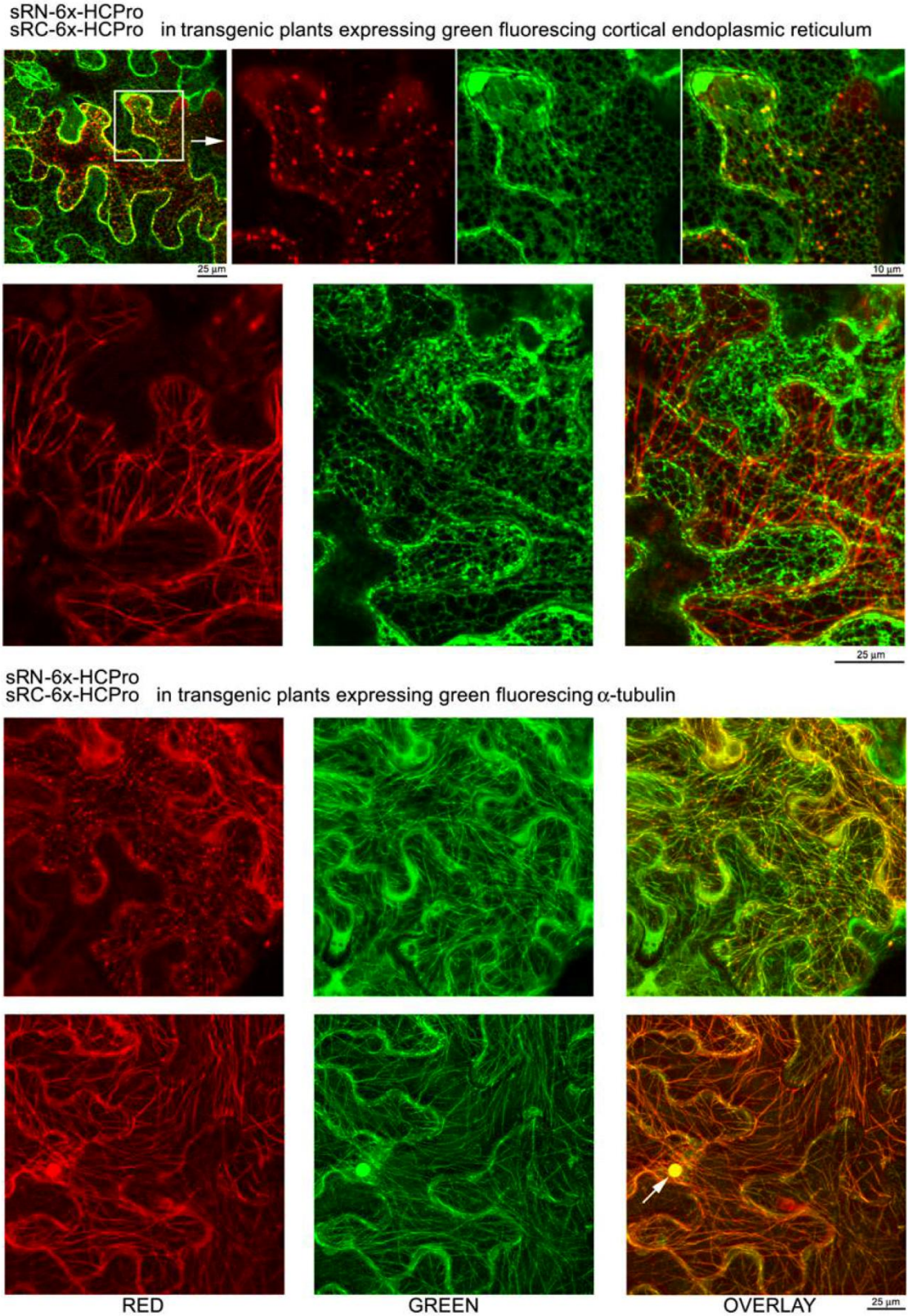

Fig. 5. Visualization of the subcellular distribution of fluorescence derived from the bimolecular fluorescence complementation (BiFC) between the two split monomeric red fluorescent protein (smRFP)-tagged HCPros (constructs sRN-6x-HCPro and sRC-6x-HCPro) transiently expressed by agroinfiltration in epidermal cells of transgenic *Nicotiana benthamiana* leaves that show their cortical endoplasmic reticulum (ER) fluorescing green (Line 16c) (Ruíz et al. 1998) or their microtubule (MT) cytoskeleton fluorescing green by expressing green fluorescent protein (GFP)-tagged α-tubulin (Tua-GFP plants) (Gillespie et al. 2002). Panels show either monochrome green (from ER or MT in transgenic plants) or red (from BiFC HCPro transiently expressed constructs) fluorescence, or overlays of both colors for colocalization studies. HCPro fluorescence either as dots (upper top left panel and enlarged area) or as filaments (upper middle panels) did not colocalize with that from the ER (middle panels). However, HCPro fluorescent dots appeared anchored to the ER scaffold (upper top panels). By contrast, HCPro distribution as filaments matched perfectly that of the MT cytoskeleton but not when distributing as dots (lower panels). Note that, interestingly, tubulin-derived green fluorescence did colocalize with that from HCPro in large irregular inclusions (arrow in lower panels). Size bars for corresponding panels appear at the bottom right corners.

MT, an interaction that is important to virus infection (Guo et al. 2003; Haikonen et al. 2013a and b). Our present work's contribution to PVY HCPro subcellular whereabouts and dynamics in vivo uses fluorescently tagged constructs whose biological activities as suppressors have been assessed (Fig. 2). Although several studies have been published involving tagged HCPros for in vivo localization or protein–protein interaction studies using confocal or epifluorescent microscopy or Y2H assays, surprisingly little has been done to assess the effect of these tags and modifications on the biological activities of the tagged constructs in planta. To our knowledge, ours is the first assessment of suppressor activity of the different tagged HCPros studied, using agropatch assays.

With our N-terminal-tagged constructs, we could visualize fluorescence derived from both single HCPro molecules and the interacting homodimers that carried complementary BiFC tags. Our work was carried out in a virus-free system and, thus, it does not replicate the infected cell environment. As a transient expression system, there was no infection front or infected rearguard to distinguish, either. Even so, our results were remarkably in agreement with previous published observations, and data from the different constructs we have used were consistent overall. PVY HCPro showed a diffuse presence throughout the cytoplasm, as well as large irregular inclusions (Fig. 3). These inclusions could be the equivalent of amorphous inclusions observed by inmunomicroscopy (Baunoch et al. 1990). We did not observe them for construct mRFP-6x-HCPro but this might be because the tag prevented their formation, the same way that the GFP tag interfered with the suppressor activity of HCPro. However, because construct mRFP-6x-HCPro displayed good suppressor activity in agropatch assays, the irregular inclusions are seemingly not required for this function. Two features of these large inclusions can be underlined. The first is that, in the presence of heterologous suppressors of gene silencing such as P19 or 2b protein, both their number and size diminish drastically (Fig. 3). We do not know the reason for this, but we could speculate that a host factor, either protein or nucleic acid, required for the formation of these inclusions is prevented from doing so by the heterologous suppressors. In any event, it shows that inclusion formation (their number and size) is dependent on factors external to HCPro itself and suggests that they may not be as irreversible or permanent as thought. The second observation is that, in Tua-GFP transgenic plants, these large inclusions contain GFP-tagged α-tubulin (Fig. 5). This suggests that these inclusions could be linked to the MT cytoskeleton. In this regard, it appears relevant to mention that caulimovirus aphid transmission helper factor P2 (the equivalent to potyviral HCPro as and aphid helper transmission factor) accumulates in a tubulin- and virion-containing large inclusion that, in response to insect probing, disperses throughout the cell cytoplasm using the MT cytoskeleton, facilitating transmission (Martiniére et al. 2013).

We also found two additional characteristic patterns of subcellular localization of PVY HCPro. One was a not previously described pattern of small dots of similar size, distributed regularly throughout the cytoplasm, which in 16c ER-fluorescent transgenic plants appeared clearly associated or anchored to the ER (Fig. 5). ER-linked structures that bear visual resemblance to these have been reported for other virus proteins such as *Tobacco mosaic virus* movement protein (Gillespie et al. 2002) which, on its way to the proteasome for degradation, also associates with MT or, in the case of potyviruses, the 6K protein (Wei and Wang 2008), which would be related to the genesis of sites of viral replication-translation. In our virus-

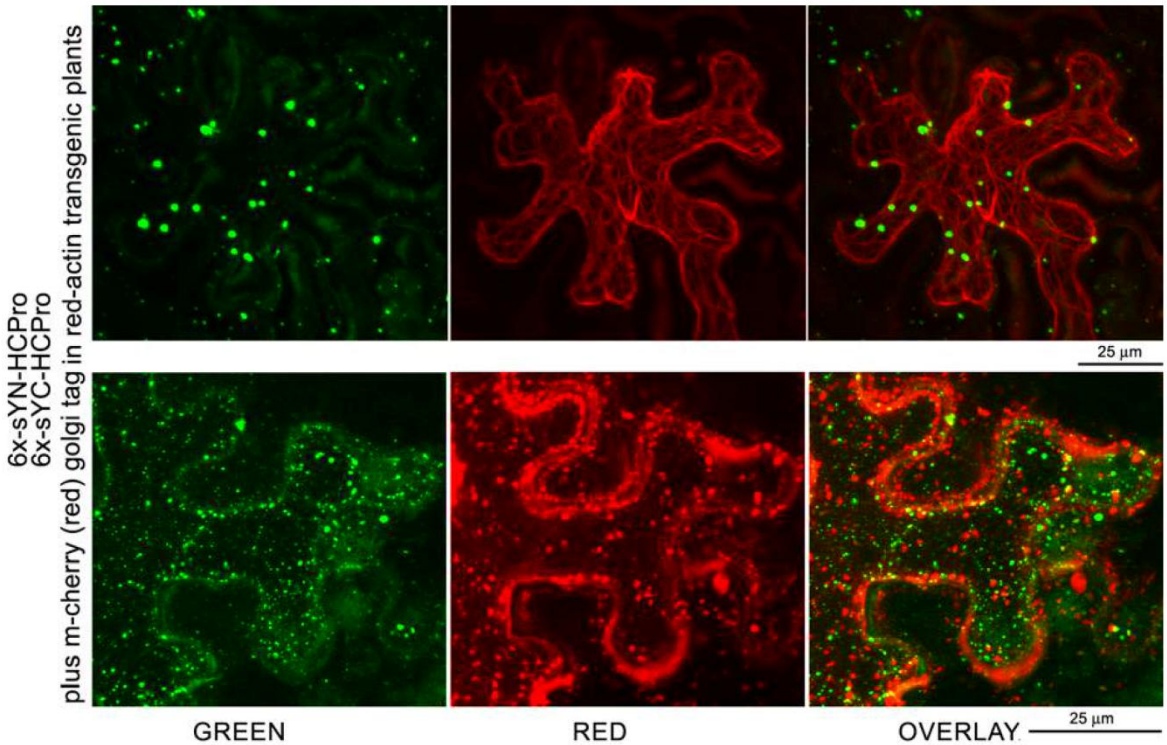

Fig. 6. Visualization of the subcellular distribution of fluorescence derived from the bimolecular fluorescence complementation (BiFC) between the two split yellow fluorescent protein (sYFP)-tagged HCPros (constructs 6x-sYN-HCPro and 6x-sYC-HCPro) transiently expressed in epidermal cells of transgenic *Nicotiana benthamiana* leaves that constitutively express a Lifeact TagRFP fusion targeting actin in the upper row of panels, or together with a binary vector that expresses mCherry protein with a targeting signal to Golgi stacks (Nelson et al. 2007) in the lower row of panels. Panels show either monochrome green (from BiFC-derived HCPro fluorescence) or red (from red actin filaments or from Golgi) fluorescence, or overlays for colocalization studies. No colocalization between green and red fluorescence was observed in both cases. Size bars for corresponding panels appear at the bottom right corners.

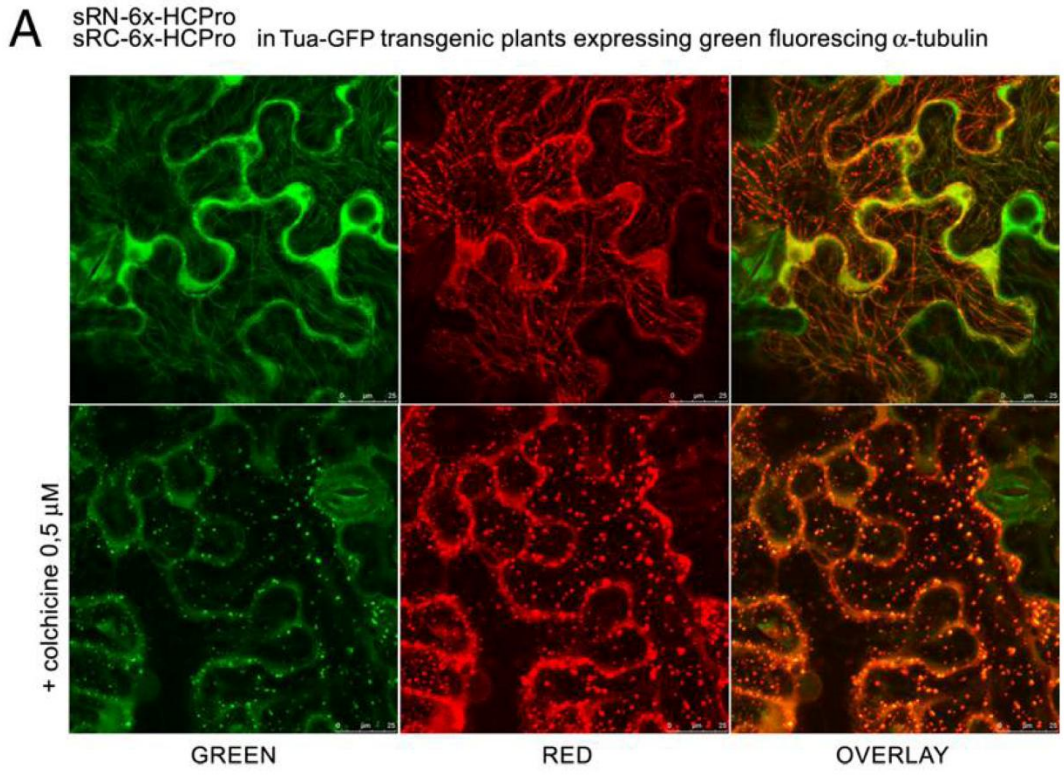

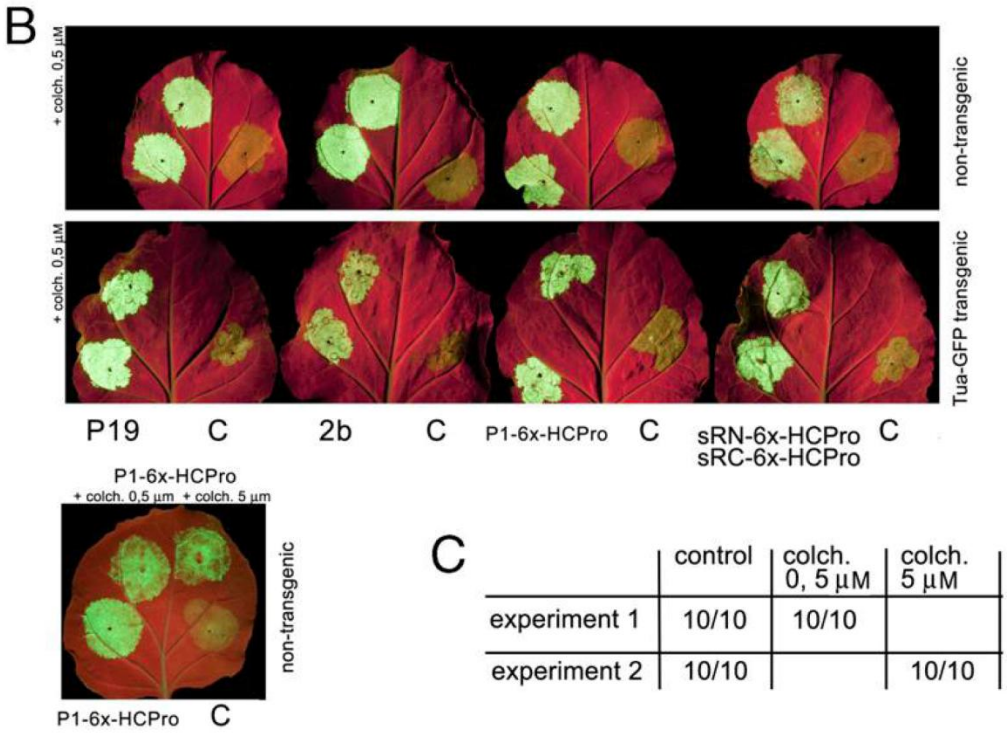

C

	control	colch. 0, 5 µM	colch. 5 µM
experiment 1	10/10	10/10	
experiment 2	10/10		10/10

Fig. 7. Disruption of the microtubule (MT) cytoskeleton and its effect on HCPro suppression of silencing activity and on its mediation of virus transmission by aphids. **A**, Visualization of the subcellular distribution of fluorescence derived from the bimolecular fluorescence complementation (BiFC) between the two split monomeric red fluorescent protein (smRFP)-tagged HCPros (constructs sRN-6x-HCPro and sRC-6x-HCPro) transiently expressed by agroinfiltration in epidermal cells of transgenic *Nicotiana benthamiana* leaves that express green fluorescent protein (GFP)-tagged α-tubulin (Tua-GFP plants) (Gillespie et al. 2002). Agrobacteria was infiltrated in the absence or presence in the agroinfiltration solution of colchicine at 0.5 µM (upper and lower rows, respectively). Colchicine had the effect of disrupting the MT cytoskeleton into dots (lower green panel). However, red fluorescence from BiFC of HCPro constructs still colocalized with that of the tubulin in those dots. **B,** Suppression of the silencing in agropatch assays of a binary vector expressing a *green fluorescent protein* (*GFP*) reporter agroinfiltrated together with the empty binary vector pROK2 (right side of leaves) or together with binary vectors expressing tombusviral P19, *Cucumber mosaic virus* 2b protein, *Potato virus Y* (PVY)-derived P1-6x-HCPro construct or the combined sRN-6x-HCPro plus sRC-6x-HCPro constructs (left side of leaves) in either the absence or presence of 0.5 µM colchicine (lower versus upper patches in left side of leaves): suppressor effects on the transient levels of fluorescence derived from the reporter did not appear affected adversely by the colchicine. **C,** Transmission by aphids of PVY from systemically infected *N. benthamiana* leaves. Leaves had been infiltrated 3 days prior to the transmission experiment with water (as control) or with colchicine (0.5 µM in experiment 1 and 5 µM in experiment 2). Five aphids were used per receptor plant. Transmission was 10 out of 10 plants in all cases.

free system, PVY HCPro localized to these structures without need of interaction with another viral factor. The second pattern showed HCPro-derived fluorescence as filaments which, in Tua-GFP plants, overlapped the fluorescent MT (Figs. 5 and 7). Interestingly, the ER-associated dots of HCPro were also connected to the MT cytoskeleton (Fig. 5, third row of images). Our results are in agreement with observations by Haikonen and associates (2013a and b) that showed, through Y2H, that HCPro from both PVY and PVA bound to the MT-associated factor HIP2. Visualization by BiFC of the PVA HCPro/HIP2 interacting pair showed a filamentous distribution (Haikonen et al. 2013b) similar to our colocalization of fluorescence from HCPro or its homodimers with that from transgenic fluorescent tubulin (Figs. 5 and 7A). Therefore, PVY HCPro BiFC homodimers may colocalize with the MT through this same host factor.

In addition to both patterns, we found numerous intermediate forms that showed both HCPro fluorescence in ER-linked dots as well as MT-linked filaments which, in our opinion, could be better explained if there was a dynamic connection between both patterns (Fig. 4). We do not know the direction of the protein transport (from dots or the diffuse cytoplasm toward MT or vice-versa) or whether it is bi- or multidirectional. An important feature of the MT-associated pattern is that it appears mainly but not exclusively after the live tissue has been subjected to stresses. Haikonen and associates (2013b) found the filamentous pattern in epidermal cells overexpressing both split YFP-tagged PVA HCPro-HIP2 BiFC constructs but not in cells expressing fluorescent HCPro, in which, instead, fluorescence spread diffusely throughout the cytoplasm. They suggest that low cellular levels of endogenous HIP2 could be responsible for the absence of a tubular pattern in the latter case. However, in our results, relocation of PVY HCPro toward the MT was extensive and took place within minutes of the added stress in those cells affected (Figs 4, 5, and 7) and, if mediated by HIP2, it would have to necessarily imply that the latter was not a limiting factor. Alternatively, HCPro coating of MT could also take place through another, HIP2-independent route. What physical process makes HCPro relocate to the MT in response to the stress? We could speculate that a host factor is released from a place where it has no contact with HCPro, or that it suffers some structural alteration that allows it to take place.

We finally tested whether the integrity of the MT cytoskeleton was required for HCPro suppressor of silencing activity or for its mediation of viral transmission by aphids. For that, we disrupted the cytoskeleton by providing colchicine as described (Wright et al. 2007). MT disruption in Tua-GFP plants did not prevent colocalization of PVY HCPro with green tubulin in dot-like structures (Fig. 7A), indicating that colocalization did not require an MT tubular architecture. In agropatch assays, we could not find a negative effect of MT disruption on the HCPro suppressor activity on the transient expression of a GFP reporter (Fig. 7B) or on the viral transmission by aphids from a PVY-infected plant (Fig. 7C); in both cases, even at doses that were 10 times higher than those needed to completely disrupt the MT. Therefore, despite the HCPro-HIP2 interaction being important to PVA infectivity (Haikonen et al. 2013b), in our experimental conditions, suppression of silencing or mediation of viral transmission by vectors functions did not require the integrity of the MT network. These results were unexpected and leave open the quest for a biological role of the binding of HCPro to MT under stress and its transit through that network for further research.

In conclusion, we have shown that, in addition to a diffuse presence throughout the cytoplasm, PVY HCPro displays several distinct subcellular localization patterns which can be influenced by the cellular environment: as large irregular, tubulin-containing inclusions; as novel, dot-sized ER- and MT-associated structures; and, finally, coating the MT in response to stresses. We also show that there is a continuum between the two latter forms that support the existence of HCPro transport between both. By contrast, in a system free from other virus components, we found no evidence of HCPro trafficking through the secretory pathway or following actin filaments. Despite its association with MT, the integrity of this tubular cytoskeleton was not necessary for HCPro suppression of silencing activity in agropatch assays or for its mediation of PVY transmission by aphids from infected plants.

MATERIALS AND METHODS

Plasmid constructs.

For transient expression in plants, proteins were cloned into the 35S promoter-polylinker-Nos terminator T-DNA cassette of pROK2-based binary vectors. Cloning of construct P1-HCPro with the *P1HCPro* sequence from PVY has already been described (Canto et al. 2002). Cloning of construct P1-6x-HCPro has also been described, as was the determination that it has suppressor activity in agropatch assays similar to that of the native protein (Tena et al. 2013). To generate constructs P1-HCPro-mRFP and P1-HCPro-GFP, the *P1-HCPro* sequence without a terminator codon was amplified by polymerase chain reaction (PCR) with appropriate oligonucleotides, digested with *Nhe*I, and cloned into *Xba*I-linearized pROK2, in frame with either the *mRFP* or *GFP* genes that had previously been inserted at the *Xba*I-*Sac*I sites of the pROK2 polylinker. For the generation of GFP- and sYFP-tagged constructs, *HCPro* sequences were amplified by PCR using appropriate oligonucleotides and cloned into pROK2 harboring *GFP* or pROK harboring sequences corresponding to sYFP N or C terminal halves already described (González et al. 2010) at the *Xba*I-*Bam*HI sites of their respective polylinkers, to generate intermediate constructs GFP-HCPro, sYN-HCPro, and sYC-HCPro. To add an N-terminal tag of methionine plus six histidines (Met-6xHis; ATG-CAT-CAC-CAT-CAC-CAT-CAC) to these three constructs as well as to construct HCPro, the sequences corresponding to the tags, if present, plus the first 5′ 330 nucleotides of the *HCPro* sequence were amplified by PCR with four appropriate 5′ oligonucleotides that contained the Met-6xHis sequence and a common 3′ oligonucleotide (nucleotides 319 to 339). The four PCR fragments were digested with *Nhe*I and *Xho*I (a unique site present at nucleotide 330 of the *HCPro* sequence) and inserted into the above-mentioned constructs and linearized with *Xba*I-*Xho*I in place of the original sequences, thus generating constructs 6x-HCPro, 6x-GFP-HCPro, 6x-sYN-HCPro, and 6x-sYC-HCPro, respectively. To insert the *Met-6xHis* sequence between the *P1* and *HCPro* sequence or between the *P1* and *GFP-HCPro* sequences, the *P1* sequence was amplified by PCR with an appropriate 5′ oligonucleotide and a 3′ oligonucleotide complementary to the end of the *P1* sequence plus a serine codon and an *Nhe*I site (CAGTTT[*P1*]AGC[serine]GCTAGC[*Nhe*I site; proline-serine]). On the other hand, two sequences from constructs 6x-HCPro and 6x-GFP-HCPro were amplified by PCR using a 5′ oligonucleotide containing the *Met-6xHis* tag sequence with an added *Nhe*I site upstream, and an appropriate 3′ oligonucleotide. These two PCR fragments were cleaned, digested with *Nhe*I, and ligated in vitro to the *Nhe*I-digested P1 PCR fragment. The ligation products were then used to amplify two PCR fusion fragments using the P1 5′ oligonucleotide and the 3′ oligonucleotide at the *HCPro* sequence (nucleotides 319 to 339). The fusion fragments thus obtained contained a *P1*-(*Ser-Pro-Ser-Met-6xHis-Met*)-*GFP* or *HCPro* sequence at the fusion

sites. The two fusion PCR products were digested with *Bam*HI and *Xho*I and cloned into equally linearized construct P1-HCPro, generating constructs P1-6x-HCPro and P1-6x-GFP-HCPro, respectively. For large-scale purifications of P1-6x-HCPro and of P1-6x-GFP-HCPro from plants, both sequences were amplified by PCR with appropriate oligonucleotides and cloned into a binary construct expressing an infectious *Potato virus X* (PVX) vector (construct pgR 107) (Lu et al. 2003), linearized with *Cla*I and *Sma*I. To obtain HCPro constructs tagged at their N-termini with the mRFP 1 or its N-terminal and C-terminal splits for BiFC, plus 6 histidines, *mRFP* or its 5′ and 3′ split part sequences were amplified by PCR with appropriate oligos and cloned into *Xba*I- and *Bam*HI-linearized pROK2 to create intermediate constructs pROK2-smRFP1, pROK2-split mRFPN (encoding the protein 168 N-terminus amino acids), and construct pROK2-split mRFPC (encoding a methionine plus the 58 C-terminus amino acids), respectively, following Zillian and Maiss (2007). On the other hand, the *HCPro* sequence was amplified by PCR from construct P1-6x-HCPro using a 5′oligo that contained a *Bam*HI site followed by *6 histidines* and a 3′oligo complementary to the 3′ end of *HCPro* coding sequence, followed by a stop codon and a *Kpn*I site. This fragment was cloned into constructs pROK2-smRFP1, pROK2-split mRFPN, and pROK2-split mRFPC and linearized with *Bam*HI and *Kpn*I to generate binary constructs mRFP-6x-HCPro, sRFPN-6x-HCPro, and sRFPC-6x-HCPro, respectively. All constructs were fully sequenced prior to experimental use. The *2b* sequence from CMV var. Fny was amplified by the PCR with appropriate oligos and cloned into *Bam*HI- and *Sac*I-linearized constructs pROK2-split mRFPN and pROK2-split mRFPC to create constructs sRFPN-2b and sRFPC-2b, respectively, which express the CMV 2b suppressor fused to the split parts of the mRFP.

Plant material.

This work used *N. benthamiana* plants, either wild-type or transgenic, for the constitutive expression of GFP targeting the cortical ER (line 16c) (Ruíz et al. 1998), of GFP fused to *A. thaliana* α-tubulin (Tua-GFP) (Gillespie et al. 2002), or a Lifeact TagRFP fusion targeting actin filaments. Lifeact TagRFP plasmid was made by primer extension PCR, as described by Berepiki and associates (2010). Gateway adapters were added by PCR with primers 5′-GGGGACAAGTTTGTACAAAAAA GCAGGCTGCATGGGTGTCGCAGATTTGATCAAG-3′ and 5′-GGGGACCACTTTGTACAAGAAAGCTGGGTCTTACT TGTACAGCTCGTCCATGCC-3′, and the resulting PCR product was recombined into pDONR207 (LifeTechnologies). After sequence verification, Lifeact TagRFP was recombined into pGRAB.TEVL (SC1046), a derivative of pGreen0229 containing a 35S promoter and a TEV leader sequence upstream of the Gateway cassette. pGRAB.TEVL Lifeact TagRFP plasmids were mobilized into *Agrobacterium* strain AGL1+psoup and used to transform *N. benthamiana* leaf segments as described by Horsch and associates (1985), with Basta-resistant plants being regenerated and screened for expression by fluorescence microscopy.

Expression of proteins in plants from binary vectors, and purification of HCPro and PVY.

For transient expression assays, binary vectors were transferred to the same batch of electrocompetent *Agrobacterium tumefaciens* C58C1 derived from a single colony, to prevent bacterial variability. Cultures were grown to exponential phase in Luria-Bertani medium with antibiotics at 28°C. For infiltration, each bacterial culture harboring a different T-DNA was diluted to a final optical density of 0.2 at 600 nm. Different cultures harboring different T-DNAs were then combined and infiltration of the mixtures was performed on fully expanded leaves of nonflowering *N. benthamiana* plants using a syringe, as described (Canto et al. 2002). Large-scale purifications of P1-6x-HCPro and of P1-6x-GFP-HCPro were performed from plants infected with constructs PVX-P1-6x-HCPro and PVX-P1-6x-GFP-HCPro, as described (Tena et al. 2013). A purified virion prep from an aphid-transmissible PVY isolate (Scottish ordinary variety PVY-O; Scottish Agricultural Science Agency), from which the *P1-HCPro* sequence used in this study derived (Canto et al. 2002), was obtained from systemically infected *N. benthamiana* plants as described, omitting the sucrose gradient final step (Moghal and Francki 1976).

Local suppression of silencing in agroinfiltration patch assays.

A free *GFP* reporter gene expressed from a binary vector under the control of the 35S promoter was expressed transiently in an *N. benthamiana* leaf, either co-infiltrated with the empty binary vector pROK2 or with another vector expressing a protein to be tested for suppression of silencing activity. To monitor the effect of the second protein on the levels of fluorescence derived from the transiently expressed free enhanced GFP, leaves were illuminated at 3 to 6 days postinoculation (dpi) with a Blak Ray long-wave UV lamp (UVP, Upland, CA, U.S.A.) and photographed as previously described (González et al. 2010).

Imaging of fluorescence from tagged proteins in live cells and tissues, and chemical treatments.

Epidermal cells in *N. benthamiana*-infiltrated leaves were monitored live for fluorescence derived from GFP-, mRFP-, smRFP-, mCherry-, or sYFP-tagged proteins transiently expressed at 3 to 5 dpi. Imaging was conducted with Leica SP2 and SP5 (Leica Microsystems GmbH, Heidelberg, Germany) confocal laser-scanning microscopes and software, using fresh leaf tissue and ×63 magnification oil immersion objectives. Excitation and emission settings in nanometers were the following: GFP (488 and 500 to 530); BiFC sYFP (514 and 530 to 550); and mRFP, BiFC smRFP, and mCherry (561 and 575 to 640). To visualize the cortical ER, actin filaments, or MT cytoskeleton transgenic *N. benthamiana* plants constitutively expressing GFP fused to *Arabidopsis thaliana* α-tubulin (Tua-GFP plants) (Gillespie et al. 2002), GFP targeting the cortical ER (16c plants) (Ruíz et al. 1998) and a Lifeact TagRFP fusion targeting actin were also used. To visualize the Golgi apparatus, a binary vector expressing mCherry protein with a targeting signal to this structure was used (Nelson et al. 2007). In colocalization studies, every single frame was imaged consecutively for green and red fluorescence. These green and red simultaneous frames were then Z-axis-stacked to create final projections.

Chemical treatments for MT disruption were performed with colchicine (Sigma-Aldrich C9754) at the dilution of 0.5 μM, as described by Wright and associates (2007), unless otherwise stated. The disrupting agent was infiltrated simultaneously with the *Agrobacterium* solutions. Exposure of infiltrated tissue to two different supermarket brands of common nail varnish (Vera Valenti, classic; Vera Valenti, San Fernando de Henares, Spain; and Deliplus, gel acabado brillo; You Cosmetics, Gava, Spain) was achieved by directly sealing the edges of the fresh tissue to the microscope slide prior to confocal viewing. Exposure of infiltrated tissue to organic solvents (n-butyl acetate and ethyl acetate) was achieved by keeping freshly cut tissue inside a wet chamber saturated with fumes from either of these two chemicals for 1 h at room temperature, prior to confocal viewing. Exposure of infiltrated tissue to saturated CO_2 atmosphere was achieved as described by Martiniére and associates (2013).

Immunoblot detection of proteins.

Total protein content from infiltrated tissue was ground with a pestle in extraction buffer (0.1 M Tris-HCl [pH 8], 10 mM ethylenediaminetetraacetic acid, 0.1 M LiCl, 1% β-mercaptoethanol, and 1% sodium dodecyl sulfate [SDS]), mixed 1:1 with 2× Laemmli buffer, and the sample was incubated for 10 min at 95°C under shaking and clarified in the bench microfuge for 5 min before fractionation in SDS polyacrylamide gel electrophoresis 10% gels. Gel proteins were wet-blotted in Tris-glycine buffer onto Hybond-P polyvinylidene diflouride membranes (Amersham, GE Healthcare, Buckinghamshire, U.K.) For immunological detection of GFP, a rabbit GFP polyclonal antiserum kindly donated by G. Cowan (James Hutton Institute, Dundee, U.K.) was used. For detection of 6x-HCPro, a mouse monoclonal antiserum to 6-histidines was used (Sigma-Aldrich, St. Louis). In the Western blot shown in Figure 5C, a rabbit polyclonal antiserum against PVY HCPro was used (Canto et al. 1995a). Blotted proteins were detected using commercial alkaline phosphatase-conjugated secondary antibodies and SigmaFast BICP/NBT substrate tablets (Sigma-Aldrich).

Aphid transmission tests and exposure of leaf tissue to aphids.

Transmission tests of PVY from either infected *N. benthamiana* fresh leaf tissue or from solutions of purified virions through stretched parafilm membranes, the latter in combination with purified HCPro, was performed using a clone of the aphid *Myzus persicae* and as described (Canto et al. 1995b). To expose infiltrated tissue to aphids, 50 aphids were harvested and placed under confinement on an infiltrated patch of approximately 15 mm in diameter for 16 h, at room temperature in a wet chamber, prior to confocal viewing.

ACKNOWLEDGMENTS

This work was supported by a joint grant between the Spanish Ministry of Economy and Competitivity (MEC; grant ACI/2009-0855) and the Department of Science and Technology of the Government of India (grant DST/INT/SPAIN/P-9/2009); by a grant from the Rural Development Administration (RDA) of the Republic of Korea "Prediction of the impact of climate change on the outcome of diseases caused by plant RNA viruses", in cooperation with the Spanish Council for Scientific Research (CSIC); and by grant BIO2013-47940-R from MEC. T. Canto acknowledges the help of former students I. González and P. Doblas at cloning steps required to obtain some of the constructs used in this work. J. Tilsner and K. M. Wright gratefully acknowledge the advice of M. Smoker (The Sainsbury Laboratory) and technical support from W. Ridley in the generation of the red-actin transgenic *N. benthamiana* plants. We also thank M. Hallett for proofreading the manuscript.

LITERATURE CITED

Ala-Poikela, M., Goytia, E., Halkonen, T., Rajamaki, M.-L., and Valkonen, J. P. T. 2011. Helper component proteinase of the genus *Potyvirus* is an interaction partner of translation initiation factors sIF(iso)4E and eIF4E and contains a 4E binding motif. J. Virol. 85:6784-6794.

Anandalakshmi, R., Pruss, G. J., Ge, X., Marathe, R., Mallory, A. C., Smith, T. H., and Vance, V. B. 1998. A viral suppressor of gene silencing in plants. Proc. Natl. Acad. Sci. U.S.A. 95:13079-13084.

Ballut, L., Drucker, M., Pugniére, M., Cambon, F, Blanc, S., Roquet, F., Candresse, T., Schmid, H.-P., Nicolas, P, Le Gall, O., and Badaoui, S. 2005. HcPro, a multifunctional protein encoded by a plant RNA virus, targets the 20S proteasome and affects its enzymatic activities. J. Gen. Virol. 88:2595-2603.

Baunoch, D. A., Das, P., and Hari, V. 1990. Potato virus Y helper component is associated with amorphous inclusions. J. Gen. Virol. 71:2479-2482.

Berepiki, A., Lichius, A., Shoji, J.-Y., Tilsner, J., and Read, N. 2010 F-actin dynamics in *Neurospora crassa*. Eukaryot. Cell 9:547-557.

Blanc, S., López-Moya, J.-J., Wang, R., García-Lampasona, S., Thornbury, D.-W., and Pirone, T. P. 1997. A specific interaction between coat protein and helper component correlates with aphid transmission of a potyvirus. Virology 231:141-147.

Brigneti, G., Voinnet, O., Li, W. X., Ding, S. W., and Baulcombe, D. C. 1998. Viral pathogenicity determinants are suppressors of transgene silencing in *Nicotiana benthamiana*. EMBO (Eur. Mol. Biol. Organ.) J. 17:6739-6746.

Canto, T., Ellis, P., Bowler, G., and López-Abella, D. 1995a. Production of monoclonal antibodies to Potato virus Y helper component-protease and their use for strain differentiation. Plant Dis. 79:234-237.

Canto, T., López-Moya, J. J., Serra-Yoldi, M. T., Díaz-Ruíz, J. R., and López-Abella, D. 1995b. Different helper component mutations associated with lack of aphid transmissibility in two isolates of Potato virus Y. Phytopathology 85:1519-1524.

Canto, T., Cillo, F., and Palukaitis, P. 2002. Generation of siRNAs by T-DNA sequences does not require active transcription or homology to sequences in the plant. Mol. Plant-Microbe Interact. 15:1137-1146.

Carrington, J. C., and Herndon, K. L. 1992. Characterization of the potyviral HC-Pro autoproteolytic cleavage site. Virology 187:308-315.

Carrington, J. C., Cary, S. M., and Dougherty, W. G. 1988. Mutational analysis of Tobacco etch virus polyprotein processing: cis- and trans-proteolytic activities of polyproteins containing the 49-kDa proteinase. J. Virol. 62:2313-2320.

Chapman, E. J., Prokhnevsky, A. I., Gopinath, K., Dolja, V. V., and Carrington, J. 2004. Viral RNA silencing suppressors inhibit the microRNA pathway at an intermediate step. Genes Dev. 18:1179-1186.

Cheng, Y.-Q., Liu, Z.-M., Xu, J., Zhou, T., Wang, M., Chen, Y.-T., Li, H.-F., and Fan, Z.-F. 2008. HC-Pro protein of sugar cane mosaic virus interacts specifically with maize ferredoxin-*5* in vitro and in planta. J. Gen. Virol. 89:2046-2054.

Chung, B. Y.-W., Miller, W. A., Atkins, J. F., and Firth, A. E. 2008. An overlapping essential gene in the Potyviridae. Proc. Natl. Acad. Sci. U.S.A. 105:5897-5902.

Dielen, A.-S., Sassaki, F. T., Walter, J., Michon, T., Menard, G., Pagny, G., Krause-Sakate, R., Maia, I., Badaoui, S., Le Gall, O., Candresse, T., and German-Retama, S. 2011. The 20S proteasome α_5 subunit of *Arabidopsis thaliana* carries and RNase activity and interacts *in planta* with the *Lettuce mosaic potyvirus* HcPro protein. Mol. Plant Pathol. 12:137-150.

Endres, M. W., Gregory, B. D., Gao, Z., Foreman, A. W., Mlotshwa, S., Ge, X., Pruss, G. J., Ecker, J. R., Bowman, L. H., and Vance, V. 2010. Two plant viral suppressors of silencing require the ethylene-inducible host transcription factor RAV2 to block RNA silencing. PLoS Pathog. 6:e1000729.

Freire, M. A. 2014. Potyviral VPg and HC-Pro proteins and the cellular translation initiation factor aIF(iso)4E interact with exoribonuclease Rrp6 and a small α-heat shock protein. Plant Mol. Biol. Rep. 32:596-604.

García, J. A., Riechmann, J. L., and Laín, S. 1989. Proteolytic activity of the Plum pox potyvirus NIa-like protein in *Escherichia coli*. Virology 170:362-369.

Gillespie, T., Boevink, P., Haupt, S., Roberts, A. G., Toth, R., Valentine, T., Chapman, S., and Oparka, K. J. 2002. Functional analysis of a DNA-shuffled movement protein reveals that microtubules are dispensable for the cell-to-cell movement of *Tobacco mosaic virus*. Plant Cell 14:1207-1222.

González, I., Martínez, L. L., Rakitina, D., Lewsey, M. G., Atienzo, F. A., Llave, C., Kalinina, N., Carr, J. P., Palukaitis, P., and Canto, T. 2010. *Cucumber mosaic virus* 2b protein subcellular targets and interactions: Their significance to its RNA silencing suppressor activity. Mol. Plant-Microbe Interact. 23:294-303.

González, I., Rakitina, D., Semashko, M., Taliansky, M., Praveen, S., Palukaitis, P., Carr, J. P., Kalinina, N., and Canto, T. 2012. RNA binding is more relevant to the suppression of silencing function of *Cucumber mosaic virus* 2b protein than nuclear localization. RNA 18:771-782.

Govier, D. A., and Kassanis, B. 1974. Evidence that a component other than the virus particle is needed for aphid transmission of Potato virus Y. Virology 57:285-286.

Guo, D., Spetz, C., Saarma, M., and Valkonen, J. P. T. 2003. Two potato proteins, including a novel RING finger protein (HIP1), interact with the potyviral multifunctional protein HCpro. Mol. Plant-Microbe Interact. 16:405-410.

Haikonen, T., Rajamäki, M.-L., Tian, Y.-P., and Valkonen, J. P. T. 2013a. Mutation of a short variable region in HCpro protein of *Potato virus A* affects interactions with a microtubule-associated protein and induces necrotic responses in tobacco. Mol. Plant-Microbe Interact. 26:721-733.

Haikonen, T., Rajamaki, M.-L., and Valkonen, J. P. T. 2013b. Interaction of the microtubule-associated host protein HIP2 with viral helper component proteinase is important in infection with *Potato virus A*. Mol. Plant-Microbe Interact. 26:734-744.

Horsch, R. B., Fry, J. E., Hoffman, N. L., Eichholtz, D., Rogers, S. G., and Fraley, R. T. 1985. A simple and general method for transferring genes into plants. Science 227:1229-1231.

Jamous, R. M., Boonrod, K., Fuellgrabe, M. W., Ali-Shetayen, M. S., Krczai, G., and Wassenegger, M. 2011. The helper component-proteinase of the *Zucchini yellow mosaic virus* inhibits the Hua Enhancer 1 methyltransferase activity in vitro. J. Gen. Virol. 92:2222-2226.

Jin, Y., Ma, D., Dong, J., Jin, J., Li, D., Deng, C., and Wang, T. 2007a. HC-Pro of *Potato virus Y* can interact with three *Arabidopsis* 20S proteasome subunits in planta. J. Virol. 81:12881-12888.

Jin, Y., Ma, D., Dong, J., Li, D., Deng, C., Jin, J., and Wang, T. 2007b. The HC-Pro protein of *Potato virus Y* interacts with NtMinD of tobacco. Mol. Plant-Microbe Interact. 20:1505-1511.

Johansen, L. K., and Carrington, J. C. 2001. Silencing on the spot. Induction and suppression of RNA silencing in the *Agrobacterium*-mediated transient expression system. Plant Physiol. 126:930-938.

Lakatos, L., Csorba, T., Pantaleo, V., Chapman, E. J., Carrington, J. C., Liu, Y.-P., Dolja, V.V., Calvino, L. F., López-Moya, J. J., and Burgyán, J. 2006. Small RNA binding is a common strategy to suppress RNA silencing by several viral suppressors. EMBO (Eur. Mol. Biol. Organ.) J. 25:2768-2780.

Lu, R., Malcuit, I., Moffett, P., Ruíz, M. T., Peart, J., Wu, A. J., Rathjen, J. P., Bendahmane, A., Day, L., and Baulcombe, D. C. 2003. High throughput virus-induced gene silencing implicates heat shock protein 90 in plant disease resistance. EMBO (Eur. Mol. Biol. Organ.) J. 22:5690-5699.

Maia, I. G., and Bernardi, F. 1996. Nucleic acid-binding properties of a bacterially expressed potato virus Y helper component protinase. J. Gen. Virol. 77:869-877.

Mangrauthia, S. K., Singh Shakya, V. P., Jain, R. K., and Praveen, S. 2009. Ambient temperature perception in papaya for *Papaya ringspot virus* interaction. Virus Genes 38:429-434.

Martinière, A., Bak, A., Macia, J.-L., Lautredou, N., Gargani, D., Doumayrou, J., Garzo, E., Moreno, A., Fereres, A., Blanc, S., and Drucker, M. 2013. A virus responds instantly to the presence of the vector on the host and forms transmission morphs. Elife 2:e00183.

Mérai, Z., Kerényi, Z., Kertész, S., Magda, M., Lakatos, L., and Silhavy, D. 2006. Double-stranded RNA binding may be a general plant RNA viral strategy to suppress silencing. J. Virol. 80:5747-5756.

Mlotshwa, S., Verver, J., Sithole-Niang, I., Gopinath, K., Carette, J., Van Kammen, A. B., and Wellink, J. 2002. Subcellular location of the helper component-protease of *Cowpea aphid-borne mosaic virus*. Virus Genes 25:207-216.

Moghal, S. M., and Francki, R. I. B. 1976. Towards a system for the identification and classification of potyviruses. Virology 73:350-362.

Nakahara, K. S., Masuta, C., Yamada, S., Shimura, H., Kashihara, Y., Wada, T. S., Meguro, A., Goto, K., Tadamura, K., Sueda, K., Sekiguchi, T., Shao, J., Itchoda, N., Matsumara, T., Igarashi, M., Ito, K., Carthew, R. W., and Uyeda, I. 2012. Tobacco calmodulin-like protein provides secondary defense by binding to and directing degradation of virus RNA silencing suppressors. Proc. Natl. Acad. Sci. U.S.A. 109:10113-10118.

Nelson, B. K., Cai, X., and Nebenführ, A. 2007. A multicolored set of in vivo organelle markers for co-localization studies in *Arabidopsis* and other plants. Plant J. 51:1126-1136.

Pasin, F., Simón-Mateo, C., and García, J. A. 2014. The hypervariable amino-terminus of P1 protease modulates potyviral replication and host defense responses. PLoS Pathog. 10:e1003985.

Plisson, C., Drucker, M., Blanc, S., German-Retama, S., Le Gall, O., Thomas, C., and Bron, P. 2003. Structural characterization of HC-Pro, a plant virus multifunctional protein. J. Biol. Chem. 278:23753-23761.

Pruss, G., Ge, X., Shi, X. M., Carrington, J. C., and Vance, V. B. 1997. Plant viral synergism: The potyviral genome encodes a broad-range pathogenicity enhancer that transactivates replication of heterologous viruses. Plant Cell 9:859-868.

Rajamaki, M.-L., Kelloniemi, J., Alminaite, A., Kekarainen, T., Rabenstein, F., and Valkonen, J. P. T. 2005. A novel insertion site inside the potyvirus P1 cistron allows expression of heterologous proteins and suggests some P1 functions. Virology 342:88-101.

Roudet-Tavert, G., German-Retama, S., Delaunay, T., Delécolle, B., Candresse, T., and Le Gall, O. 2002. Interaction between potyvirus helper component-proteinase and capsid protein in infected plants. J. Gen. Virol. 83:1765-1770.

Ruíz, M. T., Voinnet, O., and Baulcombe, D. C. 1998. Initiation and maintenance of virus-induced gene silencing. Plant Cell 10:937-946.

Ruíz-Ferrer, V., Boskovic, J., Alfonso, C., Rivas, G., Llorca, O., López-Abella, D., and López-Moya, J. J. 2005. Structural analysis of *Tobacco etch potyvirus* HC-Pro oligomers involved in aphid transmission. J. Virol. 79:3758-3765.

Sahana, N., Kaur, H., Basavaraj, Y. B., Tena, F., Jain, R. K., Palukaitis, P., Canto, T., and Praveen, S. 2012. Inhibition of the host proteasome facilitates Papaya ringspot virus accumulation and proteosomal catalytic activity is modulated by viral factor HcPro. PLoS One 7:e52546.

Sahana, N., Kaur, H., Palukaitis, P., Canto, T., and Praveen, S. 2014. The asparagine residue in the FRNK box of potyviral helper-component protease is critical for template function and subcellular localization. J. Gen. Virol. 95:1167-1177.

Shiboleth, Y. M., Haronsky, E., Leibman, D., Arazi, T., Wassenegger, M., Whitham, S. A., Gaba, V., and Gal-On, A. 2007. The conserved FRNK box in HC-Pro, a plant viral suppressor of gene silencing, is required for small RNA binding and mediates symptom development. J. Virol. 81:13135-13148.

Sorel, M., García, J. A., and German-Retana, S. 2014. The Potyviridae cylindrical inclusion helicase: A key multipartner and multifunctional protein. Mol. Plant-Microbe Interact. 27:215-226.

Tena, F., González, I., Doblas, P., Rodríguez, C., Sahana, N., Kaur, H., Tenllado, F., Praveen, S., and Canto, T. 2013. The influence of cis-acting P1 protein and translational elements on the expression of *Potato virus Y* HCPro in heterologous systems and its suppression of silencing activity. Mol. Plant Pathol. 14:530-541.

Thornbury, D. W., Hellmann, G. M., Rhoads, R. E., and Pirone, T. P. 1985. Purification and characterization of potyvirus helper component. Virology 144:260-267.

Torrance, L., Andreev, I. A., Gabrenaite-Verhovskaya, R., Cowan, G., Mäkinen, K., and Taliansky, M. E. 2006. An unusual structure at one end of potato potyvirus particles. J. Mol. Biol. 357:1-8.

Urcuqui-Inchima, S., Walter, J., Drugeon, G., German-Retama, S., Haenni, A-L., Candresse, T., Bernardi, F., and Le Gall, O. 1999. Potyvirus helper component-proteinase self-interaction in the yeast two-hybrid system and delineation of the interaction domain involved. Virology 258:95-99.

Urcuqui-Inchima, S., Maia, I. G., Arruda, P., Haenni, A.-L., and Bernardi, F. 2000. Deletion mapping of the potyviral helper component-proteinase reveals two regions involved in RNA binding. Virology 268:104-111.

Valli, A., Martín-Hernández, A. M., López-Moya, J. J., and García, J. A. 2006. RNA silencing suppression by a second copy of the P1 serine protease of *Cucumber vein yellowing ipomovirus*, a member of the Family *Potyviridae* that lacks the cysteine protease HCPro. J. Virol. 80:10055-10063.

Vargasson, J. M., Szittya, G., Burgyan, J., and Hall, T. M. 2003. Size selective recognition of siRNAs by an RNA silencing suppressor. Cell 115:799-811.

Verchot, J., and Carrington J. C. 1995a. Debilitation of plant potyvirus infectivity by P1 proteinase-inactivating mutations and restoration by second -site modifications. J. Virol. 69:1582-1590.

Verchot, J., and Carrington J. C. 1995b. Evidence that the potyvirus P1 protein functions as an accessory factor for genome amplification. J. Virol. 69:3668-3674.

Verchot, J., Koonin, E. V., and Carrington, J. C. 1991. The 35-kDa protein from the N-terminus of the potyviral polyprotein functions as a third virus-encoded proteinase. Virology 185:527-535.

Wei, T., and Wang, A. 2008. Biogenesys of cytoplamic membranous vesicles for plant potyvirus replication occurs at endoplasmic reticulum exit sites in a COPI- and CPII-dependent manner. J. Virol. 82:12252-12264.

Wei, T., Huang, T.-S., McNeil, J., Laliberté, J.-F., Hong, J., Nelson, R. S., and Wang, A. 2010a. Sequential recruitment of the endoplasmic reticulum and chloroplasts for plant potyvirus replication. J. Virol. 84:799-809.

Wei, T., Zhang, C., Hong, J., Xiong, R., Kasschau, K. D., Zhou, X., Carrington, J. C., and Wang, A. 2010b. Formation of complexes at plasmodesmata for potyvirus intercellular movement is mediated by the viral protein P3N-PIPO. PLoS Pathog. 6:e1000962.

Wei , T., Zhang, C., Hou, X., Sanfacon, H., and Wang, A. 2013. The SNARE protein Syp71 is essential for *Turnip mosaic virus* infection by mediating fusion of virus-induced vesicles with chloroplasts. PLoS Pathog. 9:e1003378.

Wright, K., Wood, N. T., Roberts, A., Chapman, S., Boevink, P., MacKenzie, K. M., and Oparka, K. 2007. Targeting of TMV movement protein to plasmodesmata requires actin/ER network: Evidence from FRAP. Traffic 8:21-31.

Zheng , H., Yan, F., Lu, Y., Sun, L., Lin, L., Cai, L., Hou, M., and Chen, J. 2011. Mapping the self-interacting domains of TuMV HC-Pro and the subcellular localization of the protein. Virus Genes 42:110-116.

Zilian, E., and Maiss, E. 2011. Detection of plum pox potyviral protein-protein interactions *in planta* using an optimized mRFP-based bimolecular fluorescence complementation system. J. Gen. Virol. 92:2711-2723.

Supplemental Material

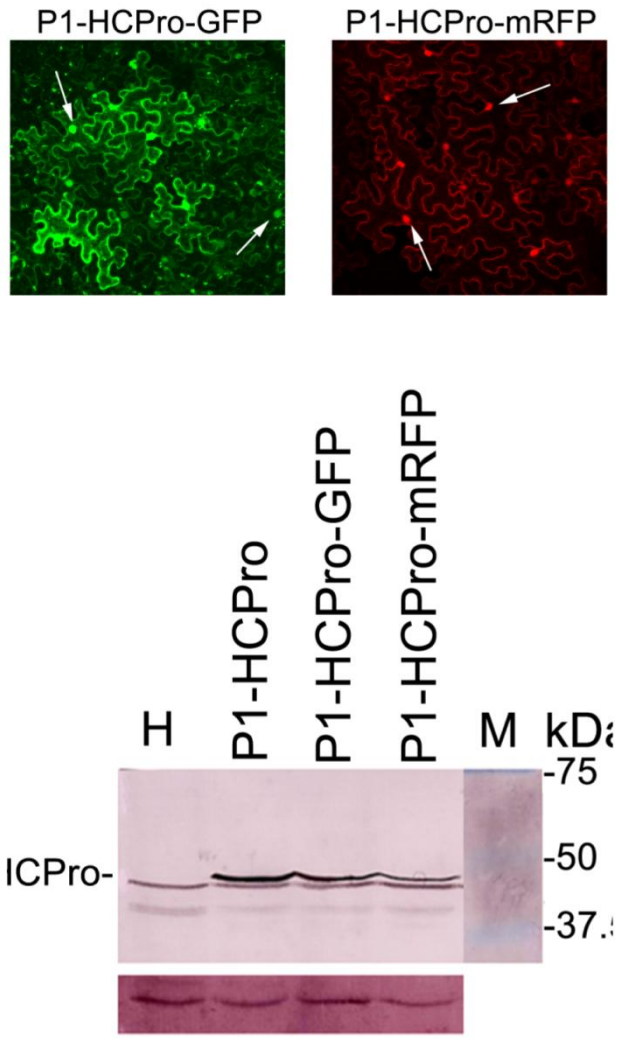

Supplementary Fig. S1. Visualization of the subcellular distribution of fluorescence derived from constructs P1HCPro-GFP and P1HCPro-mRFP transiently expressed in epidermal cells of *Nicotiana benthamiana* leaves (left and right panels, respectively). In both C-terminal fusion constructs the second glycine at the HCPro protease cleavage site (tyrosine-X-valine-**glycine/glycine**) had been replaced by tyrosine-arginine-valine-**glycine/alanine**, a motif shown previously not to be cleaved by TEV HCPro in rabbit reticulocyte lysates (Carrington and Herndon, 1992). These two constructs with C-terminal tags both showed strong suppression of silencing of the *GFP* reporter, comparable to that of the native suppressor (data not shown). Confocal microscopy also detected GFP and mRFP-derived fluorescence. However, it targeted not only cytoplasm but also nuclei, as do native GFP and mRFP (Supplemental Fig. S1, upper panels, with arrows pointing at nuclei). Western blot analysis with a rabbit anti-HCPro polyclonal antibody of protein accumulation in patches of *Nicotiana benthamiana* agroinfiltrated with constructs P1-HCPro, P1-HCPro-GFP and P1-HCPro-mRFP (lanes labeled P1-HCPro, P1-HCPro-GFP and P1-HCPro-mRFP, respectively), which should express native HCPro or HCPro fused at its C- terminus to green fluorescent protein (GFP) or monomeric red fluorescent protein (mRFP), respectively detected in the three cases a protein of the size of native HCPro, around 50 kDa. Although we cannot rule out that the fusion proteins lost their tags by the deletion of some C-terminal fragment of HCPro upstream of the protease site it appears more likely that the Gly/Ala was recognized and cleaved by PVY HCPro in planta. Published experiments on the HCPro proteolytic cleavage site were performed with TEV HCPro in vitro, using rabbit reticulocyte lysates. In this

(Contionuation of Supplementary Fig. S1) regard, although the over one hundred published sequences of members of the genus *Potyvirus*, all have an HCPro/P3 Gly/Gly cleavage site, in the closely related *Bymovirus* genus, *Barley mild mosaic virus* P1-Pro cysteine protease activity has a tyrosine-arginine-valine-glycine/alanine as cleavage site (http://www.dpvweb.net/potycleavage/). Lane H shows a sample extracted from a healthy plant, and M, pre-stained markers for molecular weight, indicated in kilodaltons (kDa). The lower panels below the Western blot shows the Ponceau S-stained membranes after blotting, as controls of loading.

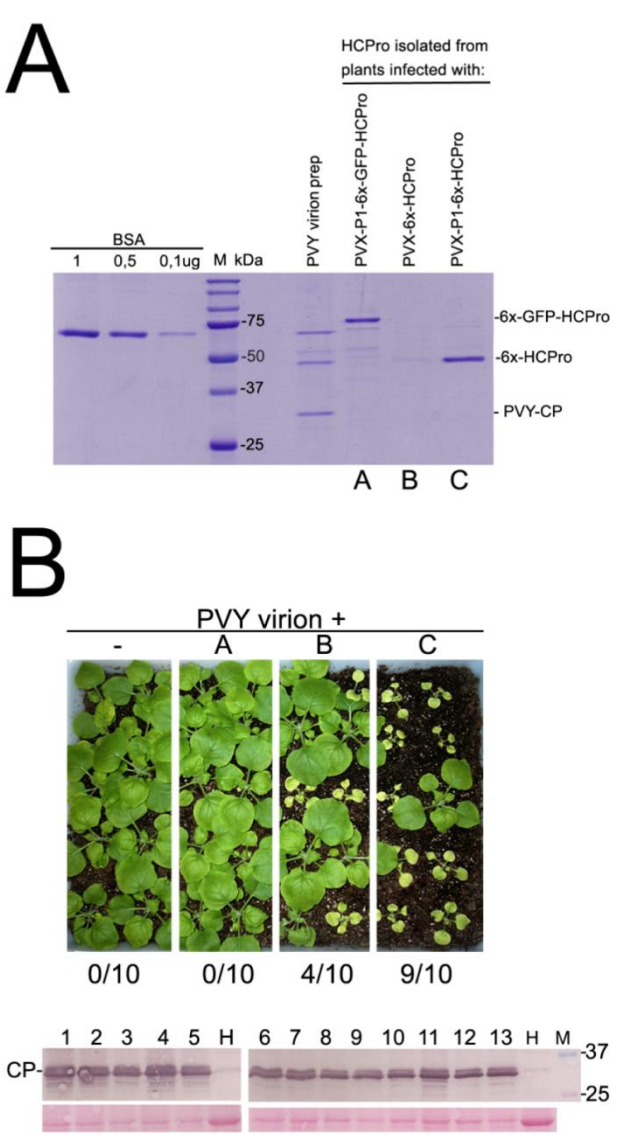

Supplementary Fig. S2. Assessment of the ability of HCPro constructs to mediate transmission by the peach aphid *Myzus persicae* of *Potato virus Y* (PVY). Purified preps from both PVY and HCPro constructs were obtained from *Nicotiana benthamiana* plants infected with PVY or with *Potato virus X* (PVX) vectors expressing P1-6x-GFP-HCPro, P1-6x-HCPro or 6x-HCPro (without P1 but with an additional N-terminal methionine). **A**, yields of purified preps resolved in an 10 % polyacrylamide SDS-APGE gel, together with bovine serum albumin (BSA) as standards for quantification of protein amounts. **B,** aphids fed through stretched parafilm membranes on 50 µl solutions containing 8 µl of virion prep and 42 µl of either buffer (sample -) or purified HCPros: A, [6x-GFP-HCPro 0.05 ug/ul]; B [6x-HCPro 0.008 ug/ul]; C [6x-HCPro 0.07 ug/ul]. Ten aphids/receptor plant were used. In those plants that showed symptoms of infection by PVY (Chlorosis, stunting) the presence of the virus was confirmed by Western blot analysis of total extracts with an

Continuation of Supplementary Fig. S2) anti PVY CP antibody (Western blot panels). While preps B and C (6x-HCPros) allowed transmission of PVY (4 out of **(**10 and 9 out of 10 plants infected, respectively), sample A (6x-GFP-HCPro) did not (no plants infected) despite its higher concentration of protein. Lanes H in Western blot panels show samples extracted from healthy plants, and M, pre-stained markers for molecular weight, indicated in kilodaltons (kDa). The lower panels below the Western blots show the Ponceau S-stained membranes after blotting, as controls of loading.

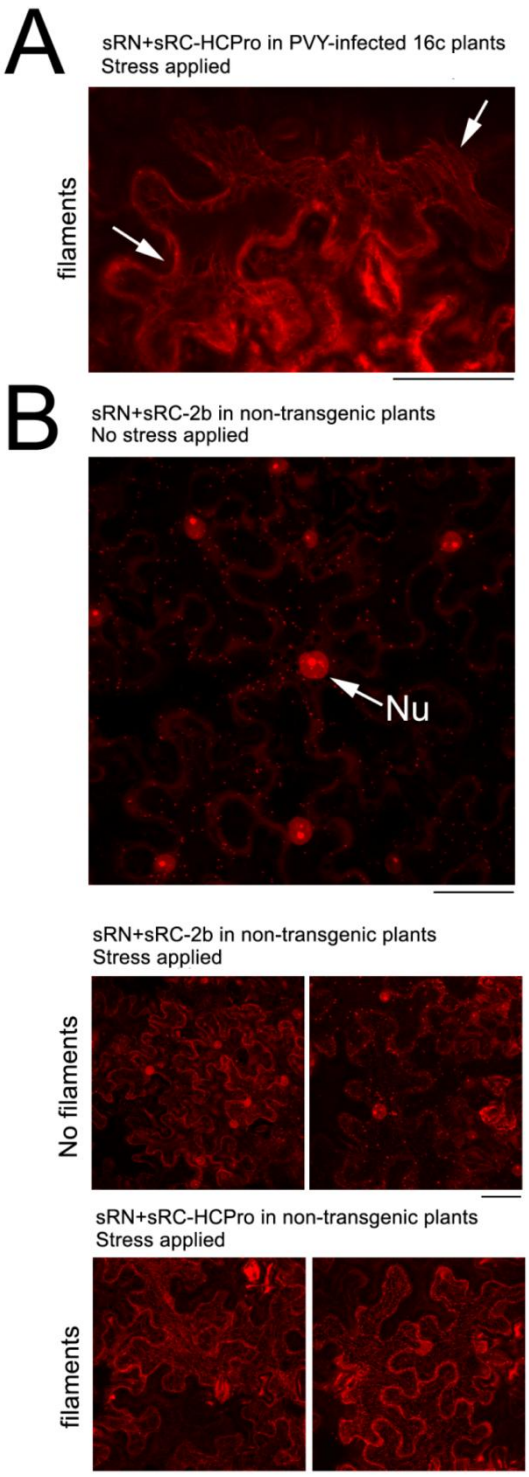

Supplementary Fig. S3. Visualization of the subcellular distribution of fluorescence derived from the bimolecular fluorescence complementation (BiFC) between the two split monomeric red fluorescent protein (smRFP)-tagged suppresors transiently expressed by agroinfiltration under different environmental conditions. **A**, (smRFP)-tagged HCPro (constructs sRN-6x-HCPro and sRC-6x-HCPro) in line 16c transgenic *Nicotiana benthamiana* leaf tissue already infected by PVY. Despite very low fluorescence derived from the BiFC-tagged HCPros, some cells displayed the filament pattern under stress conditions, indicated by arrows, suggesting that HCPro may associate with Microtubules (MT) also in a viral context. **B**, (smRFP)-tagged 2b protein transiently expressed by agroinfiltration in epidermal cells of non-transgenic *N. benthamiana* shows a nuclear and nucleolar localization pattern (Nu arrow in upper panel), but also some cytoplasmic diffuse fluorescence, as well as cytoplasmic dots not yet characterized (upper panel). Under stress conditions, fluorescence from BiFC-tagged 2b dimers did not distribute as filaments in any cell, whereas that from BiFC-tagged HCPro dimers in the same plant did (middle and lower rows of panels, respectively). This indicates that the association with MTs induced by varnish fumes is specific to HCPro. Size bars of 50 μm for corresponding panels appear at the bottom right corners.

CHAPTER 6

Potato virus Y HCPRO BINDS TO SMALL RNAS OF 21 AND 22 NTS IN LENGTH DURING INFECTION, WITH PREFERENCE OF VIRAL SEQUENCE AND WITH ADENINES AT THEIR 5'-ENDS

Manuscripts in preparation

Potato virus Y HCPro binds to small RNAs of 21 and 22 nts in length during infection, with preference of viral sequence and with adenines at their 5'-ends

FRANCISCO J. DEL TORO[1], LIVIA DONAIRE[1], EMMANUEL AGUILAR[1], FRANCISCO TENLLADO[1], BONG-NAM CHUNG[2] and TOMÁS CANTO[1]

[1]Departamento de Biología Medioambiental, Centro de Investigaciones Biológicas, CSIC. Ramiro de Maeztu 9, 28040 Madrid, Spain
[2]National Institute of Horticultural & Herbal Science. Agricultural Research Center for Climate Change. 281, Ayeon-ro, 690-150, Jeju, Jeju Island, Republic of Korea

ABSTRACT

***Potyvirus* HCPro is a much studied suppressor of RNA silencing in plants that in the case of *Turnip mosaic virus* was recently shown to bind to small RNAs (sRNAs) to viral sequences (vsRNAs) *in vivo*, likely preventing their loading into the Argonaute (AGO) effector components of the antiviral RNA-induced silencing complexes (RISCs). In this work, we have performed deep sequencing of the short RNAs of less than 500 nucleotides in length that could be bound to HCPro from *Potato virus Y* (PVY), expressed from a virus vector and purified from infected *Nicotiana benthamiana* plants. We found that PVY HCPro bound *in vivo* mainly sRNAs of 21- and 22- nucleotides (nts) in length and to a much lesser extent also some larger RNAs. Furthermore, we found a binding preference for viral over plant sequences in both cases, and within the HCPro-bound vsRNAs a bias towards those of 21 and 22 nts containing a 5' terminal adenine, not observed in the bound fraction of sRNAs to plant sequences. Our data support selective sequestering of vsRNAs and a preferential targeting of vsRNAs that could load into AGO2, a RISC effector whose antiviral role has been highlighted by recent studies, as a mode of action of HCPro in silencing suppression.**

Keywords: HCPro; small RNA; antiviral silencing; viral suppressors of RNA silencing

INTRODUCTION

Potyvirus HCPro is a multifunctional protein that has been studied since the 1980s, first because of its involvement in the horizontal transmission of these economically important viruses by their insect vectors, hence its original name of "helper component" (Pirone *et al.*

1996), and later on because of its function in the translational processing of the viral polyprotein through its protease activity (Carrington and Herndon 1992), as a pathogenicity determinant that can enhance that of other viruses, such as *Potato virus X* (PVX) in synergistic infections (Pruss *et al.* 1997), as a suppressor of silencing (Anandalakshmi *et al.*, 1998; Kasschau and Carrington, 1998; Burgyán and Havelda 2011), and because of other functions (Valli *et al.* 2014).

HCPro is of around 50 kDa in size and has three differentiated domains: an N-terminal domain, associated with aphid transmission (Canto *et al.* 1995a; Blanc *et al.* 1997) and interaction with the proteasome (Jin *et al.* 2007a; Sahana *et al.* 2014); a central domain associated to the suppression of silencing function (González-Jara *et al.* 2005; Shiboleth *et al.* 2007); and a C-terminal domain responsible of its protease activity (Carrington and Herndon 1992). In plants HCPro is a cytoplasmic protein that forms homodimers and larger soluble aggregates, as well as large cytoplasmic amorphous inclusions, the latter perhaps end-products of a translational strategy that produces equimolar amounts of each viral protein (Plisson *et al.* 2003; Ruíz-Ferrer *et al.* 2005). Inside cells, HCPro subcellular whereabouts are complex and dynamic: HCPro from *Turnip mosaic virus* (TuMV) tagged with green fluorescent protein (GFP) was found to localize to the cytoplasm of epidermal *N. benthamiana* cells as filaments, around the nucleus, and in what could be the endoplasmic reticulum (ER) (Zheng *et al.* 2011). More recent live confocal microscopy with tagged proteins have visualized the interaction of *Potato virus A* (PVA) HCPro with a protein associated to the microtubule cytoskeleton (Haikonen *et al.* 2013), as well as the association of *Potato virus Y* (PVY) HCPro homodimers biologically functional in suppression of silencing with small dot-like structures associated to the endoplasmic reticulum (ER) (Del Toro *et al.* 2014). Under certain conditions, PVY HCPro relocated in live cells from its diffuse cytoplasm/cytoplasmic structures distribution towards the cytoskeleton of microtubules, coating it completely (Del Toro *et al.* 2014). The relationships between these subcellular dynamic changes and some of the protein functions, such as silencing suppression or transmission by vectors remain to be clarified but it is likely that they have a functional significance.

The precise molecular mechanisms by which HCPro interferes with the host antiviral gene silencing defenses are not well understood either. It is not known whether it inhibits the silencing defense at one level, or like some other viral suppressors it can operate a several levels. The known interactome of HCPro is extensive and growing, and includes a host rgs-CaM factor that directs HCPro to degradation through the autophagy pathway (Anandalakshmi *et al.* 2000; Nakahara *et al.* 2012**)**, or the *Arabidopsis thaliana* transcription

factor RAV2, whose expression appears to modulate silencing and its suppression (Endres *et al.* 2010). HCPro also binds to components of the proteasome, a structure potentially involved in antiviral defense, modulating and inhibiting it (Ballut *et al.* 2005; Jin *et al.* 2007b; Sahana *et al.* 2014), as well as to translation initiation factors (Ala-Poikela *et al.* 2011) and to chloroplast factors (Jin *et al.* 2007a; Cheng *et al.* 2008). To the date only one protein interaction is known with a component of the silencing machinery: that of RNA methyl-transferase HEN1 with *Zucchini yellow mosaic virus* (ZYMV) HCPro *in vitro* (Jamous *et al.* 2011). On the other hand, HCPro binds RNAs and this property could be related to its silencing suppression function: *in vitro*, PVY HCPro interacted with 200 nucleotide (nt)-long RNAs (Maia and Bernardi 1996; Urcuqui-inchima *et al.* 2000) and both TEV and ZYMV HCPro proteins interacted with synthetic small RNAs (sRNAs; Mérai *et al.* 2006; Shiboleth *et al.* 2007). Mangrauthia and colleges (2009) demonstrated that *in vitro Papaya ringspot virus* (PRSV) HCPro had bound synthetic sRNAs in a temperature-dependent manner, and Lakatos *et al.* (2006) showed that a plant-purified TEV HCPro bound sRNAs in a size-dependent manner, with preference for those with lengths of 21 nts with 3' end overhangs, and requiring the presence of a non-identified host cofactor. One feature common to all of these HCPro-RNA interactions *in vitro* is that they required protein:RNA molar ratios much higher than the 2:1 characterized for other suppressors proposed to interfere silencing through sRNA sequestration, such as the P19 and 2b protein suppressors of *Tomato bushy stunt virus* (TBSV) and *Cucumber mosaic virus* (CMV) (Vargasson *et al.* 2003; González *et al.* 2011, respectively), thus questioning whether HCPro could be operating in the same way. However, the development of next generation sequencing (NGS) has allowed to demonstrate that TuMV HCPro binds *in vivo* sRNAs of viral sequence (vsRNAs) of 21 and 22 nts in infected arabidopsis plants, supporting sequestration of vsRNAs away from the silencing machinery by HCPro as a means of suppression of silencing (García-Ruíz *et al.* 2015). On the other hand, TuMV HCPro was shown to interfere with the biogenesis and action of microRNAs (miRNAs), but no direct binding to them was demonstrated (Chapman *et al.* 2004; García-Ruíz *et al.* 2015).

In this work, we have used NGS to characterize any short RNAs of less than 500 nts in length that could be bound to PVY HCPro purified under non-denaturing conditions from infected *Nicotiana benthamiana* plants. Our results show that PVY HCPro binds sRNAs of 21 and 22 nts in length *in vivo* in this host, and furthermore, they reveal the existence of a bias in HCPro preferences towards binding sRNAs of viral sequence over those of plant sequence, despite the latter being much more abundant in the plant,

and among the former towards those having adenines at their 5'-ends. Our results support the proposal that antiviral sRNAs are sequestered by HCPro to suppress silencing, and allow us to further propose that this could be happening through a selective targeting of the AGO2-binding antiviral sRNAs.

RESULTS

Purification of the HCPro and control samples under non-denaturing conditions, and isolation of their associated short RNAs

To determine whether PVY HCPro binds short RNAs (defined here as of less than 500 nts in length) *in vivo* we first purified this protein with a six-histidine tag at its N-terminus (6x-HCPro) from *N. benthamiana* plants infected with a PVX vector that expressed the PVY P1-6x-HPro modified bicistron through an additional subgenomic RNA (Fig. 1A). The P1 protein detaches itself post-translationally from the 6x-HCPro via proteolysis, and the latter is functionally active as suppressor of silencing in *N. benthamiana* agropatch assays (Tena Fernández *et al.* 2013). Plants infected with the PVX vector alone were used in parallel to follow the purification procedure of 6x-HCPro, as control (Fig. 1A). We performed the purification steps using Ni^{2+}-NTA resin to bind proteins with 6x-histidine tags under non-denaturing conditions in order to obtain protein as near its native state as possible, and retaining potentially associated nucleic acids. Samples from each purification step were resolved for both the HCPro and the control samples in SDS-PAGE (Fig. 1B). In both samples sequential elution of the fraction bound to the Ni^{2+}-NTA agarose showed the presence of host protein contaminants that also bound to the resin. The second elution of the HCPro sample released the bulk of 6x-HCPro and provided a preparation enriched in this protein. In both, the HCPro and control elution samples other proteins could only be detected weakly by coomasie blue-staining (Fig. 1B). However, silver staining showed that under native conditions a large number of other proteins of different sizes was also present in the 2nd elution fraction (Fig. 1B, silver-stained gel). The pattern of these proteins and their relative amounts were remarkably similar in both samples (Fig. 1B, compare the control and HCPro sample lines in the silver stained gel) Total RNAs were present in the second elution fractions from both, the control and the HCPro samples, although in larger amounts in the latter (Fig. 1D). Total RNAs were then resolved in 10% polyacrylamide-urea gels and RNAs were eluted from slices of gels containing the RNA sizes from 12 to 500 nts for their sequencing.

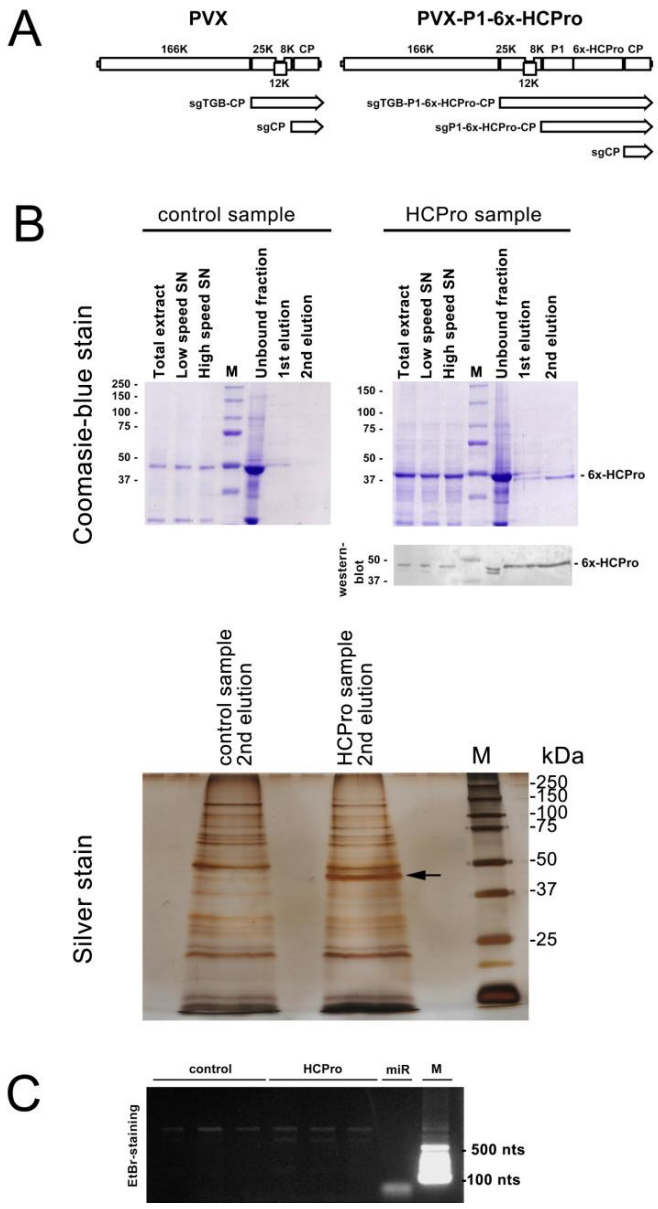

FIGURE 1. Purification under non-denaturing conditions of the HCPro and the control samples, and of their associated RNAs. (A) Schematic representation of the genomic and subgenomic RNAs (sgRNAs) of the *Potato virus X* (PVX; left) and PVX-P1-6x-HCPro (right) virus vectors, used in this study. Open reading frames are indicated as blocks and sgRNAs as block arrows. (B) Upper gels: Coomasie blue-stained SDS-PAGE of the different purification steps of the control (left gel) and HCPro samples (right gel), and western blot detection of 6x-HCPro in the latter sample (blot panel below gel). Note that as depths of stain vary between gels, band intensities between samples in both gels are indicative and cannot be directly compared. Molecular weight markers (lane M) are indicated in KDa at the left side of the gels. SN means supernatant. Lower gel: silver-stained SDS-PAGE of the 2nd elutions from the control and HCPro samples shown in the upper coomasie/stainded gels, and that were used to extract and deep-sequence their bound RNA populations of less than 500 nts in size. Both samples can be compared directly in this gel. Note that in addition to the HCPro band found only in the HCPro sample, marked by an arrow, many other bands corresponding to other proteins of different sizes are present in both samples, and that their pattern and individual amounts appear comparable. Molecular weight markers (lane M) are indicated in KDa at the right side of the gel. (C) 1.5% agarose gel electrophoresys of total RNAs isolated from second elution aliquots of control (three lanes to the left) or HCPro samples (three lanes to the right). The lane labeled miR shows a double stranded synthetic miR171 as size indicator. The lane labeled M shows RNA molecular weight markers, whose values in nucleotides (nts) are indicated to the right of the gel.

Small RNAs of 21 and 22 nts in length are the most abundant short RNA species found in both the control and HCPro samples

To investigate the composition of the different RNA species found in the 6x-HCPro and control samples and their peculiarities, a high-throughput deep sequencing

approach was followed to identify the different RNA species from ~12 nts to ~500 nts. They would include small RNAs of all types, including miRNAs, as well as other longer RNA species (i.e. long non-coding RNAs, short mRNAs, viral RNA fragments etc). We obtained 21.11 and 26.06 million sequence reads from the control and 6x-HCPro RNA samples, respectively. Reads that corresponded to ribosomal RNAs (rRNAs) were discarded, leaving 10.66 and 16.54 million reads from the control and 6x-HCPro samples for analysis, respectively (Table 1). These reads were aligned on the one hand with the genomic sequences of the viruses infecting the plants from which the samples were obtained (those of the *PVX* vector for the control sample, and of the *PVX-P1-6x-HCPro* vector for the HCPro sample), and on the other hand with the genome of *N. benthamiana*. We also aligned the reads with the sequences of the miRNAs in the PNRD.

TABLE 1. Summary of the properties of RNA reads obtained from the control and HCPro samples.

	control	HCPro
Total reads (with rRNAs)	21.11	26.06
rRNAs	10.45	9.52
Total reads without rRNAs	10.66 (100.00%)	16.54 (100.00%)
18 to 30 nt RNAs	7.50 (70.44%)	11.40 (69.94%)
21 to 24 nt sRNAs	5.06 (47.52%)	9.18 (55.53%)
21 and 22 nt sRNAs	3.94 (37.01%)	7.86 (47.51%)
matching *N. benthamiana* sequences	10.50 (98.55%)	15.17 (91.73%)
21 and 22 nt sRNAs	3.85 (36.10%)	6.65 (40.22%)
matching pre-miRNAs	31666	16859
matching mature miRNAs	400	131
matching viral sequences	0.15 (1.45%)	1.37 (8.27%)
21 and 22 nt vsRNAs	0.10 (0.91%)	1.20 (7.29%)

Table 1. Summary of the properties of RNA reads obtained from the control and HCPro samples. Reads were obtained by deep sequencing of libraries produced from RNAs isolated from either sample. Total reads are shown for the sequences matching pre-miRNAs or mature miRNAs, whereas for the rest of reads the numbers correspond to millions of reads (x10^6). After subtracting the reads corresponding to ribosomal RNAs, percentages of total reads that match *Nicotianana benthamiana* or viral sequences are shown.

In the control sample 98.55% of the reads were of plant sequence and only 1.45% of viral sequence, whereas in the HCPro sample 91.73% of the reads were of plant sequence and 8.27% of viral sequence. In both the control and HCPro samples, reads between 18 to 30 nts constituted 70.44% and 69.94% of the total, respectively. Inside this range, the small RNAs (sRNAs) from 21 to 24 nts were 47.52% of total reads for the control and 55.53% for the HCPro sample. Total reads that corresponded to sRNAs of 21 and 22 nts were the most abundant ones and constituted 37.01% and 47.51% of the total reads, respectively (all summarized in Table 1).

Very low numbers of the total reads corresponded to pre-miRNA or mature miRNA sequences in both samples, numbers that remarkably, halved (pre-miRNAs) or decreased by more than two-thirds (miRNAs) in the 6x-HCPro sample with regard to the control sample (Table 1).

Small RNAs of 21 nts in length and of viral sequence are differentially enriched in the HCPro sample

To gain insight on any potential affinity of HCPro for specific RNA species we looked for any differential enrichment of particular RNAs in the HCPro sample. For this, fold changes of their reads in this sample over those in the control sample were calculated to measure their levels of enrichment. Within the range of 18 to 30 nts in length, the total 21 nt-long RNAs of combined plant and viral sequence became enriched more than three-fold in the HCPro sample over the control sample (Fig. 2A). However, the 22 nt RNA enrichment in the HCPro over the control sample was only 1.5-fold despite being the most abundant species in both, HCPro and control samples. This ratio was similar to those observed for some of the RNA sizes in the 18 to 30 nt-long range (Fig. 2B, for example the 23,24 and 25 nt-long RNAs), suggesting a preferential enrichment of 21 nt-long over 22 nt-long RNAs in the HCPro sample.

Size distribution of the total reads from 18 to the 125 nt-long read limit shows a mayor peak in reads of 21-22 nt-long RNAs, in both the control and HCPro samples (Fig. 3A). The chart also visualizes data shown in Table 1: reads corresponding to plant sequences constitute more than 90% of the reads and outnumber those of viral sequences in both, control and HCPro samples, throughout the whole size range analyzed (Fig. 3A, upper vs. lower charts). Outside this 18-30 nt-long region that contained a defined peak with very marked fold-change increases of viral reads for 21 and 22 nt RNAs (~13 and 9 times, respectively), the number of total reads in the HCPro sample was

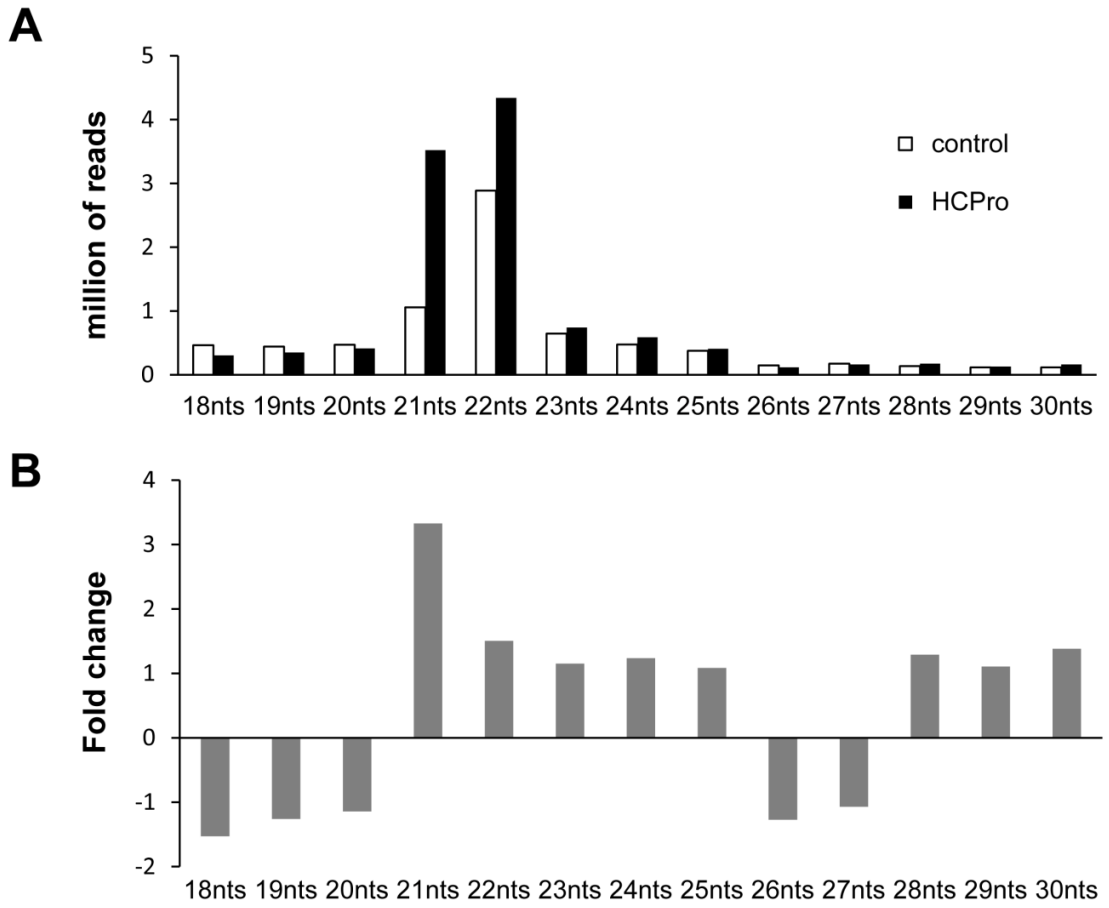

FIGURE 2. **Detail of the distribution of total reads in RNAs between 18 and 30 nts in the control and HCPro samples.** (A) Number of total reads. Scale is given in millions of reads. Reads from the control sample appear as open boxes while those from the HCPro sample appear as solid boxes. (B) Fold change values for total reads each RNA size in the HCPro sample relative to those from the control sample.

larger than in the control sample (2.22 million and 0.84 million, respectively). Accordingly, fold change values for plant reads were between 2 and 5 throughout the size range, and even larger for viral reads (Fig. 3B, fold change values in blue for plant reads vs. in red for viral reads), indicating that some bias towards enrichment in RNAs of viral sequence in the HCPro sample also occurred through the whole size range. Indeed, although the highest percentage of reads from the control and the HCPro samples corresponded mostly to the plant genome (98.55% and 91.73%, respectively; Table 1), a higher proportion of reads matched virus sequences (*PVX-P1-6x-HCPro or PVX*, depending on sample) in the HCPro sample than in the control sample (8.27% vs. 1.45%, respectively; Table 1).

Total reads that matched the plant genome in the HCPro sample (15.17 million) were 1.44 times higher than in the control sample (10.50 million), reads that matched viral sequences were 8.87 times higher (1.37 million

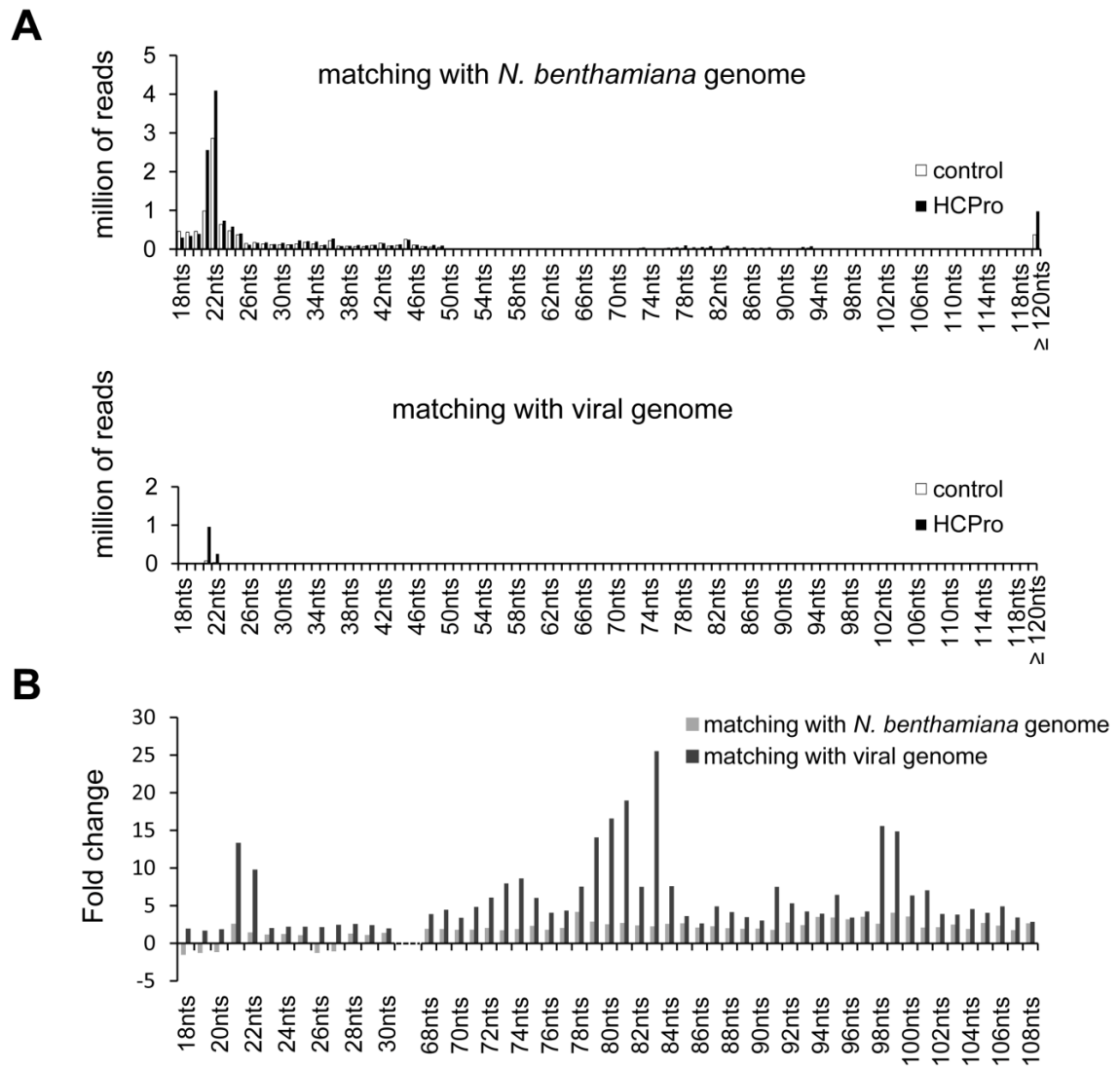

FIGURE 3. Distribution of total reads by RNA size in the control and HCPro samples. (A) Number of total reads that match either the plant genome (upper chart) or viral sequences (lower chart). Reads from the control sample appear as open boxes while those from the HCPro sample appear as solid boxes. Scale is shown in millions of reads. (B) Fold change of total reads in the HCPro sample relative to the control sample for both, viral (drak grey) and plant (light grey) sequences. Scales are shown in millions of reads.

and 0.15 million in HCPro and control sample, respectively). Therefore, in the HCPro sample RNAs of viral sequence increased their number 6.15 times more than did RNAs of plant sequence, and the bulk of them came from vsRNAs of 21 and 22 nts. Considering only these two RNA sizes in both fractions, while the number of reads corresponding to 21-nt RNAs of plant genome was 2.60 times higher in the HCPro than in the control sample, the number of reads that aligned with viral sequences went up 13.35 times, that is 5.14 times more. A similar trend was observed for the 22-nt sRNAs where the reads that aligned with the plant genome were 1.43 times higher

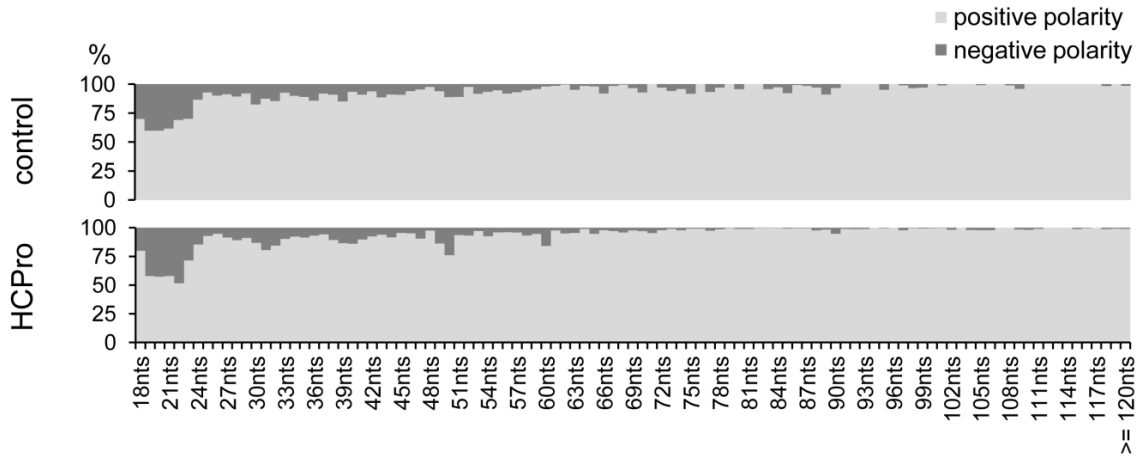

FIGURE 4. **Polarity of the reads that match with viral sequences in the control and HCPro samples.** Percentages of positive (light grey) and negative (dark grey) polarities of reads of viral sequence in the control (upper chart) and HCPro (lower chart) samples, distributed by size.

in the HCPro sample than in the control sample, but those of vsRNAs were 9.78 times higher, a net 6.84 times differential increase. The fact that neither RNAs of plant sequence in any size, nor of vsRNAs of sizes other than 21 or 22 nts experienced similar differential increases in the HCPro sample indicates that the presence of the viral suppressor introduced a bias towards RNAs of 21 and 22 nts, of viral sequence (Table 1 and Fig. 3B).

RNA reads of viral sequence were largely of positive (sense) polarity, although for some vsRNAs the negative sense reads were more abundant, around 40% (Fig. 4). In both, control and HCPro samples the RNA reads of viral sequence aligned throughout all of the viral genome, although there were genome regions with higher number of reads or hotspots that did not correlate with regions that lead to viral subgenomic RNA formation (Fig. 5A).

Considering only the most abundant vsRNAs classes of 21 and 22 nts and only those of PVX sequence (without the P1-6x-HCPro insert), 76.62% of the unique sequences found in the control sample were also found in the HCPro sample. Furthermore, 75.88% of these common unique sequences were found more times in the HCPro sample than in the control sample, with an average fold change value of 33.97. Moreover, these unique viral reads common to both samples represented only 34.58% of the unique viral reads found in the 6x-HCPro sample. This fact indicates that the HCPro sample was not only enriched in the amount of vsRNA reads but also in their sequence diversity (Fig. 5B).

Outside the range of sRNAs there were also some remarkable fold change increases of reads of viral sequence in the HCPro sample, although their absolute numbers were very small. This increment was

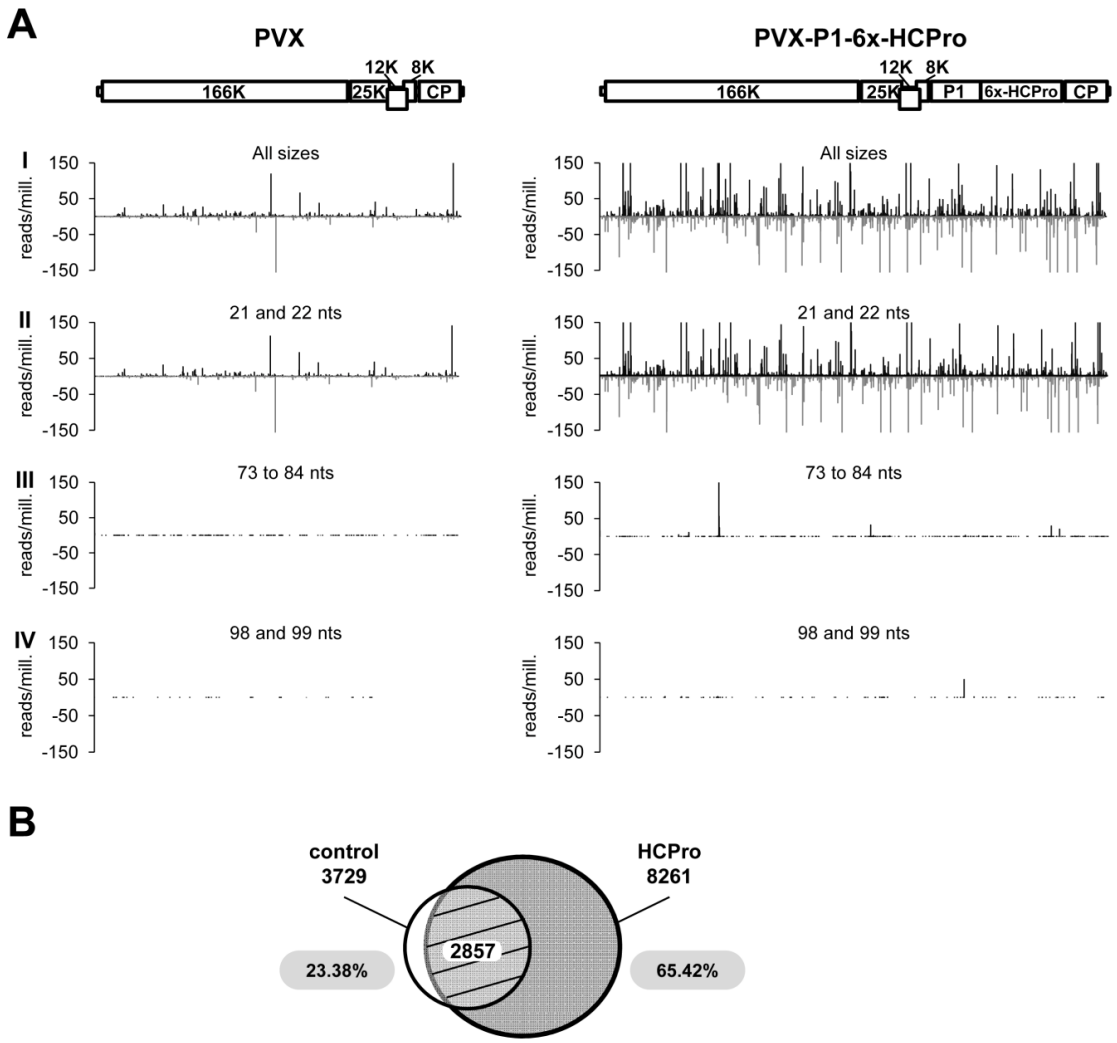

FIGURE 5. Distribution of the RNA reads of viral sequence in control and HCPro samples throughout the viral genomes. (A) Representation of reads for RNAs of all sizes [12 to 119 and 120 to 500 nucleotides (nts)] (I), 21 and 22 nts (II), 73 to 84 nts (III) and 98 and 99 nts (IV) matching with the viral genomes in control (left charts) and HCPro (right charts samples. On top of the figure the viral genomes used to match the sequences are represented schematically (PVX and PVX-P1-6x-HCPro for the control and the HCPro samples, respectively). Values are shown as reads per million (reads/mill). Positive-sense RNAs are represented in the upper side of the charts (dark grey), whereas negative-polarity RNAs are represented in the lower side (light grey). The scale was capped at 150 reads/mill. (B) Venn Diagram of unique sequences of 21 and 22 nts of viral sequence (of either polarity) in the control (white circle) and HCPro (dotted circle) samples. Numbers down the sample name represent unique reads matching PVX sequences. Numbers written over a grey oval represent the percentage of unique reads unshared between samples. The number in the overlapping area (streaked) indicates the number of unique reads found in both samples.

mainly clustered in two size-ranges, the first one in reads of RNAs from 73 to 84 nts and a second one in reads of 98-99 nts (Fig. 3B). Reads in the HCPro sample from 73 to 84 nts were about 20 times more abundant than in the control sample, and this was mainly attributable to three hotspots of sequences with more than 1000 reads each one, but

especially to one of them, only found in the HCPro sample. It corresponded to a sequence in the PVX *166K* gene, from nt 2038 to 2227 and was composed by 13000 reads of sense polarity (Fig. 5). That viral region did not correlate with a non-canonical ORF and did not form any stable secondary structure [analyzed by Mfold (Zuker 2003), data not shown] that could help explain its origin. Reads of 98 and 99 nts were also more abundant in the HCPro sample and they formed another hotspot from nucleotide 6264 to 6362 located within potyviral *P1* cistron, and therefore not present in the control sample (Fig. 5A). The existence of this hotspot with 1693 reads could not be explained either by a non-canonical ORF or by the formation of secondary structure in that viral region (analyzed by Mfold, data not shown), and its cause remains also unexplained.

In the HCPro sample, the small RNAs of viral sequence and of 21-22 nts in length appear enriched in adenine at their 5'end nucleotide, but not those of larger sizes, or of plant sequence

To test whether HCPro could show preference for loading sRNAs with a particular 5'-end nt, we performed an analysis of the 5'end nt composition of the RNA reads in the HCPro and control samples, and calculated the fold changes in the frequencies of each of the four nucleotides at the RNA 5'-ends for every RNA size between both samples (Fig. 6A). All the RNAs that matched the plant genome showed very small fold change variations in their nt composition at their 5' ends, independent of their length (Fig. 6B). However, when analyzing viral reads, the number of 21 and 22 nt-long vsRNA reads that had an adenine in their 5'-ends increased markedly in the HCPro sample in comparison to the reads in the control sample (an average fold change of adenine percentage of 10.73 times; Fig. 6C, right chart). This adenine fold change value did not occur in any other RNA size (Fig. 6C, right chart). In order to rule out that the bias to 5'-end adenines in the 21 and 22 vsRNA species was somehow specific of the PVX sequence, we analyzed separately the fold change values of vsRNAs matching the *PVX* sequence and those matching the potyviral *P1-6x-HCPro* insert sequence and found that the 5'-end adenine bias was present in both (11.25 times and 9.20 times, respectively; Supplemental Fig. 1).

Another high fold change value in 5'-end nucleotide preference towards cytosines was also observed for reads of viral RNAs of 79 to 84 nts in the HCPro sample. Those reads corresponded mainly to the hotspot in the *166K* PVX replicase gene. As a large proportion of reads in that hotspot start at their 5' end with cytosine from position 2042 in the PVX genome this is likely not a genuine bias towards this particular

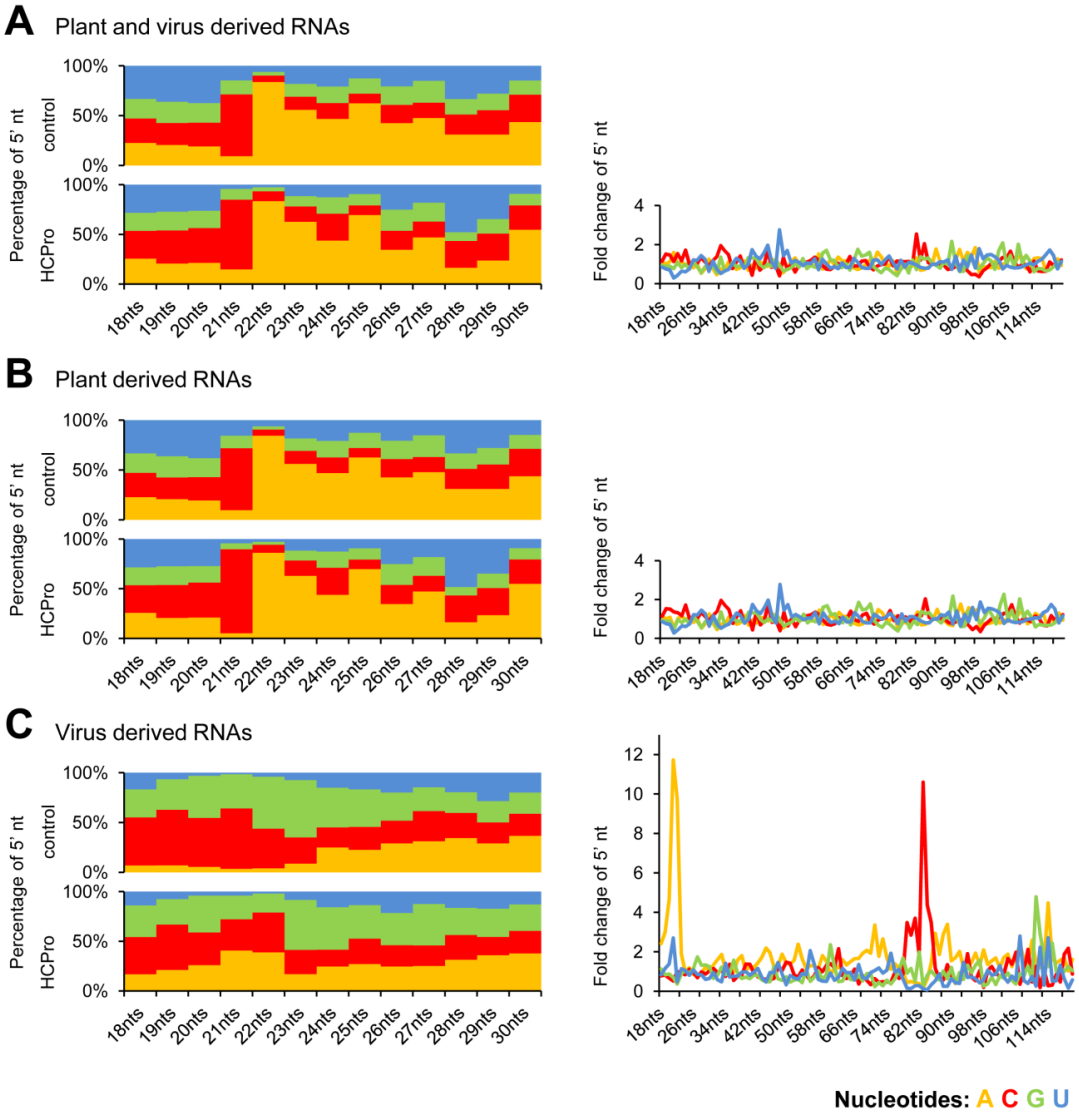

FIGURE 6. Analysis of 5'-end nucleotide prevalence in reads from control and HCPro samples. (A) Chart to the left, percentages of 5'-end nucleotide (nt) composition in total (plant and viral) RNA reads of sizes ranging from 18 to 30 nts in the control (upper chart) and HCPro (lower chart) samples. Chart to the right, corresponding fold change values in the HCPro vs. the control sample for sizes ranging from 18 to ≥ 120 nts. (B) Chart to the left, percentages of 5'-end nt composition in RNA reads of plant sequence and sizes ranging from 18 to 30 nts in the control (upper chart) and HCPro (lower chart) samples. Chart to the right, corresponding fold change values in the HCPro vs. the control sample for sizes ranging from 18 to ≥ 120 nts. (C) Chart to the left, percentages of 5'-end nt composition in viral RNA reads of sizes ranging from 18 to 30 nts in the control (upper chart) and HCPro (lower chart) samples. Chart to the right, corresponding fold change values in the HCPro vs. the control sample for sizes ranging from 18 to ≥ 120 nts.

nt, but rather caused by the existence of the hotspot reads (see Fig. 5). By contrast, the RNAs of 98 and 99 nts in the PVY *P1* cistron hotspot did not show any preference (Fig. 6). Therefore, out of the 21 and 22 nt-long vsRNAs the 5' end

composition of reads in the HCPro sample was broadly similar to that observed in the control sample, or had a very slight bias towards having an adenine.

DISCUSSION

The silencing suppression activity of HCPro was discovered soon after RNA-based gene silencing as a mechanism of defense against plant viruses started to be investigated (Anandalakshmi *et al*., 1998; Kasschau and Carrington, 1998). However, the precise mode by which this viral protein interferes with antiviral silencing remains yet to be elucidated. HCPro is a multifunctional protein, and has been shown to interact with several factors from the host. One of these is the component of the silencing machinery HEN1, whose methylation of sRNAs is inhibited by its binding with ZYMV HCPro *in vitro* (Jamous *et al*. 2011). With regard to this, it had been previously shown that in a transgenic HCPro background, the siRNA population derived from infection of tobacco plants by CMV appears to be less methylated at their 3´-ends than in normal plants (Ebhart *et al*., 2005).

An alternative mode by which HCPro could suppress silencing could be through its binding to RNAs. This property of HCPro had been shown *in vitro* for synthetic sRNAs (Urcuqui-Inchima *et al*. 2000: Mérai *et al*. 2006; Lakatos *et al*. 2006; Shiboleth *et al*. 2007; Mangrauthia *et al*. 2009), with preference for those with lengths of 21 nts with 3´end overhangs (Lakatos *et al*. 2006). However, all of those studies *in vitro* required protein:RNA molar ratios much higher than the 2:1 characterized suppressors, such as the TBSV P19 or the CMV 2b proteins that may act via sRNA sequestration. However, a recent report has demonstrated that TuMV HCPro binds *in vivo* vsRNAs of 21 and 22 nts in infected arabidopsis plants, supporting the sequestration model (García-Ruíz *et al*. 2015).

To test whether during the course of an infection PVY HCPro binds short RNAs, investigate the nature of those RNAs and explore their potential relation to its suppressor function, we expressed hexahistidine-tagged HCPro from a PVX vector in the compatible host *N. benthamiana*, purified it under non-denaturing conditions using a Ni^{2+}-NTA resin, and analyzed the RNAs associated to the purified protein of 500 nts or less in length, using high-throughput sequencing of both, viral and host sequence. This procedure was also followed with plants infected with a PVX vector, as control sample (Fig. 1A). We found short RNAs in the purified HCPro sample and also in the control sample (Fig. 1C). When the experiment was designed we were not able to predict whether there would be RNAs in the control sample and if so, in what numbers. However, it was considered that under mild native conditions, a large number of plant metalloproteins and other types of proteins of different

sizes also bind to the Ni^{2+}-NTA resin, and one such example is that of the isolation of functional CMV replicase preparations (Gal-On *et al.* 2000). Many of these proteins could carry bound nucleic acids, although that some nucleic acids could bind directly to the Ni^{2+}-NTA resin under our non-denaturing conditions cannot be ruled out either. Non-denaturing conditions could also preserve soluble multi-molecular conglomerates allowing the presence of protein components with no direct affinity for the resin. In any event, the main assumption was that the protein-RNA background in both control and HCPro samples would be comparable. For that to happen the enrichment of HCPro could not take place at the expense of other proteins. Critically, this was actually the case, as can be shown in the silver stain gel in Fig. 1B, where a similar profile of proteins can be found in the eluted fractions of both HCPro and control samples, apart from the 6xHCPro protein. They only differ in the presence or absence of 6x-HCPro, as the relative amounts of the other proteins in both samples remain rather similar. This is not surprising, because many Ni^{2+}-NTA sites would not be occupied by 6x-HCPro. The capacity of the resin to bind hexahistidine-tagged proteins is 5 to 10 mg/ml of resin (The QIAExpressionist™ handbook; Qiagen GmbH, Hilden, Germany) and we purified no more than 0.6 mg of 6x-HCPro/ml of resin, indicating that the 6x-HCPro suppressor was far from saturating the resin, leaving over 90% of the sites still available for less-specific interactions with host factors.

Our observations raise the issue of which type of control would be more adequate in the case of analyzing RNAs bound to proteins isolated from plant extracts under non-denaturing conditions, using 6x-histidine tags and Ni^{2+}-NTA resins: an input fraction that did not undergo the same resin passage as the enriched tagged protein fraction, or a fraction that did go through the purification passage, and whose background protein composition profile is identical, except for the presence or absence of the tagged protein. In our opinion we consider the latter a better control here than a total RNA from a plant extract that had not undergone the Ni^{2+}-NTA resin purification step. Any differences between the control and HCPro samples would necessarily have to be caused by, and attributable to the presence in the latter of the 6x-HCPro protein.

To ensure a normalization that would allow comparisons between RNA reads from the HCPro and the control samples, we started with identical amounts of infected plant material, obtained from plants that had been infected and kept under the same conditions. The procedures for protein purification and subsequent extraction of associated RNAs were performed in parallel. The adequate normalization of the samples analyzed by high-throughput sequencing was confirmed by the observation that reads of rRNAs were comparable in

the control and HCPro samples (10.45 and 9.52 million reads, respectively; Table 1). After discarding from analysis the rRNA sequences, the reads of sRNAs of 21- and 22-nt in length remained by far the most abundant types in the less-than 500 nt-long RNAs in both samples, indicating that 6x-HCPro did not drastically modify the RNA size profile (Table 1 and Figs. 2 and 3), although as we have shown did alter their nature and relative frequencies.

Among the entire sRNA population, 21-nt sRNAs presented the greatest enrichment in the HCPro sample (more than three times; Fig. 2B), which suggests that 6x-HCPro binds with preference to this size class of RNAs. This binding had been previously documented for synthetic sRNAs *in vitro* (Lakatos *et al.* 2006) and more recently, *in vivo*, using NGS techniques (García-Ruíz *et al.* 2015).

Although the total RNA reads obtained from the HCPro sample were higher than those from the control sample, the abundance of reads corresponding to mature or pre-mature miRNAs was lower in the HCPro samples (it roughly halved; Table 1). It has been suggested that HCPro could perform some of its biological activities or affect the host by modulating the biogenesis and/or accumulation of miRNAs. Previous studies had shown that accumulation of miRNAs increased in arabidopsis plants either infected with TuMV or transgenically expressing its HCPro (Kasschau *et al.* 2003; Dunoyer *et al.* 2004). Our results do not contradict these data but suggest that although the biogenesis/accumulation of miRNAs could be greater in the presence of HCPro, this did not lead to its increased binding by the suppressor, in agreement with recent observations (García-Ruíz *et al.* 2015) that also found this reduction of miRNAs. It should be noted that plant the most common 5'-end nt in plant miRNAs is uracile but an analysis of the 5'-ends of miRNA reads in the control and HCPro samples showed no differences in their relative frequencies (data not shown) suggesting that miRNA selection by terminal nt had not occurred. Perhaps their being of plant origin or their having sequence mismatches between both strands could be more relevant to its lack of binding by HCPro.

From the analysis of the RNA reads in the HCPro and control samples another interesting observation emerged: although both contained mainly 21 and 22 nt-long sRNAs, there was a marked differential enrichment in the HCPro sample of those that were of viral sequence over those of host sequence (Fig. 3B), despite the latter being the most abundant ones in both samples (Fig. 3A). This differential enrichment of RNAs of viral sequence also appears to lesser degrees in the other lengths of short RNAs analyzed (Fig. 3B). How could HCPro discriminate between RNAs of viral and of host sequence? We cannot provide an explanation, but we could speculate that a coincidence in the subcellular

occurrence and timing of synthesis of these vsRNAs perhaps resulting from activities by different DCLs and that of 6x-HCPro (Ding and Voinnet 2007) could favor a positive bias towards loading RNAs of viral sequences.

The viral RNAs bound to HCPro originated from the entire length of the viral genome and they were overwhelmingly of positive sense, but for the vsRNAs of 19 to 22 nts in length the percentage of positive- to negative-sense reads was around 60:40. These observations were also valid for the control sample (Fig. 4). This positive-sense bias in the polarities of vsRNAs has been observed many times in other plant-virus interactions (Donaire *et al.* 2009; Kreuze *et al.* 2009; Ding 2010; Qu 2010). The polarity of the other RNAs was almost entirely positive (Fig. 4), perhaps because of their probable origin from degradation of positive-sense viral genomic or subgenomic RNAs by the slicing activities of RISCs (Ding and Voinnet 2007; Vaucheret 2008). These longer viral RNAs distributed throughout the whole viral genome. However, there were two particular hotspots, one of RNAs of 73 to 84 nts in length that mapped to a sequence region in the PVX *166K* replicase gene, the other one of RNAs of 98-99 nts in length that mapped to a sequence region in the PVY *P1* gene (Fig. 5). The origin of these hotspots is unknown. A bioinformatic prediction analysis could not identify any secondary structure that could explain its existence. And neither was a higher presence of sRNAs derived from the flanking regions observed, although previous studies had previously shown that viral regions that are most effectively targeted by viral sRNAs do not necessarily correlate with those regions corresponding to the most abundant vsRNA formation (Szittya *et al.* 2010). Nevertheless their existence appears related to the presence of HCPro, even the more so for the hotspot of 73 to 84 nts, given that the viral genome of the vector used for expression of HCPro or the one used as control do not present any difference in that region.

Finally, our analysis of the 21- and 22-nt vsRNAs in the HCPro sample showed a specific and substantial enrichment (almost 12-fold) of those containing adenines in their 5'-ends, which was not observed in the sRNAs of plant sequence of either the same size or of different sizes (Fig. 6B), and only to a much lesser degree in some RNAs of viral sequence of other sizes (Fig. 6C).

Preferences for sRNAs with specific 5'-end nts are known to some sRNA-binding proteins, such as AGO proteins, some of them key components of plant RISCs involved in the antiviral RNA-mediated silencing (Takeda *et al.* 2008; Montgomery *et al.* 2008; Mi *et al.* 2008). HCPro binding of specific vsRNAs could then be a direct mechanism evolved by potyviruses to prevent them from loading into some AGO effectors. In this regard, García-Ruíz and colleagues (2015) recently demonstrated that the presence of an active TuMV HCPro

suppressor decreased the amount of 21-nt vsRNAs loaded into AGO1, AGO2 and AGO10 in a tissue-dependent way, while a mutant that had its binding to sRNAs abolished did not. The same work showed also that AGO2 played a key role in the defense of arabidopsis plants against infection by this *potyvirus*. This role had been observed also by others (Harvey *et al.* 2011; Zhang *et al.* 2012), and appears particularly important against potyviruses (Carbonell *et al.* 2012) or potexviruses (Jaubert *et al.* 2011). Our results with PVY HCPro confirm those of García-Ruíz *et al.* (2015) with regard to HCPro binding of 21 and 22 nt-long RNAs *in vivo*, and furthermore, show a bias towards binding vsRNAs with adenines at their 5'-ends. A preference for 21 nt-long sRNAs with 5'end adenines has been shown for AGO2 (Takeda *et al.* 2008; Montgomery *et al.* 2008; Mi *et al.* 2008). It is thus tempting to propose that HCPro targets preferentially the vsRNAs that would otherwise load into AGO2-containing RISCs, and in this way interferes with antiviral silencing. It could be argued that the enrichment of 21 nt-long vsRNAs with 5'-end adenines in the HCPro sample could derive from an interaction of HCPro with the host AGO2 and its co-purification under non-denaturing conditions, although to the date no interaction between HCPro and any of the plant AGOs has been reported. However, this would still not explain why the enrichment did not affect the 21 nt-long sRNAs of host sequence (Fig. 6B) or why the 22-nt vsRNAs with adenines at their 5'-ends also became enriched, together with a slight but clear bias towards 5'-end adenines in many of the other shorter and longer RNAs of viral sequence found in the HCPro sample (Fig. 6C). Our data instead support a complex mechanism for HCPro binding to sRNAs based on their discrimination by size, origin (viral over plant sequence) and their 5'-end nts in the case of vsRNAs, through unknown means. This selective binding by HCPro would lead to its competing mainly with AGO2 for the same antiviral sRNAs.

MATERIALS AND METHODS

Plants and viruses

N. benthamiana plants were used in this study. Plants were kept in controlled growth chambers at 25 °C day/20 °C night temperatures, with a 16/8 hours day/night photoperiod and ~2500 lux of daylight intensity. 4-5 week-old plants were agroinoculated with *Agrobacterium tumefaciens* containing the appropriate binary constructs. Two infectious PVX vectors were expressed from binary constructs: an "empty" PVX vector was expressed from binary construct pgR107 that originated from Prof. D. C. Baulcombe group (University of Cambridge, UK), which expresses an infectious PVX that contains an additional CP promoter and a polylinker for the insertion and

expression of foreign genes (Lu *et al.* 2003). Binary construct PVX-P1-6x-HCPro was derived from vector pgR107, modified to express the PVY P1 protein and hexahistidine tagged HCPro cistrons, and was already described by Tena *et al.* (2013).

Purification of HCPro from plants

Our protocol for the purification of HCPro tagged with six histidines (6x-HCPro) is similar to the one described by Tena *et al.* (2013) with minor modifications. Briefly, fully developed infected leaves were collected at seven days after their agroinoculation with either the PVX or the PVX-P1-6x-HCPro vectors. In both cases around 100 g of systemic infected tissue were collected and kept frozen until the time of use. Every step in the purification protocol for both samples was performed in parallel, at between 0º and 4º C degrees, with pre-chilled buffers and laboratory equipment. Leaves were homogenized in extraction buffer [3.3 ml of buffer/g of leaf tissue: 100 mM Tris-HCl pH 8.5, 20 mM $MgSO_4$, 500 mM NaCl, 0.5 mM, ethyleneglycol-bis(2-aminoethyl ether)-N,N,N',N'-tetra acetic acid (EGTA), 20% sucrose, supplemented with 0.2% Na_2SO_3, 0.1% polyvinylpyrrolidone-40 and 5 mM 2-mercaptoethanol]. After filtration, centrifugation and ultracentrifugation, total soluble proteins were precipitated with 40% $(NH_4)_2SO_4$. Proteins were resuspended in extraction buffer and incubated with 1ml of nickel-nitrilotriacetic acid agarose (Ni^{2+}-NTA Agarose, Qiagen GmbH, Hilden, Germany). Several rinses of the resin were performed with extraction buffer and after that two consecutive steps of elution were made with 4 ml of extraction buffer supplemented with 400 mM EGTA. The first elution contained more contaminant proteins from the host, while the second elution had a higher enrichment of 6x-HCPro (Fig. 1).

Analysis of purified proteins by SDS-PAGE plus western blot

Samples from the different purification procedure steps were mixed 1:1 with 2x Laemmli buffer (100 mM Tris-HCl, pH 6.8, 4% SDS, 20% (v/v) glycerol, 0.01% bromophenol blue, 2% 2-mercaptoethanol), boiled and fractionated by 10% SDS-PAGE. Gels were stained with a solution of 0.27% (w/v) coomassie blue in 4:4:1 (v:v:v) ethanol:water:glacial acetic acid to visualize protein bands. Silver staining of SDS-PAGE gels was performed as described (Gal-On *et al.*, 2000). In addition, HCPro was also detected in samples by western blot: SDS-PAGE-resolved proteins were wet-blotted onto Hybond-P PVDF membranes (Amersham, GE Healthcare, Buckinghamshire, UK). Detection of HCPro was performed using a mouse monoclonal antibody to PVY HCPro (Ab 1A11; Canto *et al.* 1995b) followed by commercial

alkaline phosphatase-linked secondary antibodies and SigmaFast™ BCIP/NBT substrate tablets (SIGMA Aldrich, Saint Louis, Missouri, USA).

RNA isolation and high-throughput sequencing

Total RNA was extracted from 1.5 ml aliquots from the purified second elution samples obtained from tissues infected with either PVX-P1-6x-HCPro (hereafter the HCPro sample) or with PVX (hereafter the control sample). Total RNAs were isolated with TRIzol reagent (Invitrogen, Carlsbad, CA, USA) following the instruction of the manufacturers. For visualization, total RNAs were size fractioned by electrophoresis in 1.5% Tris-acetate agarose gels. For deep-sequencing of the RNAs of 500 nts in length or less, total RNAs were fractioned by electrophoresis in 10%-PAGE containing 8M urea. The gel area resolving ~12 nts to ~500 ntsin size was sliced with a razor and RNA was eluted from the gel with 0.3 M NaCl, and precipitated with 1 ul of glycogen (20 ug/ul) (Roche, Basel, Switzerland) and 1 volume of isopropanol.

RNA sequencing was performed by Fasteris SA (Chemin du Pont-du-Centenaire, Genève, Switzerland). Briefly, RNA samples were subjected to 5' cap removing with tobacco acid pyrophosphatase (TAP) treatment and ends repair reactions, followed by single-stranded ligation of 3' and 5' indexed adapters. Afterwards, reverse transcription and PCR amplification were performed to generate the two cDNA libraries (one from the control sample and another one from the HCPro sample) that were multiplexed and sequenced in one lane of a 125 bp single-end run, using Illumina HiSeq 2500 sequencer (Illumina, San Diego, California, USA).

Analysis of RNA sequences

Sequence reads from the two RNA libraries were computationally processed by first removing adaptor sequences from the raw reads and discarding any insert reads of less than 18 nts in length, using our own Perl scripts. Reads were then mapped using Bowtie (for reads between 18 and 49 nts; Langmead *et al.* 2009) or Bowtie2 (for reads of 50 nts and higher; Langmead *et al.*, 2012) considering only perfect matches. Reads mapping to plant rRNA sequences, including mitochondrial and chloroplasts ones from NCBI database, were removed from the analysis. The remaining reads were then compared with: a) the two viral construct genomes; b) the *N. benthamiana* genome; and c) known miRNA sequences. The genomic sequence of PVX was that in the pgR107 binary construct (GenBank: AY297842.1) and that of PVX-P1-6x-HCPro was obtained by inserting the sequence of *P1-6x-HCPro* into the PVX vector *polylinker*, and confirmed by Sanger sequencing. The genome of *N. benthamiana* was obtained from the University of Sydney

(http://sydney.edu.au/), version 0.5 (Naim *et al.* 2012). For miRNAs we used the sequences of the Plant Non-coding RNA Database (PNRD; Yi *et al.* 2015) including mature, as well as pre-miRNA sequences. Sorting of sequences by length, counting of total and unique sequences, and of percentages of nucleotide identities at the RNA 5' ends were all achieved employing different Perl scripts developed in our laboratory. To measure how many times an RNA type became enriched or vice-versa in the HCPro vs. the control sample, we used fold change values. They were obtained by dividing the values in the HCPro sample by the corresponding ones in the control sample. When a fold change value (x) was lower than 1, the negative of its inverse (-1/x) was used in the charts.

Accession number

High-throughput sequencing data from this article has been uploaded into the Gene Expression Omnibus (http://www.ncbi.nlm.nih.gov/geo) with accession number GSE71921.

SUPPLEMENTAL MATERIAL

Supplemental material is available for this article

ACKNOWLEDGEMENTS

This work was supported by grant PJ00946102 "Prediction of the impact of climate change on the outcome of diseases caused by plant RNA viruses" from the Rural Development Administration (RDA) of the Republic of Korea in cooperation with the Spanish Council for Scientific Research (CSIC), and also by grant BIO2013-47940-R "Role of viral pathogenicity determinants on trade-offs established during compatible RNA virus-plant interactions" from the Spanish Ministry of Economy and Competitiveness (MINECO).

REFERENCES

Ala-Poikela M, Goytia E, Haikonen T, Rajamaki ML, Valkonen JPT. 2011. Helper component proteinase of the genus *Potyvirus* is an interaction partner of translation initiation factors sIF(iso)4E and eIF4E and contains a 4E binding motif. *J Virol* **85:** 6784-6794.

Anandalakshmi R, Pruss GJ, Ge X, Marathe R, Mallory AC, Smith TH, Vance VB. 1998. A viral suppressor of gene silencing in plants. *Proc Natl Acad Sci USA* **95**: 13079–13084

Anandalakshmi R, Marathe R, Ge X, Herr JM Jr, Mau C, Mallory A, Pruss G, Bowman L, Vance VB. 2000. A calmodulin-related protein that suppresses posttranscriptional gene silencing in plants. *Science* **290:**142–144.

Ballut L, Drucker M, Pugniére M, Cambon F, Blanc S, Roquet F, Candresse T, Schmid H-P, Nicolas P, Le Gall O, Badaoui S. 2005. HcPro, a multifunctional protein encoded by a plant RNA virus, targets the 20S proteasome and affects its enzymatic activities. *J Gen Virol* **88:** 2595-2603.

Blanc S, López-Moya JJ, Wang R, García-Lampasona S, Thornbury DW, Pirone TP. 1997. A specific interaction between coat protein and helper component correlates

with aphid transmission of a potyvirus. *Virology* **231:** 141-147.

Burgyán J, Havelda Z. 2011. Viral suppressors of RNA silencing. *Trends Plant Sci* **16:** 265-272.

Canto T, López-Moya JJ, Serra-Yoldi MT, Díaz-Ruíz JR, López-Abella D. 1995. Different helper component mutations associated with lack of aphid transmissibility in two isolates of *Potato virus Y*. *Phytopathology* **85:** 1519-1524.

Canto, T., Ellis, J. P., Bowler, G., and López-Abella, D. (1995). Production of monoclonal antibodies to Potato virus Y Helper Component protease and their use for strain differentiation. *Plant Dis* **79:** 234-237.

Carbonell A, Fahlgren N, Garcia-Ruiz H, Gilbert KB, Montgomery TA, Nguyen T, Cuperus JT, Carrington JC. 2012. Functional analysis of three Arabidopsis ARGONAUTES using slicer-defective mutants. *Plant Cell* **24:** 3613-29.

Carrington JC, Herndon KL. 1992. Characterization of the potyviral HCPro autoproteolytic cleavage site. *Virology* **187:** 308-15.

Chapman, E.J., Prokhnevsky, A.I., Gopinath, K., Dolja, V.V. and Carrington, J. 2004. Viral RNA silencing suppressors inhibit the microRNA pathway at an intermediate step. *Genes Dev* **18:** 1179-1186.

Cheng, Y-Q., liu, Z-M., Xu, J., Zhou, T., Wang, M., Chen, Y-T., Li, H-F. and Fan, Z-F. 2008. HC-Pro protein of sugar cane mosaic virus interacts specifically with maize ferredoxin-*5 in vitro* and *in planta*. *J Gen Virol* **89:** 2046-2054.

Del Toro F, Tena F, Tilsner J, Wright K, Tenllado F, Chung B-N, Praveen S, Canto T. 2014. *Potato virus Y* HCPro localization at distinct, dynamically-related and environment-influenced structures in the cell cytoplasm. *Mol Plant-Microbe Interact* **27:** 1331-1343.

Ding SW, Voinnet O. 2007. Antiviral Immunity Directed by Small RNAs. *Cell* **130:** 413-426.

Ding SW. 2010. RNA-based antiviral immunity. *Nat Rev Immunol* **10:** 632-44.

Donaire L, Wang Y, Gonzalez-Ibeas D, Mayer KF, Aranda MA, Llave C. 2009. Deep-sequencing of plant viral small RNAs reveals effective and widespread targeting of viral genomes. *Virology* **392:** 203-14.

Dunoyer P, Lecellier CH, Parizotto EA, Himber C, Voinnet O. 2004. Probing the microRNA and small interfering RNA pathways with virus-encoded suppressors of RNA silencing. *Plant Cell* **16:** 1235–1250.

Ebhart HA, Thi EP, Wang M-B, Unrau PJ. 2005. Extensive 3´ modification of plant small RNAs is modulated by helpercomponent-proteinase expression. *Proc Natl Acad Sci USA* **102**: 13398-13403.

Endres MW, Gregory BD, Gao Z, Foreman AW, Mlotshwa S, Ge X, Pruss GJ, Ecker JR, Bowman LH, Vance V. 2010. Two plant viral suppressors of silencing require the ethylene-inducible host transcription factor RAV2 to block RNA silencing. *PLoS Pathog* **6:** e1000729.

Gal-On A, Canto T, Palukaitis P. 2000. Characterisation of genetically modified cucumber mosaic virus

expressing histidine-tagged 1a and 2a proteins. *Arch Virol* **145:** 37-50.

García-Ruíz H, Carbonell A, Hoyer JS, Fahlgren N, Gilbert KB, Takeda A, Giampetruzzi A, García Ruíz MT, McGinn MG, Lowery N, Martinez Baladejo MT, Carrington JC. 2015. Roles and programming of Arabidopsis ARGONAUTE proteins during Turnip mosaic virus infection. *PLoS Pathog* **11:** e1004755.

González I, Rakitina D, Semashko M, Taliansky M, Praveen S, Palukaitis P, Carr J, Kalinina N, Canto T. 2012. RNA binding is more critical to the suppression of silencing function of *Cucumber mosaic virus* 2b protein than nuclear localization. *RNA* **18:** 771-782.

González-Jara P, Atencio FA, Martínez-García B, Barajas D, Tenllado F, Díaz-Ruíz JR. 2005. A single amino acid mutation in the plum pox virus helper component-proteinase gene abolishes both synergistic and RNA silencing suppression activities. *Phytopathology* **95:** 894-901.

Haikonen, M.T., Rajamaki, M.L., and Valkonen, J. 2013. Interaction of the Microtubule Associated Host Protein HIP2 with the Viral Helper Component Proteinase is Important in Infection with Potato Virus A. *Mol Plant-Microbe Interact* **26:** 734-744.

Harvey JJ, Lewsey MG, Patel K, Westwood J, Heimstädt S, Carr JP, Baulcombe DC. 2011. An antiviral defense role of AGO2 in plants. *PLOS One* **6:** e14639.

Jamous RM, Boonrod K, Fuellgrabe MW, Ali-Shetayen MS, Krczai G, Wassenegger M. 2011. The helper component-proteinase of the Zucchini yellow mosaic virus inhibits the Hua Enhancer 1 methyltransferase activity in vitro. *J Gen Virol* **92:** 2222-2226.

Jaubert MJ, Bhattacharjee S, Mello AF, Perry KL, Moffett P. 2011. AGO2 mediates RNA silencing anti-viral defenses against *Potato virus X* in Arabidopsis. *Plant Physiol* **156:** 1556-1564.

Jin Y, Ma D, Dong J, Jin J, Li D, Deng C, Wang T. 2007a. HCPro of *Potato virus Y* can interact with three Arabidopsis 20S proteasome subunits in planta. *J Virol* **81:** 12881-12888.

Jin, Y., Ma, D., Dong, J., Li, D., Deng, C., Jin, J. and Wang, T. 2007. The HC-Pro protein of *Potato virus Y* interacts with NtMinD of tobacco. *Mol Plant-Microbe Interact* **20:** 1505-1511.

Kasschau and Carrington 1998. A Counterdefensive Strategy of Plant Viruses: Suppression of posttranscriptional Gene Silencing. *Cell* **95**: 461–470

Kasschau KD, Xie Z, Allen E, Llave C, Chapman EJ, Krizan KA, and Carrington JC. 2003. P1/HC-Pro, a viral suppressor of RNA silencing, interferes with Arabidopsis development and miRNA function. *Dev Cell* **4:** 205–217.

Kreuze JF, Perez A, Untiveros M, Quispe D, Fuentes S. 2009. Complete viral genome sequence and discovery of novel viruses by deep sequencing of small RNAs: a generic method for diagnosis, discovery and sequencing of viruses. *Virology* **388:** 1-7.

Lakatos L, Csorba T, Pantaleo V, Chapman EJ, Carrington JC, Liu

YP, Dolja VV, Calvino LF, López-Moya JJ, Burgyán J. 2006. Small RNA binding is a common strategy to suppress RNA silencing by several viral suppressors. *EMBO J* **21:** 2768-2780.

Langmead B, Trapnell C, Pop M, Salzberg SL. 2009. Ultrafast and memory-efficient alignment of short DNA sequences to the human genome. *Genome Biol* **10:** R25.

Langmead B, Salzberg SL. 2012. Fast gapped-read alignment with Bowtie 2. *Nat Methods* **9:** 357-359.

Lu R, Malcuit I, Moffett P, Ruíz MT, Peart J, Wu AJ, Rathjen JP, Bendahmane A, Day L, Baulcombe DC. 2003. High throughput virus-induced gene silencing implicates heat shock protein 90 in plant disese resistence. *EMBO J* **22:** 5690-5699.

Maia IG, Bernardi F. 1996. Nucleic acid-binding properties of a bacterially expressed *potato virus Y* helper component protinase. *J Gen Virol* **77:** 869-877.

Mangrauthia SK, Singh Shakya VP, Jain RK, Praveen S. 2009. Ambient temperature perception in papaya for papaya ringspot virus interaction. *Virus Genes* **38:** 429-434.

Mérai Z, Kerényi Z, Kertész S, Magda M, Lakatos L, Silhavy D. 2006. Double-stranded RNA binding may be a general plant RNA viral strategy to suppress silencing. *J Virol* **80:** 5747-5756.

Mi S, Cai T, Hu Y, Chen Y, Hodges E, Ni F, Wu L, Li S, Zhou H, Long C, Chen S, Hannon GJ, Qi Y. 2008. Sorting of small RNAs into Arabidopsis argonaute complexes is directed by the 5' terminal nucleotide. *Cell* **133:** 116–127.

Montgomery TA, Howell MD, Cuperus JT, Li D, Hansen JE, Alexander AL, Chapman EJ, Fahlgren N, Allen E, Carrington JC. 2008. Specificity of ARGONAUTE7-miR390 interaction and dual functionality in TAS3 trans-acting siRNA formation. *Cell* **133:** 128–141.

Naim F, Nakasugi K, Crowhurst RN, Hilario E, Zwart AB, Hellens RP, Taylor JM, Waterhouse PM. 2012. Advanced Engineering of Lipid Metabolism in Nicotiana benthamiana Using a Draft Genome and the V2 Viral Silencing-Suppressor Protein. *PLOS One* **7:** e52717.

Nakahara KS, Masuta C. 2014. Interaction between viral RNA silencing suppressors and host factors in plant immunity. *Curr Opin Plant Biol* **20:** 88-95.

Pirone TP, Blanc S. 1996. Helper-dependent vector transmission of plant viruses. *Ann Rev Phytopathol* **34**: 227–247.

Plisson, C., Drucker, M., Blanc, S., German-Retama, S., Le Gall, O., Thomas, C. and Bron, P. 2003. Structural characterization of HC-Pro, a plant virus multifunctional protein. *J Biol Chem* **278:** 23753-23761.

Pruss, G, Ge, X, Shi, XM, Carrington, JC, Vance, VB. 1997. Plant viral synergism: the potyviral genome encodes a broad-range pathogenicity enhancer that transactivates replication of heterologous viruses. *Plant Cell* **9:** 859-868.

Qu F. 2010. Antiviral role of plant-encoded RNA-dependent RNA polymerases revisited with deep sequencing of small interfering

RNAs of virus origin. *Mol Plant-Microbe Interact* **23:** 1248-1252.

Ruíz-Ferrer, V., Boskovic, J., Alfonso, C., Rivas, G., Llorca, O., López-Abella, D. and López-Moya, J.J. 2005. Structural analysis of *Tobacco etch potyvirus* HC-Pro oligomers involved in aphid transmission. *J Virol* **79:** 3758-3765.

Sahana N, Kaur H, Palukaitis P, Canto T, Praveen S. 2014. The asparagine residue in the FRNK box of potyviral helper-component protease is critical for template function and subcellular localization. *J Gen Virol* **95**: 1167-1177.

Shiboleth YM, Haronsky E, Leibman D, Arazi T, Wassenegger M, Whitham SA, Gaba V, Gal-On A. 2007. The conserved FRNK box in HC-Pro, a plant viral suppressor of gene silencing, is required for small RNA binding and mediates symptom development. *J Virol* **81:** 13135-13148.

Szittya G, Moxon S, Pantaleo V, Toth G, Rusholme Pilcher RL, Moulton V, Burgyan J, Dalmay T. 2010. Structural and functional analysis of viral siRNAs. *PLoS Pathog* **6:** e1000838.

Takeda A, Iwasaki S, Watanabe T, Utsumi M, Watanabe Y. 2008. The mechanism selecting the guide strand from small RNA duplexes is different among argonaute proteins. *Plant Cell Physiol* **49:** 493-500.

Tena F, González I, Doblas P, Rodríguez C, Sahana N, Kaur H, Tenllado F, Praveen S, Canto T. 2013. The influence of cis-acting P1 protein and translational elements on the expression of *Potato virus Y* HCPro in heterologous systems and its suppression of silencing activity. *Mol Plant Pathol* **14:** 530-541.

Urcuqui-Inchima S, Maia IG, Arruda P, Haenni AL, Bernardi F. 2000. Deletion mapping of the potyviral helper component-proteinase reveals two regions involved in RNA binding. *Virology* **268:** 104-111.

Valli A, Gallo A, Calvo M, de Jesús Pérez J, García JA. 2014. A novel role of the potyviral helper component proteinase contributes to enhance the yield of viral particles. *J Virol* **88:** 9808-9818.

Vargasson, J.M., Szittya, G., Burgyan, J. and Hall, T.M. 2003. Size selective recognition of siRNAs by an RNA silencing suppressor. *Cell* **115:** 799-811.

Vaucheret H. 2008. Plant ARGONAUTES. *Trends Plant Sci* **13:** 350-358.

Yi X, Zhang Z, Ling Y, Xu W, Su Z. 2015. PNRD: a plant non-coding RNA database. *Nucleic Acids Res* **43**(Database issue)**:** D982-989.

Zhang X, Singh J, Li D, Qu F. 2012. Temperature-dependent survival of Turnip crinkle virus- infected arabidopsis plants relies on an RNA silencing-based defense that requires dcl2, AGO2, and HEN1. *J Virol* **86:** 6847–6854.

Zheng , H., Yan, F., Lu, Y., Sun, L., lin, L., Cai, L., Hou, M. and Chen, J. 2011. Mapping the self-interacting domains of TuMV HC-Pro and the subcellular localization of the protein. *Virus Genes* **42:** 110-116.

Zuker M. 2003. Mfold web server for nucleic acid folding and hybridization prediction. *Nucleic Acids Res* **31:** 3406-3415.

Supplemental material

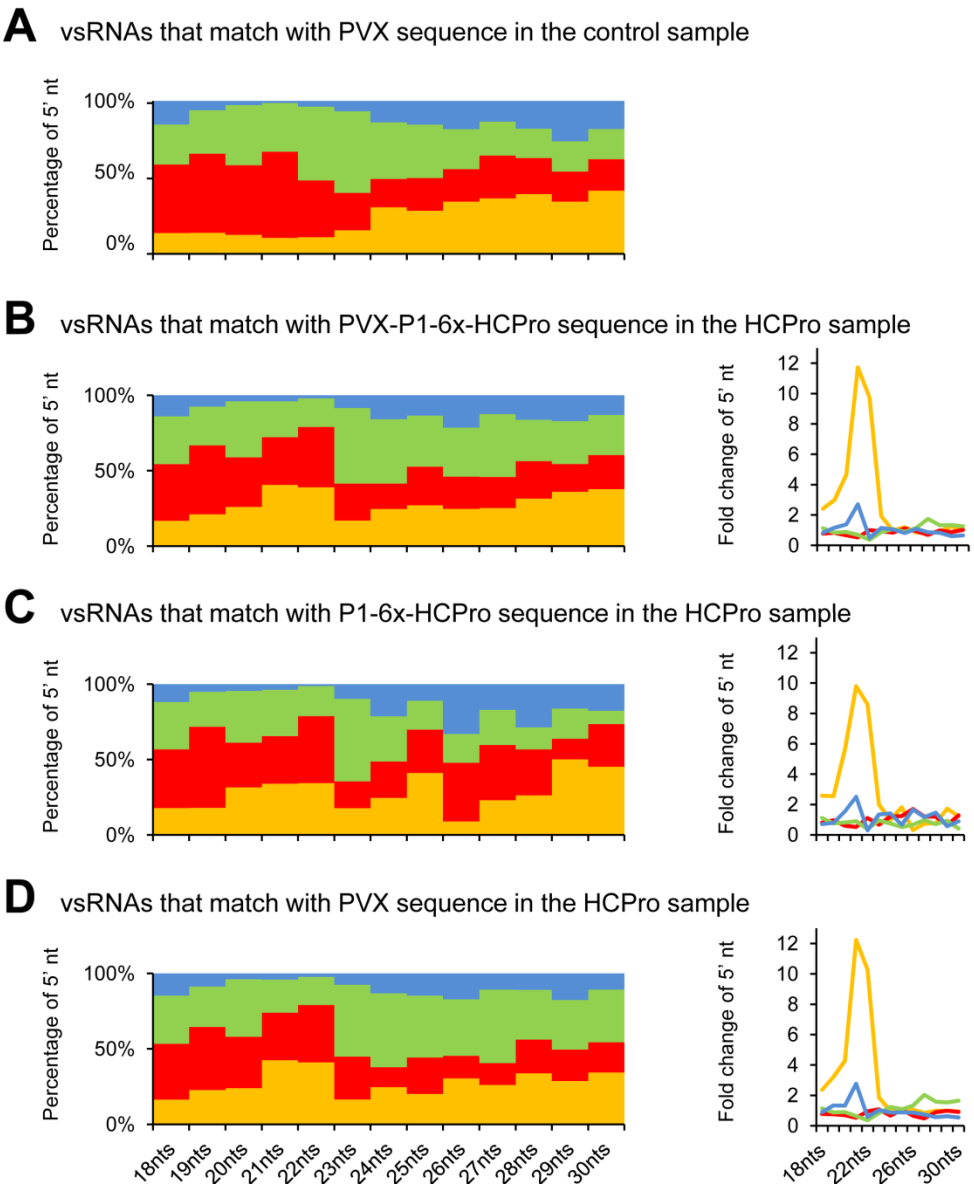

SUPPLEMENTAL FIGURE 1. Analysis of 5' end nucleotide prevalence in reads of RNA sizes ranging from 18 to 30 nts of viral sequence in the control and HCPro samples matching with either the PVX sequence or with the modified potyviral P1-6x-HCPro bicistron. (A) Upper left chart, percentage of 5'-end nucleotides (nt) RNA reads that match with PVX sequences in the control sample. (B) Left chart, percentage of 5'-end nts that match with PVX-P1-6x-HCPro sequences in the HCPro sample; right chart, corresponding fold change values in the HCPro sample relative to the control sample shown in A. (C) Left chart, percentages of 5'-end nucleotides (nt) in RNA reads that match the potyviral P1-6x-HCPro modified bi-cistron sequence in the HCPro sample; right chart, corresponding fold change values in the HCPro sample relative to the control sample shown in A. (D) Left chart, percentages of 5'-end nucleotides (nt) in RNA reads that match with the PVX genome in the control and HCPro samples, respectively; right chart, corresponding fold change values in the HCPro sample relative to the control sample shown in A.

CHAPTER 7

GENERAL DISCUSSION

Either in the wild or as part of crops, plants are components of a wider ecosystem, and have to interact with the biotic and abiotic factors of their environment. Biotic factors can range from the smallest biological entities, such as viruses, viroids or phytoplamas, to the large animal herbivores. Among the abiotic factors, temperature and CO_2 are important, as they affect plant growth and development, and also how plants respond to other environmental challenges.

Historically, plant viruses have been pathogens that cause losses in crops (Hull, 2002), and they continue to be so in the present, in spite of improvements in the prevention of virus dispersal, and of continuous efforts to introgress resistances specific to some viruses into crop varieties of high agricultural value. This is because those introgressed resistances can be overcome by the evolution through mutations, which occur fast in RNA viruses, in already genetically diverse natural virus populations, followed by the positive selection of favored variants. In addition to that, the current context in which climate change (http://www.ipcc.ch) colludes with increased global trade creates situations where new viruses-virus strains and their vectors can disperse and establish into other geographic zones with more ease than previously. This is leading to frequent outbreaks of new viral diseases in modern crops that lack resistances to them (Canto *et al.*, 2009). Crops that are the basis of modern large-scale agriculture from which global food supplies ultimately depend are genetically homogeneous, and a severe outbreak can thus have rather devastating effects on yields. Therefore, knowledge on how plants and viruses and their vectors interact at the molecular level, on how plants defend themselves from infection, on how infection leads to disease symptoms, and on how infection can affect the relationship of the plant

with its surrounding environment and *vice-versa* is relevant to the aim of creating a more sustainable, yet safe from the supply perspective, agriculture.

Compatible infections by plant viruses and how those infections relate to the interaction of a plant with its environment are being investigated by scientists at different levels; from the molecular or cellular ones, to those of the individual specimen, populations of individuals, or ecosystems. These levels of research require each their specialized approaches. This PhD Thesis investigated aspects of interactions between positive-sense RNA viruses and a compatible experimental host plant at several of those levels: at the molecular and the cellular levels, studying specific viral and host factors, sometimes in virus-free systems, and also at the individual plant level and at the population level, using whole infected plants as the investigated subject.

In plant-virus molecular interaction studies of the determination and characterization of specific protein functions is confronted with the difficulty of discerning which viral and host components are involved in specific biological mechanisms and processes during the course of a natural infection. This is because multiple factors are at play at any given moment. However, the transient expression of specific genes in plants allows the study of those particular in their natural cellular background in the absence of other elements, and to assess their specific effect in the plant, their interplay with other molecules and structures, and even to perform biological function assays. Two such systems to express specific transcripts and their encoded proteins in plants are the use of viral vectors, or their delivery as T-DNAs into plant cells by agroinfiltration. In

this PhD Thesis extensive use was made of both systems, in particular the agroinfiltration technique.

The agroinfiltration technique is widely used in plant research, and in plant virology in particular, to express ectopic genes under standard temperature conditions in the glasshouse or in plant growth chambers, usually at between 20 to 28 °C. The technique is not functional at temperatures above 29 ºC because of the failure of the bacteria to develop the physical pilus structure that will transfer the T-DNA to the plant cells (Fullner and Nester, 1996; Gelvin, 2003). However, in order to study how warmer temperatures (30 °C vs. 25°C) affect viral infections and the silencing suppression functions of some viral VSRs, an agroinfiltration procedure was developed in this PhD Thesis that allows the expression and accumulation of those genes under elevated temperature conditions, and even to perform functional studies. In our experience, expression levels of a reporter (GFP) with an empty vector or with the VSRs of either PVY, CMV or TBSV (HCPro, 2b and P19, respectively) were very poor when plants were placed at 30 ºC immediately after agroinfiltration (Chapter 3, Fig 1). Therefore, our results confirm those of the literature (Fullner and Nester, 1996). We reasoned that if we provided a window of time at 25 ºC before moving the plants to 30 ºC, pilus formation and T-DNA transfer could then proceed to some degree. Proteins could then be expressed and accumulate at the elevated temperature, and their biological properties could be studied. We tested two window periods at 25 ºC, of 12 and 24 hours, respectively, previous to placing the plants at 30 ºC, and compared the transient steady-state levels of protein accumulation in those plants, with those found in agroinfiltrated control plants that had been kept all the time at 25 °C. We studied the accumulation of a GFP reporter as well

as those of two VSRs constructs based on the 2b protein from CMV (6x-2b-HA) and HCPro from PVY (6x-HCPro). The shorter window period (12 h) proved unsatisfactory, but in the larger window period (24 h) GFP accumulation levels were comparable to those observed in the plants kept at 25 ºC (Chapter 3, Figs. 1 and S1). Time-course experiments performed to check the accumulation of these three proteins at 24, 48 and 72 hpi showed differences among them: the HCPro construct could not be detected serologically before 24 hpi using two different antibodies, GFP was detected at 24 hpi but its accumulation was a fraction of that found at 3 dpi. By contrast, the 2b construct was already detected at 24 hpi and its accumulation decreased with time (Chapter 3, Fig. 2). At one given time after infiltration (3 dpi) accumulation of GFP and of the HCPro suppressor was similar to that found in plants kept all the time at 25 °C, but not that of the 2b protein. Nevertheless, this decrease in the accumulation of the 2b construct did not correlate with a decrease in its capability as suppressor of the silencing of a GFP reporter. This suggests that in agroinfiltrations at 25 °C and at 3 dpi, this suppressor accumulates in excess of what is needed to prevent the silencing of transcripts derived from agroinfiltrated T-DNAs, or alternatively, that at the higher temperature the 2b protein suppressor activity is stronger or faster than at 25 °C, or that the protein subcellular distribution at the higher temperature is altered, making it more cytoplasmic. With regard to the latter, recent work by Du *et al.*, (2014) has shown that the balance between nuclear and cytoplasmic accumulation of the 2b protein can modulate both, its suppressor activity in agropatch assays and its pathogenicity in virus infections.

As was discussed in Chapter 3 these differences between different proteins with regard to their timings of appearance or in their subsequent accumulation kinetics may be related to different transcription and translation efficiencies, different stabilities of the mature protein products, or to some of them being differentially targeted or more susceptible to degradation processes of the host, such as those mediated by the proteasome (Ballut *et al.*, 2005; Dielen *et al.*, 2011; Jin *et al.*, 2007; Sahana *et al.*, 2012) or autophagy (Nakahara *et al.*, 2012). In any case, differences in protein expression and accumulation in agroinfiltration experiments had been observed by others (Liu *et al.*, 2010)

The capabilities of the agroinfiltrated binary constructs expressing PVX-based viral amplicons to infect plants or to express heterologous proteins through them above the restrictive temperature of 29 ºC was also investigated. Placing of plants at 30 ºC immediately after their agroinfiltration with binaries expressing PVX-based viral amplicons resulted in most but not all of them becoming infected (Chapter 3, Fig S1C). However, all the plants that had a window period of 24 h at 25 ºC became successfully infected (Chapter 3, Fig 3B). Therefore, using the viral amplicon vectors could in many cases compensate the negative effect of 30 °C on agroinfiltration delivery efficiency. However, although the placement of plants at 25 ºC was not strictly required, a period of 24 h at this temperature is advisable to ensure infection. On the other hand, amplicon-mediated expression of genes has several disadvantages, being not the least of them that plant cells become infected with a virus, or that co-expression of more than one gene inside the same cell is not possible because of cross-protection reasons.

It can therefore be concluded that the agroinfiltration procedure developed here allows the transient expression of proteins at elevated temperatures and their executing their biological activities and dynamics under those conditions, in living cells. The procedure could prove a useful tool in plant research at non-permissive temperatures. Furthermore, the procedure could potentially be also used to design means to compare accumulation kinetics of different proteins, or between those of different mutant variants of the same protein, giving an insight into their relative turnovers, although this line of investigation was not pursued further in this Thesis.

One of the goals of this PhD Thesis was to study how compatible plant-virus interactions could become affected by high temperatures, and by elevated atmospheric CO_2 levels. Plants are expected to be increasingly exposed to both if the greenhouse gas emissions and climate change projections proceed as modeled. Exposure of crops to high temperatures will become increasingly frequent as the century advances, unless compensatory measures are adopted, such as the shifting of crops to higher latitudes or altitudes, or of agricultural practices to earlier in the season. There are limits however to how far these shifts can take place in practice. The elevated ambient CO_2 will very likely become a permanent situation for some time to come.

To perform these studies the analysis of the effects of these parameters was carried out separately. Comparisons were made on defined aspects of compatible infections that took place at: a) 30 versus 25 ºC, under the current standard (st) levels of CO_2 (401 ppm); b) under st vs. elevated levels of CO_2 (970 ppm) at 25 °C. Experiments were performed in the host *N. benthamiana*, challenged with CMV, PVY or a PVX viral vector,

the latter either unaltered or expressing the 6x-2b-HA or the 6x-HCPro constructs. The parameters analyzed were the visual infection symptoms in plants, the comparative viral titers in systemic tissues at 7 days post inoculation (dpi), and the comparative activities of the corresponding viral suppressors of silencing under those environmental conditions.

The five different positive ssRNA viruses used in these studies were all able to infect systemically *N. benthamiana* plants in the three conditions tested: [normal environment conditions (25 °C and st CO_2); high temperature conditions (30 °C and st CO_2); and elevated CO_2 conditions (25 °C and 970 ppm)], but the outcomes where very different depending on the virus and the environment condition. The increase in temperatures produced a marked reduction of the visual symptoms in plants infected with PVY and a delay in their appearance that concurred with decreased viral titers (measured by the levels of viral CP and of genomic viral RNA in systemic tissue) when compared to the normal conditions (Chapter 3, Fig. 3; and Chapter 4, Figs 1 and 2).

In the case of CMV infection at elevated temperatures, neither the timing of appearance of viral symptoms nor their severity were delayed, when compared with those observed under normal conditions. Viral titers (measured as CP levels) were slightly lower at the higher temperature. However, when comparing genomic RNA 3 levels by RT-qPCR of an amplicon located inside the *MP* gene, RNA levels actually increased at the higher temperature conditions. This discrepancy between titers measured by CP levels and those measured by genomic RNA 3 levels could perhaps be caused by a slower translation of CP from subgenomic RNA 4 at elevated temperatures, or by a preferential accumulation of the RNA 3 over those of other viral RNAs.

In conclusion, the increase of temperature caused a decrease of the systemic viral accumulation of PVY and a marked attenuation of the infection symptoms that did not happen in the case of CMV. Therefore, both viruses responded in a markedly different way to high temperature during their infection of this common host.

Masking of symptoms in many virus-plant interactions at elevated temperatures (the heat masking effect) has been known since the early times of plant virology (Hull, 2002; Johnson, 1922). The reason for this effect remained unknown but has been used to advantage to for example regenerate transform plants that express viral amplicons that would otherwise prevent it or difficult it (Dujovny *et al.*, 2009). However, more recently, the discovery of gene silencing and of the viral suppressors of silencing, many of them characterized as pathogenicity determinants, opened the possibility that this plant mechanism or its suppression by viral factors could be being affected by temperature. In fact, as discussed in Chapter 4, several works showed that in different plant-virus systems elevated temperatures seemed to increase the strength of gene silencing. Some authors proposed that symptom masking occurred because of the enhanced strength of antiviral silencing (Chellappan *et al.*, 2005; Qu *et al.*, 2005; Szittya *et al.*, 2003; Velázquez *et al.*, 2010). The reasons for this enhanced strength are also discussed in that chapter and are yet not well known, but briefly, could be related to increased efficiencies of some components of the silencing machinery at the higher temperatures (Chellappan *et al.*, 2005; Zhang *et al.*, 2012; Zhong *et al.*, 2013). If this was the case, differences between viruses in their infection outcomes at elevated temperatures, such as those observed with the PVY isolate and the CMV Fny strain in this Thesis could derive from their suppressors of

silencing being or being not able to efficiently compensate silencing under those conditions. Thus, it was tested whether HCPro had a diminished functionality at elevated temperatures, and the same was tested for the 2b protein. For that we used the binary constructs that expressed these two proteins modified by the addition of tags for several research purposes (binary constructs P1-6x-HCPro and 6x-2b-HA), characterized earlier to be as functional in silencing suppression in agropatch assays as the native proteins by Tena Fernández *et al.* (2013) and González *et al.* (2010), respectively. These tests were pursued by comparing their silencing suppression activities on a GFP reporter in agropatch assays, under conditions of elevated vs. normal temperature. To do that, we took advantage of the agroinfiltration procedure for elevated temperatures that we developed in Chapter 3. The results were that at 30 ºC the HCPro construct was able to efficiently suppress silencing of the reporter, as was also the 2b construct (Chapter 4. Fig. 5). Therefore, under the physiological conditions of elevated temperature in this host, the two suppressors were able to perform their function, that is, to suppress antiviral silencing, independently of whether this defense was stronger or not than at the normal temperature. Even if this was true for the agropatch transient assays, the possibility remained that in the systemically infected plant, HCPro levels could be too low to perform their function satisfactorily. But it was found that this was not the case either, as can be seen in Fig. 5 of Chaper 4, which shows that HCPro levels in the infected plant at 30 °C were several-fold higher than in the agropatch assay. The conclusion is that the masking of PVY infection is not caused by a changed balance between silencing and its suppression. In the Discussion section of Chapter 4, other processes that could be being affected by

elevated temperature, such as the assembly and translocation of replication viral factories or viral movement are suggested.

We also analyzed the infection of *N. benthamiana* plants by PVX vectors under normal or elevated temperature conditions. We used three constructs: the "empty" vector that had an added potexviral promoter to express cloned genes from a new subgenomic RNA (Lu *et al.*, 2003) or the same vector expressing the modified VSRs of PVY, (construct P1-6x-HCPro), or of CMV (construct 6x-2b-HA), already used in this Thesis in virus-free agropatch assays. First of all it was characterized how the expression of the heterologous VSRs affected the accumulation and induction of symptoms of the three PVX constructs at normal temperature. With regard to symptoms, we observed that the expression from the vector of either of the silencing suppressors resulted in increased severity of symptoms: while PVX infection caused the typically symptoms of mosaicism and curling of leaves, stronger symptoms that included necrotic spots were observed in infections with PVX-P1-6x-HCPro and PVX-6x-2b-HA (Chapter 3, Fig 3). In contrast to the more severe symptoms, no increase in viral titers was observed in the PVX constructs that expressed the heterologous VSRs (Chapter 3, Fig. 3). Therefore, increased severity of viral symptoms in this case did not correlate with increased viral titer. This phenomenon had been observed in plants infected with a recombinant PVX expressing PPV HCPro, despite enhanced symptoms (González-Jara *et al.*, 2005). The synergism in symptoms could derive from the increased accumulation of the PVX endogenous VSR P25 in the presence of the heterologous and stronger VSRs from PVY or CMV, as was shown for *Plum pox virus* (PPV) HCPro (Aguilar *et al.*, 2015a), or by the action of the heterologous VSRs

themselves. On the other hand, failure of the heterologous VSRs to increase viral titers could be based on the increase in the genomic size of the PVX vectors that express the heterologous VSRs, very large, over 2300 nts in the case of the *P1-6x-HCPro* insert. However, the increase in genome size was smaller (less than 400 nts) in the case of *the 6x-2b-HA* insert, but still the construct failed to accumulate more. The fact that the presences of those strong heterologous suppressors of silencing failed to help PVX accumulation or its induction of symptoms at elevated temperatures also points to processes other than antiviral RNA silencing as being responsible for the viral titer and symptom outcomes.

Once the properties of the three PVX constructs were characterized under normal environment conditions we analyzed the effect of elevated temperature on them. At 30 °C all infected plants showed no visual symptoms, even when they were infected by the PVX constructs expressing the heterologous VSRs (Chapter 3, Fig. 3; and Chapter 4, Fig 1). We analyzed the systemic accumulation of the three PVX constructs by the serological quantitation of CP levels, as well as by RT-qPCR quantitation of genomic RNA levels. In all three constructs a decrease in virus levels was observed at the higher temperature (Chapter 3, Fig 3; Chapter 4, Figs. 1 and 2). Interestingly, titers of PVX at 30 °C were similar or slightly lower than those of construct PVX-P1-6x-HCPro at 25 °C (Chapter 3, Fig 3; Chapter 4, Fig. 2) in spite of the former causing no infection symptoms and of the latter causing them. Therefore, the severity of symptoms is not determined by viral titers in this case.

With regard to the activity as suppressor of silencing of the PVX P25 protein silencing suppression agropatch assays, it was tested by Aguilar and colleagues in a collaborative work (2015a). The PVX endogenous

suppressor was able to increase steady-state accumulation levels of the GFP reporter in agropatch similarly at 30 ºC and at 25 ºC.

In conclusion, elevated temperature (30 °C) decreases viral symptoms in *N. benthamiana* plants infected with PVX or with PVY, and this visual phenotype correlates with decreases in viral titers, but not necessarily the first observation depends on the second. Furthermore, it appears that this decrease in titers and symptoms is not caused by a diminished efficiency of their suppressors of silencing. Our results would also imply that efficient silencing suppression does not lead to severe symptom induction. On the other hand, CMV Fny infection was not altered by elevated temperatures, and therefore, it groups separately from PVY and PVX.

We do not know which other processes could be differentially affected by elevated temperatures in these three types of viruses. But we can speculate. One such process could be the maturation of viral replication complexes. Elevated temperatures can alter the fluidities of membranes and lead to organelles and cytoskeleton reorganization (Weis and Berry, 1988; Saidi *et al.*, 2009). Could this changes influence viral accumulation in PVY and PVX infections but not those of the PVX vectors? Replication of all these viruses take place associated to specific types of subcellular membranes (Park *et al.*, 2013; Wei *et al.*, 2010; Gal-On *et al.*, 2000; Cillo *et al.*, 2002). It should be borne in mind that all the five viruses tested were able to infect plants systemically at 7 dpi at either 25 or 30 °C, so any depressive effects of the higher temperature on replication would not have to delay their systemic dispersal.

An environment with elevated atmosphere CO_2 levels is another situation to which plants will be exposed to in the future. For this reason, in the same way as was done for elevated temperatures, the infection of *N.*

benthamiana plants with PVY, CMV or with the three PVX constructs was comparatively studied at elevated (970 ppm) vs. st. (current ~401 ppm) CO_2 levels. In elevated CO_2 environments healthy and infected plants were found to grow faster and thus larger than those kept at st CO_2 level within the time frame of our experiments. However, infection symptoms remained unaltered for all five viruses under both CO_2 conditions. Viral titers in equivalent leaf disks were also analyzed and compared using the serological quantitation of viral CPs. All viruses showed decreased titers/equivalent leaf discs in the increased CO_2 environment, except again CMV, whose accumulation increased (Chapter 4. Fig. 3).

To assess whether the efficiencies of the corresponding viral silencing suppressors in the conditions of high CO_2 levels would differ from those at st levels, silencing suppression agropatch assays were performed. The results show that the 6x-HCPro and 6x-2b-HA proteins were able to suppress RNA-mediated silencing of the reporter at similar levels than observed at standard conditions. Aguilar and colleagues in a collaborative work also confirmed the activity of the PVX P25 suppressor under the same conditions (Aguilar *et al.*, 2015a). Hence we can assume that reduction of viral titers observed for PVY or the different constructs studied of PVX elevated CO_2 environment cannot relay in a diminished ability of their respective VSRs to suppress silencing under those conditions.

These assays did not show that the 6x-2b-HA protein of CMV Fny had enhanced suppressor activity in the elevated CO_2 conditions in agropatch assays (Chapter 4. Fig. 5), suggesting that increased accumulation of CMV under those conditions does not result from increased activity of the 2b protein.

Decreased levels of Rubisco protein at elevated CO_2 levels were observed in the SDS-PAGE analysis of all protein samples. This result was unanticipated, but proved to be in agreement with previous observations by other groups that showed increased photosynthesis and C:N ratios when plants were grown in elevated CO_2 levels (Drake *et al.*, 1997; Kirschbaum and Lambie, 2015; Matros *et al.*, 2006). For this reason, total protein contents in leaf discs were measured. Results were striking. In *N. benthamiana* leaf discs total protein content halved in plants kept at elevated CO_s levels when compared to equivalent discs in plants grown at st CO_2 levels., independently of whether they were infected or not.

Interestingly, when normalizing viral titers to total protein content, rather than to leaf discs, accumulation of every virus studied increased in the high CO_2 environment (Chapter 4. Table 1). This fact could be of relevance to fields such as biotechnology, which could take advance of the relative enrichment in viral protein content in production processes such as plant molecular farming based in the use of viral-vectors (Peyret and Lomonossoff, 2015). Therefore, although *N. benthamiana* plants grew larger under high CO_2 than under normal conditions, total protein content did not follow in the increase. It is not known whether larger plant size in these experiments derives from larger cells, more water content, rather than from increased number of cells, or not, but it is something to be analyzed in the future.

In conclusion, heat masking by high temperature in the case of the PVY isolate and of the three PVX vectors should not be attributable in the plant-virus system studied to compromised silencing suppression. Reduced viral titers (in equivalent leaf discs) under elevated environmental CO_2 also cannot not be related to challenged suppressor activities of the

viral proteins. Therefore in both cases other processes must be affected by the two parameters analyzed. In-depth studies in host metabolic changes, hormonal signaling, gene expression, and in viral protein functions and their inter- and intracellular interactions would be important to answer that.

The parameters temperature and CO_2 levels were studied separately to evaluate their effect of each on infection. However, in nature, both altered parameters will occur often simultaneously. Would the effects of these two parameters on infection somewhat compensate among themselves, or by the contrary be additive, even multiplicative, or not? Preliminary results from a experiment limited to PVY indicate that both parameters combined (30 ºC and 970 ppm of CO_2 levels) have severe effect in the titers of this virus, which experience a dramatic drop to only 2-8% of the levels found in normal conditions (25 °C and st CO_2 levels), with practically no symptoms (Fig. 1 in this Chapter and data not shown). It would be interesting to see if the PVX constructs follow the PVY pattern when exposed to both altered parameters simultaneously, and if CMV still retains its ability to accumulate and induce symptoms as in the normal situation. At this point there are more questions than answers. What effects would elevated temperature and CO_2 have on the prospects of dispersal and survival of certain viruses? There could be losers and winners. In the case of the PVY isolate used here, a drop of viral titers of more than 90%, to very low levels (and also in the cellular levels of non-structural proteins, including HCPro involved in transmission) would very likely compromise its ability to be transmitted by vectors, even without considering additional effects on transmission by vectors derived from changes in attraction/repulsion of aphids by visual

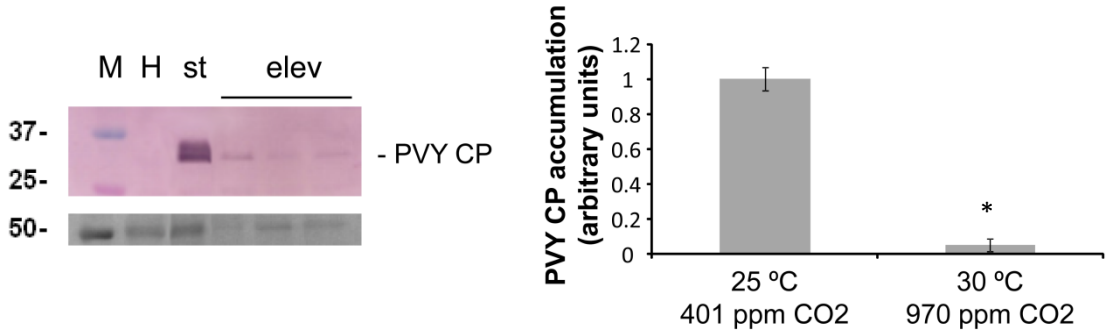

Fig 1. Systemic infection of *Nicotiana benthamiana* plants with *Potato virus Y* (PVY), at standard conditions (st; 25 °C and 401 ppm of CO_2) and elevated temperature and CO_2 conditions (elev; 30 ºC and 970 ppm of CO_2). The left coat protein (CP) western blot panel assesses viral titers in emerging systemic leaf tissue at 12 days post-inoculation: virus levels are much lower at elevated temperature and CO_2 conditions that at standard conditions, in equivalent leaf disks. Each western blot lane represents an extract from a single plant. Lane labeled H show extracts from healthy plants as negative control. Lane labeled M show molecular weight markers in kilodalton (kDa), indicated to the right of the blots. The panel below the western blot show the blotted, Ponceau S-stained membrane prior to antibody incubation as controls of loading. The chart to the right of the western blot panel displays mean CP values obtained in the densitometry analysis of the CP bands in at least 8 lanes/case with standard deviation bars relative to the average accumulation of viral CP at standard conditions, which was given an arbitrary value of 1. The asterisk in the chart indicates significant differences (Mann Whitney U-test, $P<0.05$).

infection symptoms, such as color, sap composition or volatile emission profiles. But this has not been tested yet. Against this negative outlook for some viruses exists their genetic adaptability through mutations to new conditions, but it remains to be seen if mutations and selection alone could compensate the effects of these environment changes in all types of viruses. In addition to this, in many instances plants can obtain beneficial trade-offs from compatible viral infections when under situations of biotic and abiotic stresses, such as drought or their infection by other pathogens (Fernández-Calvino *et al.*, 2014; Márquez *et al.*, 2007; Roossinck, 2011; Xu *et al.*, 2008). How would those trade-offs conferred by infection be

affected by environment situations in which viral titers in some interactions fall to very low levels?

Some of the aims of plant virologists are the understanding of mechanisms and processes involved in interactions between plants and viruses, of the responses to infection that are triggered in the host, and how the infection outcomes can be affected by the environment. In this regard, the so-called viral pathogenicity determinants influence the outcomes of plant-virus interactions and therefore, their study is important to understand those outcomes and how they could be influenced by a changing environment around them.

Viral pathogenicity determinants are associated with the disruption of host defenses, such as the RNA-mediated antiviral silencing. RNA-mediated silencing is itself a matrix of interrelated processes in plants that is involved in the regulation of gene expression during development, in the response of plants to the environment, and as a defense mechanism targeting for destruction RNAs of external infectious agents, such as viruses, with specificity of sequence. To successfully infect a plant and complete its infectious cycle a virus must overcome at least partially the antiviral silencing-based resistance. The viral factors that interfere and neutralize it are known as viral suppressors of RNA silencing (VSRs). The ways in which a viral suppressor interferes with antiviral silencing varies, and may imply either direct interaction with RNAs involved in the sequence-guided targeted silencing process, interaction/inhibition with/of any of the protein components of the plant silencing machinery, or both.

Among RNA viruses members of the genus *Potyvirus* are economically important, and some of its species have been used as experimental models in plant virology since the early times of the discipline. Research in these

particular viruses and on the functions of their encoded proteins has been going on at the CIB Plant Virology Group for over 50 years. One of the non-structural proteins that is better studied by plant virologists in general and is also subject of study by CIB virologists is HCPro. This protein has a multifunctional nature and possesses three functions that intervene directly in important processes for the virus: the proteolytic processing of the polyprotein precursor after translation, the transmission between hosts of these viruses by aphids, and the suppression of the antiviral silencing defense.

Chapters 3 and 4 of this PhD Thesis presented research that was made at the whole plant-RNA virus interaction level, studying infections of a host by several RNA viruses under different environmental conditions. One of the RNA viruses thus studied was PVY. The biological activities of the VSRs of those RNA viruses was also assessed in agropatch silencing suppression assays (Chapters 3 and 4). One of those suppressors was again PVY HCPro.

Further research on HCPro has been addressed in this PhD Thesis following other approaches, at the cellular and the molecular levels: one of them was the study of HCPro subcellular dynamics and properties in a cell biology approach that included imaging by confocal microscopy (Chapter 5). A more molecular approach studied and characterized the nucleic acid populations bound to HCPro in virus-infected plants (Chapter 6).

The study of HCPro in live differentiated plant cells by cell biology means required necessarily its expression fused to fluorescent tags of different types. This was achieved mainly by agroinfiltration, in virus-free systems. Different constructs of HCPro tagged with fluorescent proteins were developed. Initial observations showed that HCPro tagging at its C-

terminus was not feasible in our hands (Chapter 5. Fig S1), even as care was taken not to recreate published cleavage sites in the fusion region between HCPro and its tag that could be recognized and cleaved by the HCPro protease activity, as is discussed in Chapter 5. Either PVY HCPro recognizes sites that the orthologous from other potyviruses do not, or the protease cleavage specificity in an intact plant cell is different from that reported in translation assays *in vitro*, or the tag fused at the C-terminus distorts the specificity of the protease activity of the intact protein. We do not know the underlying reason, but the result was that N-terminal tagging had to be used for confocal studies of modified, fluorescent tagged HCPros in live epidermal cells of *N. benthamiana*. The fusion protein was expressed from binary vectors either by itself, or as a downstream fusion to the viral P1 protein (Chapter 5, Fig. 1) preserving the site of recognition of the P1 protease, in order to allow self-cleavage and detachment of the two protein products (P1 and tagged HCPro). In addition, to be able to establish inferences with biological significance between observations in the living cell and the HCPro suppressor function, silencing suppression agropatch assays were performed with each of the constructs used. Surprisingly, this appears to have been the first time that such characterizations of suppressor activities of tagged HCPros has been done, even though epifluorescence and confocal microscopy works using those tagged constructs have been published by others, prior to this work.

HCPro was tagged at its N-terminus with GFP, mRFP, the split parts of YFP (sYFPN and sYFPC fragments), or the split parts of mRFP (smRFPN and smRFPC fragments). The GFP and smRFP tags were used to visualize fluorescence from individual HCPro molecules. The tagging

with split fragments was used to visualize fluorescence from interacting homodimers of HCPro.

In silencing suppression agropatch assays, the suppressor activities of these constructs were determined. While the GFP-tagged construct did not display suppression of silencing activity, the mRFP-tagged HCPro, as well as the sYFP- and smRFP-tagged HCPros did retain suppressor activities (Chapter 5. Fig 2). Subcellular distribution of GFP- and sYFP-tagged showed that HCPro fluorescence was present diffusedly throughout the cytoplasm and also as small and large inclusions. Those large inclusions were absent in the presence of heterologous VSRs 2b and P19. The mRFP-tagged HCPro did not show the large inclusions in any case, whereas the smRFP-tagged constructs had only a few or just one large inclusion/cell. Therefore, the nature of the tags or of the cellular context affected the distribution of fluorescence derived from the different, tagged HCPro molecules or bimolecules, in particular the presence, number and size of irregular inclusions. Work focused on the tagged HCPros that retained suppressor activities, in particular to the smRFP-tagged constructs. A further reason for this was the availability of transgenic *N. benthamiana* plants that under confocal microscopy displayed their MT and cortical ER structures as fluorescent green, allowing for co-localization studies. Using larger magnifications other previously not reported HPro-derived fluorescence patterns were discovered, in addition to the diffuse fluorescence and to the amorphous inclusions already mentioned: one consisted in a pattern of small dot-sized structures that were associated to the ER (Chapter 5, Fig 5). Furthermore, the induction of a stress in the epidermal cells led to the redistribution of the HCPro-derived fluorescence to adopt filamentous shapes (Chapter 5, Fig 4). In

conclusion the microscopy work shows complex patterns that include inclusions of amorphous shape as well as a diffuse distribution in the cytoplasm. But in addition two other patterns were discovered: one of regular dots of similar size that seemed somehow anchored to the ER, and another filamentous pattern that appeared under stress situations. In addition, intermediates between the two patterns were observed. (Chapter 5, Fig 4). With regard to these patterns, other viral proteins have been found to associate with the ER, like the MP of TMV, which seems to lead the latter through the MT cytoskeleton to its final degradation by the proteasome (Gillespie *et al.*, 2002); or the potyviral 6K protein, involved in the formation of the ER-associated viral replication-translation factories that will later translocate towards the chloroplast periphery (Wei and Wang, 2008). The second pattern discovered was of filaments throughout the cytoplasm when under stress conditions, such as exposing the cells to varnish fumes or to a saturated CO_2 atmosphere not clearly defined yet. Intermediates between the dots pattern and the filament pattern were also observed (Chapter 5, Fig 4). These filaments were found to co-localize with the MT cytoskeleton but not to actin filaments (Chapter 5, Figs 5 and 6). The dots distribution pattern of PVY HCPro was thus also found to be linked to the MT cytoskeleton (Chapter 5, Fig 5). This coating by HCPro of MTs had been observed by other researchers but localized, and not covering the entire cellular MT cytoskeleton of the cell, as was found in this work (Haikonen *et al.*, 2013a, 2013b). Those researchers had found by yeast two-hybrid assays (Y2H) that HCPro from PVA and PVY could interact with a MT-associated factor HIP2, and visualized by bimolecular fluorescence complementation (BiFC) that this interaction followed a filamentous shape. These authors suggested that HCPro distribution on MT filaments was dependant of its interaction with HIP2, and therefore

limited by the endogenous amounts of the latter protein. They could visualize HCPro filaments only if HIP2 was transiently overexpressed. The results shown here demonstrate that HCPro can distribute along the entire MT cytoskeleton of a cell without need of overexpression of HIP2. This means that HCPro union to MTs is not limited by the amounts of endogenous HIP2, or that it happens also through other means.

What are the biological significances of these new distribution patterns of HCPro? It is known that in caulimoviruses redistribution from a large inclusion containing virions and a non-structural protein factor required for aphid transmission occurs through the MT cytoskeleton, in response to aphid probing, which in itself causes an osmotic stress in the cell. As HCPro is also a factor required for potyvirus transmission by aphids, transmission tests were performed from virus-infected tissues that had their MT cytoskeletons disrupted with colchicine. But transmission efficiencies remained high in these MT-disrupted conditions. The same happened in silencing suppression agropatch assays. The role of these subcellular localizations and translocations remain to be associated to a particular function. Despite research efforts HCPro still brings us new puzzles that require further research. In this regard, biological activities as mediators of virus transmission by aphids have been tested for the GFP-HCPro construct and proved to be negative, but have not been tested yet for the mRFP- or the smRFP-tagged constructs. This is something that should be done. Also, all the experiments described in Chapter 5 have been performed in virus-free conditions, and therefore in the absence of other potyviral factors that could be mediating, modulating or affecting HCPro subcellular whereabouts and functions. It would be most interesting to express the tagged, fluorescent HCPros used in this study

from a PVY vector, or in its defect from another potyvirus vector, in order to see how the presence of other viral proteins affect the observed subcellular dynamics and properties of HCPro.

A different approach employed in this PhD Thesis to study HCPro roles in viral infections was the analysis of the RNAs of less than 500 nts (hereinafter referred to as short RNAs) bound to this protein *in vivo*. When this work was done, it had not been published yet that HCPro was capable of binding to sRNAs *in vivo*. Multifaceted HCPro is a VSR, but the molecular means by which this protein interferes with RNA-mediated silencing is still being studied. There are two ways by which HCPro has been suggested to interfere with silencing. The first one is through its interaction with protein components of the silencing machinery. To the date no interaction with AGO proteins has been shown, either *in vivo* or *in vitro*, but interaction with the HEN1 methylase has been demonstrated *in vitro*, leading to its inhibition also *in vitro* (Jamous *et al.*, 2011) and likely causing increased levels of non-methylated small RNAs *in vivo* (Ebhardt *et al.*, 2005). Unmethylated sRNAs cannot be loaded into RISC complexes and are targeted for degradation by the host exonucleases (Boutet *et al.*, 2003; Li *et al.*, 2005; Ramachandran and Chen, 2008). The second way would be through its binding to sRNAs, preventing their loading into the antiviral response mechanism (Shiboleth *et al.*, 2007) as has been described for others VSRs. After the data shown in Chapter 6 was obtained, it was published that TuMV HCPro could bind to sRNAs *in vivo* (Garcia-Ruiz *et al.*, 2015). Whether this binding is targeted, specific and strong enough to constitute the basis of the suppressor function of the protein is being investigated.

To study the populations of short RNAs that could be bound to PVY HCPro during the course of an infection, and to characterize their nature a non-denaturing purification approach to obtain enriched fractions of HCPro tagged with 6xhistidines (6x-HCPro) was followed. Such purification procedure had been developed by the CIB group previously, and the purified protein had been found to be biologically functional in its mediation of viral transmission by aphids (Tena Fernández *et al.*, 2013), suggesting that the procedure could be enriching HCPro in its native form, and with it associated host factors, among them nucleic acids. Therefore, plants were infected with PVX vector that expressed a *P1-6x-HCPro* polycistron (construct PVX-P1-6x-HCPro; Tena Fernández *et al.*, 2013) and the suppressor protein was purified. The RNAs of less than 500 nts in length that were present in the purified fraction were sequenced by NGS technique. As a control, the same procedure was followed using plants infected with the empty PVX vector.

It is known that numerous plant proteins with metal binding sites have the ability to bind with relative high affinities to the Ni^{2+}-NTA sites under non-denaturing conditions (Gal-On *et al.*, 2000). In this purification, even when coomasie staining did not show large amounts of contaminating proteins in either the purified HCPro or in the control samples, their presence was easily detected with more sensitive methods, such as silver staining. Interestingly, the pattern of background proteins was almost identical in both samples, indicating that the enrichment of 6x-HCPro was not made at the expense of the other proteins present in the fractions (Chapter 6, Fig 1). For this reason, and given the power of deep sequencing it was not surprising to obtain millions of sequence reads to short RNAs from the control sample, even though when the experimental

approach was designed it had not been anticipated. Nevertheless, the isolation of RNAs from both samples and the subsequent generation of millions of reads allowed a detailed comparative analysis of their composition and the detection of differential biases that only the presence of the 6x-HCPro protein in the HCPro sample could introduce.

We were careful to use the same amounts of starting plant material and to perform a parallel purification of both samples. The number of reads obtained from the HCPro sample was slightly larger than that obtained from the control sample. Upon analysis it became apparent that the predominant sizes in both samples corresponded to RNAs between 21 and 24 nts, and mainly to those of 21 and 22 nts in length. Thus, presence of 6x-HCPro did not modify the RNA size profile. By comparing sRNA reads it was found that those of 21 nts in size were enriched in the HCPro sample several-fold, and this is in accordance with previously published data obtained *in vitro* by Lakatos *et al.* (2006) and more recently *in vivo* by Garcia-Ruiz *et al* (2015). The analysis of sequences corresponding to pre-miRNAs and of miRNAs showed no enrichment, in fact an impoverishment, in the HCPro sample (Chapter 6, Table 1). This could seem unexpected as in arabidopsis plants, infection with potyviruses led to increased accumulation of miRNAs (Chapman *et al.*, 2004; Kasschau *et al.*, 2003). Nevertheless, these results are in agreement with those of Garcia-Ruiz and colleagues (2015) that suggest that HCPro may not bind to miRNAs efficiently *in vivo*, at last in the presence of other types of sRNAs.

We further tested whether in the HCPro sample some bias in the composition of sRNAs could be found that would indicate a binding preference for plant or viral derived sRNAs by 6x-HCPro. This is the first work that characterized the short RNA populations of viral and of plant

origin, and compared them, as the work by García-Ruíz *et al.*, (2015) only analyzed the sRNAs of viral sequence. The characterization by origin of these sRNAs (whether of plant sequence or of viral sequence) demonstrated an enrichment of 21 and 22 nt-long sRNAs of viral origin more (vsRNAs), of over ten fold in the HCPro sample related to the levels in the control sample. This enrichment was observed not only in the amounts of vsRNAs but also in the diversity of their sequences. The preference of 6x-HCPro for vsRNAs of 21 and 22 nts in length was not observed among the plant-derived sRNAs. The vsRNAs from both, the HCPro and the control samples aligned throughout the whole viral genomes of origin and were of positive:negative polarity in a ratio of approximately 60:40, following similar observations obtained in other plant-virus interactions (Ding, 2010; Donaire *et al.*, 2008; Kreuze *et al.*, 2009; Qu, 2010).

The data obtained do not provide an explanation on how 6x-HCPro could be able to discriminate between sRNAs of plant vs. viral sequence. Some studies have indicated that plant-derived sRNAs are processed in the nucleus by DCL1 and DCL3 (Kurihara and Watanabe, 2004; Xie *et al.*, 2004), meanwhile DCL2 and DCL4 seem to have a lead role in vsRNAs generation mainly in the cytoplasm. Some subcellular co-localization of 6x-HCPro and of the vsRNAs being generated that does not occur with plant sRNAs could be taking place.

Other RNAs longer than sRNAs were found enriched in HCPro, and those also derived from viral sequences, whereas no enrichment was observed for longer RNAs of plant sequence. Those virus-derived RNAs were of positive sense and could be clustered in two groups, one of RNAs of 73 to 84 nts and another one of RNAs of 98-99 nts in length. Neither

the analysis of possible ORFs nor the prediction of possible secondary structures allowed us to infer the origin of these hotspots. In any case, the existence of RNAs bound to HCPro larger than sRNAs is in accordance with observations that revealed two distinct RNA-binding domains in the protein (Urcuqui-Inchima *et al.*, 2000), and with the ability of HCPro to bind to RNAs of 200 nts *in vitro* (Maia and Bernardi, 1996; Urcuqui-Inchima *et al.*, 2000). Although it has been proposed this short RNAs bound to HCPro could be involved in regulation of virus replication (Maia and Bernardi, 1996; Urcuqui-Inchima *et al.*, 2000), its role remains unknown. If somehow interaction HCPro could increase steady-state levels of these virus-derived short RNAs, it could be possible to speculate that they could be buffering the viral genome from RISC activity.

Because the AGO proteins of the RNA-mediated silencing machinery show binding preferences for sRNAs with specific 5' -end nts (Frank *et al.*, 2012; Mi *et al.*, 2008; Montgomery *et al.*, 2008; Takeda *et al.*, 2008), and also because such preferences have also been observed in some VSRs, such as the 2b protein of CMV (Hamera *et al.*, 2012), it was analyzed whether a similar preference could be identified for HCPro. Results showed a clear preference for an adenine base in the 5'-ends of vsRNAs of mainly 21 and 22 nts in length (Chapter 6, Fig. 6). This fact was not observed in the sRNAs of plant sequence or in the RNAs o viral sequence and more than 23 nts in length. This bias does not correlate with the existence of a particular hotspot, as the 21 and 22 nt vsRNAs distributed rather uniformly throughout the whole viral genome, and in addition, independently of whether their sequences derived from the PVX vector or from that of the P1-6x-HCPro insert. It should be noted that the biases that HCPro introduces in the associated RNA populations are of such

specific nature and so significant that they constitute additional internal controls that validate the results.

Therefore, the results from Chapter 6 show that PVY HCPro binds sRNAs as does TuMV HCPro (García-Ruíz *et al.*, 2015). But not only that, it binds preferably vsRNAs of 21 nts in length containing 5'-end terminal adenines. What biological fundament could this have? Recently, Garcia-Ruiz and colleges (2015) have shown that HCPro could be preventing vsRNAs from being loaded into different AGO proteins. The different AGO paralogous of the plant have evolved a functional diversification in their specificities for sRNAs that has led to their being implicated differentially and hierarchically in the different silencing pathways in plants (Singh *et al.*, 2015). In fact, the selective recruitment of sRNAs by AGO proteins is based on the sRNA nitrogenous base of the 5'-end nt and also on the length of the sRNA. It has been shown that AGO2 and AGO4 have both preference for loading sRNAs with 5'-end adenines, the first one of 21 nt in length, the second one of 24 nt in length (Frank *et al.*, 2012; Mi *et al.*, 2008; Montgomery *et al.*, 2008; Takeda *et al.*, 2008). It is tempting to propose that the preference of PVY HCPro towards binding 21 nt-long vsRNAs with 5'-end adenines could be the evolutive result of a selection pressure that prevent them from otherwise loading into AGO2. In this regard, several studies have demonstrated the strong antiviral role of AGO2 (Carbonell *et al.*, 2012; Harvey *et al.*, 2011; Jaubert *et al.*, 2011; Scholthof *et al.*, 2011; Wang *et al.*, 2011; Zhang *et al.*, 2012; García-Ruíz *et al.*, 2015).

CHAPTER 8

GENERAL CONCLUSIONS

1. The transient expression of proteins at temperatures above 29 ºC using the agroinfiltration technique is feasible if a 24 h window at 25 °C is provided after infiltration, before the transfer of plants to higher temperatures.

2. Infections of a common compatible host *N. benthamiana* by three types of positive-sense RNA viruses were affected differently by increases in environment temperature (25 to 30 °C) or CO_2 levels (401 to 970 ppm). These results suggest that future natural environment conditions will have different effects on different RNA virus species and/or strains.

3. In spite of the observed differences in infection outcomes, suppression of silencing in agropatch assays by the corresponding viral suppressors was not negatively affected by either high temperature (30 ºC) or high CO_2 (970 ppm). This suggests that on the one hand, those viral suppressors were capable of neutralizing the silencing resistances of the host under those environment conditions, and on the other hand, that those conditions must affect processes other than suppression of silencing, to account for the differences observed in infection outcomes.

4. The subcellular distribution in *N. benthamiana* epidermal cells of PVY HCPro modified to fluoresce was complex, and displayed also dynamic changes in response to intracellular conditions: it included a diffuse distribution throughout the cytoplasm, as well as irregular inclusions, whose number and size were affected by the presence of

heterologous protein factors (2b protein or P19 suppressors) by unknown means. In addition, two novel distribution patterns were found: one as regular dots associated to the cortical ER and also to the MTs, and another one that coated the entire MT cytoskeleton in response to some stresses. HCPro traslocated from the former to the latter, but the biological significance of these alterations remains unknown.

5. PVY HCPro was found to bind to short and to small RNAs in vivo. It was also found that HCPro has a preference for binding to sRNAs of 21 and 22 nts in length and of viral sequence over those of plant sequence. Furthermore, within the former it prefers those having adenines at their 5'-ends. These are the sRNAs that load into AGO2, which suggest that HCPro may have evolved a preference for those RNAs as a means to suppress antiviral silencing.

CHAPTER 9

GENERAL BIBLIOGRAPHY

Aguilar, E., Allende, L., del Toro, F.J., Chung, B.-N., Canto, T., Tenllado, F., 2015a. Effects of elevated CO_2 and temperature on pathogenicity determinants and virulence of *Potato virus X*/potyvirus-associated synergism. Mol. Plant-Microbe Interact. doi:MPMI-08-15-0178-R

Aguilar, E., Almendral, D., Pacheco, R., Chung, B.N., Tenllado, F., 2015b. The P25 protein of *Potato virus X* is the main pathogenicity determinant responsible for systemic necrosis in PVX-associated synergisms. J. Virol. 89, 2090–2103. doi:10.1128/JVI.02896-14

Akbergenov, R., Si-Ammour, A., Blevins, T., Amin, I., Kutter, C., Vanderschuren, H., Zhang, P., Gruissem, W., Meins, F., Hohn, T., Pooggin, M.M., 2006. Molecular characterization of geminivirus-derived small RNAs in different plant species. Nucleic Acids Res. 34, 462–471. doi:10.1093/nar/gkj447

Alam, C.M., Singh, A.K., Sharfuddin, C., Ali, S., 2014. Incidence, complexity and diversity of simple sequence repeats across potexvirus genomes. Gene 537, 189–196. doi:10.1016/j.gene.2014.01.007

Ala-Poikela, M., Goytia, E., Haikonen, T., Rajamäki, M-L., Valkonen, J.P.T., 2011. Helper component proteinase of the genus *Potyvirus* is an interaction partner of translation initiation factors eIF(iso)4E and eIF4E and contains a 4E binding motif. J. Virol. 85, 6784–6794. doi:10.1128/JVI.00485-11

Alazem, M., Lin, N.-S., 2014. Roles of plant hormones in the regulation of host-virus interactions. Mol. Plant Pathol. 16, 529–540. doi:10.1111/mpp.12204

Ali, A., Kobayashi, M., 2010. Seed transmission of *Cucumber mosaic virus* in pepper. J. Virol. Methods 163, 234–237. doi:10.1016/j.jviromet.2009.09.026

Amthor, J.S., 1995. Terrestrial higher-plant response to increasing atmospheric [CO_2] in relation to the global carbon cycle. Glob. Chang. Biol. 1, 243–274.

Anandalakshmi, R., Pruss, G.J., Ge, X., Marathe, R., Mallory, a C., Smith, T.H., Vance, V.B., 1998. A viral suppressor of gene silencing in plants. Proc. Natl. Acad. Sci. U. S. A. 95, 13079–13084. doi:10.1073/pnas.95.22.13079

Anindya, R., Chittori, S., Savithri, H.S., 2005. Tyrosine 66 of *Pepper vein banding virus* genome-linked protein is uridylylated by RNA-dependent RNA polymerase. Virology 336, 154–162. doi:10.1016/j.virol.2005.03.024

Aparicio, F., Aparicio, F., Thomas, C.L., Thomas, C.L., Lederer, C., Lederer, C., Niu, Y., Niu, Y., Wang, D., Wang, D., Maule, A.J., Maule, A.J., 2005. Virus induction of Heat Shock Protein 70 reflects a general response to protein accumulation in the plant cytosol. Plant Physiol. 138, 529–536. doi:10.1104/pp.104.058958.1

Atabekov, J., Dobrov, E., Karpova, O., Rodionova, N., 2007. *Potato virus X*: Structure, disassembly and reconstitution. Mol. Plant Pathol. 8, 667–675. doi:10.1111/j.1364-3703.2007.00420.x

Azevedo, J., Garcia, D., Pontier, D., Ohnesorge, S., Yu, A., Garcia, S., Braun, L., Bergdoll, M., Hakimi, M.A., Lagrange, T., Voinnet, O., 2010. Argonaute quenching and global changes in Dicer homeostasis caused by a pathogen-encoded GW repeat protein. Genes Dev. 24, 904–915. doi:10.1101/gad.1908710

Baebler, Š., Witek, K., Petek, M., Stare, K., Tušek-Žnidarič, M., Pompe-Novak, M., Renaut, J., Szajko, K., Strzelczyk-Zyta, D., Marczewski, W., Morgiewicz, K., Gruden, K., Hennig, J., 2014. Salicylic acid is an indispensable component of the Ny-1 resistance-gene-mediated response against *Potato virus Y* infection in potato. J. Exp. Bot. 65, 1095–1109. doi:10.1093/jxb/ert447

Balachandran, S., Hull, R.J., VaadiaA, Y., Wolf, S., Lucas, W.J., 1995. Alteration in carbon partitioning induced by the movement protein of *Tobacco mosaic virus* originates in the mesophyll and is independent of change in the plasmodesmal size exclusion limit. Plant, cell environ. 18, 1301–1310.

Ballut, L., Petit, F., Mouzeyar, S., Le Gall, O., Candresse, T., Schmid, P., Nicolas, P., Badaoui, S., 2003. Biochemical identification of proteasome-associated endonuclease activity in sunflower. Biochim. Biophys. Acta - Proteins Proteomics 1645, 30–39. doi:10.1016/S1570-9639(02)00500-9

Ballut, L., Drucker, M., Pugnière, M., Cambon, F., Blanc, S., Roquet, F., Candresse, T., Schmid, H.P., Nicolas, P., Le Gall, O., Badaoui, S., 2005. HcPro, a multifunctional protein encoded by a plant RNA virus, targets the 20S proteasome and affects its enzymic activities. J. Gen. Virol. 86, 2595–2603. doi:10.1099/vir.0.81107-0

Bamunusinghe, D., Seo, J.-K., Rao, a L.N., 2011. Subcellular localization and rearrangement of endoplasmic reticulum by *Brome mosaic virus* capsid protein. J. Virol. 85, 2953–2963. doi:10.1128/JVI.02020-10

Baumberger, N., Tsai, C.-H., Lie, M., Havecker, E., Baulcombe, D.C., 2007. The Polerovirus silencing suppressor P0 targets ARGONAUTE proteins for degradation. Curr. Biol. 17, 1609–1614. doi:10.1016/j.cub.2007.08.039

Bayne, E.H., Rakitina, D. V., Morozov, S.Y., Baulcombe, D.C., 2005. Cell-to-cell movement of *Potato Potexvirus X* is dependent on suppression of RNA silencing. Plant J. 44, 471–482. doi:10.1111/j.1365-313X.2005.02539.x

Bedoya, L.C., Daròs, J.A., 2010. Stability of *Tobacco etch virus* infectious clones in plasmid vectors. Virus Res. 149, 234–240. doi:10.1016/j.virusres.2010.02.004

Berger, S., Sinha, A.K., Roitsch, T., 2007. Plant physiology meets phytopathology: Plant primary metabolism and plant-pathogen interactions. J. Exp. Bot. 58, 4019–4026. doi:10.1093/jxb/erm298

Besong-Ndika, J., Ivanov, K.I., Hafrèn, A., Michon, T., Mäkinen, K., 2015. Cotranslational Coat Protein-mediated inhibition of *potyviral* RNA translation. J. Virol. 89, 4237–4248. doi:10.1128/JVI.02915-14

Blackman, L., Boevink, P., Cruz, S., Palukaitis, P., Oparka, K., 1998. The movement protein of *Cucumber mosaic virus* traffics into sieve elements in minor veins of *Nicotiana clevelandii*. Plant Cell 10, 525–538. doi:10.1105/tpc.10.4.525

Blanc, S., López-Moya, J.J., Wang, R., García-Lampasona, S., Thornbury, D.W., Pirone, T.P., 1997. A specific interaction between coat protein and helper component correlates with aphid transmission of a *potyvirus*. Virology 231, 141–147. doi:10.1006/viro.1997.8521

Blanco, F., Garretón, V., Frey, N., Dominguez, C., Pérez-Acle, T., Van Der Straeten, D., Jordana, X., Holuigue, L., 2005. Identification of NPR1-dependent and independent genes early induced by salicylic acid treatment in arabidopsis. Plant Mol. Biol. 59, 927–944. doi:10.1007/s11103-005-2227-x

Blevins, T., Rajeswaran, R., Aregger, M., Borah, B.K., Schepetilnikov, M., Baerlocher, L., Farinelli, L., Meins, F., Hohn, T., Pooggin, M.M., 2011. Massive production of small RNAs from a non-coding region of *Cauliflower mosaic virus* in plant defense and viral counter-defense. Nucleic Acids Res. 39, 5003–5014. doi:10.1093/nar/gkr119

Blevins, T., Rajeswaran, R., Shivaprasad, P. V., Beknazariants, D., Si-Ammour, A., Park, H.S., Vazquez, F., Robertson, D., Meins, F., Hohn, T., Pooggin, M.M., 2006. Four plant Dicers mediate viral small RNA biogenesis and DNA virus induced silencing. Nucleic Acids Res. 34, 6233–6246. doi:10.1093/nar/gkl886

Bologna, N.G., Voinnet, O., 2014. The diversity, biogenesis, and activities of endogenous silencing small RNAs in *Arabidopsis*. Annu. Rev. Plant Biol. 65, 473–503. doi:10.1146/annurev-arplant-050213-035728

Boquel, S., Ameline, A., Giordanengo, P., 2011. Assessing aphids *Potato virus Y*-transmission efficiency: A new approach. J. Virol. Methods 178, 63–67. doi:10.1016/j.jviromet.2011.08.013

Bortolamiol, D., Pazhouhandeh, M., Marrocco, K., Genschik, P., Ziegler-Graff, V., 2007. The *Polerovirus* F Box protein P0 targets ARGONAUTE1 to suppress RNA silencing. Curr. Biol. 17, 1615–1621. doi:10.1016/j.cub.2007.07.061

Boutet, S., Vazquez, F., Liu, J., Béclin, C., Fagard, M., Gratias, A., Morel, J.B., Crété, P., Chen, X., Vaucheret, H., 2003. Arabidopsis HEN1: A genetic link between endogenous miRNA controlling development and siRNA controlling transgene silencing and virus resistance. Curr. Biol. 13, 843–848. doi:10.1016/S0960-9822(03)00293-8

Bray E. A., Bailey-Serres J., Weretilnyk E. (2000) "Responses to abiotic stresses," in *Biochemistry and Molecular Biology of Plants* eds Gruissem W., Buchannan B. B., Jones R. L., editors. (Rockville: American Society of Plant Physiologists) 1158–1203

Brantley, J.D., Hunt, A.G., 1993. The N-terminal protein of the polyprotein encoded by the *potyvirus Tobacco vein mottling virus* is an RNA binding protein. J. Gen. Virol. 74, 1157–1162.

Broderick, S.R., Jones, M.L., 2014. An optimized protocol to increase virus-induced gene silencing efficiency and minimize viral symptoms in Petunia. Plant Mol. Biol. Report. 32, 219–233. doi:10.1007/s11105-013-0647-3

Bronkhorst, A.W., Van Rij, R.P., 2014. The long and short of antiviral defense: Small RNA-based immunity in insects. Curr. Opin. Virol. 7, 19–28. doi:10.1016/j.coviro.2014.03.010

Burgess, D.J., 2013. Small RNAs: antiviral RNAi in mammals. Nat. Rev. Genet. 14, 821. doi:10.1038/nrg3616

Calvo, M., Malinowski, T., García, J.A., Madrid, A. De, Ogrodnictwa, I., 2014. Single amino acid changes in the 6K1-CI region can promote the alternative adaptation of Prunus - and Nicotiana -propagated *Plum pox virus C* isolates to either host 27, 136–149. doi:10.1094/MPMI-08-13-0242-R

Canto, T., Cillo, F., Palukaitis, P., 2002. Generation of siRNAs by T-DNA sequences does not require active transcription or homology to sequences in the plant. Mol. Plant. Microbe. Interact. 15, 1137–1146. doi:10.1094/MPMI.2002.15.11.1137

Canto, T., López-Moya, J.J., Serra-Yoldi, M.T., Díaz-Ruíz, S.R., López-Abella, D., 1995. Different Helper Component mutations associated with lack of aphid transmissibility in two isolates of *Potato Virus Y*. Phytopathology 85, 1519–1524. doi:10.1094/Phyto-85-1519

Canto, T., Palukaitis, P., 2005. Subcellular distribution of mutant movement proteins of *Cucumber mosaic virus* fused to green fluorescent proteins. J. Gen. Virol. 86, 1223–1228.

Canto, T., Palukaitis, P., 1999. Are Tubules Generated by the 3a Protein Necessary for Cucumber Mosaic Virus Movement? Mol. Plant-Microbe Interact. 12, 985–993. doi:10.1094/MPMI.1999.12.11.985

Canto, T., Palukaitis, P., 1998. Transgenically expressed *Cucumber mosaic virus* RNA 1 simultaneously complements replication of cucumber mosaic virus RNAs 2 and 3 and confers resistance to systemic infection. Virology 250, 325–36. doi:10.1006/viro.1998.9333

Canto, T., Prior, D.A.M., Hellwald, K.-H., Oparka, K.J., Palukaitis, P., 1997. Characterization of *Cucumber Mosaic Virus*. Virology 237, 237–248. doi:10.1006/viro.1997.8804

Canto, T., Aranda, M.A., Fereres, A., 2009. Climate change effects on physiology and population processes of hosts and vectors that influence the spread of hemipteran-borne plant viruses. Glob. Chang. Biol. 15, 1884–1894. doi:10.1111/j.1365-2486.2008.01820.x

Carbonell, a., Fahlgren, N., Garcia-Ruiz, H., Gilbert, K.B., Montgomery, T. A., Nguyen, T., Cuperus, J.T., Carrington, J.C., 2012. Functional analysis of three arabidopsis ARGONAUTES using slicer-defective mutants. Plant Cell 24, 3613–3629. doi:10.1105/tpc.112.099945

Carbonell, A., Carrington, J.C., 2015. Antiviral roles of plant ARGONAUTES. Curr. Opin. Plant Biol. 27, 111–117. doi:10.1016/j.pbi.2015.06.013

Carrington, J.C., Dougherty, W.G., 1987. Small Nuclear Inclusion protein encoded by a plant *Potyvirus* genome is a protease. J. Virol. 61, 2540–2548.

Carrington, J.C., Freed, D.D., Sanders, T.C., 1989. Autocatalytic processing of the *potyvirus* helper component proteinase in *Escherichia coli* and *in vitro*. J Virol 63, 4459–4463.

Carrington, J.C., Herndon, K.L., 1992. Characterization of the *potyviral* HC-pro autoproteolytic cleavage site. Virology 187, 308–3015.

Carrington, J.C., Oh, C.-S., 1999. Identification of essential residues in *Potyvirus* HC-Pro by site-directed mutagenesis proteinase. Virology 173, 692–699.

Casteel, C.L., Yang, C., Nanduri, A.C., De Jong, H.N., Whitham, S. a., Jander, G., 2014. The NIa-Pro protein of *Turnip mosaic virus* improves growth and reproduction of the aphid vector, *Myzus persicae* (green peach aphid). Plant J. 77, 653–663. doi:10.1111/tpj.12417

Chapman, E.J., Prokhnevsky, A.I., Gopinath, K., Dolja, V. V., Carrington, J.C., 2004. Viral RNA silencing suppressors inhibit the microRNA pathway at an intermediate step. Genes Dev. 18, 1179–1186. doi:10.1101/gad.1201204

Chapman, S., Kavanagh, T., Baulcombe, D., 1992. *Potato virus X* as a vector for gene expression in plants. Plant J. 2, 549–557. doi:10.1046/j.1365-313X.1992.t01-24-00999.x

Chellappan, P., Vanitharani, R., Ogbe, F., Fauquet, C.M., 2005. Effect of temperature on *geminivirus*-induced RNA silencing in plants. Plant Physiol. 138, 1828–1841. doi:10.1104/pp.105.066563.1828

Chen, B., Francki, R.I.B., 1990. *Cucumovirus* transmission by the aphid *Myzus persicae* is determined solely by the viral coat protein. J. Gen. Virol. 71, 939–944. doi:10.1099/0022-1317-71-4-939

Chen, H.-Y., Yang, J., Lin, C., Yuan, Y.A., 2008. Structural basis for RNA-silencing suppression by *Tomato aspermy virus* protein 2b. EMBO Rep. 9, 754–760. doi:10.1038/embor.2008.118

Chiu, M.H., Chen, I.H., Baulcombe, D.C., Tsai, C.H., 2010. The silencing suppressor P25 of *Potato virus X* interacts with Argonaute1 and mediates its degradation through the proteasome pathway. Mol. Plant Pathol. 11, 641–649. doi:10.1111/j.1364-3703.2010.00634.x

Choi, S.K., Palukaitis, P., Min, B.E., Lee, M.Y., Choi, J.K., Ryu, K.H., 2005. *Cucumber mosaic virus* 2a polymerase and 3a movement proteins independently affect both virus movement and the timing of symptom development in zucchini squash. J. Gen. Virol. 86, 1213–1222. doi:10.1099/vir.0.80744-0

Choi, S.K., Yoon, J.Y., Canto, T., Palukaitis, P., 2011. Replication of *Cucumber mosaic virus* RNA 1 in *cis* requires functional helicase-like motifs of the 1a protein. Virus Res. 158, 271–276. doi:10.1016/j.virusres.2011.03.008

Chu, M., Lopez-Moya, J.J., Llave-Correas, C., Pirone, T.P., 1997. Two separate regions in the genome of the *Tobacco etch virus* contain determinants of the wilting response of Tabasco pepper. Mol. Plant. Microbe. Interact. 10, 472–480. doi:10.1094/MPMI.1997.10.4.472

Chung, B.Y.-W., Miller, W.A., Atkins, J.F., Firth, A.E., 2008. An overlapping essential gene in the *Potyviridae*. Proc. Natl. Acad. Sci. U. S. A. 105, 5897–5902. doi:10.1073/pnas.0800468105

Cillo, F., Roberts, I.M., Palukaitis, P., 2002. *In situ* localization and tissue distribution of the replication-associated proteins of *Cucumber mosaic virus* in tobacco and cucumber. J. Virol. 76, 10654–10664. doi:10.1128/jvi.76.21.10654-10664.2002

Cotton, S., Grangeon, R., Thivierge, K., Mathieu, I., Ide, C., Wei, T., Wang, A., Laliberté, J.-F., 2009. *Turnip mosaic virus* RNA replication complex vesicles are mobile, align with microfilaments, and are each derived from a single viral genome. J. Virol. 83, 10460–10471. doi:10.1128/JVI.00819-09

Csorba, T., Bovi, A., Dalmay, T., Burgyán, J., 2007. The p122 subunit of *Tobacco Mosaic Virus* replicase is a potent silencing suppressor and compromises both small interfering RNA- and microRNA-mediated pathways. J. Virol. 81, 11768–11780. doi:10.1128/JVI.01230-07

Csorba, T., Kontra, L., Burgyán, J., 2015. Viral silencing suppressors: Tools forged to fine-tune host-pathogen coexistence. Virology 480, 85–103. doi:10.1016/j.virol.2015.02.028

Cuellar, W.J., Kreuze, J.F., Rajamäki, M.-L., Cruzado, K.R., Untiveros, M., Valkonen, J.P.T., 2009. Elimination of antiviral defense by viral RNase III. Proc. Natl. Acad. Sci. U. S. A. 106, 10354–10358. doi:10.1073/pnas.0806042106

Cui, X., Wei, T., Chowda-Reddy, R. V., Sun, G., Wang, A., 2010. The *Tobacco etch virus* P3 protein forms mobile inclusions via the early secretory pathway and traffics along actin microfilaments. Virology 397, 56–63. doi:10.1016/j.virol.2009.11.015

Cullen, B.R., Cherry, S., Tenoever, B.R., 2013. Is RNA interference a physiologically relevant innate antiviral immune response in mammals? Cell Host Microbe 14, 374–378. doi:10.1016/j.chom.2013.09.011

Dawson WO, 1976. Synthesis of TMV RNA at restrictive high temperatures. Virology 73, 319–26.

Dawson WO, White JL, Grantham GL, 1978. Effect of heat treatment upon *Cowpea chlorotic mottle virus* ribonucleic acid replication. Phytopathology 68, 1042–8.

De Bokx, J. A. & Huttinga, H. (1981). *Potato virus Y*. CMI/AAB. Descriptions of Plant Viruses, no. 242.

Deleris, A., Gallego-Bartolome, J., Bao, J., Kasschau, K.D., Carrington, J.C., Voinnet, O., 2006. Hierarchical action and inhibition of plant Dicer-like proteins in antiviral defense. Science 313, 68–71. doi:10.1126/science.1128214

Dempsey, 2011. Salicylic Acid Biosynthesis and Metabolism. Arab. B. 1–24. doi:10.1199/tab.0156

Dielen, A.S., Sassaki, F.T., Walter, J., Michon, T., Ménard, G., Pagny, G., Krause-Sakate, R., Maia, Iv.D.G., Badaoui, S., Le Gall, O., Candresse, T., German-Retana, Sy., 2011. The 20S proteasome α5 subunit of Arabidopsis thaliana carries an RNase activity and interacts in planta with the *Lettuce mosaic potyvirus* HcPro protein. Mol. Plant Pathol. 12, 137–150. doi:10.1111/j.1364-3703.2010.00654.x

Ding, B., Li, Q., Nguyen, L., Palukaitis, P., Lucas, W.J., 1995. *Cucumber mosaic virus* 3a protein potentiates cell-to-cell trafficking of CMV RNA in tobacco plants. Virology 207, 345–353. doi:10.1006/viro.1995.1093

Ding, S. W., 2010. RNA-based antiviral immunity. Nat. Rev. Immunol. 10, 632–44. doi:10.1038/nri2824

Dolja, V. V, McBride, H.J., Carrington, J.C., 1992. Tagging of plant *potyvirus* replication and movement by insertion of beta-glucuronidase into the viral polyprotein. Proc. Natl. Acad. Sci. U. S. A. 89, 10208–12.

Donaire, L., Barajas, D., Martínez-García, B., Martínez-Priego, L., Pagán, I., Llave, C., 2008. Structural and genetic requirements for the biogenesis of *Tobacco rattle virus*-derived small interfering RNAs. J. Virol. 82, 5167–5177. doi:10.1128/JVI.00272-08

Dong, X., 2004. NPR1, all things considered. Curr. Opin. Plant Biol. 7, 547–552. doi:10.1016/j.pbi.2004.07.005

Doronin, S. V, Hemenway, C., 1996. Synthesis of *Potato virus X* RNAs by membrane-containing extracts. J. Virol. 70, 4795–4799.

Drake, B.G., Gonzalez-Meler, M. a., Long, S.P., 1997. MORE EFFICIENT PLANTS: A Consequence of Rising Atmospheric CO2? Annu. Rev. Plant Physiol. Plant Mol. Biol. 48, 609–639. doi:10.1146/annurev.arplant.48.1.609

Draper M., Pasche J., Gudmestad N. 2002. Factors influencing PVY development and disease expression in three potato cultivars. Am. J. Potato Res. 79: 155–165

Drugeon, G., Jupin, I., 2002. Stability *in vitro* of the 69K movement protein of *Turnip yellow mosaic virus* is regulated by the ubiquitin-mediated proteasome pathway. J. Gen. Virol. 83, 3187–3197.

Du, Z., Chen, A., Chen, W., Liao, Q., Zhang, H., Bao, Y., Roossinck, M.J., Carr, J.P., 2014. Nuclear-Cytoplasmic partitioning of *Cucumber Mosaic Virus* protein 2b determines the balance between its roles as a virulence determinant and an RNA-silencing suppressor. J. Virol. 88, 5228–5241. doi:10.1128/JVI.00284-14

Duan, C.-G., Fang, Y.-Y., Zhou, B.-J., Zhao, J.-H., Hou, W.-N., Zhu, H., Ding, S.-W., Guo, H.-S., 2012. Suppression of Arabidopsis ARGONAUTE1-mediated slicing, transgene-induced RNA silencing, and DNA methylation by distinct domains of the *Cucumber mosaic virus* 2b protein. Plant Cell 24, 259–274. doi:10.1105/tpc.111.092718

Dujovny, G., Valli, A., Calvo, M., García, J.A., 2009. A temperature-controlled amplicon system derived from *Plum pox potyvirus*. Plant Biotechnol. J. 7, 49–58. doi:10.1111/j.1467-7652.2008.00373.x

Ebhardt, H.A., Thi, E.P., Wang, M.-B., Unrau, P.J., 2005. Extensive 3' modification of plant small RNAs is modulated by helper component-proteinase expression. Proc. Natl. Acad. Sci. U. S. A. 102, 13398–403. doi:10.1073/pnas.0506597102

Edwardson, J.R., Christie, R.G., 1978. Use of virus-induced inclusion bodies in classification and diagnosis. Annu. Rev. Phytopathol. 16, 31–55.

Edwardson, J. R., and Christie, R. G. (1991). Cucumoviruses. In "CRC Handbook of Viruses Infecting Legumes," pp. 293–319. CRC Press, Boca Raton, FL.

Eiamtanasate, S., Juricek, M., Yap, Y.K., 2007. C-terminal hydrophobic region leads PRSV P3 protein to endoplasmic reticulum. Virus Genes 35, 611–617. doi:10.1007/s11262-007-0114-z

Fernández, A., Laín, S., García, J.A., 1995. RNA helicase activity of the *Plum pox potyvirus* CI protein expressed in *Escherichia coli*. Mapping of an RNA binding domain. Nucleic Acids Res. 23, 1327–1332.

Fernández-Calvino, L., Guzmán-Benito, I., Del Toro, F.J., Donaire, L., Castro-Sanz, A.B., Ruíz-Ferrer, V., Llave, C., 2015. Activation of senescence-associated dark-inducible genes during infection contributes to enhance susceptibility to plant viruses. Mol. Plant Pathol. doi:10.1111/mpp.12257

Fernández-Calvino, L., Osorio, S., Hernandez, M.L., Hamada, I.B., del Toro, F.J., Donaire, L., Yu, A., Bustos, R., Fernie, a. R., Martinez-Rivas, J.M., Llave, C., 2014. Virus-induced alterations in primary metabolism modulate susceptibility to *Tobacco rattle virus* in *Arabidopsis*. Plant Physiol. 166, 1821–1838. doi:10.1104/pp.114.250340

Flor, H.H., 1971. Current status of the gene-for-gene concept. Annu. Rev. Phytopathol. 9, 275–296.

Frank, F., Hauver, J., Sonenberg, N., Nagar, B., 2012. Arabidopsis Argonaute MID domains use their nucleotide specificity loop to sort small RNAs. EMBO J. 31, 3588–3595. doi:10.1038/emboj.2012.204

Fujiki, M., Kaczmarczyk, J.F., Yusibov, V., Rabindran, S., 2008. Development of a new *Cucumber mosaic virus*-based plant expression vector with truncated 3a movement protein. Virology 381, 136–142. doi:10.1016/j.virol.2008.08.022

Fujisaki, K., Iwahashi, F., Kaido, M., Okuno, T., Mise, K., 2009. Genetic analysis of a host determination mechanism of *bromoviruses* in *Arabidopsis thaliana*. Virus Res. 140, 103–111. doi:10.1016/j.virusres.2008.11.007

Fullner, K.J., Nester, E.W., 1996. Temperature affects the T-DNA transfer machinery of *Agrobacterium tumefaciens*. J. Bacteriol. 178, 1498–1504.

Gal-On, A., Meiri, E., Elman, C., Gray, D.J., Gaba, V., 1997. Simple hand-held devices for the efficient infection of plants with viral-encoding constructs by particle bombardment. J. Virol. Methods 64, 103–110. doi:10.1016/S0166-0934(96)02146-5

Gal-On, A., Meiri, E., Huet, H., Hua, W.J., Raccah, B., Gaba, V., 1995. Particle bombardment drastically increases the infectivity of cloned DNA of *Zucchini yellow mosaic potyvirus*. J. Gen. Virol. 76 (Pt 12, 3223–7. doi:10.1099/0022-1317-76-12-3223

Gal-On, A., Canto, T., Palukaitis, P., 2000. Characterisation of genetically modified cucumber mosaic virus expressing histidine-tagged 1a and 2a proteins. Arch. Virol. 145, 37–50. doi:10.1007/s007050050003

Garcia, D., Garcia, S., Voinnet, O., 2014. Nonsense-mediated decay serves as a general viral restriction mechanism in plants. Cell Host Microbe 16, 391–402. doi:10.1016/j.chom.2014.08.001

García, J. a, Riechmann, J.L., Martín, M.T., Laín, S., 1989. Proteolytic activity of the *Plum pox potyvirus* NIa-protein on excess of natural and artificial substrates in *Escherichia coli*. FEBS Lett. 257, 269–273. doi:10.1016/0014-5793(89)81550-9

García, J.A., Lucini, C., García, B., Alamillo, J.M., López-Moya, J.J., 2006. The use of *Plum pox virus* as a plant expression vector. EPPO Bull. 36, 341–345. doi:10.1111/j.1365-2338.2006.01012.x

García-Marcos, A., Pacheco, R., Manzano, A., Aguilar, E., Tenllado, F., 2013. Oxylipin biosynthesis genes positively regulate programmed cell death during compatible infections with the synergistic pair *Potato virus X-Potato virus Y* and *Tomato spotted wilt virus*. J. Virol. 87, 5769–83. doi:10.1128/JVI.03573-12

Garcia-Ruiz, H., Carbonell, A., Hoyer, J.S., Fahlgren, N., Gilbert, K.B., Takeda, A., Giampetruzzi, A., Garcia Ruiz, M.T., McGinn, M.G., Lowery, N., Martinez Baladejo, M.T., Carrington, J.C., 2015. Roles and programming of arabidopsis ARGONAUTE proteins during *Turnip mosaic virus* infection. PLOS Pathog. 11, e1004755. doi:10.1371/journal.ppat.1004755

Garcia-Ruiz, H., Takeda, A., Chapman, E.J., Sullivan, C.M., Fahlgren, N., Brempelis, K.J., Carrington, J.C., 2010. Arabidopsis RNA-dependent RNA polymerases and dicer-like proteins in antiviral defense and small interfering RNA biogenesis during *Turnip mosaic virus* infection. Plant Cell 22, 481–496. doi:10.1105/tpc.109.073056

Gassmann, W., Bhattacharjee, S., 2012. Effector-triggered immunity signaling: From gene-for-gene pathways to protein-protein interaction networks. Mol. Plant-Microbe Interact. 25, 862–868. doi:10.1094/MPMI-01-12-0024-IA

Gelvin, S.B., 2003. *Agrobacterium*-mediated plant transformation: the biology behind the "Gene-Jockeying" Tool. Microbiol. Mol. Biol. Rev. 67, 16–37. doi:10.1128/MMBR.67.1.16

Gepstein, S., Sabehi, G., Carp, M.J., Hajouj, T., Nesher, M.F.O., Yariv, I., Dor, C., Bassani, M., 2003. Large-scale identification of leaf senescence-associated genes. Plant J. 36, 629–642. doi:10.1046/j.1365-313X.2003.01908.x

Ghoshal, B., Sanfaçon, H., 2014. Temperature-dependent symptom recovery in *Nicotiana benthamiana* plants infected with *Tomato ringspot virus* is associated with reduced translation of viral RNA2 and requires ARGONAUTE 1. Virology 456-457, 188–197. doi:10.1016/j.virol.2014.03.026

Gibbs, A.J., Nguyen, H.D., Ohshima, K., 2015. The "emergence" of *Turnip mosaic virus* was probably a "gene-for-quasi-gene" event. Curr. Opin. Virol. 10, 20–26. doi:10.1016/j.coviro.2014.12.004

Gifford, R.M., Barrett, D.J., Lutze, J.L., 2000. The effects of elevated [CO_2] on the C:N and C:P mass ratios of plant tissues. Plant Soil 224, 1–14.

Gillespie, T., Boevink, P., Haupt, S., Roberts, A.G., Toth, R., Valentine, T., Chapman, S., Oparka, K.J., 2002. Functional analysis of a DNA-shuffled movement protein reveals that microtubules are dispensable for the cell-to-cell movement of tobacco mosaic virus. Plant Cell 14, 1207–1222. doi:10.1105/tpc.002303

Giner, A., Lakatos, L., García-Chapa, M., López-Moya, J.J., Burgyán, J., 2010. Viral protein inhibits RISC activity by argonaute binding through conserved WG/GW motifs. PLoS Pathog. 6, 1–13. doi:10.1371/journal.ppat.1000996

Glazebrook, J., 2005. Contrasting mechanisms of defense against biotrophic and necrotrophic pathogens. Annu. Rev. Phytopathol. 43, 205–227. doi:10.1146/annurev.phyto.43.040204.135923

Glick, E., Zrachya, A., Levy, Y., Mett, A., Gidoni, D., Belausov, E., Citovsky, V., Gafni, Y., 2008. Interaction with host SGS3 is required for suppression of RNA silencing by *Tomato yellow leaf curl virus* V2 protein. Proc. Natl. Acad. Sci. U. S. A. 105, 157–161. doi:10.1073/pnas.0709036105

González, I., Martínez, L., Rakitina, D. V., Lewsey, M.G., Atencio, F.A., Llave, C., Kalinina, N.O., Carr, J.P., Palukaitis, P., Canto, T., 2010. *Cucumber mosaic virus* 2b protein subcellular targets and interactions: their significance to RNA silencing suppressor activity. Mol. Plant-Microbe Interact. 23, 294–303. doi:10.1093/pcp/pcm074

González, I., Rakitina, D., Semashko, M., Taliansky, M., Praveen, S., Palukaitis, P., Carr, J.P., Kalinina, N., Canto, T., 2012. RNA binding is more critical to the suppression of silencing function of *Cucumber mosaic virus* 2b protein than nuclear localization. Rna 18, 771–782. doi:10.1261/rna.031260.111

González-Jara, P., Atencio, F. a, Martínez-García, B., Barajas, D., Tenllado, F., Díaz-Ruíz, J.R., 2005. A single amino acid mutation in the *Plum pox virus* Helper Component-Proteinase gene abolishes both synergistic and RNA silencing suppression activities. Phytopathology 95, 894–901. doi:10.1094/PHYTO-95-0894

Goto, K., Kobori, T., Kosaka, Y., Natsuaki, T., Masuta, C., 2007. Characterization of silencing suppressor 2b of *Cucumber mosaic virus* based on examination of its small RNA-binding abilities. Plant Cell Physiol. 48, 1050–1060. doi:10.1093/pcp/pcm074

Govier, D. a, Kassanis, B., 1974. Evidence that a component other than the virus particle is needed for aphid transmission of *Potato virus Y*. Virology 57, 285–286. doi:10.1016/0042-6822(74)90129-9

Grangeon, R., Cotton, S., Laliberté, J.-F., 2010. A model for the biogenesis of *Turnip mosaic virus* replication factories. Commun. Integr. Biol. 3, 363–365. doi:10.4161/cib.3.4.11968

Habili, N., Francki, R.I., 1974. Comparative studies on *Tomato aspermy* and *Cucumber mosaic viruses*. I. Physical and chemical properties. Virology 57, 392–401.

Habili, N., Symons, R.H., 1989. Evolutionary relationship between *luteoviruses* and other RNA plant viruses based on sequence motifs in their putative RNA polymerases and nucleic acid helicases. Nucleic Acids Res. 17, 9543–9555. doi:10.1093/nar/17.23.9543

Haikonen, T., Rajamäki, M.-L., Tian, Y.-P., Valkonen, J.P.T., 2013a. Mutation of a Short Variable Region in HCpro Protein of *Potato virus A* Affects Interactions with a Microtubule-Associated Protein and Induces Necrotic Responses in Tobacco. Mol. Plant. Microbe. Interact. 26, 721–33. doi:10.1094/MPMI-01-13-0024-R

Haikonen, T., Rajamäki, M.-L., Valkonen, J.P.T., 2013b. Interaction of the microtubule-associated host protein HIP2 with viral helper component proteinase is important in infection with *Potato virus A*. Mol. Plant. Microbe. Interact. 26, 734–44. doi:10.1094/MPMI-01-13-0023-R

Hamera, S., Song, X., Su, L., Chen, X., Fang, R., 2012. *Cucumber mosaic virus* suppressor 2b binds to AGO4-related small RNAs and impairs AGO4 activities. Plant J. 69, 104–115. doi:10.1111/j.1365-313X.2011.04774.x

Harvey, J.J.W., Lewsey, M.G., Patel, K., Westwood, J., Heimstädt, S., Carr, J.P., Baulcombe, D.C., 2011. An antiviral defense role of AGO2 in plants. PLoS One 6, e14639. doi:10.1371/journal.pone.0014639

Havelda, Z., Hornyik, C., Válóczi, A., 2005. Defective interfering RNA hinders the activity of a *Tombusvirus*-encoded posttranscriptional gene silencing suppressor. J. Virol 79, 450–457. doi:10.1128/JVI.79.1.450

Hershko, a, Ciechanover, a, 1998. The ubiquitin system. Annu. Rev. Biochem. 67, 425–479. doi:10.1146/annurev.biochem.67.1.425

Hong, Y., Hunt, a G., 1996. RNA polymerase activity catalyzed by a potyvirus-encoded RNA-dependent RNA polymerase. Virology 226, 146–151. doi:10.1006/viro.1996.0639

Huang, Y.W., Hu, C.C., Lin, C. a., Liu, Y.P., Tsai, C.H., Lin, N.S., Hsu, Y.H., 2009. Structural and functional analyses of the 3' untranslated region of *Bamboo mosaic virus* satellite RNA. Virology 386, 139–153. doi:10.1016/j.virol.2009.01.019

Huh, S.U., Kim, M.J., Ham, B.K., Paek, K.H., 2011. A zinc finger protein Tsip1 controls *Cucumber mosaic virus* infection by interacting with the replication complex on vacuolar membranes of the tobacco plant. New Phytol. 191, 746–762. doi:10.1111/j.1469-8137.2011.03717.x

Hull, R., 2002. Matthews' Plant Virology, Fourth. ed. San Diego, California, USA.

Ishibashi, K., Naito, S., Meshi, T., Ishikawa, M., 2009. An inhibitory interaction between viral and cellular proteins underlies the resistance of tomato to nonadapted *tobamoviruses*. Proc. Natl. Acad. Sci. U. S. A. 106, 8778–8783. doi:10.1073/pnas.0809105106

Itaya, A., Qi, Y., Matsuda, Y., Zhu, Y., Liang, G., Ding, B., 2002. Plasmodesma-mediated selective protein traffic between "symplasmically isolated" cells probed by a viral movement protein. Plant Cell 14, 2071–2083. doi:10.1105/tpc.003954.mitosis

Jacquemond, M., 2012. *Cucumber Mosaic Virus*, 1st ed, Advances in Virus Research. Elsevier Inc. doi:10.1016/B978-0-12-394314-9.00013-0

Jamous, R.M., Boonrod, K., Fuellgrabe, M.W., Ali-Shtayeh, M.S., Krczal, G., Wassenegger, M., 2011. The helper component-proteinase of the *Zucchini yellow mosaic virus* inhibits the Hua Enhancer 1 methyltransferase activity *in vitro*. J. Gen. Virol. 92, 2222–2226. doi:10.1099/vir.0.031534-0

Jaspars, E.M.J., Gill, D.S., Symons, R.H., 1985. Vira RNA synthesis by a particulate fraction from cucumber seedlings infected with *Cucumber mosaic virus*. Virology 144, 410–425. doi:10.1016/0042-6822(85)90282-X

Jaubert, M., Bhattacharjee, S., Mello, A.F.S., Perry, K.L., Moffett, P., 2011. ARGONAUTE2 mediates RNA-silencing antiviral defenses against *Potato virus X* in Arabidopsis. Plant Physiol. 156, 1556–1564. doi:10.1104/pp.111.178012

Jiang, J., Laliberté, J.F., 2011. The genome-linked protein VPg of plant viruses - A protein with many partners. Curr. Opin. Virol. 1, 347–354. doi:10.1016/j.coviro.2011.09.010

Jin, Y., Ma, D., Dong, J., Jin, J., Li, D., Deng, C., Wang, T., 2007. HC-Pro protein of *Potato virus Y* can interact with three Arabidopsis 20S proteasome subunits *in planta*. J. Virol. 81, 12881–12888. doi:10.1128/JVI.00913-07

Johansen, I.E., Lund, O.S., Hjulsager, C.K., Laursen, J., 2001. Recessive resistance in Pisum sativum and *potyvirus* pathotype resolved in a gene-for-cistron correspondence between host and virus. J. Virol. 75, 6609–6614. doi:10.1128/JVI.75.14.6609-6614.2001

Johansen, L.K., Carrington, J.C., 2001. Silencing on the spot. Induction and suppression of RNA silencing in the Agrobacterium-mediated transient expression system. Plant Physiol. 126, 930–938. doi:10.1104/pp.126.3.930

Johnson, J., 1922. The relation of air temperature to the mosaic disease of potatoes and other plants. Phytopathology 12, 438–440.

Kadioglu, A., Terzi, R., Saruhan, N., Saglam, A., 2012. Current advances in the investigation of leaf rolling caused by biotic and abiotic stress factors. Plant Sci. 182, 42–48. doi:10.1016/j.plantsci.2011.01.013

Kang, B.-C., Yeam, I., Jahn, M.M., 2005. Genetics of plant virus resistance. Annu. Rev. Phytopathol. 43, 581–621. doi:10.1146/annurev.phyto.43.011205.141140

Karran, R., Sanfacon, H., 2014. *Tomato ringspot virus* coat protein binds to ARGONAUTE 1 and suppresses the translation repression of a reporter gene. Mol. Plant. Microbe. Interact. 27, 1–32. doi:10.1094/MPMI-04-14-0099-R

Kasschau, K.D., Carrington, J.C., 1998. A counterdefensive strategy of plant viruses: suppression of posttranscriptional gene silencing. Cell 95, 461–470. doi:http://dx.doi.org/10.1016/S0092-8674(00)81614-1

Kasschau, K.D., Xie, Z., Allen, E., Llave, C., Chapman, E.J., Krizan, K.A., Carrington, J.C., 2003. P1/HC-Pro, a Viral Suppressor of RNA Silencing, Interferes with Arabidopsis Development and miRNA Function. Dev. Cell 4, 205–217. doi:10.1016/S1534-5807(03)00025-X

Kendall, A., McDonald, M., Bian, W., Bowles, T., Baumgarten, S.C., Shi, J., Stewart, P.L., Bullitt, E., Gore, D., Irving, T.C., Havens, W.M., Ghabrial, S. a, Wall, J.S., Stubbs, G., 2008. Structure of flexible filamentous plant viruses. J. Virol. 82, 9546–9554. doi:10.1128/JVI.00895-08

Kim, M.J., Kim, H.R., Paek, K.H., 2006. Arabidopsis tonoplast proteins TIP1 and TIP2 interact with the *Cucumber mosaic virus* 1a replication protein. J. Gen. Virol. 87, 3425–3431.

Kim, S.H., Kalinina, N.O., Andreev, I., Ryabov, E. V, Fitzgerald, A.G., Taliansky, M.E., Palukaitis, P., 2004. The C-terminal 33 amino acids of the *Cucumber mosaic virus* 3a protein affect virus movement, RNA binding and inhibition of infection and translation. J. Gen. Virol. 85, 221–230.

Kirschbaum, M.U.F., Lambie, S.M., 2015. Re-analysis of plant CO 2 responses during the exponential growth phase : interactions with light , temperature , nutrients and water availability. Funct. Plant Biol. 42, 989–1000.

Kovač, M., Müller, a., Milovanovič Jarh, D., Milavec, M., Düchting, P., Ravnikar, M., 2009. Multiple hormone analysis indicates involvement of jasmonate signalling in the early defence of potato to *Potato virus* Y^{NTN}. Biol. Plant. 53, 195–199. doi:10.1007/s10535-009-0034-y

Kreuze, J.F., Perez, A., Untiveros, M., Quispe, D., Fuentes, S., Barker, I., Simon, R., 2009. Complete viral genome sequence and discovery of novel viruses by deep sequencing of small RNAs: a generic method for diagnosis, discovery and sequencing of viruses. Virology 388, 1–7. doi:10.1016/j.virol.2009.03.024

Kurihara, Y., Watanabe, Y., 2004. Arabidopsis micro-RNA biogenesis through Dicer-like 1 protein functions. Proc. Natl. Acad. Sci. U. S. A. 101, 12753–8. doi:10.1073/pnas.0403115101

Laín, S., Martín, M.T., Riechmann, J.L., García, J. a, 1991. Novel catalytic activity associated with positive-strand RNA virus infection: nucleic acid-stimulated ATPase activity of the *Plum pox potyvirus* helicaselike protein. J. Virol. 65, 1–6.

Laín, S., Riechmann, J.L., García, J. a, 1990. RNA helicase: a novel activity associated with a protein encoded by a positive strand RNA virus. Nucleic Acids Res. 18, 7003–7006. doi:10.1093/nar/18.23.7003

Lakatos, L., Csorba, T., Pantaleo, V., Chapman, E.J., Carrington, J.C., Liu, Y.-P., Dolja, V. V, Calvino, L.F., López-Moya, J.J., Burgyán, J., 2006. Small RNA binding is a common strategy to suppress RNA silencing by several viral suppressors. EMBO J. 25, 2768–2780. doi:10.1038/sj.emboj.7601164

Larkindale, J., Hall, J.D., Knight, M.R., Vierling, E., Larkindale J., Hall J.D., Knight M.R., E., V., 2005. Heat stress phenotypes of Arabidopsis mutants implicate multiple signaling pathways in the acquisition of thermotolerance. Plant Physiol. 138, 882–897. doi:10.1104/pp.105.062257.882

Larkindale, J., Huang, B., 2004. Thermotolerance and antioxidant systems in *Agrostis stolonifera*: involvement of salicylic acid, abscisic acid, calcium, hydrogen peroxide, and ethylene. J. Plant Physiol. 161, 405–413. doi:10.1078/0176-1617-01239

Lawson, R.H., Hearon, S.S., 1971. The association of pinwheel inclusions with plasmodesmata. Virology 44.

Lewandowski, D.J., 1993. A single amino acid change in *Tobacco mosaic virus* replicase prevents symptom production. Mol. Plant-Microbe Interact. doi:10.1094/MPMI-6-157

Li, H.W., Lucy, A.P., Guo, H.S., Li, W.X., Ji, L.H., Wong, S.M., Ding, S.W., 1999. Strong host resistance targeted against a viral suppressor of the plant gene silencing defence mechanism. EMBO J. 18, 2683–2691. doi:10.1093/emboj/18.10.2683

Li, Y., Jinfeng, L., Yanhong, H., Xiaoxu, F., Shou-Wei, D., 2013. RNA interference functions as an antiviral immunity mechanism in mammals. Science (80). 342, 231–234. doi:10.1016/j.biotechadv.2011.08.021.Secreted

Li, J., Yang, Z., Yu, B., Liu, J., Chen, X., 2005. Methylation protects miRNAs and siRNAs from a 3'-end uridylation activity in Arabidopsis. Curr. Biol. 15, 1501–7. doi:10.1016/j.cub.2005.07.029

Li, Y.I., Chen, Y.J., Hsu, Y.H., Meng, M., 2001. Characterization of the AdoMet-dependent guanylyltransferase activity that is associated with the N terminus of *Bamboo mosaic virus* replicase. J. Virol. 75, 782–788. doi:10.1128/JVI.75.2.782-788.2001

Li, Y.I., Cheng, Y.M., Huang, Y.L., Tsai, C.H., Hsu, Y.H., Meng, M., 1998. Identification and characterization of the *Escherichia coli*-expressed RNA-dependent RNA polymerase of *Bamboo mosaic virus*. J. Virol. 72, 10093–10099.

Linnik, O., Liesche, J., Tilsner, J., Oparka, K.J., 2013. Unraveling the structure of viral replication complexes at super-resolution. Front. Plant Sci. 4, 6. doi:10.3389/fpls.2013.00006

Lot, H., Kaper, J.M., 1976. Further studies on the RNA component distribution among the nucleoproteins of *Cucumber mosaic virus*. Virology 74, 223–226.

Love, A.J., Geri, C., Laird, J., Carr, C., Yun, B.W., Loake, G.J., Tada, Y., Sadanandom, A., Milner, J.J., 2012. *Cauliflower mosaic virus* protein P6 inhibits signaling responses to salicylic acid and regulates innate immunity. PLoS One 7. doi:10.1371/journal.pone.0047535

Lózsa, R., Csorba, T., Lakatos, L., Burgyán, J., 2008. Inhibition of 3' modification of small RNAs in virus-infected plants require spatial and temporal co-expression of small RNAs and viral silencing-suppressor proteins. Nucleic Acids Res. 36, 4099–4107. doi:10.1093/nar/gkn365

Lu, R., Malcuit, I., Moffett, P., Ruiz, M.T., Peart, J., Wu, A.-J., Rathjen, J.P., Bendahmane, A., Day, L., Baulcombe, D.C., 2003. High throughput virus-induced gene silencing implicates heat shock protein 90 in plant disease resistance. EMBO J. 22, 5690–5699. doi:10.1093/emboj/cdg546

Lucy, A.P., Guo, H.S., Li, W.X., Ding, S.W., 2000. Suppression of post-transcriptional gene silencing by a plant viral protein localized in the nucleus. EMBO J. 19, 1672–1680. doi:10.1093/emboj/19.7.1672

Maia, I.G., Bernardi, F., 1996. Nucleic acid-binding properties of a bacterially expressed *Potato virus Y* helper component-proteinase. J. Gen. Virol. 77, 869–877. doi:10.1099/0022-1317-77-5-869

Madsen, E. 1971. Cytological changes due to the effect of carbon dioxide concentration on the accumulation of starch in chloroplasts of tomato leaves. Royal Veterinary and Agriculture University, Copenhagen. Yearbook:1971:191-194.

Madsen, E. 1973. Effect of CO_2 concentration on the morphological, histological and cytological changes in tomato plants. Acta Agr. Scand. 220:428-429.

Márquez, L.M., Redman, R.S., Rodriguez, R.J., Marilyn J.Roossinck, 2007. A Virus in a Fungus in a Plant: Science (80). 315, 513–516. doi:10.1126/science.1136237

Matros, A., Amme, S., Kettig, B., Buck-Sorlin, G.H., Sonnewald, U., Mock, H.-P., 2006. Growth at elevated CO_2 concentrations leads to modied profiles of secondary metabolites in tobacco cv. SamsunNN and to increased resistance against infection with *Potato virus Y*. Plant, Cell Environ. 29, 126–137.

Mauck, K.E., De Moraes, C.M., Mescher, M.C., 2010. Deceptive chemical signals induced by a plant virus attract insect vectors to inferior hosts. Proc. Natl. Acad. Sci. 107, 3600–3605. doi:10.1073/pnas.0907191107

Mayers, C.N., Palukaitis, P., Carr, J.P., 2000. Subcellular distribution analysis of the *Cucumber mosaic virus* 2b protein. J. Gen. Virol. 81, 219–226.

Mérai, Z., Kerényi, Z., Kertész, S., Magna, M., Lakatos, L., Silhavy, D., 2006. Double-stranded RNA binding may be a general plant RNA viral strategy to suppress RNA silencing. J. Virol. 80, 5747–5756. doi:10.1128/JVI.01963-05

Merits, a, Guo, D., Järvekülg, L., Saarma, M., 1999. Biochemical and genetic evidence for interactions between *Potato A potyvirus*-encoded proteins P1 and P3 and proteins of the putative replication complex. Virology 263, 15–22. doi:10.1006/viro.1999.9926

Mi, S., Cai, T., Hu, Y., Chen, Y., Hodges, E., Ni, F., Wu, L., Li, S., Zhou, H., Long, C., Chen, S., Hannon, G.J., Qi, Y., 2008. Sorting of small RNAs into Arabidopsis argonaute complexes is directed by the 5' terminal nucleotide. Cell 133, 116–27. doi:10.1016/j.cell.2008.02.034

Mlotshwa, S, Verver, J, Sithole-Niang, I, Gopinath, K, Carette, J, Van Kammen, AB, Wellink, J. 2002. Subcellular location of the helper component-protease of *Cowpea aphid-borne mosaic virus*. Virus Genes 25:207-216.

Molnár, A., Csorba, T., Lakatos, L., Várallyay, E., Lacomme, C., Burgyán, J., 2005. Plant virus-derived small interfering RNAs originate predominantly from highly structured single-stranded viral RNAs. J. Virol. 79, 7812–7818. doi:10.1128/JVI.79.12.7812-7818.2005

Montgomery, T.A., Howell, M.D., Cuperus, J.T., Li, D., Hansen, J.E., Alexander, A.L., Chapman, E.J., Fahlgren, N., Allen, E., Carrington, J.C., 2008. Specificity of ARGONAUTE7-miR390 interaction and dual functionality in TAS3 trans-acting siRNA formation. Cell 133, 128–41. doi:10.1016/j.cell.2008.02.033

Mysore, K.S., Ryu, C.M., 2004. Nonhost resistance: How much do we know? Trends Plant Sci. 9, 97–104. doi:10.1016/j.tplants.2003.12.005

Nagano, H., Mise, K., Furusawa, I., Okuno, T., 2001. Conversion in the requirement of coat protein in cell-to-cell movement mediated by the *Cucumber mosaic virus* movement protein. J. Virol. 75, 8045–8053. doi:10.1128/JVI.75.17.8045-8053.2001

Nakahara, K.S., Masuta, C., Yamada, S., Shimura, H., Kashihara, Y., Wada, T.S., Meguro, a., Goto, K., Tadamura, K., Sueda, K., Sekiguchi, T., Shao, J., Itchoda, N., Matsumura, T., Igarashi, M., Ito, K., Carthew, R.W., Uyeda, I., 2012. Tobacco calmodulin-like protein provides secondary defense by binding to and directing degradation of virus RNA silencing suppressors. Proc. Natl. Acad. Sci. 109, 10113–10118. doi:10.1073/pnas.1201628109

Napoli, C., Lemieux, C., Jorgensen, R., 1990. Introduction of a chimeric chalcone synthase gene into Petunia results in reversible co-suppression of homologous genes in trans. Plant Cell 2, 279–289. doi:10.1105/tpc.2.4.279

Ng, J.C., Liu, S., Perry, K.L., 2000. *Cucumber mosaic virus* mutants with altered physical properties and defective in aphid vector transmission. Virology 276, 395–403. doi:10.1006/viro.2000.0569

Ng, J.C.K., Josefsson, C., Clark, A.J., Franz, a. W.E., Perry, K.L., 2005. Virion stability and aphid vector transmissibility of *Cucumber mosaic virus* mutants. Virology 332, 397–405. doi:10.1016/j.virol.2004.11.021

Nienhaus, F., Stille, B., 1965. Übertragung des *Kartoffel-X-Virus* durch Zoosporen von Synchytrium endobioticum. J. Phytopathol. 54, 335–337. doi:10.1111/j.1439-0434.1965.tb04104.x

Nieto, C., Rodríguez-Moreno, L., Rodríguez-Hernández, A.M., Aranda, M. a., Truniger, V., 2011. *Nicotiana benthamiana* resistance to non-adapted *Melon necrotic spot virus* results from an incompatible interaction between virus RNA and translation initiation factor 4E. Plant J. 66, 492–501. doi:10.1111/j.1365-313X.2011.04507.x

Nitta, N., Takanami, Y., Kuwata, S., Kubo, S., 1988. Inoculation with RNAs 1 and 2 of *Cucumber mosaic virus* induces viral RNA replicase activity in tobacco mesophyll protoplasts. J. Gen. Virol. 69, 2695–2700. doi:10.1099/0022-1317-69-10-2695

Norse, D., Gommes, R., 2003. Climate change and agriculture: physical and human dimensions, in: World Agriculture Towards 2015/2030: An FAO Perspective. Earthscan Publications Ltd, London, UK, pp. 357–372.

O'Reilly, E.K., Wang, Z., French, R., Kao, C.C., 1998. Interactions between the structural domains of the RNA replication proteins of plant-infecting RNA viruses. J. Virol. 72, 7160–7169.

Okano, Y., Senshu, H., Hashimoto, M., Neriya, Y., Netsu, O., Minato, N., Yoshida, T., Maejima, K., Oshima, K., Komatsu, K., Yamaji, Y., Namba, S., 2014. *In planta* recognition of a double-stranded RNA synthesis protein complex by a potexviral RNA silencing suppressor. Plant Cell 26, 2168–2183. doi:10.1105/tpc.113.120535

Pacheco, R., García-Marcos, A., Barajas, D., Martiáñez, J., Tenllado, F., 2012. PVX-*potyvirus* synergistic infections differentially alter microRNA accumulation in *Nicotiana benthamiana*. Virus Res. 165, 231–235. doi:10.1016/j.virusres.2012.02.012

Padmanabhan, M., Dinesh-Kumar, S.P., 2009. Virus-induced gene silencing as a tool for delivery of dsRNA into plants. Cold Spring Harb. Protoc. 4, 1–5. doi:10.1101/pdb.prot5139

Palukaitis, P., Carr, J.P., 2008. Plant resistance responses to viruses. J. Plant Pathol. 90, 153–171.

Palukaitis, P., García-Arenal, F., 2003. *Cucumoviruses*. Adv. Virus Res. 62, 241–323.

Palukaitis, P., Roossinck, M.J., Dietzgen, R.G., Francki, R.I., 1992. *Cucumber mosaic virus*. Adv. Virus Res. 41, 281–348.

Park, M.R., Seo, J.K., Kim, K.H., 2013. Viral and Nonviral Elements in Potexvirus Replication and Movement and in Antiviral Responses, 1st ed, Advances in Virus Research. Elsevier Inc. doi:10.1016/B978-0-12-407698-3.00003-X

Park, M.-R., Jeong, R.-D., Kim, K.-H., 2014. Understanding the intracellular trafficking and intercellular transport of *potexviruses* in their host plants. Front. Plant Sci. 5, 60. doi:10.3389/fpls.2014.00060

Pasin, F., Simón-Mateo, C., García, J.A., 2014. The hypervariable amino-terminus of P1 protease modulates potyviral replication and host defense responses. PLoS Pathog. 10. doi:10.1371/journal.ppat.1003985

Peyret, H., Lomonossoff, G.P., 2015. When plant virology met Agrobacterium□: the rise of the deconstructed clones. Plant Biotechnol. J. n/a–n/a. doi:10.1111/pbi.12412

Pita, J.S., Morris, V., Roossinck, M.J., 2015. Mutation and recombination frequencies reveal a biological contrast within strains of *Cucumber Mosaic Virus*. J. Virol. 89, 6817–6823. doi:10.1128/JVI.00040-15

Potters, G., Pasternak, T.P., Guisez, Y., Palme, K.J., Jansen, M. a K., 2007. Stress-induced morphogenic responses: growing out of trouble? Trends Plant Sci. 12, 98–105. doi:10.1016/j.tplants.2007.01.004

Pruss, G., Ge, X., Shi, X.M., Carrington, J.C., Bowman Vance, V., 1997. Plant viral synergism: the potyviral genome encodes a broad-range pathogenicity enhancer that transactivates replication of heterologous viruses. Plant Cell 9, 859–868. doi:10.1105/tpc.9.6.859

Pumplin, N., Voinnet, O., 2013. RNA silencing suppression by plant pathogens: defence, counter-defence and counter-counter-defence. Nat. Rev. Microbiol. 11, 745–60. doi:10.1038/nrmicro3120

Puustinen, P., Mäkinen, K., 2004. Uridylylation of the *potyvirus* VPg by viral replicase NIb correlates with the nucleotide binding capacity of VPg. J. Biol. Chem. 279, 38103–38110. doi:10.1074/jbc.M402910200

Qu, F., Ye, X., Hou, G., Sato, S., Clemente, T.E., Morris, T.J., 2005. RDR6 has a broad-spectrum but temperature-dependent antiviral defense role in Nicotiana benthamiana. J. Virol. 79, 15209–15217. doi:10.1128/JVI.79.24.15209-15217.2005

Qu, F., 2010. Antiviral role of plant-encoded RNA-dependent RNA polymerases revisited with deep sequencing of small interfering RNAs of virus origin. Mol. Plant. Microbe. Interact. 23, 1248–1252. doi:10.1094/MPMI-06-10-0124

Qu, F., Ye, X., Morris, T.J., 2008. Arabidopsis DRB4, AGO1, AGO7, and RDR6 participate in a DCL4-initiated antiviral RNA silencing pathway negatively regulated by DCL1. Proc. Natl. Acad. Sci. U. S. A. 105, 14732–14737. doi:10.1073/pnas.0805760105

Quirino, B.F., Normanly, J., Amasino, R.M., 1999. Diverse range of gene activity during *Arabidopsis thaliana* leaf senescence includes pathogen-independent induction of defense-related genes. Plant Mol. Biol. 40, 267–278. doi:10.1023/A:1006199932265

Radcliffe, E.B., Ragsdale, D.W., 2002. Aphid-transmitted potato viruses: The importance of understanding vector biology. Am. J. Potato Res. 79, 353–386. doi:10.1007/BF02870173

Ramachandran, V., Chen, X., 2008. Degradation of microRNAs by a family of exoribonucleases in Arabidopsis. Science (80). 321, 1490–1492. doi:10.1126/science.1163728.Degradation

Reichel, C., Beachy, R.N., 2000. Degradation of *Tobacco mosaic virus* movement protein by the 26S proteasome. J. Virol. 74, 3330–3337. doi:10.1128/JVI.74.7.3330-3337.2000

Requena, a, Simón-Buela, L., Salcedo, G., García-Arenal, F., 2006. Potential involvement of a cucumber homolog of phloem protein 1 in the long-distance movement of *Cucumber mosaic virus* particles. Mol. Plant. Microbe. Interact. 19, 734–746. doi:10.1094/MPMI-19-0734

Restrepo-Hartwig, M. a, Carrington, J.C., 1994. The *Tobacco etch potyvirus* 6-kilodalton protein is membrane associated and involved in viral replication. J. Virol. 68, 2388–2397.

Riechmann, J.L., Laín, S., García, J.A., 1992. Highlights and prospects of *potyvirus* molecular biology. J. Gen. Virol. 73 (Pt 1), 1–16. doi:10.1099/0022-1317-73-1-1

Robatzek, S., Somssich, I.E., 2001. A new member of the Arabidopsis WRKY transcription factor family, AtWRKY6, is associated with both senescence- and defence-related processes. Plant J. 28, 123–133. doi:10.1046/j.1365-313X.2001.01131.x

Rodrigo, G., Carrera, J., Ruiz-Ferrer, V., del Toro, F.J., Llave, C., Voinnet, O., Elena, S.F., 2012. A meta-analysis reveals the commonalities and differences in arabidopsis thaliana response to different viral pathogens. PLoS One 7. doi:10.1371/journal.pone.0040526

Rodriguez, M., Conti, G., Zavallo, D., Manacorda, C., Asurmendi, S., 2014. TMV-Cg Coat Protein stabilizes DELLA proteins and in turn negatively modulates salicylic acid-mediated defense pathway during *Arabidopsis thaliana* viral infection. BMC Plant Biol. 14, 210. doi:10.1186/s12870-014-0210-x

Rogers, H.H., Dahlman, R.C., 1993. Crop responses to CO_2 enrichment. Plant Ecol. 104, 117–131.

Roossinck, M.J., 2011. The good viruses: viral mutualistic symbioses. Nat. Rev. Microbiol. 9, 99–108. doi:10.1038/nrmicro2491

Roossinck, M.J., 1999. *Cucumoviruses* (*Bromoviridae*) General Features, in: Encyclopedia of Virology. Elsevier, pp. 315–320. doi:10.1006/rwvi.1999.0059

Rozanov, M.N., Koonin, E. V, Gorbalenya, A.E., 1992. Conservation of the putative methyltransferase domain: a hallmark of the "Sindbis-like" supergroup of positive-strand RNA viruses. J. Gen. Virol. 73, 2129–2134.

Ruan, Y.L., Jin, Y., Yang, Y.J., Li, G.J., Boyer, J.S., 2010. Sugar input, metabolism, and signaling mediated by invertase: Roles in development, yield potential, and response to drought and heat. Mol. Plant 3, 942–955. doi:10.1093/mp/ssq044

Rubio-Huertos, M., López-Abella, D., 1966. Ultraestructura de células de pimiento infectadas con un virus y su localización en las mismas. Microbiol. Española 19, 1–77.

Ruiz, M., Voinnet, O., Baulcombe, D., 1998. Initiation and maintenance of virus-induced gene silencing. Plant Cell 10, 937–46. doi:10.2307/3870680

Ruiz-Ferrer, V., Boskovic, J., Alfonso, C., Rivas, G., Llorca, O., López-Abella, D., López-Moya, J.J., 2005. Structural analysis of *Tobacco etch potyvirus* HC-pro oligomers involved in aphid transmission. J. Virol. 79, 3758–3765. doi:10.1128/JVI.79.6.3758-3765.2005

Sahana, N., Kaur, H., Basavaraj, Tena, F., Jain, R.K., Palukaitis, P., Canto, T., Praveen, S., 2012. Inhibition of the host proteasome facilitates *Papaya Ringspot Virus* accumulation and proteosomal catalytic activity is modulated by viral factor HcPro. PLoS One 7. doi:10.1371/journal.pone.0052546

Saidi, Y., Finka, A., Muriset, M., Bromberg, Z., Weiss, Y.G., Maathuis, F.J.M., Goloubinoff, P., 2009. The heat shock response in moss plants is regulated by specific calcium-permeable channels in the plasma membrane. Plant Cell 21, 2829–2843. doi:10.1105/tpc.108.065318

Scholthof, K.B.G., Adkins, S., Czosnek, H., Palukaitis, P., Jacquot, E., Hohn, T., Hohn, B., Saunders, K., Candresse, T., Ahlquist, P., Hemenway, C., Foster, G.D., 2011. Top 10 plant viruses in molecular plant pathology. Mol. Plant Pathol. 12, 938–954. doi:10.1111/j.1364-3703.2011.00752.x

Schwartz, M., Chen, J., Janda, M., Sullivan, M., Den Boon, J., Ahlquist, P., 2002. A positive-strand RNA virus replication complex parallels form and function of retrovirus capsids. Mol. Cell 9, 505–514. doi:10.1016/S1097-2765(02)00474-4

Schwinghamer, M.W., Symons, R.H., 1977. Translation of the four major RNA species of *Cucumber mosaic virus* in plant and animal cell-free systems and in toad oocytes. Virology 79, 88–108.

Senshu, H., Ozeki, J., Komatsu, K., Hashimoto, M., Hatada, K., Aoyama, M., Kagiwada, S., Yamaji, Y., Namba, S., 2009. Variability in the level of RNA silencing suppression caused by triple gene block protein 1 (TGBp1) from various potexviruses during infection. J. Gen. Virol. 90, 1014–1024. doi:10.1099/vir.0.008243-0

Shiboleth, Y.M., Haronsky, E., Leibman, D., Arazi, T., Wassenegger, M., Whitham, S. a, Gaba, V., Gal-On, A., 2007. The conserved FRNK box in HC-Pro, a plant viral suppressor of gene silencing, is required for small RNA binding and mediates symptom development. J. Virol. 81, 13135–13148. doi:10.1128/JVI.01031-07

Shimura, H., Pantaleo, V., Ishihara, T., Myojo, N., Inaba, J.I., Sueda, K., Burgyán, J., Masuta, C., 2011. A viral satellite RNA induces yellow symptoms on tobacco by targeting a gene involved in chlorophyll biosynthesis using the RNA silencing machinery. PLoS Pathog. 7, 1–12. doi:10.1371/journal.ppat.1002021

Shukla, D.D., Ward, C.W., Brunt, A.A., 1994. The *Potyviridae*, CAB Intern. ed. Wallingford, Oxfordshire.

Sikorskaite, S., Vuorinen, A.L., Rajamäki, M.-L., Nieminen, A., Gaba, V., Valkonen, J.P.T., 2010. HandyGun: An improved custom-designed, non-vacuum gene gun suitable for virus inoculation. J. Virol. Methods 165, 320–4. doi:10.1016/j.jviromet.2010.02.025

Silhavy, D., Burgyán, J., 2004. Effects and side-effects of viral RNA silencing suppressors on short RNAs. Trends Plant Sci. 9, 76–83. doi:10.1016/j.tplants.2003.12.010

Silhavy, D., Molnar, a, Lucioli, a, Szittya, G., Hornyik, C., Tavazza, M., Burgyan, J., 2002. A viral protein suppresses RNA silencing and binds silencing-generated, 21-to 25-nucleotide doube-stranded RNAs. Embo J. 21, 3070–3080.

Singh, R.K., Gase, K., Baldwin, I.T., Pandey, S.P., 2015. Molecular evolution and diversification of the Argonaute family of proteins in plants. BMC Plant Biol. 15, 23. doi:10.1186/s12870-014-0364-6

Simmons, H.E., Dunham, J.P., Zinn, K.E., Munkvold, G.P., Holmes, E.C., Stephenson, A.G., 2013. *Zucchini yellow mosaic virus* (ZYMV, *Potyvirus*): vertical transmission, seed infection and cryptic infections. Virus Res. 176, 259–64. doi:10.1016/j.virusres.2013.06.016

Smith, K.M., 1931. On the composite nature of certain potato virus diseases of the mosaic group as revealed by the use of plant indicators and selective methods of transmission. Proc. R. Soc. London 109, 251–267.

Sorel, M., Garcia, J. a, German-Retana, S., 2014. The *Potyviridae* cylindrical inclusion helicase: a key multipartner and multifunctional protein. Mol. Plant. Microbe. Interact. 27, 215–26. doi:10.1094/MPMI-11-13-0333-CR

Soumounou, Y., Laliberté, J.F., 1994. Nucleic acid-binding properties of the P1 protein of *Turnip mosaic potyvirus* produced in *Escherichia coli*. J. Gen. Virol. 10, 2567–2573.

Spoel, S.H., Johnson, J.S., Dong, X., 2007. Regulation of tradeoffs between plant defenses against pathogens with different lifestyles. Proc. Natl. Acad. Sci. U. S. A. 104, 18842–18847. doi:10.1073/pnas.0708139104

Stav, R., Hendelman, A., Buxdorf, K., Arazi, T., 2010. Transgenic expression of *Tomato bushy stunt virus* silencing suppressor P19 via the pOp/LhG4 transactivation system induces viral-like symptoms in tomato. Virus Genes 40, 119–129. doi:10.1007/s11262-009-0415-5

Szittya, G., Silhavy, D., Molnár, A., Havelda, Z., Lovas, Á., Lakatos, L., Bánfalvi, Z., Burgyán, J., 2003. Low temperature inhibits RNA silencing-mediated defence by the control of siRNA generation. EMBO J. 22, 633–640. doi:10.1093/emboj/cdg74

Takács, A., Horváth, J., Gáborjány, R., Kazinczi, G., Mikulas, J., 2014. Hosts and non-hosts in plant virology and the effects of plant viruses on host plants, in: Plant Virus–Host Interaction Molecular Approaches and Viral Evolution. Academic Press, Oxford, pp. 105–122. doi:10.1016/B978-0-12-411584-2.01001-5

Takeda, A., Iwasaki, S., Watanabe, T., Utsumi, M., Watanabe, Y., 2008. The mechanism selecting the guide strand from small RNA duplexes is different among argonaute proteins. Plant Cell Physiol. 49, 493–500. doi:10.1093/pcp/pcn043

Talbot, N.J., 2004. Plant-pathogen Interactions. CRC Press, Victoria, Australia.

Tena Fernández, F., González, I., Doblas, P., Rodríguez, C., Sahana, N., Kaur, H., Tenllado, F., Praveen, S., Canto, T., 2013. The influence of *cis* -acting P1 protein and translational elements on the expression of *Potato virus Y* helper-component proteinase (HCPro) in heterologous systems and its suppression of silencing activity. Mol. Plant Pathol. 14, 530–541. doi:10.1111/mpp.12025

Thornbury, D.W., Hellmann, G.M., Rhoads, R.E., Pirone, T.P., 1985. Purification and characterization of *potyvirus* helper component. Virology 144, 260–267. doi:10.1016/0042-6822(85)90322-8

Tilsner, J., Linnik, O., Louveaux, M., Roberts, I.M., Chapman, S.N., Oparka, K.J., 2013. Replication and trafficking of a plant virus are coupled at the entrances of plasmodesmata. J. Cell Biol. 201, 981–995. doi:10.1083/jcb.201304003

Tilsner, J., Linnik, O., Wright, K.M., Bell, K., Roberts, a. G., Lacomme, C., Santa Cruz, S., Oparka, K.J., 2012. The TGB1 movement protein of *Potato virus X* reorganizes actin and endomembranes into the X-body, a viral replication factory. Plant Physiol. 158, 1359–1370. doi:10.1104/pp.111.189605

Torres, M.A., Jones, J.D.G., Dangl, J.L., 2006. Reactive oxygen species signaling in response to pathogens. Plant Physiol. 141, 373–378. doi:10.1104/pp.106.079467.conjunction

Trębicki, P., Nancarrow, N., Cole, E., Bosque-Pérez, N. a., Constable, F.E., Freeman, A.J., Rodoni, B., Yen, A.L., Luck, J.E., Fitzgerald, G.J., 2015. Virus disease in wheat predicted to increase with a changing climate. Glob. Chang. Biol. 21, 3511–3519. doi:10.1111/gcb.12941

Urcuqui-Inchima, S., Maia, I.G., Arruda, P., Haenni, a L., Bernardi, F., 2000. Deletion mapping of the potyviral helper component-proteinase reveals two regions involved in RNA binding. Virology 268, 104–111. doi:10.1006/viro.1999.0156

Urcuqui-Inchima, S., Walter, J., Drugeon, G., German-Retana, S., Haenni, a L., Candresse, T., Bernardi, F., Le Gall, O., 1999. *Potyvirus* helper component-proteinase self-interaction in the yeast two-hybrid system and delineation of the interaction domain involved. Virology 258, 95–99. doi:10.1006/viro.1999.9725

Van der Krol, a R., Mur, L. a, Beld, M., Mol, J.N., Stuitje, a R., 1990. Flavonoid genes in petunia: addition of a limited number of gene copies may lead to a suppression of gene expression. Plant Cell 2, 291–299. doi:10.1105/tpc.2.4.291

Van Loon, L.C., Rep, M., Pieterse, C.M.J., 2006. Significance of inducible defense-related proteins in infected plants. Annu. Rev. Phytopathol. 44, 135–162. doi:10.1146/annurev.phyto.44.070505.143425

Vance, V.B., 1991. Replication of *Potato virus X* RNA is altered in coinfections with *Potato virus Y*. Virology 182, 486–94.

Vance, V.B., Berger, P.H., Carrington, J.C., Hunt, A.G., Shi, X.M., 1995. 5' proximal potyviral sequences mediate *Potato virus X/potyviral* synergistic disease in transgenic tobacco. Virology 206, 583–90.

Vaquero, C., Liao, Y.C., Nähring, J., Fischer, R., 1997. Mapping of the RNA-binding domain of the *Cucumber mosaic virus* movement protein. J. Gen. Virol. 78, 2095–2099.

Vaquero, C., Sanz, A., Serra, M.T., García-Luque, I., 1996. Accumulation kinetics of CMV RNA 3-encoded proteins and subcellular localization of the 3a protein in infected and transgenic tobacco plants. Arch. Virol. 141, 987–999.

Velázquez, K., Renovell, a., Comellas, M., Serra, P., García, M.L., Pina, J. a., Navarro, L., Moreno, P., Guerri, J., 2010. Effect of temperature on RNA silencing of a negative-stranded RNA plant virus: Citrus psorosis virus. Plant Pathol. 59, 982–990. doi:10.1111/j.1365-3059.2010.02315.x

Verchot, J., Carrington, J.C., 1995. Debilitation of plant potyvirus infectivity by P1 proteinase-inactivating mutations and restoration by second-site modifications. J. Virol. 69, 1582–1590.

Verchot, J., Koonin, E. V., Carrington, J.C., 1991. The 35-kDa protein from the N-terminus of the potyviral polyprotein functions as a third virus-encoded proteinase. Virology 185, 527–535. doi:10.1016/0042-6822(91)90522-D

Vijayapalani, P., Maeshima, M., Nagasaki-Takekuchi, N., Miller, W.A., 2012. Interaction of the trans-frame *potyvirus* protein P3N-PIPO with host protein PCaP1 facilitates *potyvirus* movement. PLoS Pathog. 8. doi:10.1371/journal.ppat.1002639

Vlot, a C., Dempsey, D.A., Klessig, D.F., 2009. Salicylic acid, a multifaceted hormone to combat disease. Annu. Rev. Phytopathol. 47, 177–206. doi:10.1146/annurev.phyto.050908.135202

Vogler, H., Akbergenov, R., Shivaprasad, P. V, Dang, V., Fasler, M., Kwon, M.-O., Zhanybekova, S., Hohn, T., Heinlein, M., 2007. Modification of small RNAs associated with suppression of RNA silencing by tobamovirus replicase protein. J. Virol. 81, 10379–10388. doi:10.1128/JVI.00727-07

Voinnet, O., 2009. Origin, Biogenesis, and Activity of Plant MicroRNAs. Cell 136, 669–687. doi:10.1016/j.cell.2009.01.046

Voinnet, O., Lederer, C., Baulcombe, D.C., 2000. A viral movement protein prevents spread of the gene silencing signal in *Nicotiana benthamiana*. Cell 103, 157–167. doi:10.1016/S0092-8674(00)00095-7

Wallis, C.M., Stone, A.L., Sherman, D.J., Damsteegt, V.D., Gildow, F.E., Schneider, W.L., 2007. Adaptation of *Plum pox virus* to a herbaceous host (*Pisum sativum*) following serial passages. J. Gen. Virol. 88, 2839–2845. doi:10.1099/vir.0.82814-0

Walters, H.J., 1952. Some relationships of the three plant viruses in the differential grasshopper, *Melanopus differentialis*. Phytopathology 42, 355.

Wang, X.-B., Jovel, J., Udomporn, P., Wang, Y., Wu, Q., Li, W.-X., Gasciolli, V., Vaucheret, H., Ding, S.-W., 2011. The 21-nucleotide, but not 22-nucleotide, viral secondary small interfering RNAs direct potent antiviral defense by two cooperative argonautes in *Arabidopsis thaliana*. Plant Cell 23, 1625–1638. doi:10.1105/tpc.110.082305

Wang, Y., Bao, Z., Zhu, Y., Hua, J., 2009. Analysis of temperature modulation of plant defense against biotrophic microbes. Mol. Plant. Microbe. Interact. 22, 498–506. doi:10.1094/MPMI-22-5-0498

Ward, C.W., Shukla, D.D., 1991. Taxonomy of *potyviruses*: current problems and some solutions. Intervirology 32, 269–296.

Weaver, L.M., Gan, S., Quirino, B., Amasino, R.M., 1998. A comparison of the expression patterns of several senescence-associated genes in response to stress and hormone treatment. Plant Mol. Biol. 37, 455–469. doi:10.1023/A:1005934428906

Wei, T., Huang, T.-S., McNeil, J., Laliberté, J.-F., Hong, J., Nelson, R.S., Wang, A., 2010a. Sequential recruitment of the endoplasmic reticulum and chloroplasts for plant *potyvirus* replication. J. Virol. 84, 799–809. doi:10.1128/JVI.01824-09

Wei, T., Wang, A., 2008. Biogenesis of cytoplasmic membranous vesicles for plant *potyvirus* replication occurs at endoplasmic reticulum exit sites in a COPI- and COPII-dependent manner. J. Virol. 82, 12252–12264. doi:10.1128/JVI.01329-08

Wei, T., Zhang, C., Hong, J., Xiong, R., Kasschau, K.D., Zhou, X., Carrington, J.C., Wang, A., 2010b. Formation of complexes at plasmodesmata for *potyvirus* intercellular movement is mediated by the viral protein P3N-PIPO. PLoS Pathog. 6. doi:10.1371/journal.ppat.1000962

Wei, T., Zhang, C., Hou, X., Sanfaçon, H., Wang, A., 2013. The SNARE protein Syp71 is essential for *Turnip mosaic virus* infection by mediating fusion of virus-induced vesicles with chloroplasts. PLoS Pathog. 9, e1003378. doi:10.1371/journal.ppat.1003378

Weis E., Berry J. A. (1988) Plants and high temperature stress. *Symp. Soc. Exp. Biol.* 42329–346

Wen, R.H., Hajimorad, M.R., 2010. Mutational analysis of the putative pipo of *Soybean mosaic virus* suggests disruption of PIPO protein impedes movement. Virology 400, 1–7. doi:10.1016/j.virol.2010.01.022

Whitham, S. a, Yang, C., Goodin, M.M., 2006. Global impact: elucidating plant responses to viral infection. Mol. Plant. Microbe. Interact. 19, 1207–1215. doi:10.1094/MPMI-19-1207

Wise, R.P., Moscou, M.J., Bogdanove, A.J., Whitham, S. a, 2007. Transcript profiling in host-pathogen interactions. Annu. Rev. Phytopathol. 45, 329–369. doi:10.1146/annurev.phyto.45.011107.143944

Xie, Z., Johansen, L.K., Gustafson, A.M., Kasschau, K.D., Lellis, A.D., Zilberman, D., Jacobsen, S.E., Carrington, J.C., 2004. Genetic and functional diversification of small RNA pathways in plants. PLoS Biol. 2, E104. doi:10.1371/journal.pbio.0020104

Xu, P., Chen, F., Mannas, J.P., Feldman, T., Sumner, L.W., Roossinck, M.J., 2008. Virus infection improves drought tolerance. New Phytol. 180, 911–921. doi:10.1111/j.1469-8137.2008.02627.x

Yang, Y., Kim, K.S., Anderson, E.J., 1997. Seed transmission of *Cucumber mosaic virus* in spinach. Phytopathology 87, 924–931. doi:10.1094/PHYTO.1997.87.9.924

Yoon, J.Y., Ahn, H. Il, Kim, M., Tsuda, S., Ryu, K.H., 2006. *Pepper mild mottle virus* pathogenicity determinants and cross protection effect of attenuated mutants in pepper. Virus Res. 118, 23–30. doi:10.1016/j.virusres.2005.11.004

Yue, R., Lu, C., Sun, T., Peng, T., Han, X., Qi, J., Yan, S., Tie, S., 2015. Identification and expression profiling analysis of calmodulin-binding transcription activator genes in maize (*Zea mays* L.) under abiotic and biotic stresses. Front. Plant Sci. 6, 1–15. doi:10.3389/fpls.2015.00576

Zhang, S., Li, X., Sun, Z., Shao, S., Hu, L., Ye, M., Zhou, Y., Xia, X., Yu, J., Shi, K., 2015. Antagonism between phytohormone signalling underlies the variation in disease susceptibility of tomato plants under elevated CO_2. J. Exp. Bot. 66, 1951–1963. doi:10.1093/jxb/eru538

Zhang, X., Yuan, Y.-R., Pei, Y., Lin, S.-S., Tuschl, T., Patel, D.J., Chua, N.-H., 2006. *Cucumber mosaic virus*-encoded 2b suppressor inhibits Arabidopsis Argonaute1 cleavage activity to counter plant defense. Genes Dev. 20, 3255–3268. doi:10.1101/gad.1495506

Zhang, X., Zhang, X., Singh, J., Li, D., Qu, F., 2012. Temperature-dependent survival of *Turnip crinkle virus*-infected arabidopsis plants relies on an RNA silencing-

based defense that requires DCL2, AGO2, and HEN1. J. Virol. 86, 6847–6854. doi:10.1128/JVI.00497-12

Zheng, H., Yan, F., Lu, Y., Sun, L., Lin, L., Cai, L., Hou, M., Chen, J., 2011. Mapping the self-interacting domains of TuMV HC-Pro and the subcellular localization of the protein. Virus Genes 42, 110–116. doi:10.1007/s11262-010-0538-8

Zhong, S.-H., Liu, J.-Z., Jin, H., Lin, L., Li, Q., Chen, Y., Yuan, Y.-X., Wang, Z.-Y., Huang, H., Qi, Y.-J., Chen, X.-Y., Vaucheret, H., Chory, J., Li, J., He, Z.-H., 2013. Warm temperatures induce transgenerational epigenetic release of RNA silencing by inhibiting siRNA biogenesis in Arabidopsis. Proc. Natl. Acad. Sci. 110, 9171–9176. doi:10.1073/pnas.1219655110

Zhu, F., Xi, D.-H., Yuan, S., Xu, F., Zhang, D.-W., Lin, H.-H., 2014. Salicylic acid and jasmonic acid are essential for systemic resistance against *Tobacco mosaic virus* in *Nicotiana benthamiana*. Mol. Plant. Microbe. Interact. 27, 567–77. doi:10.1094/MPMI-11-13-0349-R

Zhu, S., Gao, F., Cao, X., Chen, M., Ye, G., Wei, C., Li, Y., 2005. The *Rice dwarf virus* P2 protein interacts with ent-kaurene oxidases *in vivo*, leading to reduced biosynthesis of gibberellins and rice dwarf symptoms. Plant Physiol. 139, 1935–45. doi:10.1104/pp.105.072306

Ziebell, H., Murphy, A.M., Groen, S.C., Tungadi, T., Westwood, J.H., Lewsey, M.G., Moulin, M., Kleczkowski, A., Smith, A.G., Stevens, M., Powell, G., Carr, J.P., 2011. *Cucumber mosaic virus* and its 2b RNA silencing suppressor modify plant-aphid interactions in tobacco. Sci. Rep. 1, 1–7. doi:10.1038/srep00187

Zilian, E., Maiss, E., 2011. Detection of *Plum pox potyviral* protein-protein interactions *in planta* using an optimized mRFP-based bimolecular fluorescence complementation system. J. Gen. Virol. 92, 2711–2723. doi:10.1099/vir.0.033811-0